



HAL
open science

High performance cellulosic materials to increase the life and reliability of power transformers

Enrique Felix Quesada Saavedra

► **To cite this version:**

Enrique Felix Quesada Saavedra. High performance cellulosic materials to increase the life and reliability of power transformers. Material chemistry. Université Grenoble Alpes [2020-..], 2023. English. NNT : 2023GRALI042 . tel-04210645

HAL Id: tel-04210645

<https://theses.hal.science/tel-04210645>

Submitted on 19 Sep 2023

HAL is a multi-disciplinary open access archive for the deposit and dissemination of scientific research documents, whether they are published or not. The documents may come from teaching and research institutions in France or abroad, or from public or private research centers.

L'archive ouverte pluridisciplinaire **HAL**, est destinée au dépôt et à la diffusion de documents scientifiques de niveau recherche, publiés ou non, émanant des établissements d'enseignement et de recherche français ou étrangers, des laboratoires publics ou privés.

THÈSE

Pour obtenir le grade de

DOCTEUR DE L'UNIVERSITÉ GRENOBLE ALPES

École doctorale : I-MEP2 - Ingénierie - Matériaux, Mécanique, Environnement, Energétique, Procédés, Production

Spécialité : 2MGE - Matériaux, Mécanique, Génie civil, Electrochimie

Unité de recherche : Laboratoire de Génie des Procédés pour la Bioraffinerie, les Matériaux Biosourcés et l'Impression Fonctionnelle

Matériaux cellulosiques de haute-performance pour accroître la durée de vie et la fiabilité de transformateurs de puissance

High performance cellulosic materials to increase the life and reliability of power transformers

Présentée par :

Enrique Felix QUESADA SAAVEDRA

Direction de thèse :

Gérard MORTHA

PROFESSEUR DES UNIVERSITES, Université Grenoble Alpes

Directeur de thèse

Nathalie MARLIN

MAITRE DE CONFERENCES, Université Grenoble Alpes

Co-encadrante de thèse

Olivier LESAIN

DIRECTEUR DE RECHERCHE, CNRS

Co-encadrant de thèse

Rapporteurs :

Anne-Laurence DUPONT

DIRECTRICE DE RECHERCHE, CNRS délégation Paris Centre

Thierry PAILLAT

PROFESSEUR DES UNIVERSITES, Université de Poitiers

Thèse soutenue publiquement le **12 juin 2023**, devant le jury composé de :

Gérard MORTHA

PROFESSEUR DES UNIVERSITES, Grenoble INP

Directeur de thèse

Anne-Laurence DUPONT

DIRECTRICE DE RECHERCHE, CNRS délégation Paris Centre

Rapporteuse

Thierry PAILLAT

PROFESSEUR DES UNIVERSITES, Université de Poitiers

Rapporteur

María GONZALEZ MARTÍNEZ

ASSISTANT PROFESSOR, IMT Mines Albi-Carmaux

Examinatrice

Alain SYLVESTRE

PROFESSEUR DES UNIVERSITES, Université Grenoble Alpes

Président

Invités :

Nathalie MARLIN

MAITRE DE CONFERENCES, Grenoble INP

Olivier LESAIN

DIRECTEUR DE RECHERCHE, CNRS



General introduction

With the invention of the lightbulb and the development of electrical machinery, the industrial world developed an appetite for an ever-increasing electrical power consumption. Over all the solution developed to meet this demand, the alternative current power grid eventually triumphed. This type of grid represents the vast majority of the power grids today. The power grid is an interconnected network made to transport electricity from producers to consumers. Central to the power grid are power transformers that are passive electrical devices which can rise and lower the voltage in electrical grids, in order to transport electricity with minimum losses. A higher voltage going through electrical lines will lead to lower power losses and thus allow the place of electricity generation to be far away to the place of energy consumption.

Power Transformer (PT) are particular types of transformers, found at the beginning of electrical networks. They are directly coupled with alternators in power plants and perform the first step-up in current sent to the rest of the grid. PT have among the highest power ratings of all the transformer and are therefore massive and expensive machines, considered of strategic importance. On average, transformers are designed to last at least 30 to 40 years. An important proportion of the PT present in western countries date back to peak installation that occurred in the 1970s, and therefore, a lot of them are reaching today their designed life expectancy. These are custom made machines that cannot be easily or quickly replaced. This growing concern has fueled research by electrical utility companies to further develop ageing assessment methods that can predict when a transformer will fail.

Transformers can change the voltage by using the Faraday's induction law. A varying current in any of the transformer coil produces a varying magnetic flux in the transformer's core, which induces a varying electromotive force across any other coil wound around the same core. On average, transformers have an efficiency ratio of 99%, and power ratings of the order of 1000 MVA. A loss of only 1% of this energy represents an important amount of heat and vibrations. Within a transformer, particularly between the windings, there are components with an extensive voltage difference that are spatially adjacent to each other. The combination of these two factors means that a PT requires an insulation system with excellent thermal and dielectric properties. A combination of mineral oil and cellulosic insulation (Kraft paper and pressboard immersed in the oil) is used in power transformers. Oil acts as the main insulation and dissipates heat while cellulosic insulation breaks the stress in the oil and provides a mechanical support.

Paper-oil insulation in PT will degrade over time and, while oil can be periodically renewed, cellulosic insulation cannot be replaced. In normal working conditions, the first component of a PT that will fail is the paper insulation. Once paper loses its mechanical properties, it will become brittle and fail under stress. Therefore, assessment methods of PT focus on evaluating the state of the cellulosic insulation.

The present work is the result of a partnership of the LGP2 (Laboratoire de Génie des Procédés pour la Bioraffinerie, les Matériaux Bio-sourcés et l'Impression Fonctionnelle) and the G2Elab (Laboratoire de Génie Electrique de Grenoble). This collaboration combined two different types of expertise, LGP2 allowed to work on chemical modifications and characterizations of paper and G2Elab added extensive dielectric characterization expertise and equipment to the project.

The combination of expertise allowed studying both chemical changes and dielectric properties changes during paper ageing in oil, at laboratory scale. The study did not focus on oil behavior.

The presented research is divided in four chapters.

In the first chapter, a general bibliographic survey provides the necessary information to present the global topic. This chapter starts by a general introduction of transformers history, with an overview of transformer insulation, its structure and function. The chemistry of insulation materials, paper and oil, is also presented with a description of the general ageing behavior of Kraft insulation. Since only a general literature focus is provided in this first chapter, each following chapter will contain its own literature review, precisely related to the studied topic and results obtained in each chapter.

The second chapter focuses on the use of methanol as an ageing marker for cellulose degradation in PT. This is an indirect method that relates the dosage of a dissolved substance (methanol) to the state of degradation of the cellulose insulation inside a PT. Extensive literature at laboratory and field level exists on the method, but the method has not been normalized yet. A review of the relevant literature on the subject and description of the experimental methods which have been used to validate methanol as an ageing marker are presented. In our study, a particular focus was brought on the chemical role of paper main components (cellulose, hemicelluloses, lignin) in the production of methanol during ageing, among which the particular role of lignin, in relation to its monomeric structure, has been revealed.

In the next chapters, the same set of samples was studied. It was selected to represent the possible variations in the organic and inorganic composition of paper. Variation in organic composition were achieved by simply using paper samples of different types. Variations in inorganic composition was achieved by ion exchange, to substitute some cations present in Kraft pulps, and enrich the paper with other metal ions.

The third chapter aimed at studying the damage created by the oxidation of the lignocellulosic matrix during ageing, and how it relates to the DPv test, classically applied on electrotechnical papers (viscosity average degree of polymerization of cellulose). Assessing oxidation damage could add further information, not available with other assessment methods. Only a small literature exists on the subject, mostly at laboratory scale. Our study provided a particular focus on the role of paper composition in relation to pulp oxidation. It also showed some clear relationships between the oxidation behavior of the pulp and its depolymerization.

The fourth chapter evaluated some dielectric properties of the lignocellulosic matrix during ageing. Changes in dielectric properties were related to oxidation and it could be another tool to assess the state of Kraft insulation. The measurement method used in the study, field dielectric spectroscopy, is rather original and literature is not extensive on the subject (mostly at a laboratory scale with a few field tests). The start of the chapter gives a background and survey of materials dielectric properties and the most relevant literature on insulation papers is presented. The particular role of substrate enrichment in moisture, which accompanies oxidation, was also focused during paper ageing, revealing some contradictions found in literature about the role of moisture and ageing in the dielectric response.

Chapter 1 - Table of content

General introduction.....	1
Introduction	12
1) Power Transformers and their oil/paper insulation	13
a) Power Transformers	13
i) History of transformers in the power grid	13
ii) Power transformers typical ratings	14
iii) Structure of Power Transformers	14
iv) Thermal management.....	15
v) Dielectric insulation	16
vi) Mechanical role of insulating materials	17
b) Insulation materials	17
i) Paper / oil insulation system	17
c) Structure and fabrication of Kraft Insulation	18
i) Kraft pulping.....	18
ii) Chemical Structure of Kraft insulation	20
iii) Different types of electrotechnical paper	24
2) Ageing of Power Transformers Kraft insulation	25
a) Monitoring degradation of Kraft insulation	25
i) Ageing conditions for Kraft insulation	25
ii) Methods used to monitor the state of Kraft insulation.....	26
b) Mathematical models describing ageing	27
i) Depolymerization of cellulose.....	27
ii) Experimental data	28
iii) Theoretical models.....	30
c) Chemical pathways of degradation	33
i) Defects of new Kraft insulation.....	33
ii) Cellulose oxidation	33
iii) Acid hydrolysis	34
iv) Pyrolysis.....	35
v) Summary	36
Conclusion and perspectives	37
References	38

Chapter 2 - Table of content

Introduction	45
1) Understanding Dissolved Gas Analysis (DGA).....	46
a) Monitoring Power Transformers.....	46
b) Cellulose depolymerization through DGA	47
c) Methanol as a marker of cellulose depolymerization	48
i) Correlation experiments.....	49
ii) Stability and partition coefficient experiments.....	53
iii) Origin of the methanol production experiments	56
d) Kinetics of methanol production.....	58
2) Materials and methods	61
a) Materials	61
i) Chemical products.....	61
ii) Instruments and standardized methods for characterizations	61
b) Methods.....	62
i) Method development	62
ii) Correlation experiments on paper samples	63
iii) Partition coefficient experiments on paper samples.....	64
• Partition coefficient with a change in methanol concentration.....	64
• Partition coefficient with a change in paper degradation.....	65
iv) Origin experiments on model compounds	65
• Lignin model compounds	65
• Cellulose and hemicelluloses model compounds.....	66
3) Results and discussion.....	67
a) Understanding the experimental approach.....	67
b) Origin experiments on model compounds	68
i) Lignin model compounds	68
ii) Cellulose model compounds	74
iii) Hemicelluloses model compounds.....	75
iv) Discussion of results.....	76
c) Correlation experiments paper samples	80
i) Ageing of cotton linters (CL)	80
ii) Ageing of BKP	81
iii) Ageing of UKP.....	82

iv) Discussion of results.....	82
d) Partition coefficient experiments	84
i) Effect of methanol concentration and paper composition	84
ii) Effect of ageing	86
iii) Effect of moisture content	87
iv) Discussion of results.....	88
e) Contrasting results with literature	88
Conclusion.....	92
References	94

Chapter 3 - Table of content

Introduction	101
1) Dielectric and chemical properties during ageing	102
a) Metallic cations in wood pulps.....	102
i) Role of metallic cations	102
ii) Metal binding to cellulose fibers	104
b) Chemical study of paper ageing	105
i) Depolymerization cellulose and oxidation in paper	105
ii) Oxidation of the cellulose chain	106
iii) Chromatographic and spectroscopic assessment of paper	108
2) Materials and methods	110
a) Materials.....	110
i) Chemical products	110
ii) Instruments used for chemical characterization	110
b) Methods.....	111
i) Method development of ion exchange.....	111
ii) Ion exchange experiments	111
iii) Size exclusion chromatography experiments.....	112
iv) Infrared experiments.....	112
3) Results and discussion	113
a) Ion exchange of paper	113
b) Effect of paper chemical composition on cellulose depolymerization during ageing	115
i) Quantifying the depolymerization of cellulose	115

ii) Effect of pulp polymers composition.....	115
iii) Ion exchange with main metal ions	118
iv) Ion exchange with transition metal ions	120
c) Effect of paper chemical composition on polymers oxidation during ageing.....	121
i) Oxidation of the cellulose chain	121
ii) Effect of pulp composition	122
iii) Ion exchange with main metal ions.....	126
iv) Ion exchange with transition metal ions	128
v) Synthesis on depolymerization and oxidation results.....	129
Conclusion.....	134
References	136

Chapter 4 - Table of content

Introduction	143
1) Bibliographic study: dielectric study of paper ageing	144
a) Dielectric properties of an insulator: main characteristic parameters	144
i) General considerations	144
ii) Resistivity	144
iii) Permittivity.....	145
iv) Loss angle.....	146
v) Dielectric strength.....	148
b) Previous measurements and analyses of dielectric spectroscopy of Oil - Paper systems 148	
i) A cautionary statement about FDS results	148
ii) Xie et al.; Physical Model for Frequency Domain Spectroscopy of Oil–Paper Insulation in a Wide Temperature Range by a Novel Analysis Approach (2020).....	149
iv) Jadav et al.; Understanding the Impact of Moisture and Ageing of Transformer Insulation on Frequency Domain Spectroscopy (2014).....	154
v) Xia et al.; A New Method for Evaluating Moisture Content and Aging Degree of Transformer Oil-Paper Insulation Based on Frequency Domain Spectroscopy (2017). 156	
2) Materials, experimental methods, and experiments carried out.....	157
a) Materials and experimental methods.....	157
i) Chemical products	157
ii) Sample preparation and chemical characterizations.....	157

iii)	Instruments used for chemical characterization	158
iv)	Instruments used for dielectric spectroscopy.....	158
v)	Instruments used for breakdown measurements	159
b)	Measurements carried out	160
i)	Dielectric spectroscopy experiments in oil.....	160
ii)	Dielectric breakdown experiments	161
3)	Influence of paper chemical and residual metal composition on dielectric properties during ageing	161
a)	Objectives.....	161
b)	Preliminary results.....	162
i)	Calibration of measurements	162
ii)	Dielectric properties of oil and non-impregnated UKP paper	162
iii)	Dielectric properties of unaged impregnated UKP	163
iv)	Influence of water content	168
c)	Dielectric properties of impregnated UKP during ageing.....	171
i)	Influence of ageing during 46 days	171
ii)	Evolution of permittivity and water content during ageing.....	172
iii)	Characterization of aged oil and aged UKP paper alone	175
iv)	Discussion of results.....	176
d)	Influence of paper composition on ageing	178
i)	Effect of paper composition on unaged samples	178
ii)	Effect of paper composition on aged samples	179
e)	Effect of ion exchange during ageing	179
i)	Effect of ion exchange on unaged samples	180
ii)	Effect of ion exchange on aged samples	181
f)	Dielectric breakdown	182
i)	Dielectric strength of paper of different compositions (UKP, BKP and CL).....	183
ii)	Dielectric strength of paper after ion exchanges	183
	Conclusion.....	185
	References	187

Annex

1) SEC Results.....	193
a) Samples List	193
b) Results per samples	194
i) UKP.....	194
(1) UKP D0.....	194
(2) UKP D2.....	196
(3) UKP D5.....	197
(4) UKP D7.....	199
ii) BKP	200
(1) BKP D0.....	200
(2) BKP D2.....	202
(3) BKP D5.....	203
(4) BKP D7.....	205
iii) CL.....	206
(1) CL D0.....	206
(2) CL D2.....	208
(3) CL D5.....	209
(4) CL D7.....	211
2) Analysis technique	212
a) Head Space Gas Chromatography with a Flame Ionization Detector.....	212
b) Size Exclusion Chromatography (SEC).....	215
c) Viscometric degree of polymerization	216
d) Karl Fischer titration	217
e) Soxhlet extraction.....	218
References	218

Chapter 1: Bibliographic review of Kraft insulation roles and ageing mechanisms in Power Transformers.

Table of content

General introduction.....	1
Introduction	12
1) Power Transformers and their oil/paper insulation	13
a) Power Transformers	13
i) History of transformers in the power grid	13
ii) Power transformers typical ratings	14
iii) Structure of Power Transformers	14
iv) Thermal management.....	15
v) Dielectric insulation	16
vi) Mechanical role of insulating materials	17
b) Insulation materials	17
i) Paper / oil insulation system.....	17
c) Structure and fabrication of Kraft Insulation	18
i) Kraft pulping.....	18
ii) Chemical Structure of Kraft insulation	20
iii) Different types of electrotechnical paper	24
2) Ageing of Power Transformers Kraft insulation.....	25
a) Monitoring degradation of Kraft insulation	25
i) Ageing conditions for Kraft insulation	25
ii) Methods used to monitor the state of Kraft insulation.....	26
b) Mathematical models describing ageing	27
i) Depolymerization of cellulose.....	27
ii) Experimental data	28
iii) Theoretical models.....	30
c) Chemical pathways of degradation	33
i) Defects of new Kraft insulation.....	33
ii) Cellulose oxidation	33
iii) Acid hydrolysis	34
iv) Pyrolysis.....	35
v) Summary	36
Conclusion and perspectives	37
References	38

Introduction

The industrial world relies on the power grid to light up everything from homes to industries. Yet seldom do we think about this country wide infrastructure and its maintenance. The power grid is an interconnected network made to transport electricity from producers to consumers. Central to the power grid are Power Transformers that are passive electrical devices that rise voltage in electrical grids in order to transport electricity with minimum losses. Today, most Power Transformers in the power grid of western countries are reaching the end of their life expectancy, while it is not easy and quite expensive to quickly replace them. If correctly maintained, the first thing that will decide users to stop a transformer will be its insulation system. An important practical feature of mineral oil / Kraft insulation system is that oil can be renewed, while Kraft insulation cannot be replaced.

For the past 70 years there has been important research in the field of Kraft insulation ageing. The aim of this study is to better understand the ageing process with the objective to better predict the remaining life expectancy of a Power Transformer, provide parameters able to quantify ageing, and check ageing properties of various modified papers. In this context, the first part of this chapter explains what are Power Transformers, their role and structure. A focus is given on insulation and specially on Kraft insulation. In the second part, the monitoring procedures of utility operators is explained. Power Transformers are routinely checked to test any potential ongoing or future issue. The monitoring of transformers aims to characterize the ageing of insulation. From the information obtained, it is possible to use mathematical models in order to quantify cellulose depolymerization. Behind ageing of Kraft insulation, a complex chemistry of cascading reactions occurs, and will be explained.

1) Power Transformers and their oil/paper insulation

a) Power Transformers

i) History of transformers in the power grid

Electricity now seen as a ubiquitous part of life started to appear in the late 19th century. From the beginning, efficient transport was one of the main hurdles towards the democratization of electricity. The main problem behind transport of electricity is that the voltage used by most appliances (100-220 V) is so low that heat dissipation due to high currents would make transporting electricity for long distances inefficient. Therefore, long distance power lines rely on higher voltage and lower current to transport electricity with minimal losses. This in turn allows building massive power stations that can cheaply generate electricity through economies of scale. Transformers are at the heart of the alternative current grids, they allow changing voltage in a simple and very efficient way. They initially competed against mechanical solutions involving motors and alternators, but finally triumphed thanks to their better simplicity, reliability, and energy efficiency (> 98 %).

Although the working principles behind transformers were discovered in the mid-19th century, the first transformer with a modern design was built in 1885 by William Stanley (Figure 1a). By 1891 the first line using alternative current was built for the Frankfurt Electrical Exhibition, it ran for 120 km at 25 KV. By start of the 20th century, electrical lines linked a single power station to a city or a factory, but with time, lines became interlinked and gave birth to country wide power grids. After the second world war, a massive increase in the use of electrical consumption arose in housing and industry with almost every house having some sort of electrical appliance. Networks in the western countries can trace most of their growth, up to an installation peak from the 1970s. Today power grids span continents where electricity is sold between countries. As an example, the latest massive transformers (Figure 1b) used in 1100 KV line in China allows transporting electricity for a distance of 3400 km.

Power grids are divided into three parts: generation, high voltage transmission network over long distances, and medium voltage distribution network to consumers. Different types of transformers in terms of voltage and power are used in power grids.


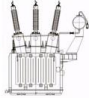





Figure 1: a: Picture of the first transformer demonstrator unit made by William Stanley in 1883. b: Picture of the new Siemens 1100 KV HVDC power transformer from 2016. Extracted from a Siemens brochure [1].

ii) Power transformers typical ratings

Transformers design and weight will vary from a few kilos to thousands of tons depending on the amount of power they can handle. The power rating of a transformer corresponds to the power they can deliver, without exceeding internal temperature limitations of 65°C on average and 80°C on hotspots [2]. As can be seen in Table 1, transformers used in electrical distribution can be divided into three main types:

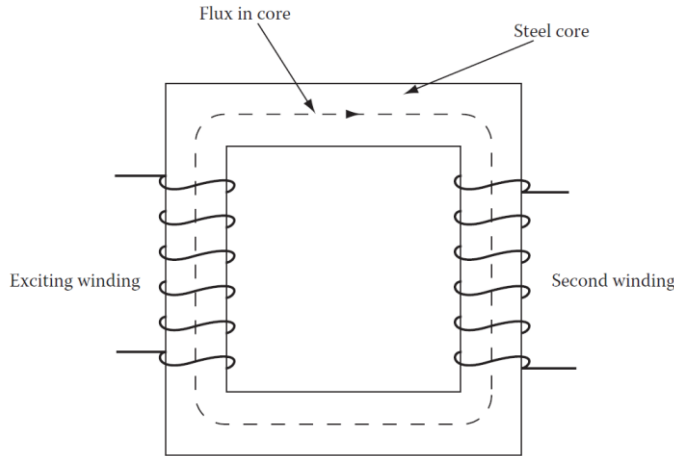
Table 1: Schematic summary of the types of transformers found in the electrical grid.

	Generator	Power Transformer	Transmission transformer	Distribution transformer	Home appliance
Typical voltages used	 1 - 25 kV	 400 kV	 90 kV	 33 kV	 220 V
Power rating	800 MVA	1000 MVA	100-300 MVA	2.5-100 MVA	

Power Transformers (PT) are coupled to a generator, show the highest power ratings and voltage in the electrical grid, and are considered strategic assets in the power grid. They get a power rating 10-20% higher than the generator for safety and durability. They are normally run at 100% capacity and are rarely subjected to overloads since they are coupled to a single generator. To date, the biggest Power Transformers have a 1000 MW rated power and their weight exceeds 500 tons. Transmission transformers are found in substations that regulate the transport of electricity and allow their conversion to medium voltages. Distribution transformers handle the flow of electricity at city level until private housing or industrial clients. With the highest power ratings and voltage, power transformers insulation has to handle harder thermal and dielectric constraints.

iii) Structure of Power Transformers

Transformers use the Faraday's induction law, discovered in the 19th century, allowing to change the voltage between a primary and secondary winding (Figure 2). The ratio between the number of turns for the primary and secondary winding determines the voltage ratio between primary and secondary.



$$V_E = -N_E \frac{d\phi}{dt}$$

$$V_S = -N_S \frac{d\phi}{dt}$$

$$\text{turn ratio} = \frac{V_E}{V_S} = \frac{N_E}{N_S} = a$$

Figure 2: Transformer core and Faraday's induction law (V : Volt, N : is the number of turns around the core; $d\Phi/dt$ is the derivative of the magnetic flux Φ through one turn of the winding over time (t), the derivative of the magnetic flux Φ through one turn of the winding over time (t)). Extracted from the *Electrical Power Transformer Engineering Handbook* [3]

Between the windings a large voltage difference (several 100 kV) may exist, and efficient insulation is needed to prevent short circuits. In addition, various energy losses (magnetic, Joule heating) induce heat inside the transformer that needs to be evacuated. The insulation of power transformers and other transformers with high power ratings [4] is made of oil and paper (Figure 3), constituting the focus of this study. The magnetic core of the transformer and windings are submerged in an airtight steel tank.

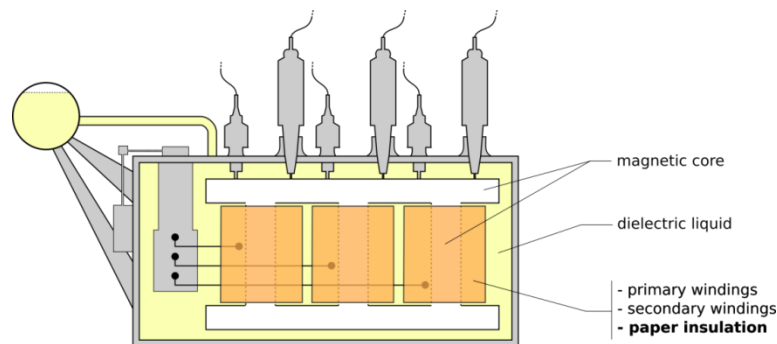


Figure 3: Schematic view of a three-phase core type Power Transformer. The insulation is immersed in oil in an airtight metallic container.

iv) Thermal management

In addition to electrical insulation, the oil has a very important role of heat transfer toward external radiators, with requires its circulation within the transformer. Power transformer are equipped with pumps, radiators and coolers (Figure 4). Depending on their quality, some papers immersed in oil can endure temperatures up to 105°C without significant loss of life (thermal rating A), but in general transformers are designed to never reach temperatures above 98°C in hot spots. Another critical threshold of 120/180°C exists, after which a dielectric failure can occur because of bubble formation.

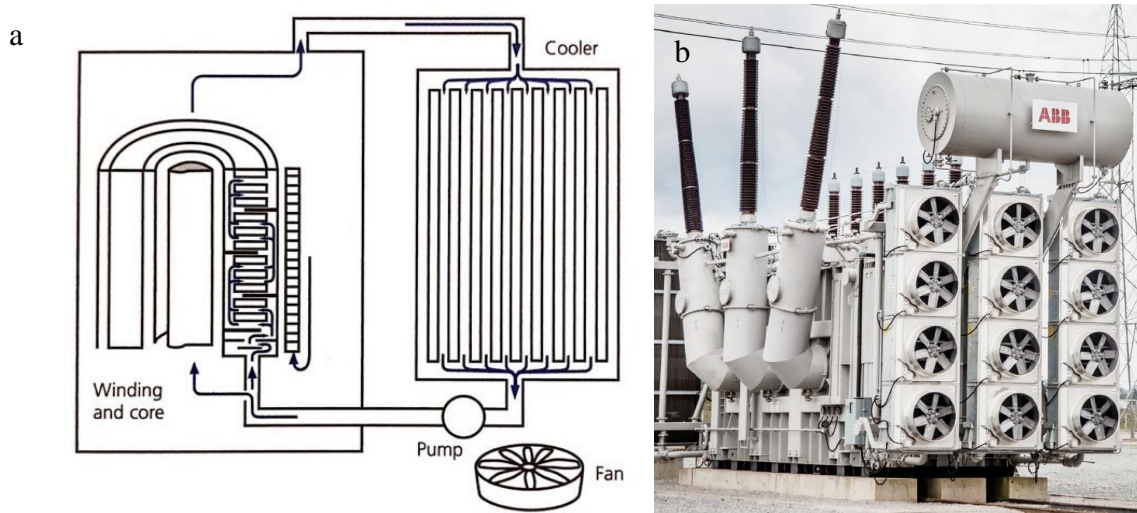


Figure 4: Schematic (a) and exterior (b) view of the cooling system inside a Power Transformers. Extracted from the Transformers oil handbook and a ABB brochure [5,6]

v) Dielectric insulation

Dielectric stress is present between materials with significant voltage difference (Figure 5). Particular areas of stress are located in the space between windings, between low voltage winding and the high voltage winding, and between the winding and the core. For these zones, the dielectric insulation is provided by solid pressboard barriers that subdivide highly stressed oil. Barriers are arranged vertically along field lines. In this way, discharges that may occur accidentally hit perpendicularly the barrier and are stopped.

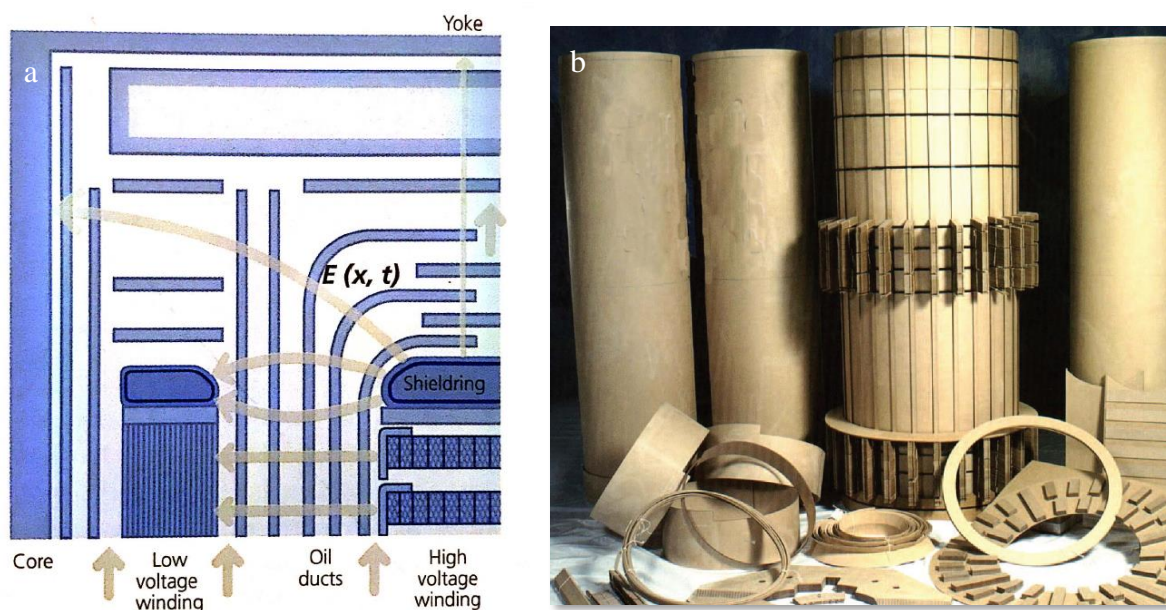


Figure 5: Schematic (a) view of the insulation system inside a Power Transformer, the arrows represent the electric field. Picture (b) of the cylindrical boards that separate the windings between them and the windings from the core. Extracted from the Transformers oil handbook and from Oommen et al. [4,6].

vi) Mechanical role of insulating materials

Solid insulation holds the windings and supports most of the weight of all the components. In addition, it must endure vibrations and mechanical stress coming from short circuit forces (Figure 6a). The axial forces are supported by the spacers (Figure 6b). To survive these forces, recompressed pressboards were invented, they are able to bend under stress and comes back to their original shape. Axial spacers have shaped edges to avoid cutting the conductors.

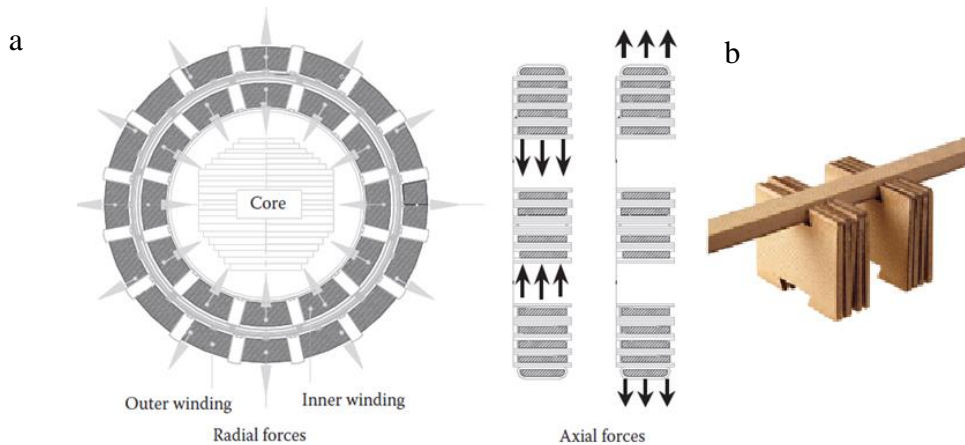


Figure 6: Schematic view of the mechanical forces imposed on the transformer winding during operations and picture of a Kraft spacer used in transformers. Extracted from the *Electrical Power Transformer Engineering Handbook* and from Oommen et al. [3,5].

b) Insulation materials

i) Paper / oil insulation system

The combination of mineral oil and Kraft based insulation (paper and pressboards) has been the backbone of Power Transformer insulation for over a century [7]. Today, paper and mineral oil insulation still provides the highest performance, as compared to other more modern solid and liquid materials (e.g. polymers, synthetic liquids). Kraft based materials can bend under axial and radial forces, and then return to their original shape, a quality not found on other synthetic alternatives. Mineral oil provides excellent ultra-high voltage properties that get almost no equivalent. For lower voltage ranges (e.g. distribution transformers), ester liquids of either natural or synthetic origin are however being increasingly used, taking advantage of their better resistance to fire, and biodegradability.

Mineral oil is obtained from distillation of light and naphtha fractions of petroleum, and contains three different types of molecules: paraffinic, naphthenic and aromatic. Figure 7 represents the typical molecule structure. Only polyaromatic and alkanes occur in a single molecule with the rest being always a mixture of the three. High fraction of naphthenics are often preferred because of their lower viscosity at low temperature (important for oil flow) and better thermal properties than paraffinic structures. Aromatic structures mainly serve as oxygen inhibitors and allow a higher oxygen absorption in the oil. Oxidation inhibitors can also be added to oil to increase its service life, the oils are then called inhibited oils. In terms of cost, mineral oil represents between 15 to 20% of the cost of a transformer, while ester oils are more expensive.

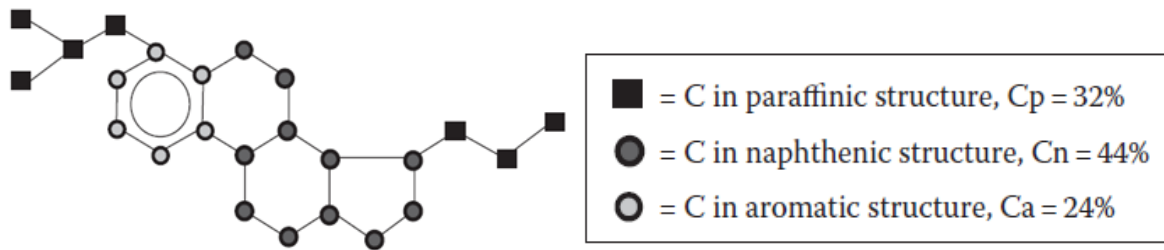


Figure 7: Chemical structure of the model molecule for mineral oil along the average amounts of paraffinic, naphthenic and aromatic structures. Extracted from the electrical Power Transformer Engineering Handbook [3].

Kraft insulation is present in two forms; paper that is wrapped around conductors and pressboards that hold the winding and the core (Figure 8). Paper has no mechanical role and only provides an insulation between windings. Pressboards can be of low or high density. High density pressboards constitute structural supports, and handles axial and radial forces. In places where no mechanical support is needed, low density pressboards are placed only for dielectric purposes. In some designs, pressboards also have a thermal role because they are arranged with the purpose of directing oil flow. The manufacture and types of Kraft insulation will be discussed in detail in the next part of the chapter.

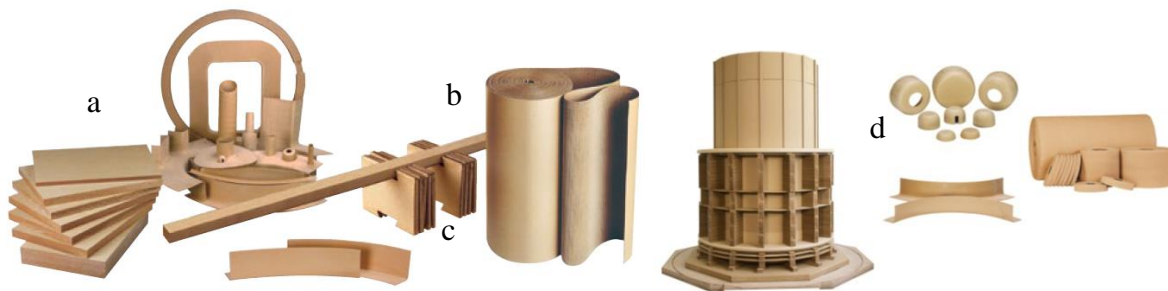


Figure 8: Pictures of Kraft insulation used in Power Transformers. Among the components pressboards (a), paper (b), spacers for winding (c) and molded components (d) are visible. Extracted from an ABB brochure [5].

The advantages of Kraft insulations are that they are widely available, bio-based, cheap, have excellent dielectric and mechanical properties that make them able to compete with more modern materials. When paper is impregnated with oil, it has a dielectric constant of 3.5 to 4. Other modern materials such as synthetic aramid-based papers are prohibitively expensive and are therefore only used in hot spots. Thermally upgraded Kraft insulation uses alkaline additives added to the cellulosic pulp to hinder the degradation of cellulose. These compounds are of synthetic origin, and current research focuses on trying to find bio-based alternatives to them.

c) Structure and fabrication of Kraft Insulation

i) Kraft pulping

Transformer insulation is made of pure unbleached Kraft pulp. The Kraft process is the most common one to manufacture paper and board pulp. Pulping allows the transformation of natural wood into paper pulp. Kraft means strength in German; because this process allows to obtain a

pulp with the strongest mechanical properties. Natural wood fibers contain important amounts of lignin (25-30% of the mass of wood) that mainly forms a binder for lignocellulosic fibers. Kraft pulping separates the individual fibers and dissolves most of the lignin. Around 3-5% of residual lignin remains in the fiber wall after pulping. Alkaline pulping also contributes to a mechanical reinforcement of the fiber wall, making paper less brittle and more flexible.

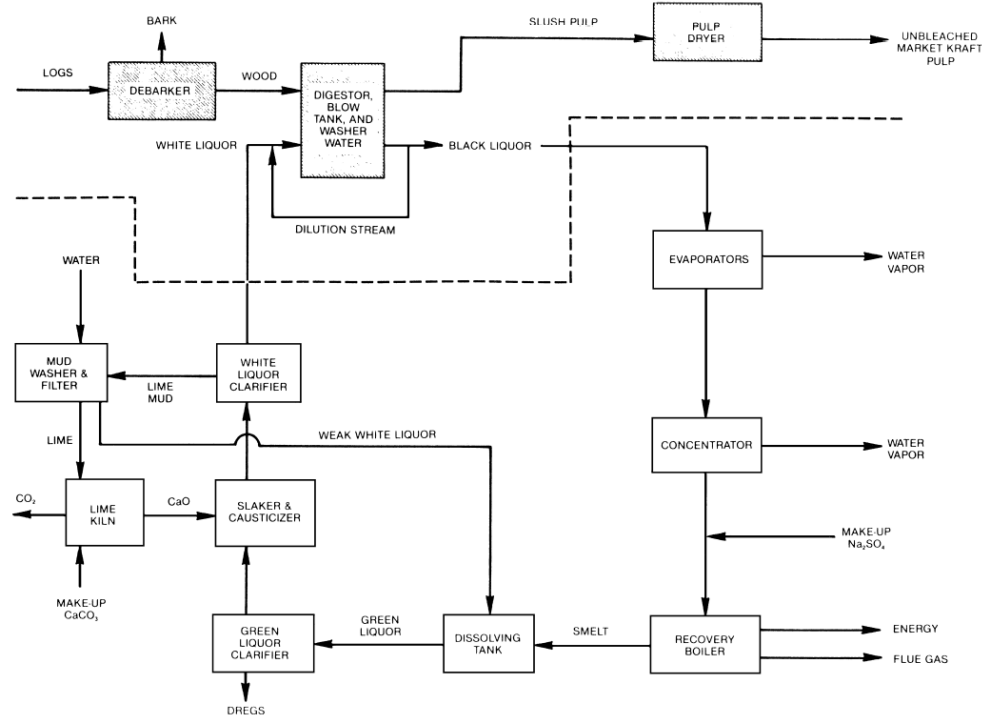


Figure 9: Flowsheet of an unbleached Kraft pulp mill focusing on chemical flows [8].

The Kraft process is a complex process (Figure 9). Wood trunks are debarked, cut into chips that are steamed, then mixed with white liquor (containing water, NaOH and Na₂S) in a short hot impregnation step. This is followed by chemical cooking at a temperature of 150-170°C and a pressure of 5-7 bars. During cooking, wood lignin is strongly degraded and partly released into the cooking solution called black liquor. Polysaccharides (cellulose and hemicelluloses) are partially depolymerized and short chains of hemicelluloses are partly dissolved in the black liquor, which also contain wood extractives and minerals. After mechanical defibration, the delignified fibers in water suspension are washed in diffusers to remove the black liquor. Fibers are then dried in the form of thick pulp sheets that are formatted to make the end products such as paper or pressboards. Kraft pulps are often associated with brown color because they are mainly used for packaging or other mechanically oriented purposes where the color of the pulp doesn't matter. Since cellulose and other remained polysaccharides in fibers are white, if a white color is desired, an additional bleaching step is applied to remove the residual lignin that is responsible for the brown color.

Electrotechnical paper is made of classical Kraft pulp, on top of the Kraft pulping it is made with a process where additional washing steps are used to fully remove the sodium and residual metal cations found in classical Kraft pulps. Insulating papers are generally manufactured from softwood species (mostly Black Spruce). This is because these species contain very few impurities and have long cellulose fibers (1 to 4 mm) that lead to strong thermal and mechanical properties. For the insulating paper, the pulp used must contain few metal cations. These

impurities originate from pulping or are naturally present in the wood [9]. The concentration of Na^+ is checked at all the stages after pulping because this element is considered to increase the dielectric dissipation factor. Metal cations, particularly iron, catalyze hydroxyl radical formation in the presence of O_2 , that leads to depolymerization of cellulose by oxidation. To obtain the purest possible pulp, an additional chemical treatment is added after Kraft pulping, such as acid washing (pH 2, 90°C for 2 hours), the use of chelating reagents (sequestering metals), or a washing stage which substitutes sodium by another ion, like calcium. The ideal pulp should have as few sodium, iron and other metal ions as possible, but it is actually impossible to remove all of them which remain in residual amounts (ppm).

Electrotechnical grade paper is obtained from purified Kraft pulp with some added steps [10]. The first universal step is to resuspend the pulp in weakly ionized water (so as not to add more residual cations). Afterwards, mechanical refining in disk refiners at a suited level is applied to promote fiber wall fibrillation and hydration. Refining reinforces the linkages between fibers after drying, and thus the strength of the paper and board. During the sheet forming stages on the paper machine, water is gradually removed from the wet sheet by dripping, then pressing, and finally it is dried on hot metal cylinders. Fibers on the paper machine are therefore oriented. Hydrogen bonds between fibers and microfibrils at the surface of the fibers are formed as water is removed during drying, thus conferring strength and cohesion of the paper. Kraft multilayer pressboards are manufactured by assembling wet paper layers which are dried under pressing in plateau dryers.

ii) Chemical Structure of Kraft insulation

Paper pulp is made of hollowed wood fibers that are flattened during the forming and drying process on paper machines (Figure 10). Paper is a porous material and there is a lot of empty space between the fibers that is filled by oil in transformers. Fibers themselves are made of microfibrils that are an assembly of cellulose chains. Kraft fibers contain around 80% of cellulose, 15-20% of hemicelluloses, 3-5% of lignin and less than 0.5% of residual materials, mainly minerals.

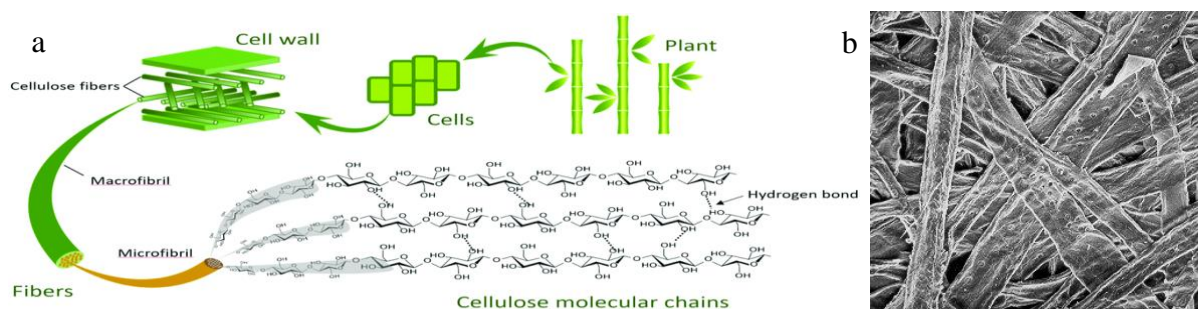


Figure 10: a: Structure of lignocellulosic materials at macroscopic, microscopic and atomic level. B: Electron microscope picture of flattened macroscopic fibers in a paper sample [8]. Extracted from Emsley et al. [11].

- Cellulose:

Cellulose is a polymer made of joining D-glucose units through 1,4- β -D-glycosidic bonds (Figure 11). Cellobiose which consists of two anhydroglucose units (AGUs) is the repeating

unit in the cellulose chain. In addition to the three hydroxyl groups (two secondary alcohols in positions C2 and C3, and one primary alcohol at C6), a hemiacetal is present on each AGU of the chain, and each cellulose chain contains a non-reducing hydroxyl group at one end, and a reducing hemiacetal (presence of an aldehyde group) at the other end. These chemical functions give to cellulose a particular reactivity. It is also considered that the presence of these functions –OH and –CH₂OH are responsible for its hygroscopic nature [4]. The degree of polymerization (DP) of cellulose represents the chain length of cellulose which can be determined by the number of AGUs. Native cellulose chains in wood have a degree of polymerization (DP) between 5000 and 15000. For new insulation paper, the viscosity average degree of polymerization (DP_v) of cellulose can be in the 1100-1600 range, but the DP_v can drop down after drying and oil impregnation by about 10% of the initial value.

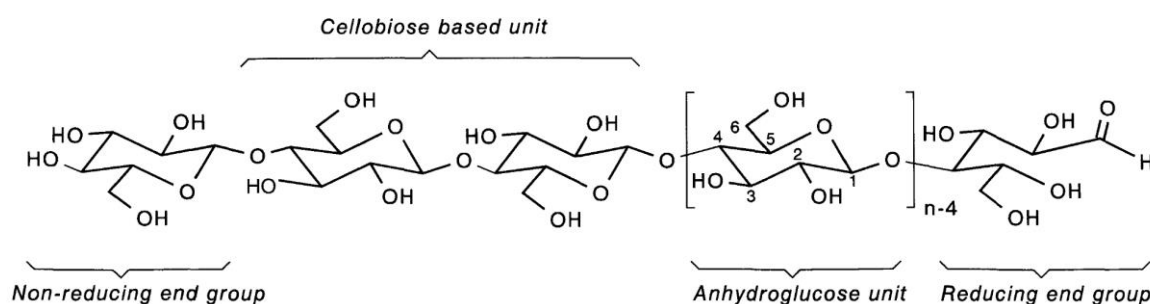


Figure 11: Representation of a cellulose chain in chair conformation in the non-reducing and reducing end groups. Extracted from Bonfiglio et al. [12].

In microfibrils, cellulose chains can either be well aligned or randomly organized to have crystalline or amorphous zone. Crystalline and amorphous zones alternate within the same cellulose chain. Amorphous regions are considered to be more reactive [10], because their random organization makes chemical functions more accessible and therefore more reactive. Crystalline zones are pack tightly and on top of that hydroxyl groups less reactive since they make hydrogen bonds between them. Depending on how the chains are organized, crystalline zones can form different allomorphs: cellulose I (native cellulose; α or β type), II, III and IV, but in transformer paper or board cellulose, only cellulose I is found as in the original wood fibers.

- **Hemicelluloses:**

The other main components of paper are hemicelluloses. They are heterogeneous and short (100-200 repeating units) carbohydrate-based polymers that are branched. Their structure and proportions will vary depending on the wood species. They are either 6-carbon carbohydrates, such as glucose or mannose, or 5-carbon carbohydrates, such as xylose, arabinose. Hemicelluloses also have naturally oxidized or reduced forms of hexoses and pentoses. Hemicelluloses found in the softwood pulps used for electrotechnical paper are mainly composed of glucomannans (Figure 12a) and xylans (Figure 12b), with glucomannans being the most common. These are copolymers composed of mannose and glucose, whose side chains are galactose or acetylated groups (regularly present in the C2 position).

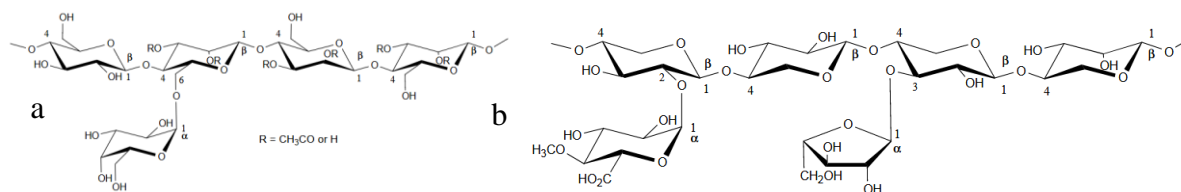


Figure 12: a: Representation of glucomannans from softwood b: Representation of xylans from softwood. In the native state in wood, hemicelluloses are covalently bound to cellulose and to lignin.

Hemicelluloses have a structural role in cellulose fibers, they act as binders between cellulose fibers. Inside the fiber wall, hemicelluloses interact with the cellulose chains by cross-linking the microfibrils: they fill the void between the microfibrils (microfibrils being formed of cellulose chains bundles) and can make covalent bonds with lignin. A part of hemicelluloses is lost during the Kraft pulping but most remain in the final product.

- **Lignin:**

Lignin is a complex macromolecule which is present in almost all wood-based cellulosic materials and which constitutes a hydrophobic matrix or glue that incorporates in the wall of the carbohydrate fibers. Unlike cellulose, lignin is not a polymer made up by the same monomer repeating unit. Instead, lignin is formed by the irregular coupling of several aromatic monomers (Figure 13) that form an amorphous 3D network. This structure will vary greatly from one specie to the other but can be characterized as a specific blend of aromatic monomers, functional groups and bond types. Lignin can therefore be considered as a copolymer of phenylpropane-type units linked together by weak ether bonds and strong carbon-carbon bonds. [13]. The bond most frequently encountered in softwood lignin is the β -O-4 bond, representing 50-60% of the ether bonds (Figure 14). Free phenolic groups are grafted by 10-20 % of the aromatic rings in the native lignin, but they reach more than 50 % in Kraft pulp residual lignin. Guaiacyl-type lignin, the single constituent of softwoods, contains more than 90% of guaiacyl repeating units which bear only one methoxy groups (OCH_3). The other types of aromatic units, present in hardwoods and in annual plants, are syringyl-type (two methoxy groups) and hydroxyphenyl-type (no methoxy group).

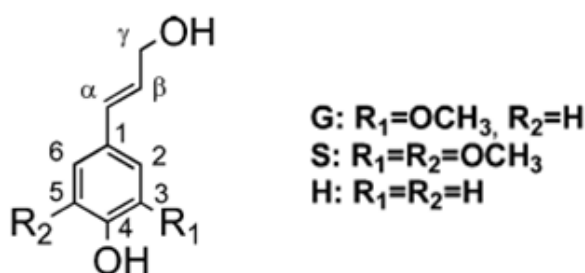


Figure 13: Schematic representation of aromatic monomer motif with the corresponding chemical structure for: α -hydroxyphenol residue (H), syringyl residue (S); guaiacyl residue (G). Extracted from Crestini et al. [13].

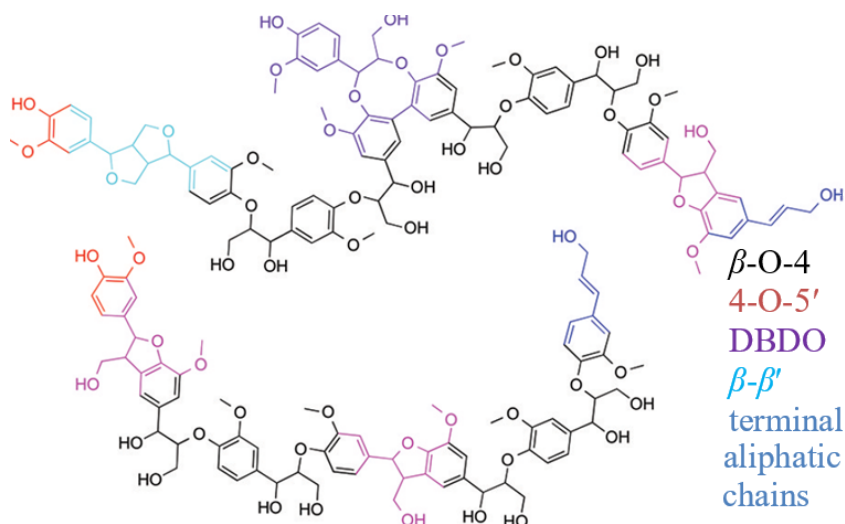


Figure 14: Schematic representation of an average lignin structure of lignin. The types of bonds are color coded. Extracted from Crestini et al. [13].

Chemical bonds of different types exist between lignin and carbohydrates (cellulose and hemicelluloses): weak bonds (hydrogen, van der Waals) and covalent bonds (benzyl-ether, benzyl-ester and phenyl-glycoside bonds). It is considered that lignin has a mechanical role acting as a binder of cellulose and a biological role acting as a water and pathogen repellent in the wood [14]. Lignin extracted during pulping is a heavily modified lignin called Kraft lignin, it is burned in pulp mills to produce electricity. Despite some progress, little chemical valorization of lignin exists today except for vanillin (a food additive), from bisulfite pulp liquors (and not Kraft liquors). In electrotechnical paper, the residual lignin is the same as in common Kraft pulps, meaning that it is altered (partially depolymerized and enriched in free phenolic groups, and also conjugated quinonic and phenolic structures), as compared to the original lignin structure in softwoods.

- **Extractives and Residuals:**

Minor components (extractives, residuals) are present in Kraft pulps. They are either originally present in the wood or introduced during the pulping process. Wood contains structural proteins and pectin, most of them are removed during the pulping process, and very few residuals are found in the pulp. Other extractives molecules like fatty acids, resins, terpenes, soaps, ... are present in Kraft pulps as traces. Some cations are originally present in wood (Ca, Mn), others are introduced during the pulping process (Fe, Cu, Mn, Ni, Na), or during the washing steps (Na is mostly removed and replaced by Ca, Mg). Electrotechnical-grade pulp requires several washing stages for pulp purification of the cations, it is a very important operation for producing electrotechnical papers. For a standard electrotechnical grade Kraft pulp, the following metal ions contents can be given as an example:

Table 2: Dissolved metals present in electrotechnical grade pulp.

Metal	Sodium	Calcium	Potassium	Magnesium	Manganese	Iron
Amount in ppm	180	850	8	111	50	4



iii) Different types of electrotechnical paper




Different types of electrotechnical Kraft insulation exist: standard and thermally upgraded Kraft insulation. Thermally upgraded insulation paper is made with standard Kraft pulp with added nitrogen-based compounds, in which nitrogen content represents about 1.7 to 2.5 % of the total weight of the pulp. The three main types of compounds added are dicyandiamide (DICY), melamine and polyacrylamide. Most manufacturers use a combination of the three and only DICY is used alone. Basic compounds react with acids created during cellulose degradation that leads to a higher thermal rating. Synthetic fibers can also be blended with pulp. These synthetic blends are most often made of polyaramid papers. For Kraft papers and pressboards, the density and the grammage can vary, and also surface conditioning. For immersed-in-oil power transformers, the main standard used is IEC 60076. The main parameters controlled during the manufacture are porosity, thickness, moisture content, apparent density, tensile strength, grammage and nitrogen content for TU papers.

Papers can be classified according to changes during finition. Paper is optionally creped (creation of tight folds) or calendered (strong crushing by passing between two rollers). Crepe paper has a higher stretch (the extra elongation is useful to wrap around copper wiring). The weights typically targeted for application in power transformers are approximately 60-70 g/m². Water content of electrotechnical papers is typically around 6% at 23°C and 50% relative humidity in air. New types of paper include a thin layer of epoxy resin coated over the paper; the epoxy layers fuse when exposed to the heat inside transformers. The extra layers contribute to the mechanical and dielectric strength of the rolled paper around copper wires.

A synthesis of the type of papers found in transformers can be seen below: standard Kraft paper, crepe paper, diamond dotted paper, thermally upgraded paper and synthetic paper. Pressboards are almost exclusively made of standard Kraft pulp, they vary in density and thickness.

Table 3: Types of papers used in Power Transformers. The thermal classes are NEMA / UL Letter Class: the indicated temperature is the temperature after which a significant loss of life expectancy will appear.

Paper type	Production	Characteristics	Thermal class	Picture
Kraft paper	Kraft process.	<ul style="list-style-type: none"> The most common electrical grade paper; Cheaper than all the other alternatives but more vulnerable to thermal, mechanical, and electrical stress. 	Class A (105°C)	
Crepe paper	Kraft process ¹ with and extra creeping step.	<ul style="list-style-type: none"> Higher stretch (elongation) capacity to wrap around copper wiring without tearing. More expensive than standard Kraft paper 	Class A (105°C)	

Diamond dotted paper	Kraft process ² with an epoxy layer.	<ul style="list-style-type: none"> • Epoxy layer provides internal strengthening of the coil for a better adhesion to the conductor. • More expensive than standard Kraft paper 	Class A (105°C)	
Thermally upgraded paper (TUP)	Kraft process with additional nitrous compound.	<ul style="list-style-type: none"> • Better thermal properties than standard Kraft pulp. • Dicyandiamide is the most common additive used for TU. • More expensive than standard Kraft paper 	Class B (130°C)	
Synthetic paper	Blend of wood pulp, synthetic fibers and a binder ³ .	<ul style="list-style-type: none"> • Better thermal properties • Mostly polyaramid based papers (Nomex®) • Low moisture adsorption; • More expensive than other alternatives. 	Nomex 910 Class B (130°C) Nomex 410 Class C (220°C)	

¹: Crepe paper can be made from thermally upgraded paper. ²: Diamond dotted paper can be made from thermally upgraded paper or synthetic based paper (Nomex®).³: Multiple types of synthetic paper exist, some are a blend of polyaramid paper with cellulose fibers (Nomex 910) while others can be made of pure polyaramide fibers (Nomex 410).

2) Ageing of Power Transformers Kraft insulation

a) Monitoring degradation of Kraft insulation

i) Ageing conditions for Kraft insulation

The duo between mineral oil and Kraft insulation will have excellent performances as long as it is protected from the atmosphere. There are multiple design philosophies to keep the insulation hermetically sealed. All transformers rely on a steel box to protect the insulation from the atmosphere but differ in how they handle the expansion of oil from heating. They can either be sealed tanks that have positive pressure systems or expansion tank systems at atmospheric pressure. Transformers can have a hydrogen blanket added on top of the oil that allows oil volume expansion with fluctuating temperatures. Expansion tanks can be added outside of the main transformer body (Figure 15a). For transformers with air, free breathing apparatus contain desiccant canisters that dry the air that can come inside the transformer. Another widely used solution is the use of a rubber bladder inside the expansion tanks (Figure 15b), they stretch to compensate changes in volume² and allow for evacuation of gases. The actual structure will vary depending on the price and availability, with some design specific to individual manufacturers. Most transformers in Europe are of the free breathing type.

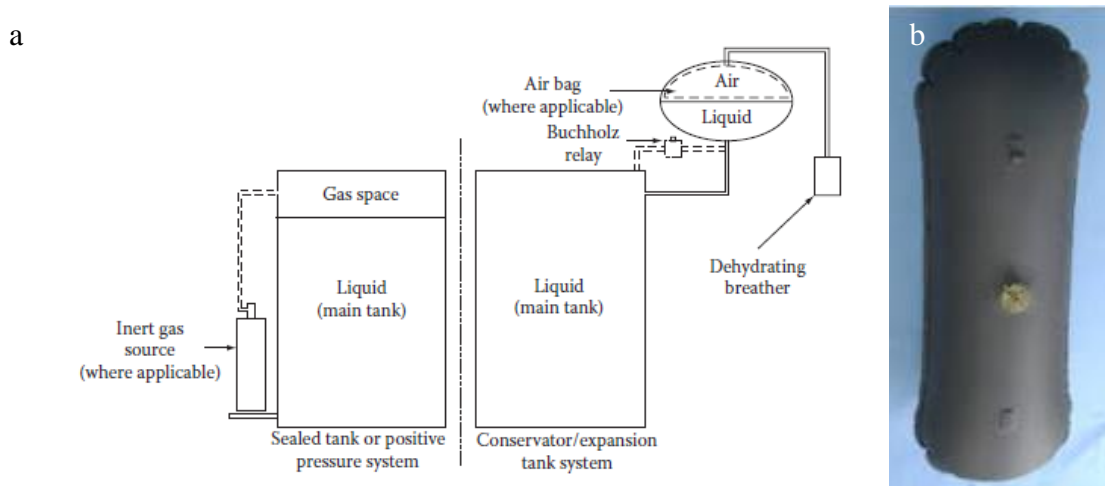


Figure 15: a: Schematic view of liquid preservation systems in Power Transformers, b: rubber bladder found inside the expansion tanks. Extracted from the *Electrical Power Transformer engineering handbook* [3].

Although there are many variations in the preservation systems, some conditions are universal. Water is always purged from transformers but the main difference is that some systems are free breathing (meaning that oxygen is in contact with oil) while others have an inert gas nitrogen blanket. Other conditions, such as temperature, can vary from one transformer to another. Given these variations, there is a large panel of ageing conditions used in thermally accelerated laboratory experiments [15]. Temperatures range from 60 to 210°C depending on the focus of the study. In accelerated thermal ageing experiments, low temperature studies (around 60-90°C) focus on the oxidation reactions undergone by cellulose, medium temperatures focus on the acid hydrolysis of cellulose (around 90-150°C), while temperatures above 150°C mostly focus on the pyrolysis phenomena undergone by the different polymers, in addition to the acid hydrolysis phenomena. In these experiments, Kraft insulation is immersed in oil and then aged at constant temperatures. Most experiments use dry Kraft insulation and non-oxidative conditions (absence of air). The paper to oil mass ratio used in the experiments varies from 4 to 121. Some experiments also include copper to simulate winding. The main issue is the control of moisture, since water is created during ageing reactions and accumulated in closed autoclaves. In non-closed systems, water can be released by evaporation and the oil-paper medium can be kept dry.

In our study, non-oxidative conditions were used for ageing paper in closed, stainless steel or glass autoclaves, containing dry oil at the beginning. Paper was aged with a paper and oil mass ratio of 1:19 (the closest value to the ratio in most power transformers), and temperature was chosen at 130°C to focus on acid hydrolysis reactions undergone by the polysaccharides leading to cellulose depolymerization.

ii) Methods used to monitor the state of Kraft insulation

Utility operators have comprehensive monitoring methods used to assess the state of the solid insulation of transformers. As already mentioned, ageing of the insulation paper is governed by the combination of three mechanisms, namely oxidation, hydrolysis and pyrolysis. Each mechanism dominates in a certain temperature range and can be catalyzed by metals, water, acids, etc. In normal working conditions (70°C), hydrolysis is the main mechanism involved in

depolymerization of cellulose. It is calculated from the measure of the viscosity of a cellulose solution at a given concentration dissolved in copper-ethylenediamine at 20°C or 25°C, depending on the standard method used. This standard methodology is described in the appendix section. This method is widely used by industry because it is simple and fast and does not require an expensive equipment. Other methods to follow cellulose depolymerization are mainly based on size exclusion chromatography, they are more common in research laboratories.

Most utility operators agree that Kraft insulation has reached the end of its life when reaching a DP_v of 200. The limit of 200 corresponds to the moment when the paper loses almost all of its mechanical strength [11]. Even after paper reaches a DP_v of 200, a transformer can still work properly for a long time but will be very vulnerable to any mechanical stress that could shear off the now brittle paper. The criteria used to describe the end of life of Kraft insulation can be found in IEEE C57.91-2011 standard. Yet in literature, DP_v is rarely used directly, instead it is often preferred to show the number of scissions of glycosidic bonds or the number of scissions per chain as a function of time. Using scission instead of DP_v allows to have normalized unit that can compare samples with different starting DP_v . The number of scissions per chain is the most widely used because it minimizes the influence of the variability from the samples [17].

- The number of scissions per number of anhydroglucose unit in a cellulose chain (also called Scission Fraction of Cellulose Unit) has been defined from the DP_n :

$$S = \frac{1}{DP_{n(t)}} - \frac{1}{DP_{n(0)}}$$

Here; S is the number of scissions per anhydroglucose chain, $DP_{n(0)}$: initial number-average degree of polymerization, and $DP_{n(t)}$: number-average degree of polymerization at time t.

- The number of scissions per initial cellulose chain (also called Chain Scission Number).

$$S = \frac{DP_{n(0)}}{DP_{n(t)}} - 1$$

This second expression for S (Chain Scission Number) is simply the value of the (Scission Fraction of Cellulose Unit) multiplied by the initial DP_n of the polymer ($DP_{n(0)}$).

ii) Experimental data

In the particular environment of transformers, the DP_v of the cellulose decreases over time, leading to a decay of the mechanical properties of paper. Dielectric properties of paper will also degrade. At higher temperatures than normal conditions (70°C), the life expectancy of paper will start to decrease significantly.

Data show that for standard Kraft or thermally insulated (TU) paper aged in mineral oil, DP_v value is generally a decreasing exponential curve tending towards a horizontal asymptote. Correspondingly, the number of scissions per initial cellulose chain shows a first linear phase that tends towards an asymptote (Figure 17). This behavior greatly increases with temperature. It can be explained by the chemical structure of cellulose; the first linear phase corresponds to a fast degradation of the amorphous phase of cellulose, which is followed by a slower degradation of the crystalline phase of cellulose chains in fibrils bundles. Cellulose chains in

the amorphous phase are more accessible than in the crystalline phase. Amorphous cellulose contains some free space between chains while crystalline cellulose is compact with almost no free space between chains. Therefore, cellulose from the amorphous phase will degrade along the chain while crystalline cellulose tends to degrade at chain ends, which is the only place where this cellulose can interact with solvents and degrade. When amorphous cellulose is completely degraded, any more scissions in this phase will not affect the average length of cellulose and only crystalline cellulose degradation will change the average degree of polymerization. In this final situation, the DP reaches what is called the LODP (Levelling-Off Degree of Polymerization) where degradation starts to be very slow.

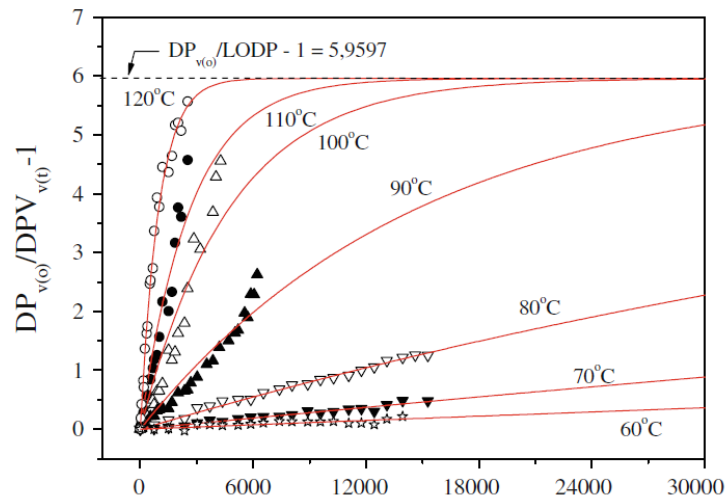


Figure 17: Depolymerization of cellulose for thermal isotherms from 60 to 120°C. Extracted from Jalbert et al. [18].

The fall of cellulose DP_v is followed because it is a fundamental property that is directly correlated to mechanical properties. The main reason behind the loss of mechanical properties is that a loss of DP_v will lead to a loss of chain entanglement. Chain entanglement is a critical property; chains are bonded together and the movement of one chain is impeded by other chains. A loss of DP_v means less interaction between chains and more free volume. Experimental data of Figure 18, obtained for standard or TU Kraft papers, show that the tensile strength remains constant with the fall of DP_v until a value of about 600. After that, the tensile strength decreases linearly with DP_v . In some reports, it is considered that Kraft insulation has reached its end of life when the tensile strength has reached 50% of its initial value [19].

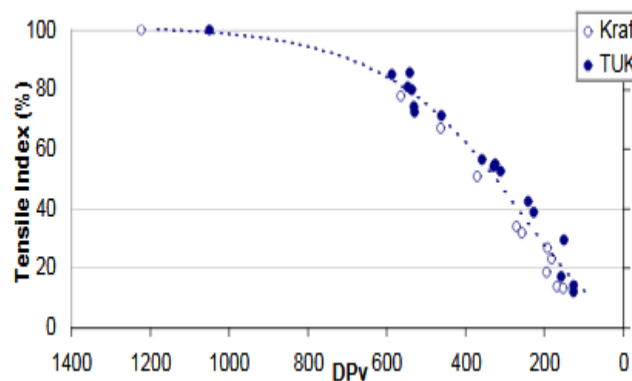


Figure 18: Evolution of tensile index with the fall of DP_v . Extracted from Arroyo et al. [19].

The loss of dielectric properties is not directly related to the DP_v . Yet, because it is used as a reference, DP_v is often plotted against changes in dielectric properties (Figure 19). Dielectric properties used to characterize Kraft insulation are described in the third chapter. During ageing, the resistivity of the insulation degrades over time but it does display a linear relationship with DP_v . The loss of dielectric properties will usually not fully degrade the transformers but it leads to higher losses and more heat produced in the insulation. The reason for the loss of permittivity is thought to be correlated to the increase in water content of insulation.

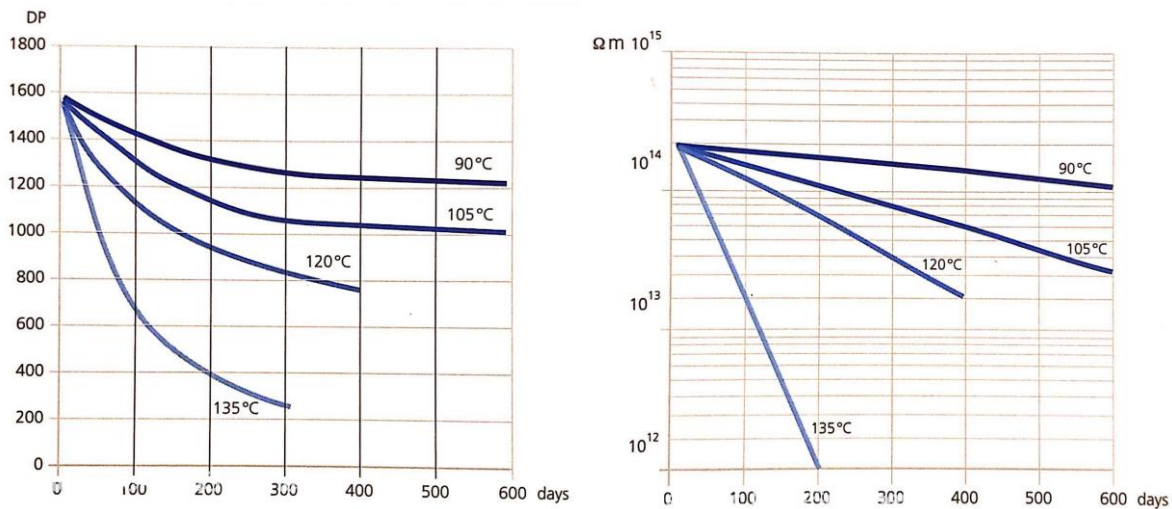


Figure 19: Loss of permittivity during ageing and the corresponding fall of DP_v . Extracted from the Transformer oil handbook [6].

iii) Theoretical models

Models that describe cellulose depolymerization can be divided into zero (or pseudo zero) rate order models, that consider the rate of depolymerization is constant and independent of the concentration of the reacting substances, and in first-order models. In the latter, the rate of reaction is proportional to the concentration of the reactant.

- Zero-order model

The basic description of cellulose degradation kinetics (depolymerization) is described by Enkenstam's first-order kinetic law considering cellulose as a single type of linear and homogeneous polymer:

$$\frac{dN}{dt} = -k'N$$

Where: N , the number of unbroken glycosidic bonds at time t and k' the first-order rate constant. Because the number of scissions is very low compared to the overall number of bonds, a zero-order kinetic law can be derived, which gives after time-integration:

$$\frac{1}{DP_{n(t)}} - \frac{1}{DP_{n(0)}} = \alpha kt$$

In this equation, α measures the accessibility of the bonds and k the scission rate constant. As seen in Figure 17, the initial rate of cellulose degradation follows a first-order kinetic law that transitions into a second order kinetic law after reaching the LODP value. Cellulose is not a homogeneous polymer since it contains crystalline and amorphous phases that have distinct accessibilities and depolymerization kinetics.

A better fitting equation was introduced by Emsley [17] to introduce a change in the depolymerization kinetics during ageing. A second rate constant k_2 is added to account for the rate at which the initial rate constant decreases.

$$\frac{1}{DP_{n(t)}} - \frac{1}{DP_{n(0)}} = \frac{k_{10}}{k_2} \times (1 - e^{-k_2 t})$$

Here, k_{10} is the initial rate constant and k_2 is the rate at which k_{10} decreases. This model was successfully applied to accelerated ageing temperature experiments of Kraft insulation in laboratory experiments. Yet, the limit of this equation is that it only mathematically corrects a change in the depolymerization kinetics but does not describe the chemical origin of this difference. Over the decades, the zero-order model has been modified and some authors, based on new approaches, have gradually made improvements to it. An additional variant was introduced by Calvini [20]. This model introduces the existence of a limiting LODP. The decrease of the initial rate constant can therefore be correlated to an exponential function of time involving the LODP.

$$\frac{DP_{n(0)}}{DP_{n(t)}} - 1 = \left(\frac{1}{LODP} - \frac{1}{DP_0} \right) \cdot (1 - e^{-k \cdot t})$$

Calvini *et al.* further introduced the concept of initial number (n^o) of reacting glycosidic linkages in weak (n_w^o), amorphous (n_a^o), and crystalline (n_c^o) regions. Three kinetics are therefore considered, they represent scissions of glycosidic bonds with different reactivities: weak (easily accessible and degradable), amorphous (degradation is still rather easy), and crystalline bonds. The role of weak bonds is sometimes omitted because of the claim that they may not exist because they would not resist the chemical treatments during Kraft pulp manufacturing. Differences in pulping process parameters of each manufacturer could be the reason why they are not always present. For crystalline cellulose, chemical studies showed that acid-depolymerization of the crystalline phase happens by end-chain spot wise degradation, meaning linear degradation is a more accurate model for the crystalline phase. The resulting kinetics can be uncoupled from each other as seen in Figure 20, depolymerization of the crystalline region can be separated from the amorphous region. After time-integration, the proposed equation includes the simultaneous occurrence of these three types of degradation which do not take place at the same rate:

$$\frac{DP_{n(0)}}{DP_{n(t)}} - 1 = n_w^o(1 - e^{-k_w t}) + n_a^o(1 - e^{-k_a t}) + n_c^o(1 - e^{-k_c t})$$

The left side of the equation represents the number of scissions per chain; n_w^o , n_a^o and n_c^o are the initial numbers of weak, amorphous and crystalline region bonds; k_w , k_a and k_c are the corresponding reaction rate constants. In practice, experimental data show that weak bonds do not play an important role in the overall equation and can be omitted, and that depolymerization of the crystalline phase is better represented by a linear model.

Considering the latter assertion, the best-fitting model can be represented by:

$$\frac{DP_{n(0)}}{DP_{n(t)}} - 1 = n_a^o(1 - e^{-k_a t}) + n_c^o k_c t$$

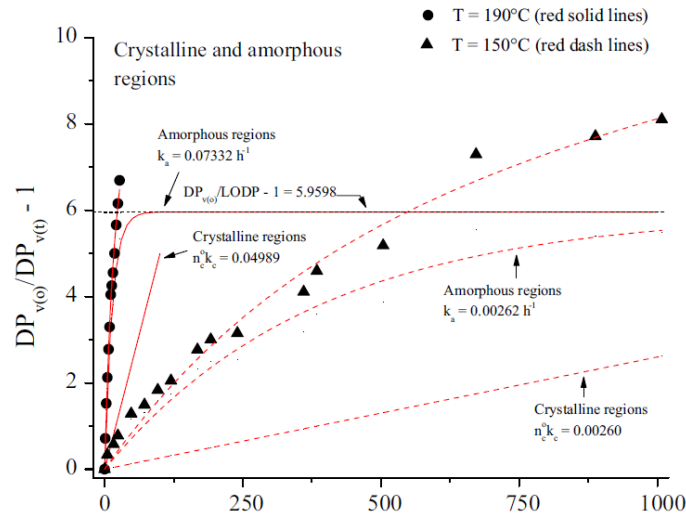


Figure 20: Depolymerization of cellulose at 190 and 150°C with the corresponding independent depolymerization of the amorphous and crystalline regions. Extracted from Jalbert et al. [21].

Independently, Ding and Wang [22] described cellulose depolymerization with another approach:

$$1 - \frac{DP_{n(t)}}{DP_{n(0)}} = \omega_{DP}^* \times (1 - e^{-kt})$$

Here, ω_{DP}^* describes a “capacity of the DP reservoir”. This constant was contested in the literature because it does not have a clearly defined physical meaning. Critics argue that this model does not describe a purely hydrolytic mechanism (the main chemical pathway of degradation) but a spot wise degradation of cellulose. This mechanism might only be predominant in the crystalline phase of cellulose.

- **First order model**

In the first-order degradation model, the rate of depolymerization is considered proportional to the length of the cellulose chain.

$$DP_{n(t)} = DP_{n(0)} e^{-kt}$$

This model did not correlate to experimental data [23]. Chemical reactions and the multiplicity of chemical pathways in degradation means that a direct proportional law is inaccurate. In comparison, zero-order and pseudo-zero models can better subdivide the multiple reactions that are responsible for the overall change in DP.

c) Chemical pathways of degradation

i) Defects of new Kraft insulation

Kraft insulation contains defects that will be at the source of cellulose depolymerization. They are of two types; impurities and network imperfections. No matter what engineers do, insulation will always have traces of impurities of three types: water, traces of oxygen and metal cations. Imperfections are present in all cellulose chains in the form of oxidative damage coming from pulping and any errors causing overcooking. Although these defects are only present in small quantities of parts per million, they are at the first step of depolymerization. Only one cleavage is needed to reduce the average DP of cellulose chains from 1000 to 500; meaning that on average, very few numbers of cleavages can have a very important impact on Kraft insulation.

Water and oxygen traces are impossible to remove from paper. The most significant transition metals are: iron (that comes mainly from pulping) and copper (more present in paper in contact with wiring, but also found in other layers of papers). Other metal ions are calcium, magnesium and sodium. During ageing, transition metal ions are more critical than other metal ions because they are known to trigger oxidative cellulose degradation by catalyzing the formation of reactive oxygen species (hydroxyl radicals) and hydroxyl anions in the presence of oxygen and water [24].

Regarding imperfections, oxidative damage is evenly distributed through the cellulose chain, they come from dehydration of hydroxyl groups at the high temperatures found during finition. Oxidation of cellulose causes introduction of carbonyl groups in cellulose. Cellulose monomer (AGU) damage by oxidation can be of three types:

- Keto groups at C2, C3
- Aldehyde function at C6
- Carboxyl groups at C6

An example of oxidative damage of a C2 carbon can be seen in Figure 21. Cellulose with oxidation damage is susceptible to further cleavage by oxidation or hydrolysis.

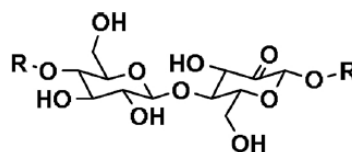


Figure 21: Anhydroglucose repeating unit with an oxidized C2 unit. Extracted from Jusner et al. [16].

ii) Cellulose oxidation

Kraft insulation in power transformers is aged in a dry and non-oxidative environment, but the small impurities inside the Kraft pulp will be at the origin of oxidative cleavages of cellulose. The β -alkoxy elimination degradation is the nucleophilic attack of hydroxyl groups. The glycosidic bond cleavage forms a new reducing end group and an unstable counterpart that rearranges to more stable products. The most common type of rearrangement is of the

saccharinic acid type. These acids are also known to attack copper in winding. The overall reaction is presented below:

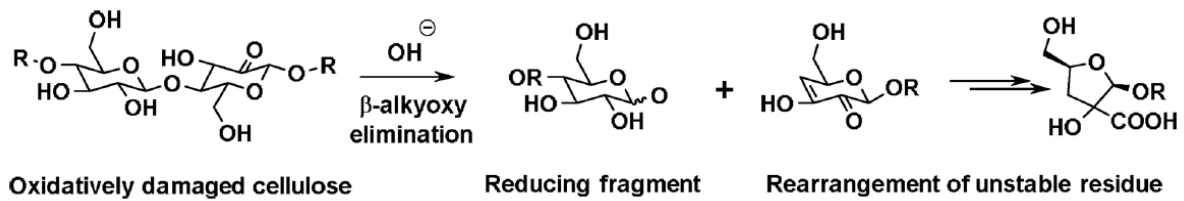


Figure 22: β -alkoxy elimination of oxidized cellulose in Kraft insulation. Extracted from Jusner et al. [16].

In general, oxidative cellulose degradation does not contribute much to the absolute degradation of oil when oxidative factors (oxygen, transition metals) are reliably excluded (which is generally the case in Power Transformers). It can only become more influential in the case of oxidatively pre-damaged (overbleached) celluloses, which is not the case of the unbleached Kraft pulp used for insulation paper. In practice, this reaction is self-inhibiting because the acid products of the reaction react with the hydroxyl ions responsible for the reaction. However, β -alkoxy elimination is at the start of an acid build up in Kraft insulation, which in-turn will be at the start of a much more destructive reaction: acid hydrolysis.

iii) Acid hydrolysis

Unlike oxidation, acid hydrolysis can cleave non-oxidized cellulose, which represents the vast majority of repeating units. The hydrolytic chain scission starts by the protonation of either the oxygen of any β -(1-4)-glycosidic bond along the cellulose backbone or by protonation of the ring-oxygen of any pyranose. After the scission, further acid hydrolysis attacks degrade cellulose up to the level of organic acids. In practice this does not always happen, degradation can stop before total degradation. When cellulose AGU only degrades to 5-hydroxymethylfurfural, the overall reaction is net positive in water production. When cellulose degrades up to levulinic and formic acids, the net reaction is neutral in water production but increases the acidity of the system. On top of the organic acids, while pure water has a pH of 7 at room temperature, the neutral pH value at 100°C is about 6, meaning that water dissociation and hydronium ion concentration are increased by a factor of 10. The overall reaction scheme is described below:

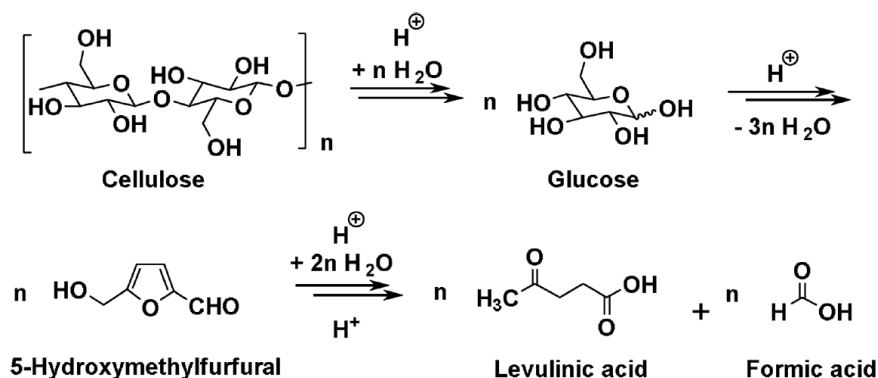


Figure 23: Acid hydrolysis of non-oxidized cellulose in Kraft insulation. Extracted from Jusner et al. [16].

The initial kinetics of this reaction is kinetically determinant, since the production of water and acid byproducts makes that the reaction will become auto-catalytic. Indeed, new Kraft insulation does not have the initial acidity to start acid hydrolysis but β -alkoxy elimination slowly leads to the growth of the acidity, which in turn leads to the start of a vicious cycle of acid hydrolysis. Acid hydrolysis will therefore represent the main degradation pathway of cellulose in power transformer conditions. In normal working temperatures (70°C) acid hydrolysis is the only reaction that will contribute significantly to cellulose degradation. Moreover, temperature spikes and hot spots can dramatically increase the process of degradation in some locations.

iv) Pyrolysis

Finally, in some hot spots at very high temperature, pyrolysis of cellulose might occur. The latter starts to become predominant for temperatures above 150°C (Figure 24). Between 150 and 240°C, healthy carbohydrates dehydration becomes dominant, leading to oxidized cellulose and water production. Oxidized cellulose can then be cleaved for temperatures above 200°C and release even more water. After 240°C, healthy reducing ends of cellulose can be degraded and produce even more water in the process. Degradation is mostly located in the amorphous phase of cellulose because of the higher chain mobility, unlike in the highly ordered crystalline phase. These reactions do not need alkali or acidic catalysts. In parallel, hemicelluloses, less stable than cellulose, are more likely to degrade at lower temperatures than cellulose and increase water production.

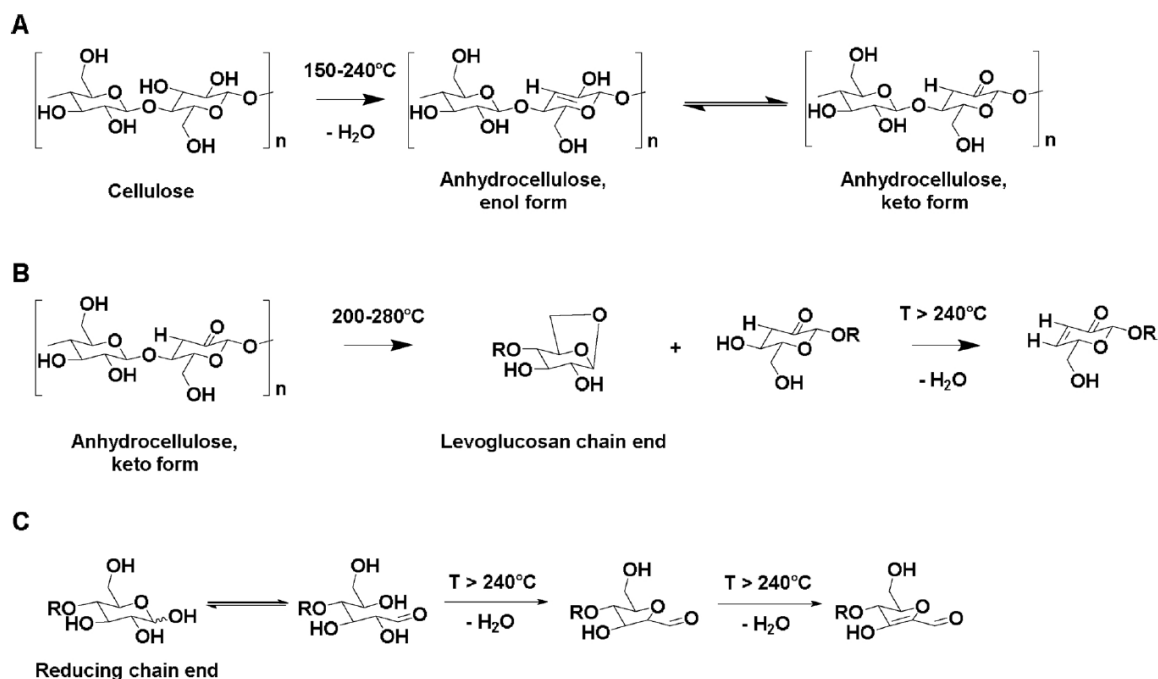


Figure 24: Pyrolysis reaction of oxidized and non-oxidized cellulose in Kraft insulation. Three pathways of oxidation are shown; from cellulose (A), cellulose with oxidative damage (B) and reducing end groups (C). Extracted from Jusner et al. [16].

It does happen that a transformer is subjected to a higher load and spots in the transformer are temporarily at a much higher temperature. Environmental stress or failure of the cooling system can also increase the temperature in the insulation. The importance of these reactions is the high

production of water content and oxidation damage to the cellulose chain. After high loads, it is common for utility operators to detect significant amounts of water in the transformer.

v) Summary

Insulation in Power Transformers degrades through a combination of multiple reactions. Degradation pathways are too numerous and extensive to be fully understood but it is commonly accepted that Kraft insulation starts to build up acidity from β -alkoxy eliminations, this reaction is self-inhibiting but slowly increases the acidity that will be at the source of an unavoidable depolymerization of cellulose by acid hydrolysis. Pyrolysis at locally very hot spots can also add to this process by additionally feeding water and oxidative damage during punctual events. With all of these phenomena having a higher impact on amorphous cellulose than on crystalline cellulose.

Conclusion and perspectives

Power transformers today are at a crossroad, their insulation was designed to have a working life of a minimal of 30-40 years. Yet, most transformers found today (in western countries) date back to a peak of installation that happened during the 1970s, therefore massive number of machines are reaching their expected working life with no means to quickly replace them. Utility operators are still in the need of new methods that can accurately follow cellulose depolymerization. With current technology, it is impossible to fully understand and follow the complex reactions that govern cellulose depolymerization. It is known that impurities and imperfections in Kraft insulation lead to local acidification of cellulose, which starts a vicious cycle of cellulose depolymerization by acid hydrolysis. Models may try to predict how the depolymerization of cellulose will evolve with time and will affect key properties of the insulation. Understanding these phenomena can help to the formulation of additives to extend insulation lifetime. It can also help utility operators to develop improved monitoring methods to prevent insulation failures.

In our study, the main objectives are to improve the understanding and the follow-up of cellulose ageing in order to improve monitoring techniques. The following themes will be investigated:

Investigations on the origin of methanol production in power transformers during paper ageing.

Dissolved gas analysis in oil is an indirect monitoring method related to the state of Kraft insulation in transformers. Analysis of the concentration of some focused degradation by-products in oil can be related to cellulose depolymerization. In recent years, methanol dissolved in oil was shown to be a promising tracer molecule for this purpose. The first part of our study focuses on investigating the origin of this molecule to improve the accuracy of this method.

Investigations on the role of organic and mineral components during ageing and their effect on dielectric and chemical properties of the oil-insulation couple.

As discussed previously, the chemical composition of paper plays an important role in paper ageing. In particular, the role of some cations that can affect the buffering capacity of paper and its capacity to retain acidity, will be investigated. The second part of this study will focus on the analysis of the evolution of the dielectric properties of paper during ageing, in relation to its chemical composition in terms of cellulose, hemicelluloses, lignin and minerals.

References

1. Siemens brochure, Electrical Power Transformers, 2017.
2. Myers, S.D., Kelly, J.J., and Parrish, R.H., A Guide to Transformer Maintenance, Transformer Maintenance Institute, Akron, 1981.
3. Harlow JH. Electric power transformer engineering. 3rd ed. Boca Raton, FL: CRC Press; 2012.
4. Prevost TA, Oommen TV. Cellulose insulation in oil-filled power transformers: Part I - history and development, IEEE Electr Insul Mag, 2006, (1):28–35.
5. ABB Brochure, Insulation in Transformers, 2020.
6. Nynas. Transformer oil handbook. 2010.
7. Sheppard H. A Century of Progress in Electrical Insulation 1886-1986. IEEE Electr Insul Mag, 1986, (5):20–30.
8. Gilot B, Pautou G, Moncada E, Ain G., Ecological study of *Ixodes ricinus* (Linné, 1758) (Acarina, Ixodoides) in southeastern France, Acta Trop. 1975, 32(3):232–58.
9. Huang C, Chu Q, Xie Y, Li X, Jin Y, Min D, et al. Effect of Kraft Pulping Pretreatment on the Chemical Composition, Enzymatic Digestibility, and Sugar Release of Moso Bamboo Residues, BioResources, 2014, 17;10(1):240–55.
10. Valette P, Choudens C de. Le bois, la pâte, le papier. 3e éd. rev. et augm. Grenoble: Centre technique de l'industrie des papiers, cartons et cellulose, 1992.
11. Emsley AM, Stevens GC. Kinetics and mechanisms of the low-temperature degradation of cellulose. Cellulose, 1994, 1(1):26–56.
12. Bonfiglio F. Reactivity of Dissolving Pulps: A measure based on Acetylation kinetics, 2015.
13. Crestini C, Melone F, Sette M, Saladino R. Milled Wood Lignin: A Linear Oligomer. Biomacromolecules, 2011, 14;12(11):3928–35.
14. Solihat NN, Sari FP, Falah F, Ismayati M, Lubis MAR, Fatriasari W, et al. Lignin as an Active Biomaterial: A Review. J Sylva Lestari, 2021, 29;9(1):1.
15. Barnet A. Compréhension des phénomènes de vieillissement des papiers électrotechniques dans les transformateurs de puissance et recherche de solutions industrielles. 2020.
16. Jusner P, Schwaiger E, Potthast A, Rosenau T. Thermal stability of cellulose insulation in electrical power transformers – A review. Carbohydr Polym, 2021, 252:117196.
17. Gilbert R, Jalbert J, Tétreault P, Morin B, Denos Y. Kinetics of the production of chain-end groups and methanol from the depolymerization of cellulose during the ageing of paper/oil systems. Part 1: Standard wood kraft insulation. Cellulose, 2009, 16(2):327–38.
18. Gilbert R, Jalbert J, Duchesne S, Tétreault P, Morin B, Denos Y. Kinetics of the production of chain-end groups and methanol from the depolymerization of cellulose during the ageing of paper/oil systems. Part 2: Thermally-upgraded insulating papers. Cellulose, 2010, 17(2):253–69.

19. Arroyo OH, Fofana I, Jalbert J, Ryadi M. Relationships between methanol marker and mechanical performance of electrical insulation papers for power transformers under accelerated thermal aging. *IEEE Trans Dielectr Electr Insul*, 2015, 22(6):3625–32.
20. Calvini P. On the meaning of the Emsley, Ding & Wang and Calvini equations applied to the degradation of cellulose. *Cellulose*, 2014, 21(3):1127–34.
21. Jalbert J, Rodriguez-Celis E, Duchesne S, Morin B, Ryadi M, Gilbert R. Kinetics of the production of chain-end groups and methanol from the depolymerization of cellulose during the ageing of paper/oil systems. Part 3: extension of the study under temperature conditions over 120 °C, *Cellulose*, 2015, 22(1):829–48.
22. Hongzhi D. Degradation phenomenology and life modelling of paper [Internet]. In *Advances in Pulp and Paper Research*, Oxford, 2018.
23. Hill DJT, Le TT, Darveniza M, Saha T. A study of degradation of cellulosic insulation materials in a power transformer, part 1. Molecular weight study of cellulose insulation paper. *Polym Degrad Stab*, 1995, 48(1):79–87.
24. L. L. The limits of metal removal from Kraft pulp by acid treatment. *Journal of pulp and paper science*, 1997.

Chapter 2: Investigations on the origin of methanol production during Kraft paper ageing in Power Transformers.

Table of content

Introduction	45
1) Understanding Dissolved Gas Analysis (DGA).....	46
a) Monitoring Power Transformers.....	46
b) Cellulose depolymerization through DGA	47
c) Methanol as a marker of cellulose depolymerization	48
i) Correlation experiments.....	49
ii) Stability and partition coefficient experiments.....	53
iii) Origin of the methanol production experiments	56
d) Kinetics of methanol production.....	58
2) Materials and methods	61
a) Materials	61
i) Chemical products	61
i) Instruments and standardized methods for characterizations	61
b) Methods.....	62
i) Method development	62
ii) Correlation experiments on paper samples	63
iii) Partition coefficient experiments on paper samples.....	64
• Partition coefficient with a change in methanol concentration.....	64
• Partition coefficient with a change in paper degradation.....	65
iv) Origin experiments on model compounds	65
• Lignin model compounds	65
• Cellulose and hemicelluloses model compounds.....	66
3) Results and discussion.....	67
a) Understanding the experimental approach.....	67
b) Origin experiments on model compounds	68
i) Lignin model compounds	68
ii) Cellulose model compounds	74
iii) Hemicelluloses model compounds.....	75
iv) Discussion of results.....	76
c) Correlation experiments paper samples	80
i) Ageing of cotton linters (CL)	80
ii) Ageing of BKP	81
iii) Ageing of UKP.....	82

iv) Discussion of results.....	82
d) Partition coefficient experiments	84
i) Effect of methanol concentration and paper composition	84
ii) Effect of ageing	86
iii) Effect of moisture content	87
iv) Discussion of results.....	88
e) Contrasting results with literature	88
Conclusion.....	92
References	94

Introduction

Power transformers are the Achilles' heel of the power grid. Following a peak in the 1970s, addition of new power transformers in the grid has steadily declined to the point where today most transformers in western countries are around 40 years old and are reaching their designed life expectancy.

A combination of mineral oil and cellulosic insulation is used in power transformers acting as the main electrical insulation for metal parts. Circulating oil dissipates heat while oil-impregnated paper prevents direct contact between metal conductors. Cellulosic insulation degrades over time through a combination of thermal and mechanical stresses (from vibrations, oil flow), a process in which moisture, acidity and temperature are the main contributors. Central to this problem is that, while oil can be periodically dried, purified and renewed, cellulosic insulation cannot be replaced during the transformer's lifetime. Paper and pressboard insulation will be the critical factor of the transformer's life expectancy.

The ageing process of lignocellulosic materials in transformers is still not fully understood. This topic will be herein further explored, studying the effect of wood fiber composition on the degradation products from paper ageing. Through the Dissolved Gas Analysis (DGA), some of these degradation products are used as chemical markers to indicate the state of the paper insulation in a working transformer. Of particular interest is lignin, present as a residue in original Kraft paper, who might play an unsuspected role in the production of markers used to follow cellulose depolymerization. Gas markers in the oil can be analyzed by HSGC-FID (Head space Gas Chromatography with a Flame Ionization Detector).

Methanol was recently identified as a main chemical marker to evaluate the rate of cellulose depolymerization (cellulose DP_v decay) in the Kraft insulation during long-time thermal ageing. Methanol was recently identified as a main chemical marker to evaluate the rate of cellulose depolymerization (cellulose DP_v decay) in the Kraft insulation during long-time thermal ageing. In this chapter, the contribution of lignin to the production of methanol will be studied. This will be done by comparing the behavior of unbleached Kraft pulp, bleached Kraft pulp, and bleached cotton linters pulp, since bleaching operations fully eliminates lignin from the lignocellulosic matrix. As a complement, some lignin and cellulose model compounds will be also investigated, to identify the functional groups contributing in the generation of methanol. In addition, paper's affinity towards methanol will be studied, in particular the methanol paper/oil partition coefficient in relation to the presence of lignin in paper.

1) Understanding Dissolved Gas Analysis (DGA)

a) Monitoring Power Transformers

Although power transformers (PT) are static electrical machines with no moving parts, they still require constant care during their service, which requires an important care and maintenance by electrical utility companies to detect faults and prevent failures. Operators constantly scan their machines for potential problems that could develop into a serious issue [1]. Entire books detail PT care and maintenance, but for the purpose of our study, it should be pointed out that insulation media will be the first component to fail under normal working conditions, and therefore, monitoring its state will be of paramount importance. Two types of monitoring exist; on-line and off-line monitoring, where transformers are energized or deenergized respectively [2]. On-line monitoring is preferred by utility companies since it increases the availability of transformers and allows the transition to condition-based maintenance instead of time-based maintenance. On-line monitoring covers the most critical parts of transformers; the insulation system, the coil and core assembly and the bushings, where faults are the ones that most often lead to system failure. The most critical parameters are checked, such as temperature, moisture in oil, partial discharge detection, and dissolved gas analysis (DGA). The latter only requires a simple valve on the transformer tanks to collect oil without interfering with operations.

The idea that gases formed in transformers could be monitored to prevent faults from developing, dates from the late 1920s, when Bucholz relays, installed on transformer tanks, gave the pressure of free gas generated in the transformer. A rise in pressure indicated an imminent or developing fault. It wasn't until the early 1960s that chromatography was applied as an analytical technique to correlate the presence of a specific gas to a particular fault. In the 1980s, the development of gas chromatography (GC) allowed to have reliable and fast analysis of gas content dissolved in the oil. At first, some gases were used to detect characteristic faults on PT, for example, carbon oxides indicate conductor overheating, and acetylene the presence of arcing. Then, tabulated concentrations allowed utility companies to rule the severity of the fault and the action to be taken. DGA is not only useful to punctual problems but also to assess the health of the solid and liquid insulation. Today, three methods are used to quantify dissolved gases in the oil; gas chromatography, hydrogen on-line monitoring, and photo-acoustic spectroscopy [3]. Although gas chromatography is the most precise and reliable method, it is also the longest and most expensive one, therefore it performs less frequently or if significant faults are detected in other routine tests.

Technology combined with research led to normalization of three main methods to extract dissolved gases from oil for gas chromatography analysis (ASTM D3612); vacuum, stripper and headspace extraction [4]. Of these ones, headspace extraction is the main type used for research because it requires less manipulation and is less susceptible to contamination [5]. After extraction, gases are separated using gas chromatography columns and detected through either Mass Spectrometry (MS) or Flame Ionization Detectors (FID). The development of robust DGA quantification allowed to seriously consider its possible use to analyze the state of degradation of solid Kraft insulation, *i.e.* cellulose depolymerization. It was used to correlate a concentration of a depolymerization product in oil to the long-term evolution of the inaccessible solid insulation. A sample of the gas blanket could also be taken to perform gas analysis but it

is seldom used because handling and analysis of the gas is more complicated. The gas blanket is a term used to designate the gas phase that sits on top of the oil in transformers.

b) Cellulose depolymerization through DGA

Materials scientist know that cellulose depolymerization is the main factor behind the loss of mechanical properties of lignocellulosic substrates. Yet, since Kraft insulation cannot be sampled in working transformers, direct analysis is impossible. DGA is an indirect analysis that attempts to correlate the concentration of a tracer molecule dissolved in oil to the Viscometric Degree of Polymerization (DP_v) of the cellulosic insulation. Since cellulose degradation is a complex process that produces many degradation by-products, the main challenge is to find the ideal tracer.

From the literature, it can be summarized that the ideal tracer should have the following properties:

- It should be stable in oil, high temperature and oxidative conditions so as not to degrade after its formation.
- It should come only from the degradation of paper (preferably from cellulose).
- Its production should be independent of the type of paper (*i.e.* pure Kraft or thermally upgraded (TU) Kraft paper).
- It should arise during all stages of ageing.
- It should have a foreseeable partition coefficient between the paper/oil/gas phase inside the transformer. The partition coefficient refers to the fraction of methanol that will be in each paper/oil/gas phase.

In practice, utility operators will measure the concentration of tracers annually and then apply a mathematical model that fits the evolution of a particular transformer [6]. The model should be able to predict the ageing time when cellulose DP_v will reach the value of 200, a critical value where the transformer should be removed from service. For a given tracer, multiple mathematical models might exist that each prioritize a different aspect of the tracer formation [7]. The accuracy of each model will depend on the transformer construction parameters and its environment.

Three generations of tracers in oil (markers) have been used since DGA appeared in the 1980s [8]. The first generation is the measurement of carbon oxides (CO/CO₂), since their concentration could be linked to cellulose depolymerization. However further experiments showed that these molecules could also originate from the long-term oxidation of oil [9]. The second generation of markers were furanic compounds, produced from the dehydration of pyranose cycles of carbohydrates. Therefore they should only originate from cellulose or hemicelluloses degradation [7]. Five compounds were defined as chemical markers; 2-Furfural (2-FAL), 2-Furfurol (2-FOL), 5-Hydroxy methyl 2-furfural (5-HMF), 5-Methy-2-furfural (5-MEF), and 2-Acetylfuran (2-ACF). Among these, 2-FAL is the most commonly used tracer [10]. Furanic compounds can easily be analyzed by HPLC (High-Performance Liquid

Chromatography) and are still widely used in the industry. The main limits of using furanic compounds come from the facts that:

- 2-FAL tracer is inaccurate in TU paper. The presence of alkaline inhibitors in TU paper influences the acid hydrolysis reaction that is responsible for the formation of the 2-FAL and therefore dramatically reduces furan production.
- 2-FAL can come from any pyranose-based compound. Therefore, hemicelluloses degradation, and not only cellulose degradation, can also produce furanic compounds.
- 2-FAL is only accurate in the later stages of degradation, when acid hydrolysis has led to a cellulose DP_v of around 500 or below.

Given the limitations of 2-FAL and carbon oxides, another chemical marker was searched. The ever-increasing use of TU papers in transformers limits the use of 2-FAL as a reliable marker. Methanol (and also ethanol) were then identified as potential tracers and became “third-generation markers” that, since 2007, promised to solve the limitations of previous markers.

c) Methanol as a marker of cellulose depolymerization

Methanol as a chemical indicator for cellulose depolymerization was first revealed by Jalbert *et al.* in 2007 [8]. It was noticed that methanol and ethanol were detected in significant amounts during paper aging in insulating oil between 60 °C and 120 °C. It was postulated that there is a linear relationship between methanol production and the breakage of 1,4-β-glycosidic bonds in cellulose, *i.e.* the depolymerization of cellulose. This proposal came after extensive studies of the behavior of 50 DGA byproducts by HSGC-MS (Headspace Gas Chromatography coupled to Mass Spectrometry). Acetaldehyde, acetone, methanol, butanol, 2-butanone, ethanol and carbon disulfide were included among the molecules detected. However, only acetone, methanol, butanol and ethanol were selected because they came mostly from paper degradation. The thermal stability of these compounds was tested at different temperatures in mineral oil, and methanol was found to be the most stable. Thus, methanol in oil became the focused compound for the control of aged paper depolymerization, and attempts were made to correlate its concentration in oil with the DP_v of the paper insulation.

The initial studies showed that the main advantage of methanol over 2-FAL is that it is generated with any type of insulating paper, *i.e.* both Kraft and TU paper. Disadvantages are the high volatility of methanol and the possible esterification with low molecular mass acids formed with paper and oil [11]. In practice, there is a long path between the time a compound of interest is found and when it is used; the compound is identified, extensive literature is built on its potential applicability and then standardization is made. For methanol, after 15 years of scientific research on the subject, international committees (ASTM WG D27 WK30948 and IEC TC10 WG 63025) are working on a normalization standard for methanol analysis [5]. Even though there is no standard yet, methanol is already used by utility companies around the globe. Yet, it is important to understand what experiences were made that led international working groups to be created.

Multiple experiment types are needed to demonstrate that methanol is a valid tracer. The most fundamental one is to correlate the concentration of methanol to a parameter that measures the state of the solid insulation, such as paper DPv or tensile strength. Correlation with other tracers and the effect of temperature should also be studied. Once a correlation is established, “stability” and “methanol partition” experiments between oil/paper/gas can be investigated to understand how the tracer will behave in the transformer and how it will be distributed among the different phases inside (solid: paper / liquid: oil / gas: nitrogen). Complementary, “origin” experiments can give clues to what components of the insulation are responsible for methanol production. All experiments can either be done at laboratory scale or by field sampling on working or post-mortem transformers. The literature review below will present a summary of these experiments and the establishment of mathematical models to describe methanol production in relation to cellulose ageing.

i) Correlation experiments

The first in-depth analysis of the relationship between cellulose depolymerization and the formation of methanol was reported by Jalbert *et al.*'s original publication [8] as illustrated in Figure 25. Since Kraft pulp from different manufacturers can have different starting DP, most studies present depolymerization as a function of $1/DP$, in this manner a clear picture of degradation will be visible independently of the original DP. Three sections are expected for the curves in Figure 25a: the first one corresponds to a fast-initial rate period, followed by a moderate rate period, and then by an extremely slow rate period. The fast rate section is considered to represent an attack on a small fraction of 1,4- β -glycosidic bonds of the cellulosic fibrils that are very accessible and particularly sensitive to rupture. The second section of the curves implies the rupture of the 1,4- β -glycosidic bonds between β -D-glucopyranose units located in the amorphous regions (the most accessible part) of the cellulosic fibrils. The third section corresponds to an attack of the crystalline regions of the cellulosic fibrils (this is the less accessible part of cellulose chains, and this section is only visible when paper is aged at 100 - 120°C). In Figure 25b there is a corresponding linear increase of methanol concentration in the oil, which allows to postulate a linear relation between the rupture of glycosidic bonds between the AGUs (anhydroglucose units of the cellulose chain) and the generation of methanol. This appears especially verified at the beginning of the curves.

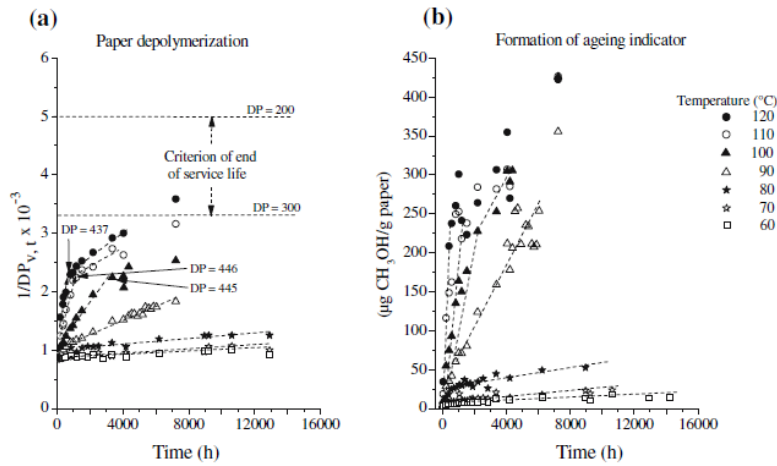


Figure 25: Overall results for the relationship between paper depolymerization (a), expressed as a function of $1/DP_v$, and formation of tracer with time (b) expressed as the concentration of methanol in oil in $\mu\text{g/g}$ of paper. Extracted from Jalbert et al. [8].

Besides DP_v , mechanical properties of paper are generally followed. Due to the combination of heat, radial and axial forces that cause contractions and elongations of the coils, the Kraft insulation paper becomes stiff and brittle. It can tear under stress and lead to equipment failure. To follow mechanical properties, tensile strength is used as a reference test, it is the maximum stress that a material can withstand while being stretched or pulled before breaking. Tensile index is used because it normalizes tensile strength, allowing for sample width and grammage. Tensile index is defined as the breaking force per width and grammage unit of paper [70]. Grammage is defined as the mass per unit area of paper (grams per square meter).

Experimentally, tensile index does not vary until a DP_v of about 700 and then it starts a linear decline until a DP_v of 200. It is generally considered as a criterion that Kraft insulation has reached its end of life when the initial tensile index has dropped down to between 50 % to 20 % of its original value. The limits of tensile index as a criterion are that humidity, temperature and small imperfections can cause wide variations leading to important standard deviations. Nonetheless, correlation experiments were performed to explore the relationship with methanol production in ageing experiments. Not surprisingly, a linear correlation was found between methanol production and tensile index as shown in Figure 26. Temperature dependence is visible and TU paper also validates this model. Based on these results, methanol was retained to predict the remained mechanical strength of paper insulation. Yet, these are laboratory results in which closed samples were aged individually, and not as part of an ensemble of paper aged at different temperature simultaneously, like in real transformers. More analysis on field-equipment would be needed to further explore this parameter.

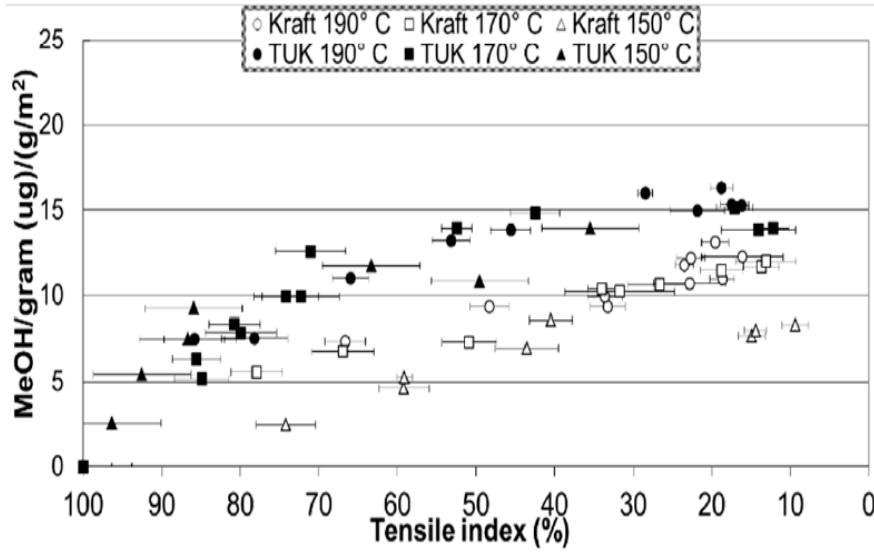


Figure 26: Overall results for the relationship between the tensile index, and formation of tracer during ageing, expressed as the concentration of methanol in oil in $\mu\text{g}/(\text{g}/\text{m}^2)$ of paper. Extracted from Arroyo *et al.* [12].

Further experiments have been carried out by Jalbert *et al.* and by other researchers. A summary is presented below, gathering major publications where methanol production was studied against another variable in a correlation experiment (Table 4, Table 5 and Table 6). Experiments were done at laboratory scale or by field measurements. Methanol concentration is plotted against either ageing time or change in DPv, or a variable derived from DPv variation, such as mean number of scissions, fraction of scissions or number of chain end groups. The following table gives a list of the other variables that were measured in some studies. For field measurements, methanol is plotted against the transformer's service time at the time of sampling.

Table 4: Variables tested in literature (with their acronym)

Variable	Acronym
Temperature	TE
Moisture of paper or oil	MO
Tensile Index	TI
Paper Weight	PW
Fourier Transform Infrared Spectroscopy	FTIR
Acidity of Oil	AO
Nitrogen Content of paper (ageing inhibitors of TU paper)	NC
Pressboard Samples	PS
Type of Cap used to seal the ageing vessel	TC

All publications relate the use of unbleached Kraft papers or TU Kraft papers.

Table 5: Main correlation experiments done at a laboratory scale

1 st Author / Year	Temperature (°C)	Duration (days)	Other tracers tested	Variable(s) tested against methanol concentration in oil	Ref
Jalbert 2007	60 - 120	540	2-FAL	TE/MO	[8]
Jalbert 2009	60 - 130	660		TE/MO	[13]
Jalbert 2010	60 - 130	660	2-FAL	TE/NC	[14]
Schaut 2011	100	210	2-FAL / Propanal / butanal / 2-methoxy-propanol / 2-butanol / 2-propanon	TC	[15]
Jalbert 2013	20 - 90	200	2-FAL / H ₂ O / Ethanol	TE	[10]
Laurichesse 2013	98/110/122	180	2-FAL	TE/MO	[16]
Arroyo 2014	140	101	2-FAL / Ethanol	TI	[17]
Arroyo 2015	170	54		TI/NC	[18]
Matharge 2015	120	100	Ethanol	No other variables were tested	[19]
Rodriguez-Celis 2015	60/130/250	250: 20 seconds 60/130: 1 week		FTIR/PW	[20]
Perrier 2015	105/122/130	380	2-FAL	NS/PS	[21]
Matharge 2016	120	275	2-FAL / Ethanol	TI/MO/AO	[22]
Arroyo 2017	170	145		NC/TI/FTIR	[12]
Arroyo 2018	150	330	2-FAL	TI/AO/MO	[23]
Matharge 2018	80-120	357	2-FAL	TI/AO/comparison between different types of oil ¹	[24]

1: All the experiments were done in inhibited mineral oil (Gemini X) and synthetic ester oil (MIDEL7131).

Table 6: Main correlation experiments done with field transformers

1 st Author / Year	Transformer's age (years)	Other tracers tested	Transformer's situation	Origin of samples	Ref
Jalbert 2007	1 - 80	2-FAL	Online	Unspecified	[8]
Schaut 2011	4/30+	2-FAL	Online	Unspecified	[15]
Jalbert 2012	0-36	2-FAL CO/CO ₂	Online	Unspecified	[25]
Ryadi 2013	0	2-FAL	Online	Unspecified	[26]
Laurichesse 2013	25-55	2-FAL	Online	Unspecified	[16]
Ryadi 2014	Unknown	2-FAL CO/CO ₂	Online and post mortem	Low and High Voltage windings	[27]
Jalbert 2015	57	2-FAL / H ₂ O / Ethanol	Post Morten	Low and High Voltage windings	[28]
Jalbert 2018	37-61		Post Morten	Low and High Voltage windings	[29]

ii) Stability and partition coefficient experiments

An oil-tracer analyzed by DGA should be stable in the operating conditions of the transformer and it should have a predictable paper/oil/gas partition coefficient. Reports have shown that methanol fulfills these properties. Stability experiments were done in closed vessels by adding methanol under accelerated ageing conditions. Partition coefficient experiments are characterized by adding known quantities of methanol in an oil/paper system and quantifying how much remains in the oil. Jalbert *et al.* [8] monitored the changes in methanol concentration in sealed ampoules placed in an oven at 70, 90, 110 and 130°C. The inhibited oil Nynas 10 CX was analyzed at different time intervals of up to 1505 hours. The results are shown in Figure 27. The concentration of methanol remained reasonably stable over the duration of the test at 70 and 90°C. At 110 and 130°C, methanol concentration decreased after 16 days. This decline was attributed to a modification of the matrix polarity by the presence of oil oxidation by-products, enhanced by the higher temperatures. Since the gas/oil partitioning of methanol declines with time, fewer molecules are accessible to HS-GC-MS analysis.

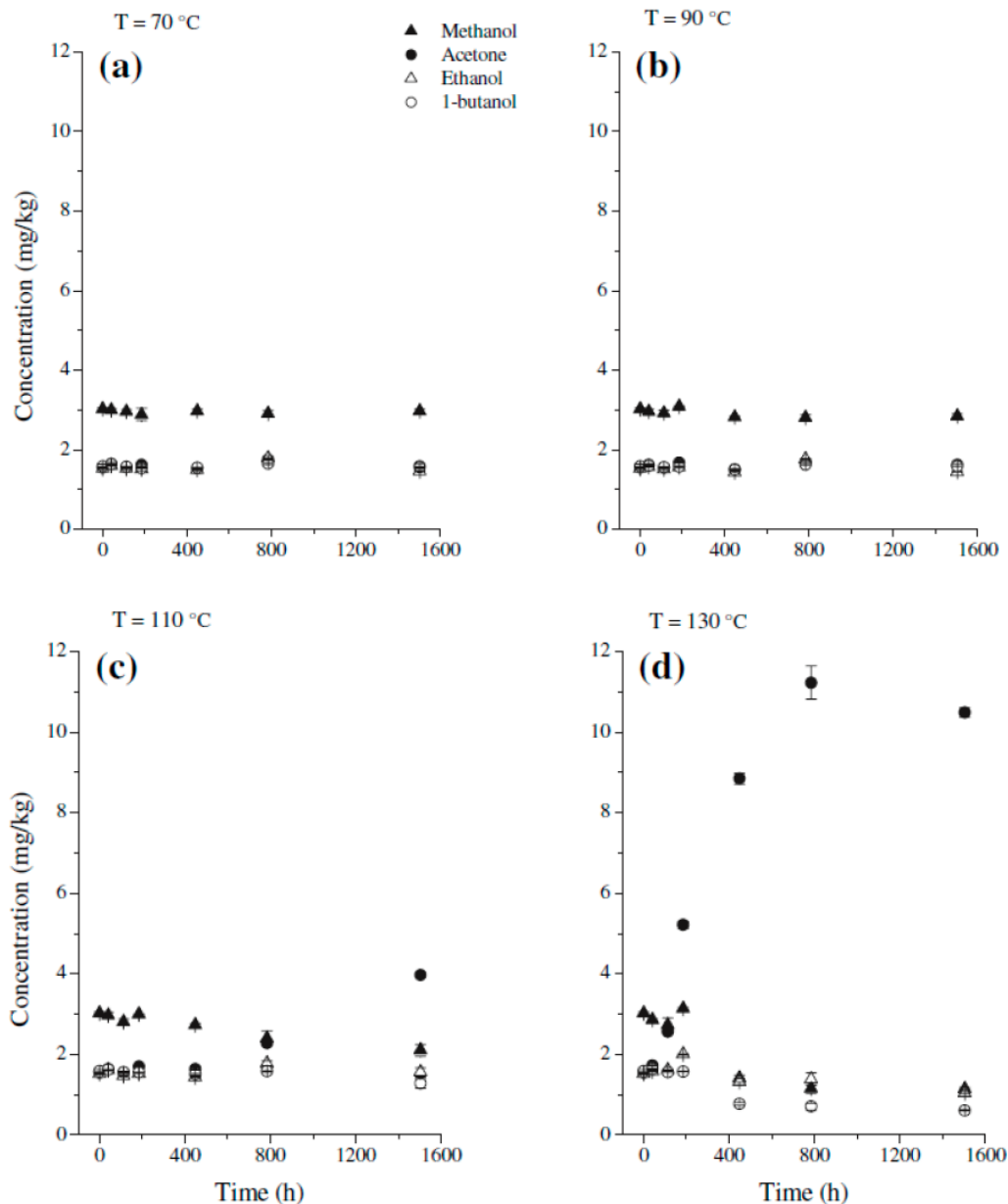


Figure 27: Stability with time for methanol, acetone, ethanol and 2-FAL under conditions prevailing for open-breathing equipment at different temperatures (a)70°C, (b)90°C, (c)110°C, (d)130°C. Extracted from Jalbert et al. [8].

Further experiments consisted in immersing a paper sample in the oil and then, adding methanol to the solution. The concentration of methanol in the oil was followed every 2 hours. In Figure 28 it is shown that over 58 % of the methanol in the oil migrated into the paper after 15 hours. This is relevant because if most of the tracer remains in the paper, then an equilibrium will be regained quickly after an oil change (around 3 months is needed for methanol against 1 year for 2-FAL [25]). When most of the tracer remains in the paper, it takes less time for the new oil to reach the same equilibrium that it had before the oil change.

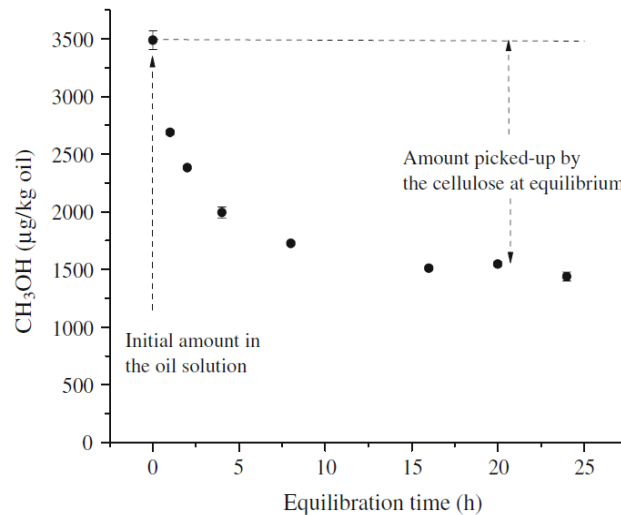


Figure 28: Evolution of MeOH concentration in oil during the equilibration time with paper for 25 hours after spiking at 40°C. Extracted from Jalbert et al. [14].

Further experiments from different authors and studies regarding stability and partition coefficients are listed in Table 7 and Table 8. The cited publications contain other type of data and experiments, which are not mentioned below.

Table 7: Main stability experiments found in literature.

1 st Author / Year	Temperature (°C)	Duration	Other tracers or conditions tested	Ref
Jalbert 2007	60 -120	540 days	2-FAL / Acetone / Ethanol / Butanol	[8]
Schaut 2011	120	220 days	Propanal / Butanal / Butanone / 2-propanol / Ethanol / 2-pentanone	[15]
Souza 2016	75	7-21 days		[11]
Matharage 2018	130	168 days	Comparison between different types of oil ¹	[24]

1: All the experiments were done in inhibited mineral oil (Gemini X) and synthetic ester oil (MIDEL7131).

Table 8: Main partition coefficient experiments found in literature.

1 st Author / Year	Temperature (°C)	Duration (hours)	Other oils tested	Origin of methanol	Ref
Jalbert 2009	40	0 - 25		Spiking of the oil	[13]
Jalbert 2010	20	0 - 250		Ageing at 130°C for 168h	[14]
Jalbert 2012	40/60/80	0 - 25		Spiking of the oil	[25]
Matharage 2018	20	2040	Synthetic esters	Spiking of the oil	[24]

All the partition coefficient experiments shown were measured in a laboratory setting.

iii) Origin of the methanol production experiments

Only three publications report about the origin of the methanol production. The first two [8,20] focused on studies on model compounds of paper, while the third one [24] focused on methanol production coming from oil.

The first report came from Jalbert *et al.* original publication in 2007 [8]. This study aimed to find the origin of methanol from the different polymers present in Kraft paper: α -cellulose, lignin, and hemicelluloses. Each compound was added in equimolar amounts and aged at 130°C for 168 h under oxidative conditions. Methanol, ethanol, butanol and 2-FAL were quantified in oil. Results in Table 9 are the mean values found after 5 measurements.

*Table 9: Methanol production (in μg of methanol/kg of oil/g of component) of model compounds of paper based on five replicas heated at 130°C for 168 hours (D.L.: Detection Limit). Extracted from Jalbert *et al.* [8].*

Components of Kraft paper	Model compound studied	CH ₃ OH detected (μg of methanol/kg of oil/g of component)
α -cellulose	Microcrystals from cotton linters	8 940
	Whatman paper No.41	1 730
Lignin	Alkali Kraft Lignin	153200
Hemicelluloses from softwoods	Mannan isolated from <i>Saccharomyces cerevisiae</i>	<D.L.
Hemicelluloses from hardwoods	Xylan isolated from birch	227 500
Major by-product from α -cellulose hydrolysis	D-(+)-glucose	<D.L.
Major by-product from α -cellulose hydrolysis	1,6-anhydro- β -D-glucopyranose	1 750
Blank oil	Mineral oil	440

Results in these experiments showed that alkali lignin produced significant amounts of methanol compared to other products, as for instance, 17 times more methanol than from α -cellulose (per gram of component). Because lignin constitutes 3-5% of the paper weight and has a good stability during paper ageing, it was concluded that its presence should not impact the tracer. Regarding carbohydrates, α -cellulose produced significant amounts of methanol and since it composes at least 75-80 % of the paper, it was seen as a positive result to show that cellulose should be the major contributor to methanol production. Another point of interest was that softwood hemicelluloses did not produce methanol in detectable amounts, contrary to hardwood hemicelluloses. The explanation given is that xylans, mostly contained in hardwoods,

have large amounts of acetyl and methoxy groups that are liable to be cleaved. Since only softwood pulp is used to produce transformer paper or board, and xylans are not a major component in them, hemicelluloses in the Kraft paper should not contribute significantly to methanol production. Concurrently, cellulose degradation products were tested; 1,6-anhydro- β -D-glucopyranose produced as much methanol as Whatman paper, and D-(+)-glucose produced no detectable amount. No explanation is given for such differences.

Another series of experiments was included in Rodriguez-Celis *et al.* (2015) publication [20]. It compared methanol and ethanol production during paper-oil ageing. Cellobiose is the repeating unit in cellulose chains. Glucose is also tested, and levoglucosan, a well-known byproduct of cellulose thermal ageing, or pyrolysis. The ageing protocol was the same as in the previous experiments except for the addition of another ageing temperature of 60°C. Results can be found in Table 10.

Table 10: Methanol production (in μg of methanol/kg of oil/g of component) of model compounds heated at 60 and 130°C for 168 hours (D.L.: Detection Limit). Extracted from Rodriguez-Celis *et al.* [20].

Component	Ageing (168h) (°C)	CH ₃ OH detected (μg of methanol/kg of oil/g of component)
Glucose	60	< D.L.
	130	< D.L.
Cellobiose	60	28
	130	23
Levoglucosan	60	8
	130	6

Again, glucose produced no detectable amount of methanol in oil. This study does not present any results for oil blanks meaning that for results with small concentrations it is difficult to know how much methanol comes from oil or from model compounds. It is mentioned that water content, acidic conditions, and an inert atmosphere (N₂) do not change the results. Because this study mainly focused on ethanol, there are no comments on methanol production for cellobiose and levoglucosan.

The third series of experiments is part of Matharage *et al.* (2017) publication [24] that focused on methanol production coming from oil. It was compared the oil acidity and methanol production in accelerated ageing conditions at 110, 120 and 130°C for 70 days in sealed flasks. Partial oxidation of oil produced detectable amounts of methanol. Production of methanol was inversely related to the acidity of the oil: when acidity was low, higher amount of methanol was detected. This behavior could come from the methanol consumption, by the esterification with the acidic byproducts from oil degradation. In the interpretation of these results, it is important to understand that in practice, oil is checked periodically and never reaches the acidity level as in this laboratory study. Nonetheless, this study shows that it is possible to have some methanol reactions by esterification in acidic conditions. This should be further investigated and verified, and some cautions should be taken during methanol analysis to avoid these phenomena.

d) Kinetics of methanol production

Methanol was identified as a promising tracer to be analyzed in DGA. A proper kinetic law of methanol generation should be identified for field usage by the operators. At the time of writing, no standardization has yet been published by the IEC or ASTM work groups and only some publications [5,13,14,30] give preliminary models.

The basic description of cellulose degradation kinetics (depolymerization) is described by Ekenstam's first order kinetic law (Equation 1) that considers cellulose as a single type of linear and homogeneous polymer:

$$\frac{dN}{dt} = -k'N \quad (1)$$

Where: N, the number of unbroken glycosidic bonds at time t and k' the first-order rate constant.

The number of scissions of the polymer chain, S, is considered: $S = DP_{n(0)} [1/DP_{n(t)} - 1/DP_{n(0)}]$

where $DP_{n(t)}$ and $DP_{n(0)}$ correspond to the number-average degree of polymerization (DP_n) of cellulose at the measured time t, and at the beginning of the experiment (t = 0), respectively.

Because S is very low compared to the overall number of bonds, a zero-order kinetic law can be derived, which gives after time-integration:

$$\frac{1}{DP_{n(t)}} - \frac{1}{DP_{n(0)}} = \alpha kt \quad (2)$$

In Equation 2, α measures the accessibility of the bonds and k the specific rate of the scission of glycosidic bonds constant, both constants are defined as the product of the first-rate constant degradation of cellulose in the air.

Cellulose is not a homogeneous polymer since it contains crystalline and amorphous phases that have distinct depolymerization kinetics. As seen in Figure 29, the initial rate of cellulose degradation follows a first-order kinetic law that transitions into a second order kinetic law. Experimentally, depolymerization is most often followed through the viscometric degree of polymerization (DP_v) while the number average degree of polymerization (DP_n) is most often used in in mathematical models. DP_n is calculated using the average molecular masses of the individual cellulose chains while DP_v uses the empirical relation between viscosity of a solution with dissolved cellulose and the degree of polymerization. Both methods are accurate, the main difference is DP_n gives priority to the number of chains while DP_v gives priority to their weight. This comes from the fact that the amorphous phase is responsible for the initial, fast and linear degradation that further stagnates into a slow, leveling-off degree of polymerization (LO-DP) where only the crystalline phase remains and slowly degrades.

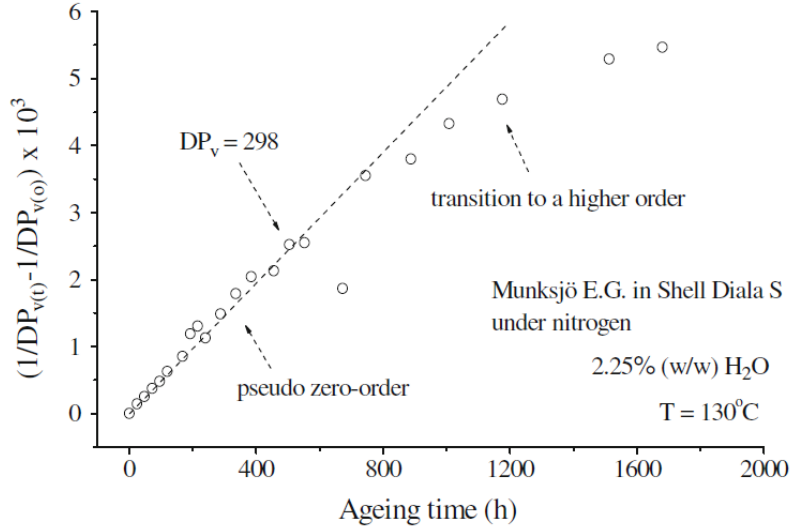


Figure 29: Transition of the depolymerization reaction from a zero-order to a higher order kinetic law. Extracted from Jalbert et al. [14].

A better fitting equation was proposed by Emsley [31] to introduce the change in the depolymerization kinetics during ageing (Equation 3). A second constant k_2 is added to account for the rate at which the initial rate constant decreases.

$$\frac{1}{DP_{n(t)}} - \frac{1}{DP_{n(0)}} = \frac{k_{10}}{k_2} \times (1 - e^{-k_2 t}) \quad (3)$$

Here, k_{10} is the initial rate constant and k_2 is the rate at which k_{10} decreases. This model was successfully applied to accelerated ageing temperature experiments of Kraft insulation in laboratory experiments. Yet, the limit of this equation is that it only corrects mathematically a change in the depolymerization kinetics but does not describe the origin of this difference.

Another equation was introduced by Calvini [31]. Three kinetics are considered, they represent scissions of different types of glycosidic bonds: weak (easily accessible and degradable), bonds in the amorphous zones of the chains, and bonds in the crystalline regions of the chains. After time-integration, the proposed Equation 4 includes the simultaneous occurrence of these three kinds of degradations which do not take place at the same rate:

$$\frac{DP_{n(0)}}{DP_{n(t)}} - 1 = n_w^o(1 - e^{-k_w t}) + n_a^o(1 - e^{-k_a t}) + n_c^o(1 - e^{-k_c t}) \quad (4)$$

The left side of the equation represents the number of scissions per chain; n_w^o , n_a^o and n_c^o are the initial numbers of weak, amorphous and crystalline region bonds; k_w , k_a and k_c are the corresponding reaction rate constants. The role of weak bonds is sometimes omitted because of the claim that they may not exist because they would not resist the chemical treatments during Kraft pulp manufacturing [32]. Differences on the pulping process of each manufacturer could be the reason why they would not always be present. Moreover, chemical studies showed that acid-depolymerization of the crystalline regions happens by chain end spot wise degradation, meaning linear degradation is a more accurate model for the crystalline phase. Considering the latter assertion, model curves could be made that had a better fit to experimental data (Equation 5):

$$\frac{DP_{n(0)}}{DP_{n(t)}} - 1 = n_a^o(1 - e^{-k_a t}) + n_c^o k_c t \quad (5)$$

Jalbert *et al.* [29] proposed a transposed kinetic law that would link cellulose depolymerization to methanol production:

$$\frac{DP_{n(0)}}{DP_{n(t)}} - 1 = J_a(1 - e^{-k_a t}) + J_c k_c t \quad (6)$$

In the Equation 6, the production of one methanol molecule is assumed to represent one scission. The coefficients J_a and J_c represent the number of methanol molecules produced by chain scissions in the amorphous and crystalline regions, respectively, with their corresponding rate constants k_a and k_c . This equation was used to plot the weight-average number of scissions against the methanol concentration in samples coming from a real power transformer. The results of the investigations of 20 transformers are shown in Figure 30. Values that fit the model equation were marked in blue, red ones were those outside the observed tendency.

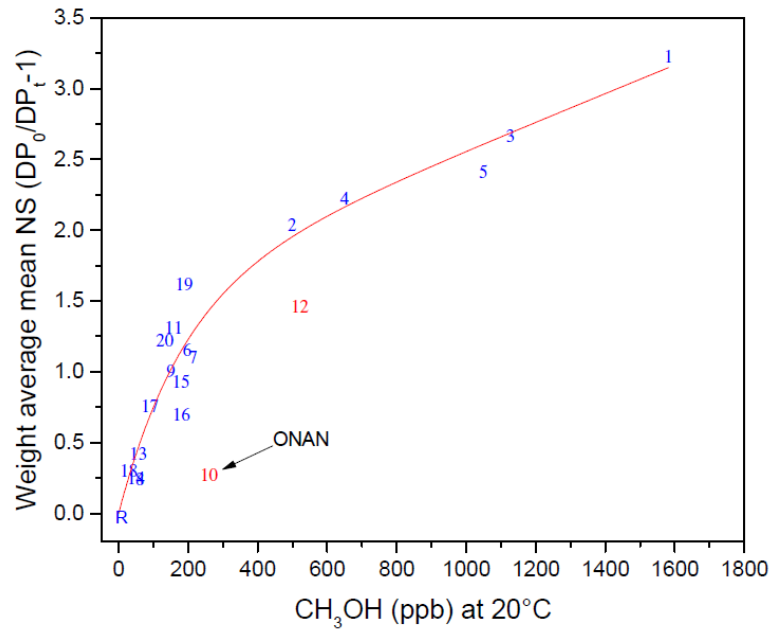


Figure 30: Results for the methanol prediction model used on a real-life core-type transformer. Extracted from Jalbert *et al.* [29].

Since the paper or oil affinity for methanol will vary with temperature, the concentration of methanol is normalized at 20°C. Normalization was done by plotting the variations of methanol concentrations for varying temperatures. The validity of the model was shown, with a high linear correlation coefficient of $R^2=0.941$. It was also possible to create a set of threshold values for methanol concentration in transformers, as seen in Table 11. These values were calculated based on tabulated data that are used for 2-FAL.

Table 11: Ethanol threshold levels and the corresponding paper conditions; using a temperature correction factor of 20°C. Extracted from Jalbert *et al.* [29].

[CH ₃ OH] (ppb)	Mean calculated DPv	Paper condition
0-50	1000-700	Healthy
51-200	700-450	Moderate deterioration
201-1440	450-250	Extensive deterioration
>1440	<250	End-of-life criteria

e) Conclusion

There are still some unknowns about the origin of methanol generation during transformer paper ageing. The investigations that will be presented aim at elucidating some of the points discussed above from the literature, more especially the molecular origin of methanol, *i.e.* the chemical reactions yielding methanol. A special insight will be on the role of lignin.

2) Materials and Methods

- Materials

- i) Chemical products*

Oil: NYTRO 10XN and NYTRO Taurus oils are the inhibited and uninhibited transformer mineral oil. They were supplied by NYNAS Company.

Kraft and cotton pulps: Unbleached Kraft Pulp (**UKP**) and Bleached Kraft Pulp (**BKP**) originate from ASPA mill in Sweden. Cotton Linters (**CL**) were obtained from CELSUR in Spain. TAPPI handsheets were made with a grammage of 130 g.m² from these raw pulps using deionized water (180 µm thickness, 14 cm diameter).

Model compounds and chemicals: vanillyl alcohol (98%), vanillin (99%), vanillic acid (97%), anisole (99%), guaiacol (98%), syringol (99%), methyl- α -D-glucopyranoside (99%, CAS: 97-30-3, Reference number: M9376) and phenol (99%) were purchased from Sigma Aldrich. Toluene (99%) was bought from Chimie-Plus, and sulfuric acid (95%) was from Fluka. Methanol (98%), D-(+)-cellobiose (98%, CAS:528-50-7, Reference number:10176711-08), xylan (95%), Galactomannan from softwood (98%, CAS: 1078-30-1, Reference number:1018111-31), D-(+)-glucose and n-pentane (99%) were purchased from Roth. Ethanol was bought from Revol. Hydranal Coulomat E was used for Karl Fischer titrations.

- ii) Instruments and standardized methods for characterizations*

The following instruments were used for these experiments:

HSGC-FID (Headspace gas chromatography with flame ionization detector): PerkinElmer, Clarus 690 gas chromatogram with a TurboMatrix 40 headspace sampler.

Viscometric Degree of polymerization (DP_v): depolymerization of cellulose was also followed by viscometric degree of polymerization. Pulps were grinded (using a Forplex) and dissolved in a solution of cupriethylenediamine. After degassing with nitrogen, the cellulose solutions were measured for their viscosity using Ubelhode-type capillary viscosimeters. Through the intrinsic viscosity it is possible to calculate the DP_v of the dissolved cellulose.

Karl-Fischer analysis: water in oil and in impregnated paper was measured by Karl-Fischer analysis coupled to thermal desorption of the sample (oven temperature 140°C), under dry air flow, and water content analysis by coulometric titration (Metrohm 831 KF coulometer coupled to Metrohm 832 thermoprep oven).

- **Methods**

An important part of the work was focused on developing an experimental technique suited to the available equipment in LGP2 and allowing many samples to be tested. An ageing approach with minimum handling and good repeatability was developed. Experiments included “correlation experiments” on paper samples (UKP, BKP and cotton linters bleached pulp), “origin experiments” on model compounds (model compounds of cellulose, hemicelluloses and lignin) and “partition coefficient experiments” on paper samples (UKP). Nynas Nytro Taurus oil was used in the experiments for paper samples, and Nynas 10XN was used for experiments on model compounds. The reason for this is that Nynas 10XN was not available and no distributor was willing to sell volumes inferior to one barrel (180 kg). Both oils are the same except that Nynas 10XN contains an inhibitor to control oxidation. This should not play a significant role in the conditions chosen for the ageing tests. For all experiments, HSGC-FID was used to quantify methanol in oil. For samples with paper, additional steps were needed to measure water content in oil and paper (Karl Fischer titration), to extract oil from paper (Soxhlet extraction) prior to cellulose DP_v measurement.

i) Method development

Initially, thermal ageing of model compounds or paper samples was done using open bottles placed in stainless steel reactors. Reactors were hermetically closed and placed in an oven at 140°C for 24 hours (Figure 31). These experiments were meant to reproduce the most common experiments in literature which is ageing in sealed glass ampoules.

Once aged, the metal bottles were quickly cooled with water flow and compressed air flow, they were opened and the oil was sampled. This method proved inadequate for two main reasons. First, the speed of cooling had an effect on the results because gases inside the bottle could condensate on the walls. It was impossible to have a completely homogenous cooling meaning reproducibility was poor. Secondly, this method required much more handling and an exposure of oil to the outside atmosphere, therefore leading to more time-consuming process and a risk of methanol loss or sample contamination.



Figure 31: Original steel glass and steel bottles used for ageing in an oven.

Given these limitations, multiple variations of the steel metal bottles were tested but none system was adapted. However, in one previous study [15], 20 mL headspace vials were used as vessels for thermal ageing, and then, oil was pipetted to fill 10 mL headspace vials for analysis. Then, we had the idea to do the ageing and headspace analysis in the same vial. It would remove

many steps and allow for the oil to never be exposed to the outside air. The problem then came that vial caps could not withstand the stress of prolonged ageing at 130°C inside an oven since they became unable to hold pressure in the headspace sampler. Therefore, an oil bath (Figure 32) was used instead of an oven to prevent vial caps from heating in the oven.

Final tests were done to compare the reproducibility of ageing in headspace-vials with either screwed caps or crimped caps (with silicon/Teflon and butyl rubber seals), in the oven or in silicon oil bath, under the same condition (130 °C for 24 hours). Silicon/Teflon seals with crimped caps were shown to resist thermal ageing conditions. Reproducibility was tested in 5 vials aged under the same conditions, it showed a standard deviation of about 10 ppm of methanol in oil.



Figure 32: On the left; ageing of head space vials in oil bath (the first batch was protected from light by adding boxes on top of the stirrers; for the other experiments vials were wrapped in aluminum foil). On the right; vials of BKP samples aged from 3 hours to 13 days at 130 °C.

Because paper samples were in the oil during headspace sampling, there was a concern that some of the methanol detected from the GC also came from paper. Therefore, a test was done to ensure that the detected methanol only came from oil. For this purpose, an ageing was performed on oil & paper samples and 1/10 of the oil was pipetted from the vial with paper & oil to be spiked into a vial that only contained oil. Results showed that the spiked vial contain 1/10 of the signal of the original vial, showing that the signal only comes from methanol in oil.

ii) Correlation experiments on paper samples

Methanol production of the 3 types of papers (UKP, BKP and cotton linters) was studied in thermally-accelerated ageing conditions (130 °C) for a relatively short time (0-240 h). Change in the cellulose DP_v was studied in order to correlate it to methanol production in oil. Despite using high temperatures, a change in matrix polarity of the oil should not have an effect on methanol detection because, in our case, even the longest experiments can be considered still too short. Indeed, the literature shows (Figure 27) that some matrix polarity effects may appear only after 400 h ageing.

The paper handsheets made of UKP, BKP, and CL were cut into 2 cm wide narrow strips. Then, 0.4 g of each strip was weighted, rolled, and put in 20 mL HS-vials. A total of 10 samples were prepared for cotton samples and 13 samples for BKP and UKP (Table 12). Before adding the oil, paper drying was done by placing each vial in an oven at 93°C for 24 hours under vacuum. Then, they were immediately impregnated by pouring 10 mL of NYTRO Taurus oil using a 10 mL pipette; then they were degassed under vacuum for an hour. To protect them from light, vials were covered with an aluminum foil after they were sealed with crimped Silicon/Teflon cap. Finally, these samples were placed in a silicon oil bath with the controlled temperature of

130°C for 3 to 240 h. To avoid damaging the caps, vials were submerged up to a level below the neck of the vial.

Table 12: Ageing time for each tipe of paper sample (BKP, UKP, and cotton linters).

Ageing time for each sample (h)				
3	6	9	24	28
34	48	120	144	168
192	216	240		

The maximum ageing time for cotton linters was 168 h (7 days), and 240 h (10 days) for UKP and BKP. Samples were removed according to the times set in Table 9, the exterior of the vials was cleaned to remove heating oil from the oil bath, and prepared for the GC analysis. Opening of the vial was done only after HSGC-FID analysis, then paper was removed and prepared for Soxhlet extraction, followed by DPv measurement.

iii) Partition coefficient experiments on paper samples

Three effects were investigated for the measurement of paper/oil partition coefficient of methanol: (1) effect of paper type (BKP, UKP, and cotton linters) at different methanol concentrations; (2) on UKP only, effect of paper ageing, and (3), on UKP only, effect of varying paper moisture.

- *Partition coefficient with a change in methanol concentration*

Calibration solutions were prepared with methanol and ethanol concentration range of 0 to 24 000 ng/g for oil, oil and BKP, oil and UKP, and oil and cotton linters. Stock solution was prepared by adding 10.3 mg (13 µL) of methanol and ethanol to 128 g (160 mL) of NYTRO Taurus oil to reach the concentration of 80 µg/gin µg methanol and ethanol per g of oil.

Paper sheets were cut into 2 cm wide narrow strips, weighted for 0.4 g, rolled and placed in HS-vials. Then, these vials were placed for drying under vacuum at 93°C for 24 h in an oven. After drying, these papers were immediately impregnated by 10 mL oil and then different amount of stock solution were added to prepare the desired concentration (Table 13). All of the prepared calibration solutions were left at room temperature for 48 hours to reach the equilibrium before analyzing with HSGC-FID.

Table 13: Stock solutions used to spike methanol in partition coefficient experiments.

Concentration of methanol and ethanol (ng/g)	Required volume of stock solution (µl)		Concentration of methanol and ethanol (ng/g)	Required volume of stock solution (µl)
0	0		13600	1700
1600	200		16000	2000
4000	500		17600	2200
5600	700		20000	2500
8000	1000		21600	2700

9600	1200		24000	3000
12000	1500			

- *Partition coefficient with a change in paper degradation*

After ageing, UKP paper samples were kept for studying the partition coefficient. Oil was removed through soxhlet extraction, aged samples were dried in identical conditions and impregnated in oil using the same method as for the ageing experiments. Then, oil was spiked at the same methanol concentration for all the samples used in this experiment (5600 ng/g). After impregnation, all samples were hermetically sealed and stored for 48 hours to allow methanol reaching an equilibrium with paper before GC analysis.

iv) Origin experiments on model compounds

Methanol production by lignin model compounds, including vanillyl alcohol, anisole, guaiacol, syringol, phenol, and toluene, was studied. Each compound was chosen to represent a key structure in lignin. Thermal accelerated ageing conditions were 130 °C for 24 hours. Ageing was done with 0.3% and 1.5% mass ratio of model compound to oil. The mass ratio was calculated by using Kraft lignin as a reference; for a mass ratio of 1.5 and 0.3 % mass of lignin per mass of oil, the molar amount of aromatic cycle was calculated to obtain the number of moles of model compounds that were added in each sample. Lignin model compounds were tested under neutral and acidic conditions (sulfuric acid or a mixture of 1/3 formic acid and 2/3 acetic acid). Polysaccharide model compounds were only tested in neutral conditions.

- *Lignin model compounds*

For experiments in neutral conditions, lignin model compounds (at a lignin compound/oil mass ratio of 1.5% and 0.3%) were added to HS-vials (Table 14). These compounds were then impregnated with 10 mL of NYTRO 10XN oil (using a pipette). The vials were sealed with silicon/Teflon crimped caps to obtain a perfect seal. A silicone oil bath was placed on a heater-stirrer, at controlled temperature of 130°C. Temperature was homogenized in the bath by magnetic stirring. The HS-vials were covered by aluminum foils and partially submerged in a silicone oil bath for 24 hours before the analysis of the dissolved gas.

Table 14: Amounts of lignin model compounds used for ageing tests in neutral conditions.

Sample	Oil (mL)	Compound	Compound per sample (mg)	
			1.5% lignin	0.3% lignin
1	10	Blank oil	-	-
2	10	Guaiacol	38.8 (34.4 µl)	7.75 (6.85 µl)
3.1 et 3.2 (Doublet for repeatability)	10	Syringol	48.2	9.63
4	10	Vanillyl alcohol	48.2	9.63
5	10	Phenol	29.4	5.88
6	10	Anisole	33.8 (33.8 µl)	6.75 (6.78 µl)

7	10	Toluene	28.8 (33.2 μ l)	5.75 (6.63 μ l)
---	----	---------	---------------------	---------------------

Complementary experiments were done using the same preparation and ageing protocol with vanillin, vanillic acid and vanillyl alcohol, 3 weeks after the trials presented in Table 11. These experiments are described in Table 15.

Table 15: Complementary ageing tests using vanillin, vanillyl alcohol and vanillic acid in neutral conditions.

Sample	Oil (mL)	Compound	Compound per sample (mg)	
			1.5% lignin	0.3% lignin
1	10	Blank oil	-	-
2	10	Vanillin	47.6	9.51
3	10	Vanillic acid	52.5	10.5
4	10	Vanillyl alcohol	48.2	9.63

Experiments in acidic conditions followed the same protocol except that, for the addition of 0.01 mol of sulfuric acid per mol of model compound, acid was introduced in the oil after the model compound. Ageing experiments done with weak acids used a mixture of 1/3 formic acid and 2/3 acetic acid, with acid/oil mass ratio ranging from 0.1 to 1 mg/g and at 115, 120 and 130°C, only 1.5% lignin compound/oil mass ratio in the case for experiments with guaiacol. Experiments carried out to calculate the activation energy used only guaiacol with a ratio of 1 mg/g of acid/oil. The experiments were the same as for acidic conditions except 118 and 23.5 μ l of sulfuric acid were added to samples of 1.5 and 0.3 % lignin mass ratio, respectively. Also, an acid blank sample was added where 118 μ l of sulfuric acid was added.

After ageing, the samples were removed from the oil bath, cooled down in cold water, and then vials were cleaned before analysis. The HSGC-FID was launched and the calibration solutions in HS-vials followed the method of Jalbert *et al.* [33].

- *Cellulose and hemicelluloses model compounds*

Experiments carrying out on polysaccharide model compounds used the same protocol as for lignin model compounds in neutral conditions. D-(+)-cellobiose, D-(+)-glucose, and methyl-alpha-D-glucopyranoside, were used and added at a 1.5% and 0.3% cellulose compound/oil mass ratio. The desired amount of model compounds (Table 16) was mixed with NYTRO 10XN oil in HS-vials, sealed, and aged at 130°C for 24 hours in stirred silicone-oil bath before HSGC-FID analysis.

Table 16: Amounts of cellulose model compounds used for ageing tests.

Sample	Oil (mL)	Compound	Cellulose model compound per sample (mg)	
			1.5%	0.3%
1	10	Blank oil	-	-
2	10	Cellobiose	106	21.4

3	10	Glucose	56.3	11.3
4	10	Methyl Glucose	60.5	12.0
5	10	Glucose/Cellobiose (50%/50%)	56.3/106	11.3/21.4
6	10	Glucose/Methyl Glucose (50%/50%)	56.3/60.5	11.3/12.0

Experiments to evaluate the reactivity of glucose with methanol used the same protocol as for lignin model compounds in neutral conditions. D-(+)-glucose was added with a 1.5% glucose molecules/oil mass ratio and methanol was spiked to obtain a concentration of 1500 ng of methanol/g of oil. The desired amount of glucose (Table 17) was mixed with NYTRO 10XN, sealed, and aged at 130 °C for 20 and 24 h before HSGC-FID analysis.

Table 17: Amount of glucose used to test its reactivity with methanol.

Sample	Oil (mL)	Compound	Cellulose model compound per sample (mg)	
			1.5%	
1	10	Blank oil	-	
2	10	Glucose	56.3	

Experiments for hemicelluloses model compounds used the same protocol as for lignin model compounds in neutral conditions. Xylan and galactomannan were added with a 1.5% and 0.3% hemicellulose compound/oil mass ratio. The desired amount of model compounds (Table 18) was mixed with NYTRO 10XN, sealed, and aged at 130 °C for 24 hours before HSGC-FID analysis.

Table 18: Amount of model compounds used for hemicelluloses model compounds ageing.

Sample	Oil (mL)	Compound	Hemicellulose model compound per sample (mg)	
			1.5%	0.3%
1	10	Blank oil		
2	10	Xylan	30.8	6.21
3	10	Galactomannan	40.4	8.12

3) Results and discussion

a) Understanding the experimental approach

Insulation papers in transformers are made of one single component, softwood Kraft pulp. TU Kraft paper also contains some nitrogen-containing additives in minor amounts, typically dicyandiamide, melamine and some other amine-related components. Kraft pulp is made of 3 macromolecules: cellulose (75-80 %), hemicelluloses (15-20 %) and lignin (< 5%). Cellulose is a well-defined linear polymer made of anhydroglucose units (AGU) interlinked with 4-β-glycosidic linkages. Hemicelluloses are a family of cross-linked polysaccharides containing 5

elemental sugars in wood: glucose, mannose, galactose, xylose, arabinose; and lignin is a complex and variable assembly of phenyl propane units (C₉ units), which differ by their sequential arrangement, attached functional groups and bond types. Lignin chemistry has been widely investigated in the frame of chemical pulping and bleaching processes applied on wood and annual plants. The main features of the transformations that happen during these operations are currently rather well known. However, its chemical behavior during thermal ageing processes in oil transformers has not been specifically investigated.

In this study, investigations were carried out with three different approaches:

- First, origin experiments looked into the behavior of some selected model compounds, that represent the main chemical functions in lignin, cellulose and hemicelluloses. For each model compound, methanol production was measured during ageing experiments.
- Secondly, correlation experiments used papers of varying polysaccharides and lignin composition to examine the influence on methanol production.
- Thirdly, methanol partition coefficients were measured to study whether the presence of lignin, or ageing phenomena, modifies the paper affinity for methanol.

b) Origin experiments on model compounds

i) *Lignin model compounds*

The model compounds, presented in Table 19, were selected to simulate different functional groups attached to the aromatic ring: methoxy, hydroxyl, aldehyde and alkyl groups.

Ageing was carried out either in neutral conditions, or with two sets of acidic conditions (Table 20). A first set aimed to produce strongly acidic conditions by adding 0.01 moles of sulfuric acid per mol of model compound. A second set used a lighter acidity to better fit the acidity created during ageing of paper, by introducing varying concentration (from 0.1 mg to 1 mg/g in oil) of a mixture of 1/3 formic acid and 2/3 acetic acid. In total, five types of experiments were carried out.

Results for methanol production from ageing experiments of lignin model compounds are presented in Figure 33 and Figure 39. In all the experiments, blank samples did not produce detectable amounts of methanol or ethanol in neutral or acidic conditions.

Table 19: Lignin model compounds and their chemical structure.

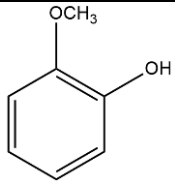
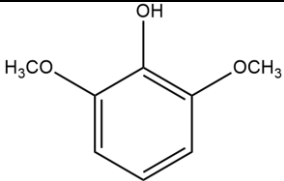
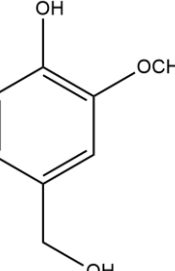
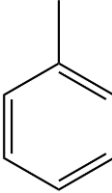
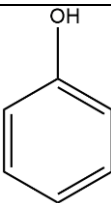
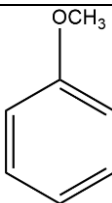
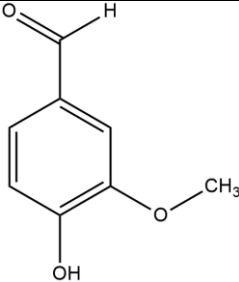
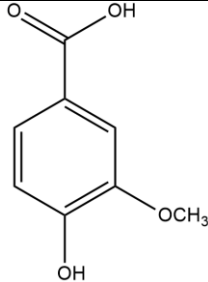
Compound	Structure	Compound	Structure
Guaiacol		Syringol	
Vanillyl Alcohol		Toluene	
Phenol		Anisole	
Vanillin		Vanillic acid	

Table 20: Summary of the experiments carried out on lignin model compounds.

Conditions	Temperatures (°C)	Compounds tested
Neutral	130	Guaiacol, syringol, vanillyl alcohol, toluene, phenol, anisole
Neutral	130	Vanillin, vanillic acid, vanillyl alcohol
Acidic - Sulfuric acid	130	Guaiacol, syringol, vanillyl alcohol, toluene, phenol, anisole
Acidic - Formic and acetic acid	130	Guaiacol
Acidic - Formic and acetic acid	115/125/130	Guaiacol

- Neutral conditions

The first experiments were done using 1.5% and 0.3% mass ratio of model compound to oil without adding acid, *i.e.* in neutral conditions. In these experiments, vanillyl alcohol did not completely dissolve in oil before heating (130°C), phenol and guaiacol needed shaking and

heating (40-50°C) for dissolution, but the other compounds dissolved easily. Syringol samples were done in doublets to verify the reproducibility of the results.

Methanol and ethanol production after ageing is presented in Figure 33a and Figure 34a. To better compare the methanol production between the different tested models, Figure 33b and Figure 34b only shows the methanol production (the ethanol production is removed).

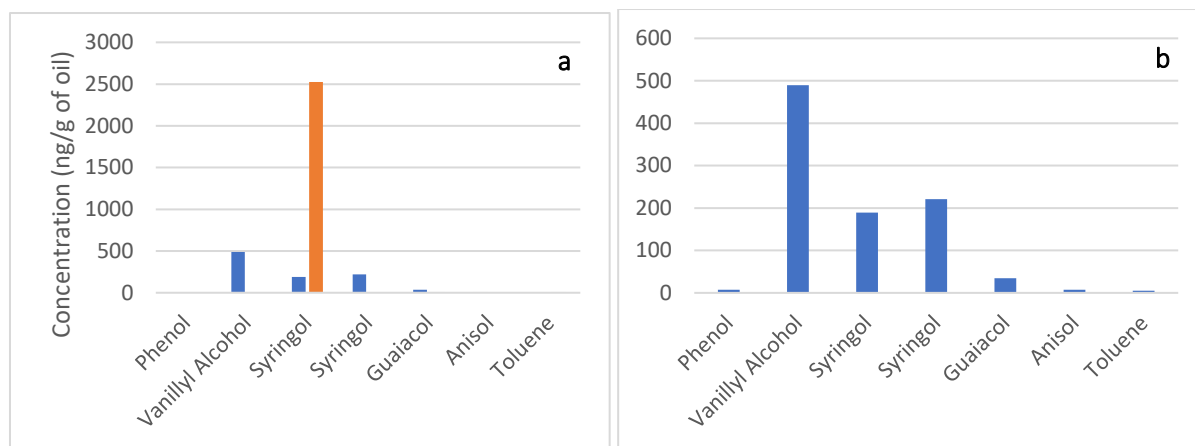


Figure 33: a) Methanol (■) and ethanol (■) b) methanol (■) production from *lignin model compounds* at 1.5% mass ratio to oil, in neutral conditions. Figure b is a closeup of the methanol production of figure a.

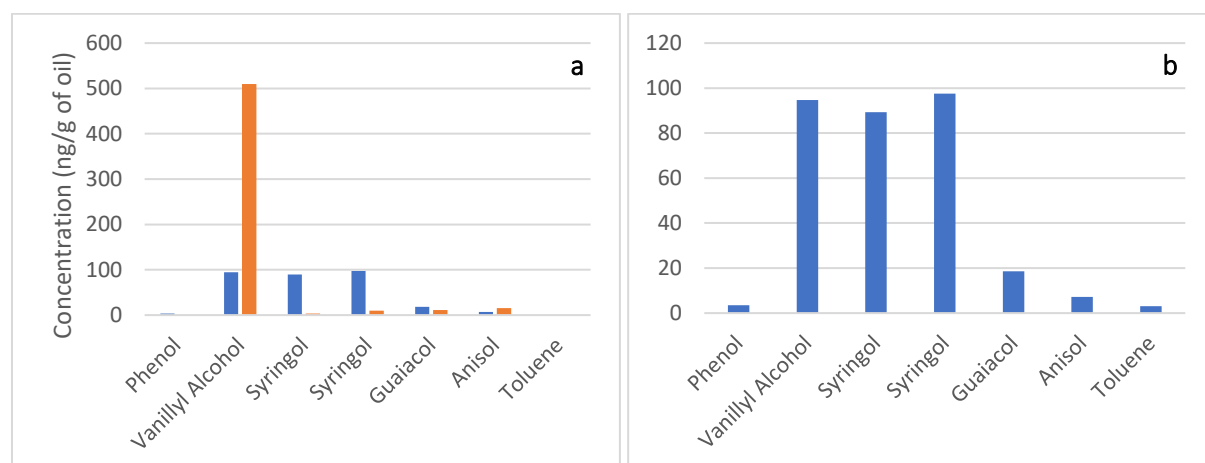


Figure 34: a) Methanol (■) and ethanol (■), b) methanol (■) production from *lignin model compounds* at 0.3% mass ratio to oil, in neutral conditions. Figure b is a closeup of the methanol production of figure a.

First of all, blank samples (without model compound) did not lead to detectable amount of methanol nor ethanol. Thus, the oil alone is not responsible for methanol or ethanol release.

Results of the first set of experiments (Figure 33 and Figure 34), in neutral conditions, showed that syringol, guaiacol and vanillyl alcohol produced significant amounts of methanol. Good reproducibility was found, as seen from the analysis of the syringol samples. Samples with a 1.5% mass ratio produced about 5 times more methanol than samples with a 0.3% mass ratio (except for syringol). Vanillyl alcohol completely solubilized during ageing as the temperature of the oil increased, but it precipitated again once the experiment was over and the oil cooled

down. Ethanol production was important for vanillyl alcohol but minor for the other model compounds.

A second set of experiments (Figure 35), also in neutral conditions, allowed a comparison between vanillin with its reduced form (vanillyl alcohol) and with its oxidized form (vanillic acid). Ageing was performed under identical conditions as previous experiments but 3 weeks after. All compounds tested did not completely dissolved until the vials were added to the heated bath.

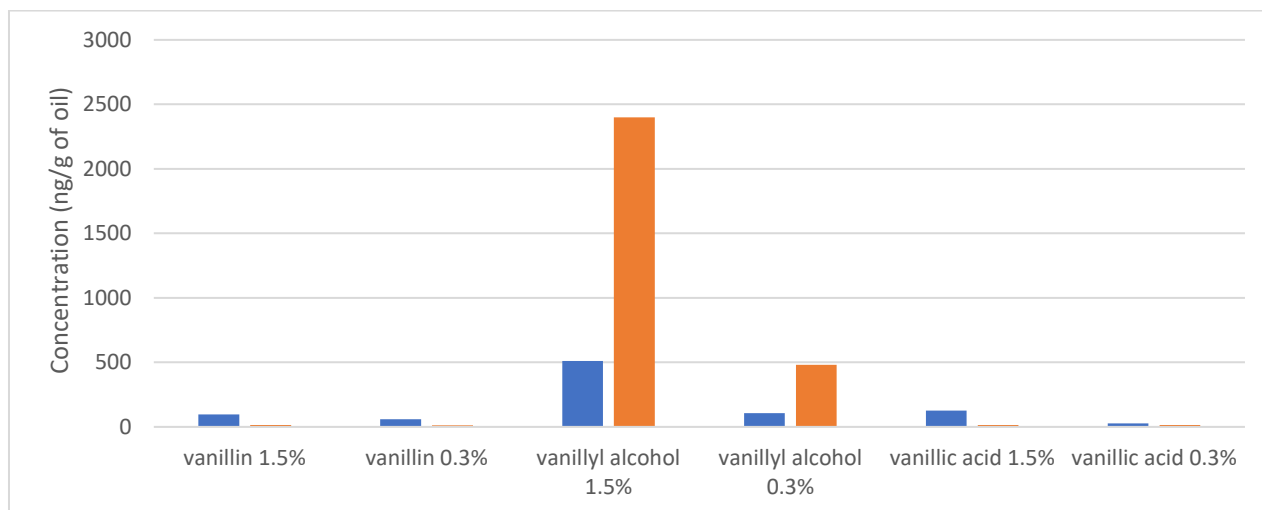


Figure 35: Methanol (■) and ethanol (■) production from vanillin, vanillyl alcohol and vanillic acid, in neutral conditions.

Results for vanillyl alcohol mirrored those of the previous experiments (Figure 35). Again, samples with 1.5% mass ratio produced around 5 times more methanol than samples with 0.3% mass ratio. While all samples completely solubilized during ageing, vanillyl alcohol precipitated once the experiment was over and the oil cooled down. And again, only vanillyl alcohol produced significant amounts of ethanol.

- Acidic conditions

Then, after following an identical protocol, strong acids were spiked into each vial. The addition of sulfuric acid to the samples containing oil and model compounds changed the color of samples (even for the blank oil) while samples without acid addition did not show any color change. All samples became darker after ageing under acidic conditions. Vanillyl alcohol solubility was similar as in neutral conditions. Methanol and ethanol productions are presented in Figure 36 and Figure 37 (figures (a): methanol and ethanol, figures (b): only ethanol).

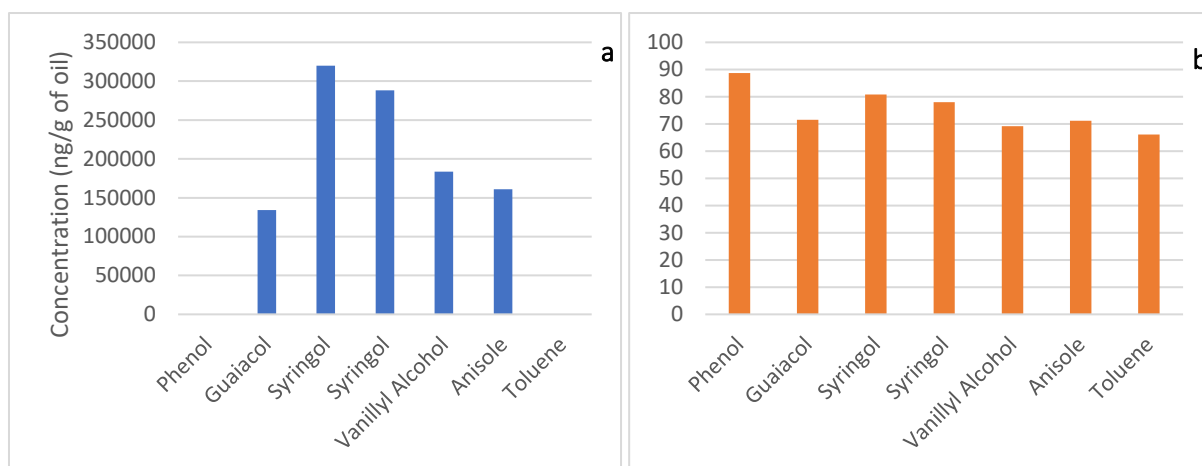


Figure 36: a) Methanol (■), b) ethanol (■) production from lignin model compounds at 1.5% mass ratio to oil, in strong acidic conditions (sulfuric acid).

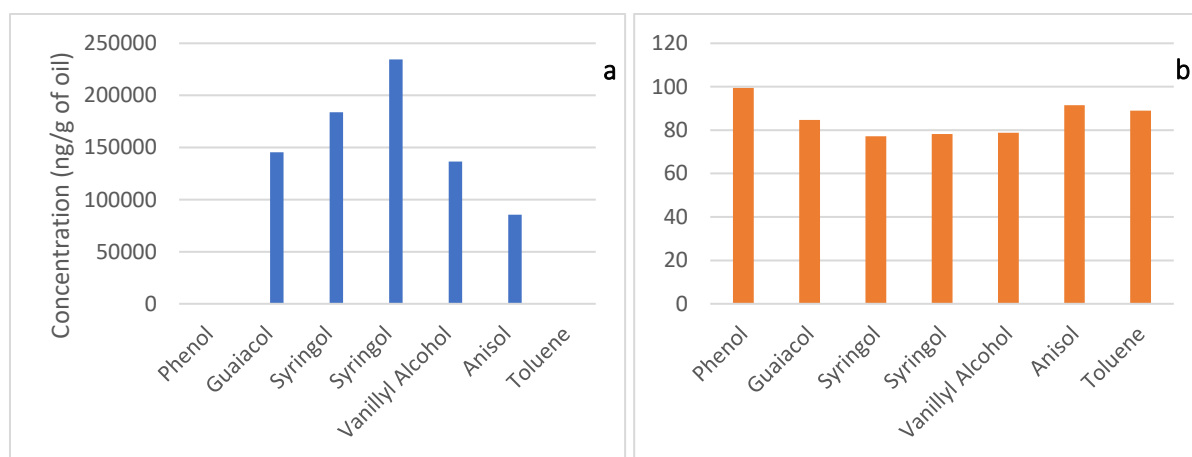


Figure 37: a) Methanol (■), b) ethanol (■) production from lignin model compounds at a 0.3% mass ratio to oil, in strong acidic conditions (sulfuric acid).

Results in strong acid conditions show that methanol production is extremely important for guaiacol, syringol, vanillyl alcohol and anisole with two orders of magnitude higher than in neutral conditions (Figure 33 and Figure 34). Syringol produces around twice as much methanol as other model compounds. In contrast to methanol, ethanol production was small and lower than in neutral medium, but it was present for all samples. It can be noticed that duplication of syringol 1.5% experiments gave similar results, and that methanol production was similar between samples with a mass ratio of 0.3 and 1.5%.

Trials were also conducted in weak acid conditions. Methanol production is presented in Figure 38 and Figure 39. Each experiment was done with two blank references, one with only oil and one with oil and acid. In all cases, methanol was not detected.

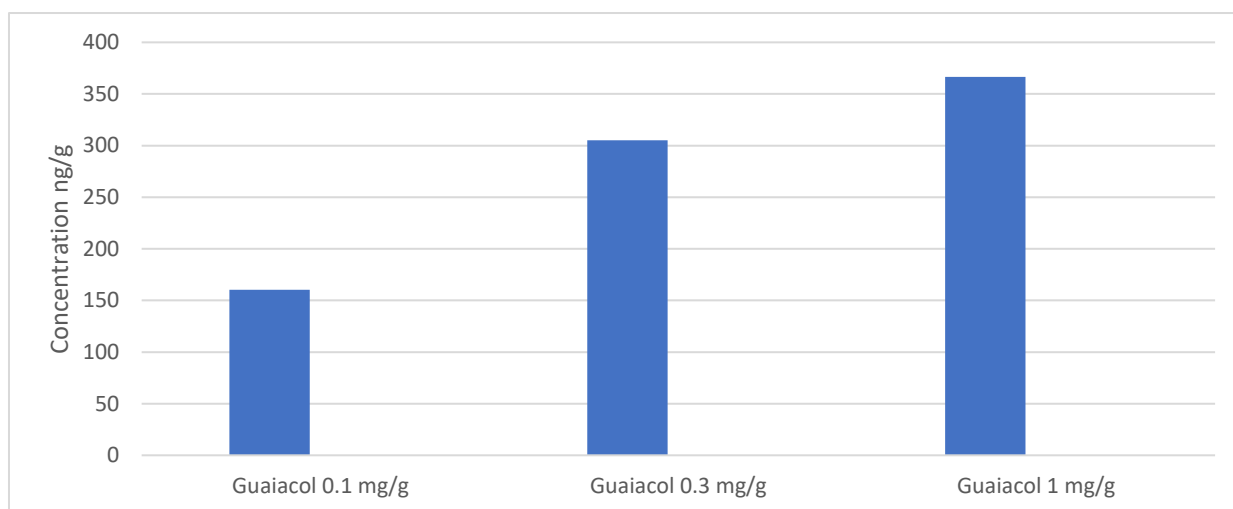


Figure 38: Methanol production from guaiacol after 24 hours at 130°C. Weak acidic mixture made of 1/3 formic acid and 2/3 acetic acid, at 0.1, 0.3 and 1 mg acid/g of oil.

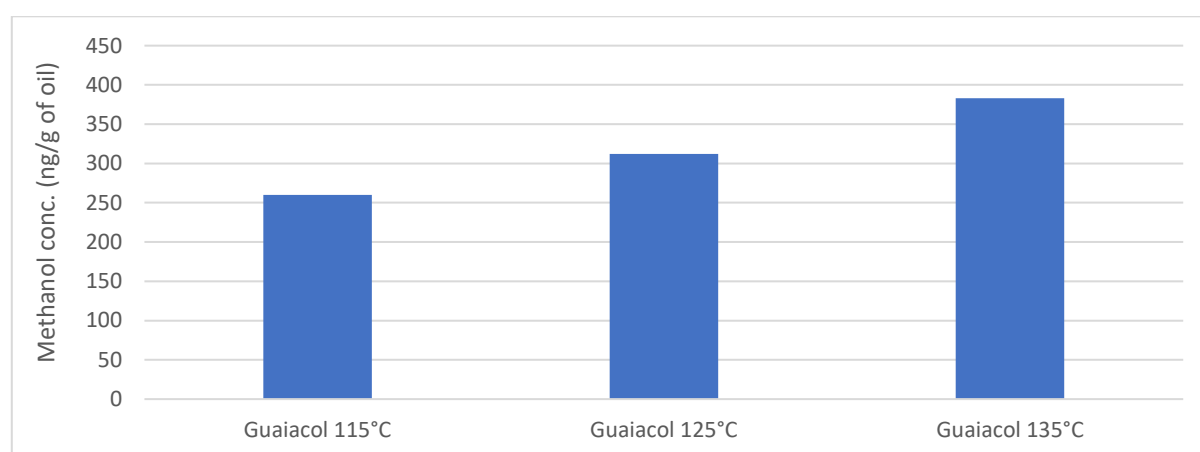


Figure 39: Methanol production from guaiacol at varying temperatures (24 h ageing at 115, 125 and 130°C). Weak acidic mixture made of 1/3 formic acid and 2/3 acetic acid at 1 mg of acid per g in oil.

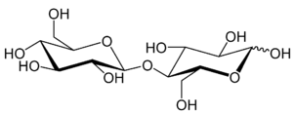
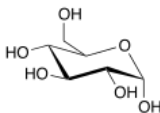
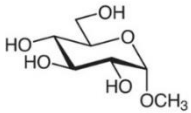
Experiments (Figure 38 and Figure 39) with a weak acid mixture (formic acid: acetic acid at a weight ratio of 1:2) were done with guaiacol only, at a 1.5% mass ratio in oil, varying the amount of weak acid mixture between 0.1 to 1 mg/g of oil. In samples with weak acids (formic and acetic acid) a change of color was barely noticeable. The second set of experiments (Figure 39) using guaiacol in acidic conditions investigated the effect of the temperature (115, 125 and 135°C). Each experiment was done with two blank references, one with only oil and the other with oil and acid; none produced detectable amounts of methanol.

Results show that methanol production increased with temperature and acidity (Figure 38 and Figure 39). Still, compared to neutral conditions, weak acidic conditions and increased temperature only multiplied the methanol production by a factor between 1.5 to 3, which can be compared to the two orders of magnitude obtained with sulfuric acid. It was also noticed that under acidic conditions, all samples became darker after ageing.

ii) Cellulose model compounds

In these experiments, the aim was to test the correlation between the methanol production and the degradation of some cellulose model compounds. Three model compounds were tested, cellobiose (the repeating unit of glucose), glucose (as base monomer, and also reaction byproduct of the chain scission of cellobiose) and methyl glucose (Table 21). An emphasis was placed on methyl glucose, the methylated form of glucose. Indeed, methylation of the C1 carbon of glucose suppresses the reactivity of the reducing end group (aldehyde group) of the molecule, which potentially inhibits sugar ring opening. All experiments were done under neutral conditions. Some experiments were carried out with an initial addition of methanol.

Table 21: Cellulose model compounds and their chemical structure.

Compound	Cellobiose	Glucose	Methyl glucose
Structure			

- Without adding methanol

In this first set of experiments, the three cellulose model compounds were compared, without addition of extra methanol (Figure 40). Trials with a mix of two model compounds have been also carried out.

It was impossible to completely solubilize cellobiose, but glucose immediately dissolved and methyl glucose dissolved with some shaking. For the purpose of this experiment, it was not necessary that they completely dissolve in any case.

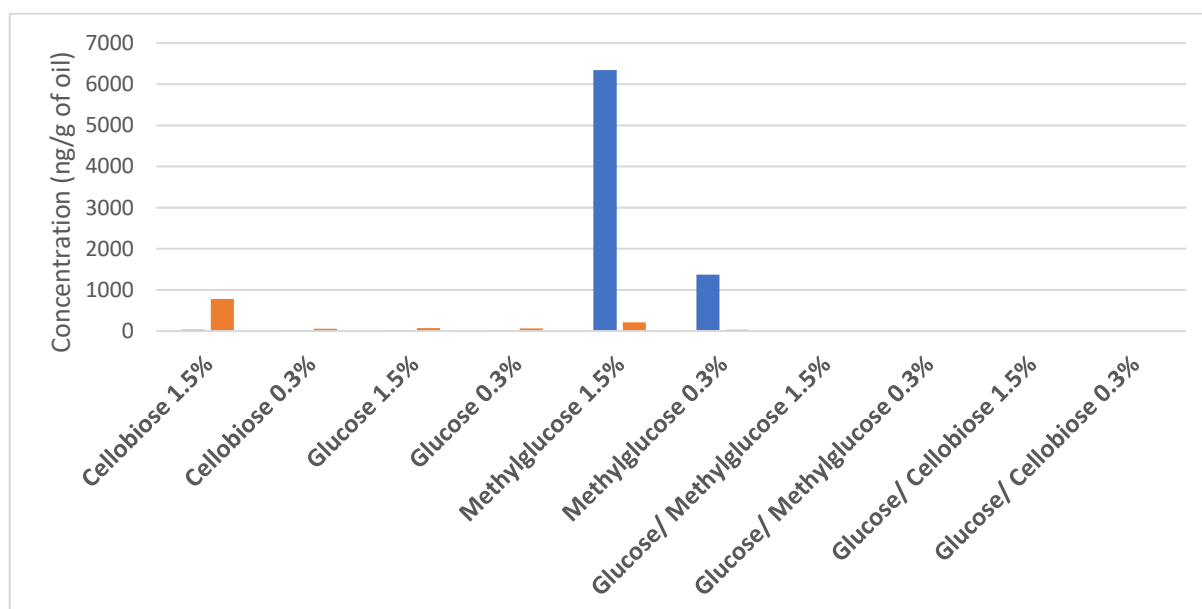


Figure 40: Methanol (■) and ethanol (■) production for cellulose model compounds at 0.3% and 1.5% by weight in oil.

Results show that methanol production is only detectable in a significant amount from the ageing of methyl glucose (Figure 40). A minor quantity was also detected with cellobiose, at the highest dosage. Methyl glucose at 1.5% mass ratio produced about 5 times more methanol than at 0.3%. Even during ageing, cellobiose never completely dissolved in oil.

- With an addition of methanol

Since methanol was not generated from glucose alone, and only very slightly generated from cellobiose, the possible reaction of glucose with methanol was investigated. A second set of experiments was carried out, where an oil solution containing glucose was spiked with methanol. Each sample was contrasted with a reference vial aged under the same conditions where methanol was also spiked. The aim was to study whether methanol could react with glucose in the present medium, since this possible reaction is mentioned in the literature [34].

Results in Figure 41, repeated twice, show that methanol concentration slowly declined in samples containing glucose, while methanol kept at the same concentration in samples without glucose, spiked with the same amount of methanol. Compared to the reference samples of methanol, 51.5% of methanol was consumed after 24 hours; the concentration of methanol went from 1600 ng/g to 776 ng/g of oil.

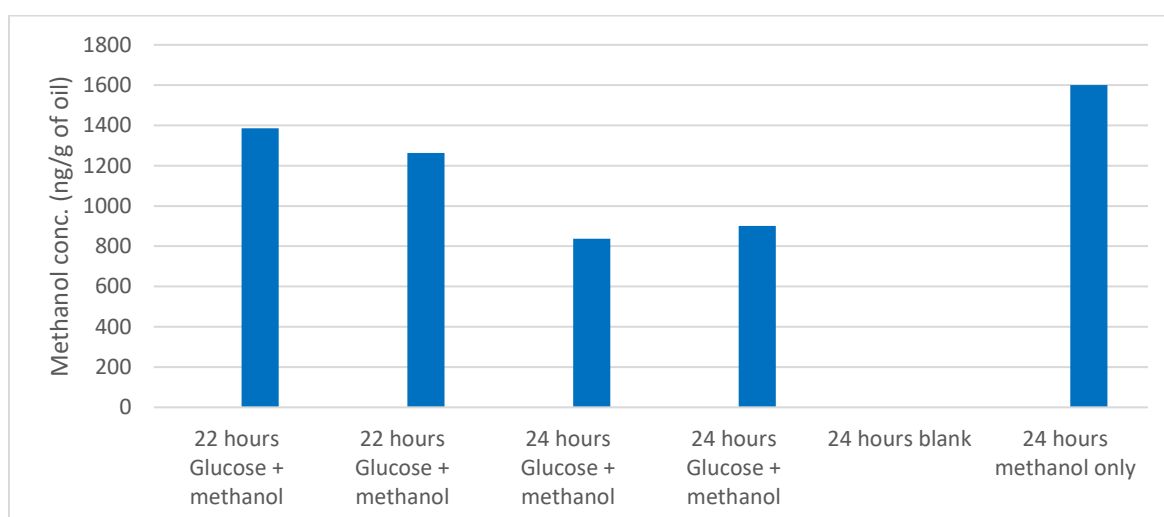


Figure 41: Methanol concentration in vials containing glucose at 1.5% by weight in oil. Each vial was spiked at the beginning of experiment with 1600 ng methanol/g of oil.

iii) Hemicelluloses model compounds

Xylans and galactoglucomannans samples were investigated under identical experimental conditions as the ones for lignin model compounds, under neutral conditions. In the form of white powder, they were not solubilized in oil. No detectable amount of methanol was obtained with these two kinds of hemicelluloses model compounds.

iv) Discussion of results

Experiments on lignin model compounds aimed to understand the origin of methanol production by lignin. Results show, under neutral conditions, that the only compounds that produce significant amount of methanol are the compounds that contained a methoxy group. The only exception is anisole whose methoxy group is not activated by any substituent on the aromatic ring, and therefore much more stable. This is also confirmed in acidic conditions where sulfuric acid catalyzes the acid hydrolysis of methoxy groups. In this case, methanol production was proportional to the number of methoxy groups per aromatic ring, regardless of the activating or deactivating effects coming from other substituents (Figure 42). Since electrotechnical papers are manufactured with unbleached softwood Kraft pulp, in which the residual lignin (at a content of about 3 to 5%) is composed of guaiacyl units (containing 1 MeO per C6 unit), methanol could be potentially generated from lignin for a very long release time during long-term ageing, due to the progressive increase of the acidity of paper (partly but not fully dissolved in the oil), which in turn increases the rate of methanol production.

The following calculation provides an evidence of the latter assertion:

Assuming paper contains 4% of guaiacyl lignin (with an average molar mass of 180 g/mol), 1g of paper contains $0.04/180 = 2.22 \times 10^{-4}$ mol = 222 μ mol of MeO unit.

Looking at Figure 47, about 6 μ g of methanol per g of oil was generated during the total ageing time (240 h) at 130°C. Since paper samples were placed in vials at a paper:oil ratio of 0.4 g paper:10 mL of oil, the oil:paper ratio is 25 mL/g paper. Thus, the amount of methanol generated is equal to $6 \times 25 \times 0.8 = 120$ μ g of methanol per g of paper (assuming an oil density of 0.8 g/mL). This corresponds to $120/32 = 3.75$ μ mol methanol/g paper (molar mass of methanol is 32g/mole). Thus, comparing the amount of generated methanol (3.75 μ mol) and the amount of guaiacyl units (222 μ mol) in one gram of paper, only $3.75/222 \times 100 = 1.7\%$ of guaiacyl groups in lignin were demethylated. This value is probably an overestimation of the released methanol by lignin, since in the same ageing conditions (Figure 46 and Figure 47), about 1/6th of the methanol would come from polysaccharides degradation since BKP paper samples produced around 1/6th of the methanol that UKP produced under similar conditions, this difference can only attributed to lignin

To conclude, the above numbers show that lignin exhibits an important methanol production, and thus, a potential methanol release during a very long time, compared to methanol production from cellulose depolymerization.

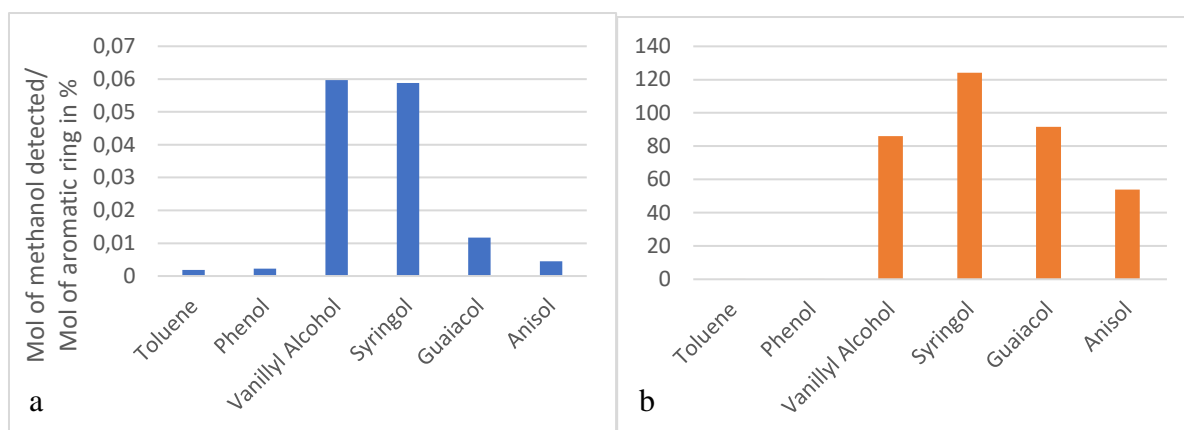


Figure 42: Molar ratio between the number of methanol molecules detected on each sample and the number of aromatic groups detected after 24h at 140°C, shown as a percentage. Results are shown under neutral (a) and acidic (b) conditions. Y scale: represents the mols of methanol detected in the oil against the mols of aromatic rings introduced in the oil.

Further, weak acid experiments confirmed that even a small increase in acidity affects greatly the methanol production.

The amount of methanol produced during ageing at three different temperatures was quantified and used to calculate the reaction rate constant and the activation energy of the reaction. Results are presented in Figure 43.

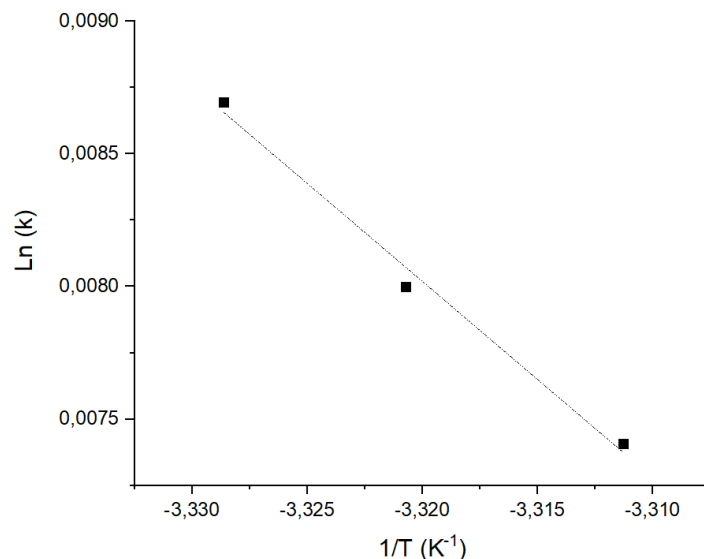
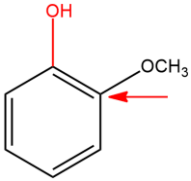
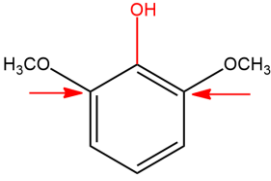
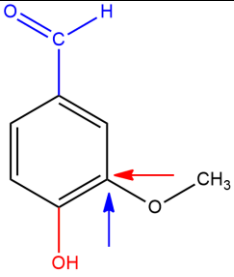
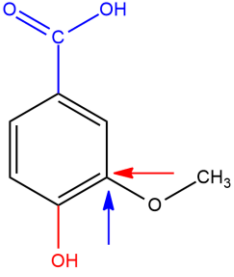
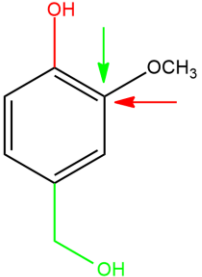


Figure 43: The Arrhenius expressions of the constant production rate table is visible below for methanol production from guaiacyl ageing after 24 hours at 115, 125 and 135°C. The linear regression has a curve of $y = -13.411x - 3.2125$ with $R^2=0.9907$.

The activation energy of the reaction of methanol production was calculated from the advancement of the reaction after 24 hours at 115, 125 and 135°C. It was calculated to be 111 kJ/mol, close to the activation energy for the acid hydrolysis of cellulose, given to be around 109 kJ/mol in most published papers.

Considering the formula of the selected lignin model compounds, it is shown that for aromatic groups with multiple substitutions, inductive effects and donor-acceptor effects from the different substituents can affect methanol production by activating or deactivating the reactions of methoxy groups during the acid hydrolysis. The selected models exhibited three different functional groups, with varying inductive effects (Table 22):

Table 22: Functional groups in lignin model compounds.

Chemical group substituted on the C6	Type of effect and position
Hydroxyl group (HG)	Strong – donor (activating) – ortho/para
Methoxy group (MG)	Medium – donor (activating) – ortho/para
Alkyl group (AG)	Weak – donor (activating) – ortho/para
Carbonyl groups (CG)	Medium – acceptor (deactivating) – meta
Model compound	Chemical function
Guaiacol	 <p>Strong donor Ortho/para</p>
Syringol	 <p>Strong donor Ortho/para</p>
Vanillin	 <p>CG: Medium acceptor Meta HG: Strong donor Ortho/para</p>
Vanillic acid	 <p>CG: Medium acceptor meta HG: Strong donor ortho/para</p>
Vanillyl alcohol	 <p>HG: Strong donor Ortho/para AG: Weak acceptor Meta</p>

The effect of the functional groups present on lignin are found to be in accordance with the experimental results of methanol release. For instance, in the case of syringol, the two methoxy groups in syringol are strongly activated by the hydroxyl group present on the aromatic ring, this means they are more likely to be cleaved by acid hydrolysis. Methanol release for guaiacol is not half the value of syringol, suggesting other factors are present. In vanillic acid and vanillin, a carbonyl group (carboxylic acid and an aldehyde, respectively) deactivates the methoxy group while nothing strongly deactivates methoxy groups in vanillyl alcohol, this difference explains why vanillyl alcohol produced higher amounts of methanol. In strongly acidic conditions, (Figure 42b) where acid hydrolysis is catalyzed by sulfuric acid, methanol production was directly proportional to the number of methoxy groups per aromatic rings. Results show that syringol, with its two methoxy groups per C6, produced around twice more methanol than anisole, guaiacol, and vanillyl alcohol which have one methoxy substituent per C6. Toluene and phenol which do not bear methoxy substituent did not produce methanol even under acidic condition, further confirming that the methoxy group is the sole group that forms methanol. Vanillin, vanillic acid also followed inductive and donor-acceptor effects with C=O or COOH that deactivated the methoxy group for vanillin and vanillic acid, and therefore a lowered methanol production compared to vanillyl alcohol (Table 22).

Regarding ethanol, it was only produced in significant quantity by vanillyl alcohol (Figure 33 and Figure 34) since it is the only model compound that contains a substituent long enough to be cleaved into ethanol. In acidic conditions, ethanol detection is very low, suggesting that the produced ethanol is consumed in reactions to generate acids (with the postulate that it oxidizes to form carboxylic acids).

Our observations on the two lignin-free pulp substrates (CL and BKP) confirmed that carbohydrates in pulps also generate methanol (Figure 45, Figure 46 and Figure 47), as reported by Jalbert and coworkers [8]. However, the two cellulosic model compounds in Figure 40, cellobiose and glucose, did not produce any methanol after ageing at 130°C for 24 h. The literature reports that methyl glucose is synthesized from a reaction between glucose and methanol in acidic conditions [34] visible below in Figure 44:

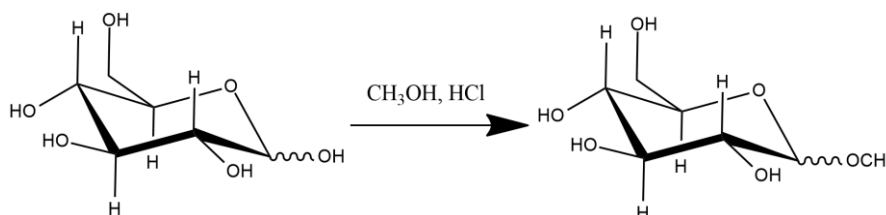


Figure 44: Schematic representation of the methylation of glucose with methanol. Extracted from Heleferich *et al.* [34].

It is thus suggested that under the ageing conditions in oil, this reaction also happens with glucose, and that it would also happen with cellobiose which possesses the same terminating reducing unit as glucose. This is also in line with the observation of Jalbert *et al.* [8, 20] who did not find any methanol production during ageing of D-(+)-glucose. Conversely, methyl glucose doesn't have a reducing unit that could react with methanol, and therefore, all the methanol it produces isn't lost in a methylation reaction with glucose. It was then suspected that D-(+)-glucose and cellobiose did produce methanol (probably in similar quantities to methyl glucose), but it was not detectable since it reacted with the open ring carbohydrates. It is also interesting to notice that under identical equimolar and neutral pH conditions (Figure

40), methyl glucose produced about ten times more methanol than lignin model compounds, showing an easier reaction regarding carbohydrate degradation when compared to demethylation of the lignin aromatic rings in the same conditions.

This result leads to the fact that, in paper, reducing end aldehyde groups might consume some of the methanol that is produced by lignin demethylation or carbohydrates depolymerization. This should at least partly contribute to the relationship between cellulose depolymerization and methanol production. However, such contribution in the initial phase of cellulose depolymerization should be rather minor, due to the high cellulose DP_v (and thus, low number of chain end reducing units). Its contribution might increase at lower cellulose DP_v, when the accessibility and the number of chain end reducing groups is rising. Then methanol consumption increases also.

To further understand the reaction between glucose and methanol under these conditions, an equimolar amount of glucose and methyl glucose was aged under the same conditions as before (Figure 40). Results showed that methanol was undetectable. Since glucose or methyl glucose are monomers, none of the methanol molecules originated from depolymerization. Another test under the same conditions consisted in directly spiking methanol in vials containing glucose. It was found that the concentration of methanol rapidly declined. The only explanation is that methanol reacts with glucose. This proves that methanol produced from demethylation is consumed by glucose.

Experiments on hemicelluloses model compounds were carried on xylans and galactomannans. Neutral conditions and the same procedure as described for the other model compounds were applied. No methanol was detected in this case. It can be hypothesized that given the rather short size of the polymer chains of hemicelluloses, about 100 to 200 repeating units, compared to 1203 for UKP, there are 5 to 6 times more repeating end groups for every repeating unit of cellulose. Again, in literature, methanol was not detected with mannan, although there was some methanol production for xylan, which was not observed in this study. The heterogenous nature of xylan structure can change depending on the type of wood it was sourced from; this can account for a difference in the chemistry and structure that could change methanol production between the samples in this study and those from literature.

c) Correlation experiments paper samples

Methanol production from paper pulp samples was also studied. Pulps with different compositions were selected to represent each of the main components of paper: bleached cotton linters pulp (pure cellulose), softwood bleached Kraft pulp (cellulose and hemicelluloses), and softwood unbleached Kraft pulp (cellulose, hemicelluloses and lignin). The same amounts of samples were aged in identical conditions, at 130°C with long ageing times (1 to 13 days) to compare the methanol production of each sample.

i) Ageing of cotton linters (CL)

As bleached cotton linters pulp is composed of pure cellulose, its behavior was particularly interesting. It was aged at 130°C for 7 days; a shorter ageing time was chosen because the initial DP_v of cotton linters was 883, which is lower than those of UKP and BKP, *i.e.* 1205 and 950

respectively. The relationship between methanol production and change of cellulose DPv is shown on Figure 45.

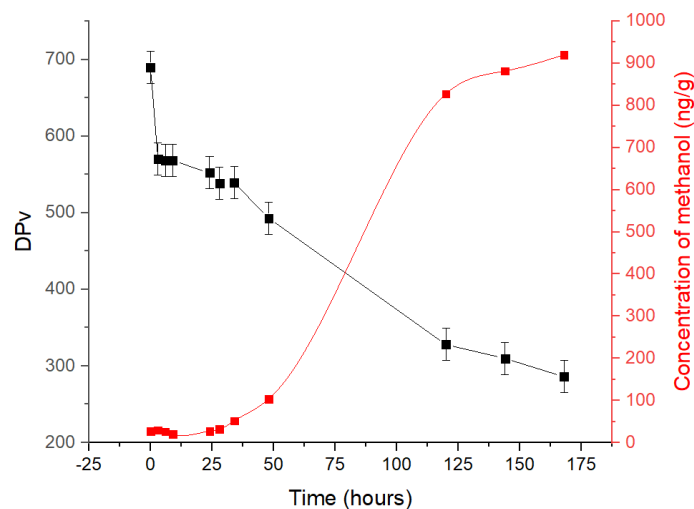


Figure 45: Evolution of methanol concentration (■) in vials and the DPv (■) of cotton linters (CL) samples aged till to 168 hours at 130°C.

Results show that ageing can be divided in three phases. In the first few hours a sharp decline of cellulose DPv is observed with no corresponding production of methanol. A brief stagnation is followed, after about 30 h, by the appearance of a linear relationship between methanol formation and cellulose depolymerization.

ii) Ageing of BKP

As BKP is composed of cellulose and hemicelluloses, the role of hemicelluloses should be visible by contrasting these results to those of cotton linters. BKP was aged at 130°C for 10 days. The relationship between methanol production and change of cellulose DPv is shown in Figure 46.

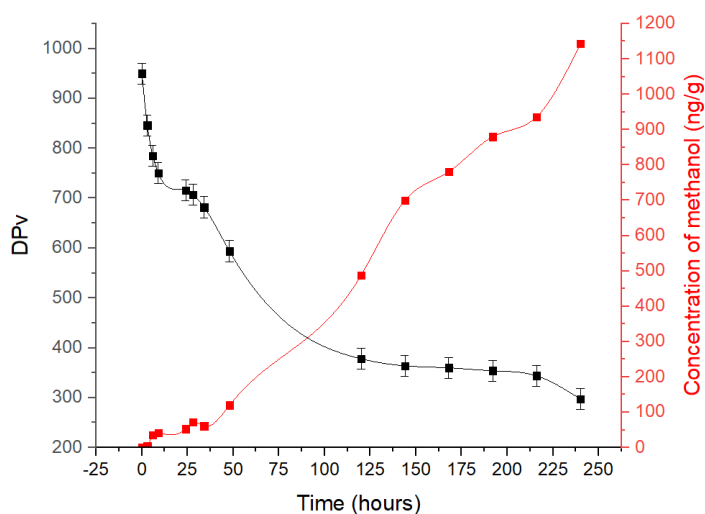


Figure 46: Evolution of methanol concentration (■) in vials and corresponding cellulose DPv (■) of BKP samples aged till to 240 hours at 130°C.

Results show a rather similar pattern at the beginning of ageing, as compared to cotton linters pulp, since in the first part, a sharp decrease of cellulose DP_v is observed with almost no formation of methanol. Then, in the following part, cellulose DP_v stagnation without formation of methanol is again observed, but for a longer period of time. Finally, the more or less linear relationship between methanol concentration and cellulose depolymerization only starts after about 50 h, but it is followed by a period of cellulose DP_v stagnation (or at least, a much slowest drop of cellulose DP_v), while methanol production still increases at a rather similar rate.

iii) Ageing of UKP

As UKP is composed of cellulose, hemicelluloses, and lignin, the ageing behavior of this substrate is to be contrasted to the ageing behavior of BKP. The same kind of curves were plotted, as shown in Figure 47.

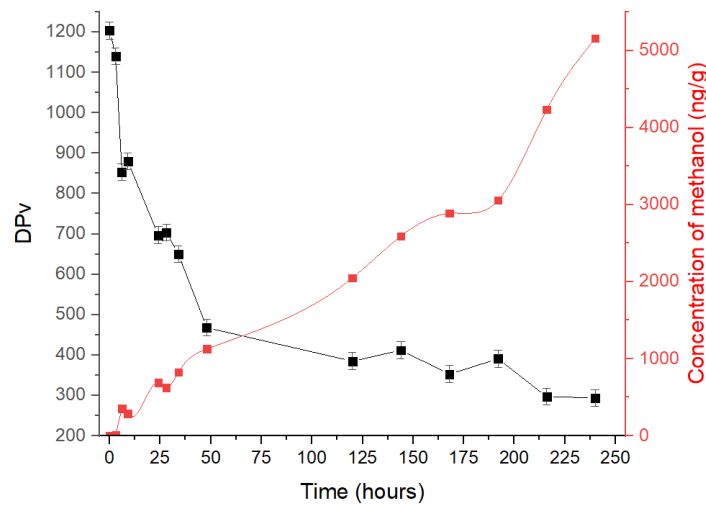


Figure 47: Evolution of methanol concentration (■) in vials, and corresponding cellulose DP_v (■) of UKP samples aged till to 240 hours at 130°C.

Results for unbleached Kraft pulp show a very different behavior. No initial plateau for methanol formation is observed, and an almost immediate linear relationship is visible between methanol formation and cellulose DP_v decay. Rate of methanol production at given cellulose degradation is also much higher than for the BKP or CL cases, at all stages of the degradation: about 2 to 3 times more at the early stages, and until about 5 times more at the later stages.

iv) Discussion of results

Trials with papers scaled up this approach by providing direct quantification of methanol production from actual paper with and without lignin. Here the amount methanol produced per gram of paper is contrasted with the average number of cellulose chain scission calculated from Equation 7 below:

$$\text{Average number of chain scission} = DP_{n \text{ initial}} \times \left(\frac{1}{DP_{n(t)}} - \frac{1}{DP_{n \text{ initial}}} \right) \quad (7)$$

where: DP_n(t) = cellulose DP_n value after paper ageing time t; DP_{n, initial} = initial cellulose DP_n before paper ageing.

Under the assumption that the ratio DP_v/DP_n keeps constant along the depolymerization process during paper ageing, this formula can be re-written in Equation 8 as follows:

$$\text{Average number of chain scission} = DP_{v \text{ initial}} \times \left(\frac{1}{DP_{v(t)}} - \frac{1}{DP_{v \text{ initial}}} \right) \quad (8)$$

In Figure 48, the relation between methanol production and the average number of scissions per chain is plotted. It is seen that the rate of methanol production highly depends on the pulp substrate. UKP produced, on average, about five times more methanol than BKP or CL pulp. Such differences can only be attributed to lignin present in UKP.

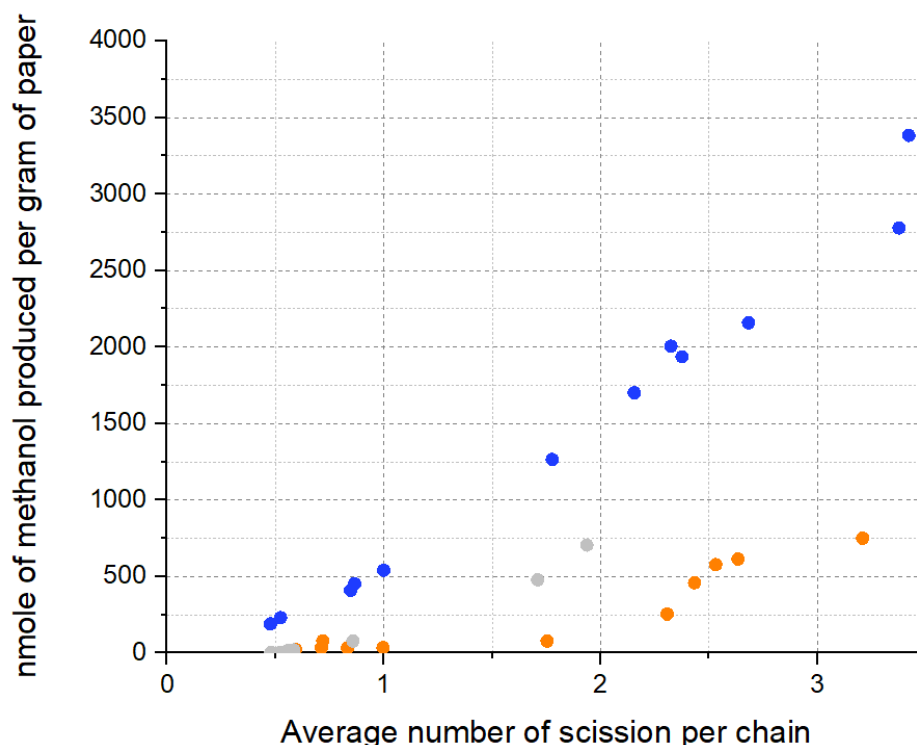


Figure 48: Methanol production from different cellulosic samples versus average number of scissions per chain; Cotton wads (●), unbleached (●) and bleached (●) Kraft paper samples during accelerated thermal ageing in oil (130°C; 0 to 13 days), results are given in nmole of methanol detected per chain scission.

These results not only show that lignin plays an important role in methanol production, but also that its role tends to increase during paper ageing. Indeed, it is shown in Figure 48 that, while methanol production keeps rather small for the lignin-free substrates (BKP and CL) until a chain scission number of about 2, it increases continuously and linearly for UKP since the beginning of ageing.

It was shown previously that the molar amount of methanol release by guaiacyl lignin (G-lignin), when reaching paper end-of-life (cellulose $DP_v \approx 200$), was of the order of 1.7% of the total molar amount of lignin aromatic G-units. Therefore, since 98.3% of G-units still have a methoxy group that could be cleaved, the potential for methanol production by lignin in UKP looks very important.

Furthermore, it is observable that a linear methanol production starts at the beginning of ageing time in the case of UKP. Conversely, the formation of methanol is delayed for CL, and even more for BKP. It can be postulated that this is related to the number of chain ends reducing groups that are present in each paper. Once chain-end groups have all reacted with the generated methanol, the latter accumulates. New chain end groups are formed along depolymerization, but nevertheless, this produces approximately a linear accumulation of methanol in the oil. Given that UKP has a high production of methanol coming from lignin, methanol can quickly overwhelm the initial chain-end reducing groups of polysaccharides. Because of the presence of hemicelluloses chains in BKP (containing chain-end reducing groups), methanol accumulation arose later in BKP than in CL pulp. Moreover, the raise of the acidity of the medium should play a double role: it will increase methanol production from lignin demethylation, and catalyze polysaccharides chain-end group reactivity with methanol.

d) Partition coefficient experiments

Paper-oil samples have different interactions with the various by-products generated during ageing. Mineral oils in transformers are not polar, whereas polysaccharides and lignin in the cellulosic substrate are polar. The difference in their polarity is responsible for partitioning of ageing products between oil and paper [5]. Experiments reported here, compared UKP, BKP, and Cotton Linters (CL) pulps, to establish whether paper composition could also play a role in the air/solid/liquid partition coefficient. Further experiments were also carried out to study the effect of ageing on the partition coefficient. For all the partition coefficient experiments, methanol was spiked in samples that contained oil and paper. Methanol partition between oil and paper is not instantaneous so 48 hours were waited before analysis for all samples since literature showed that an equilibrium between the methanol in oil and the methanol in paper was reached after 48 hours [13].

i) Effect of methanol concentration and paper composition

0.4 g of paper sample was dried at 105°C for 24 h and then, impregnated in oil. A mixture of methanol and ethanol was then spiked in each vial to obtain a concentration ranging from 0 to 24 µg of methanol and ethanol per gram of oil. For the same alcohol concentration, results in vials with oil and paper were then contrasted with vials with oil only. UKP, BKP and CL samples were tested in parallel. Oil/substrate partition coefficients of methanol and ethanol for unaged UKP, BKP and CL are presented in Figure 49 and Figure 50:

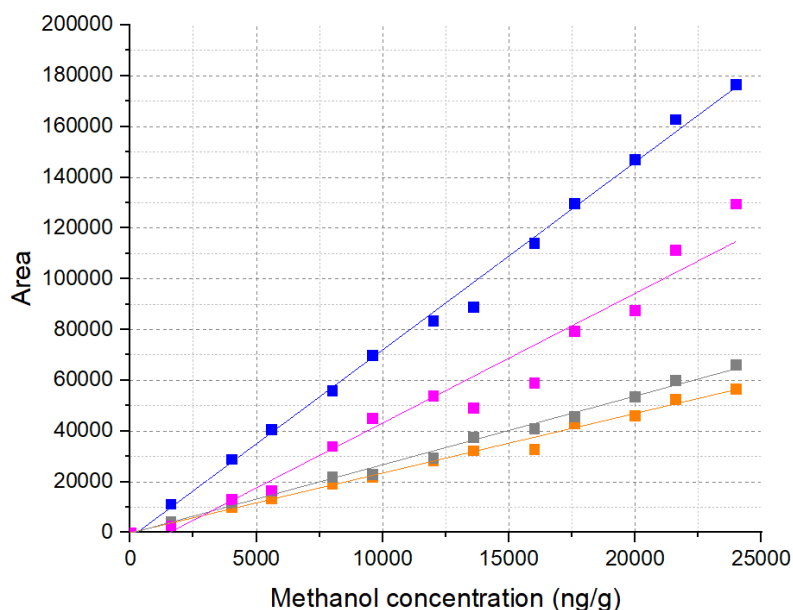


Figure 49: *Oil/substrate partition coefficient of methanol for unaged UKP (■), BKP (■), and cotton linters pulps (■). Methanol/ethanol was spiked at different concentrations. Oil without paper was also spiked with methanol/ethanol (■). Y-scale: the area corresponds to the calculated area of methanol's signal detected by a Flame Ionization Detector. X-scale: the concentration of the spiked methanol in the oil.*

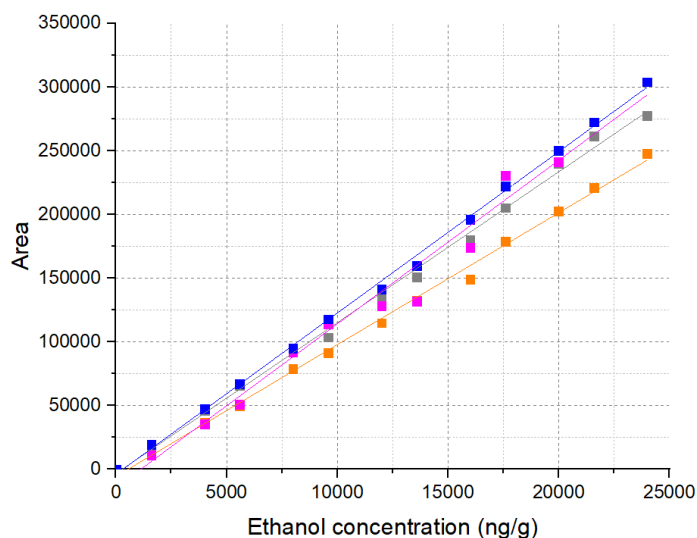


Figure 50: *Oil/substrate partition coefficient of ethanol, for unaged UKP (■), BKP (■), and cotton linters pulp (■). Methanol/ethanol was spiked at different concentrations. Oil without paper was also spiked with methanol/ethanol (■). Y-scale: the area corresponds to the calculated area of ethanol's signal detected by a Flame Ionization Detector. X-scale: the concentration of the spiked ethanol in the oil.*

Samples with the same amount of spiked methanol showed much lower concentrations of methanol in oil when paper was present, this is because a part of the oil was absorbed by paper; therefore, creating a partition coefficient.

In the case of methanol (Figure 49), results show that among the two wood pulps, UKP has a slightly higher affinity for methanol compared to BKP. But the difference is small when

compared to CL pulp which has a much lower affinity for methanol. Comparing the different slopes, the calculated oil/paper partition coefficient for UKP is about 32-33%; then it is 35-36% for BKP, and 61-64% for cotton linters pulp. The percentage of methanol that remained in the oil, and that was therefore not absorbed by papers, was calculated by dividing the detected amount of detected methanol in the oil for samples with paper samples by the amount of methanol detected in the oil for samples without paper. Methanol detected in the oil for samples with paper represents the methanol that did not migrate into paper while methanol in oil only samples represents the total amount of methanol added to each vial.

In the case of ethanol (Figure 50), a less polar molecule than methanol, a lower affinity to paper is observed, as compared to methanol. UKP has a slightly higher affinity for ethanol than the two other substrates, which can be caused by the presence of lignin in UKP. About 10% of ethanol is absorbed in UKP, while BKP and CL absorbed about 1% of the ethanol spiked in oil. These values were calculated in the same manner as for methanol.

ii) Effect of ageing

The effect of ageing on the partition coefficient was more difficult to test. Indeed, in a direct test in which methanol is spiked before ageing the sample, the methanol production during ageing interferes. Therefore, to avoid interference from methanol and water produced during ageing, it was decided to age the sample first, then clean it by Soxhlet extraction with pentane, and finally proceed to a spike test after new oil introduction, following the same testing procedure as without ageing. This ensures that only changes in the chemical structure of paper can affect the partition coefficient.

Only UKP sample was tested at different ageing times. All samples were spiked with the same concentration of methanol in oil (5.6 $\mu\text{g/g}$). Oil/substrate methanol partition coefficient of UKP, as function of the cellulose DPv after thermal ageing is presented in Figure 51.

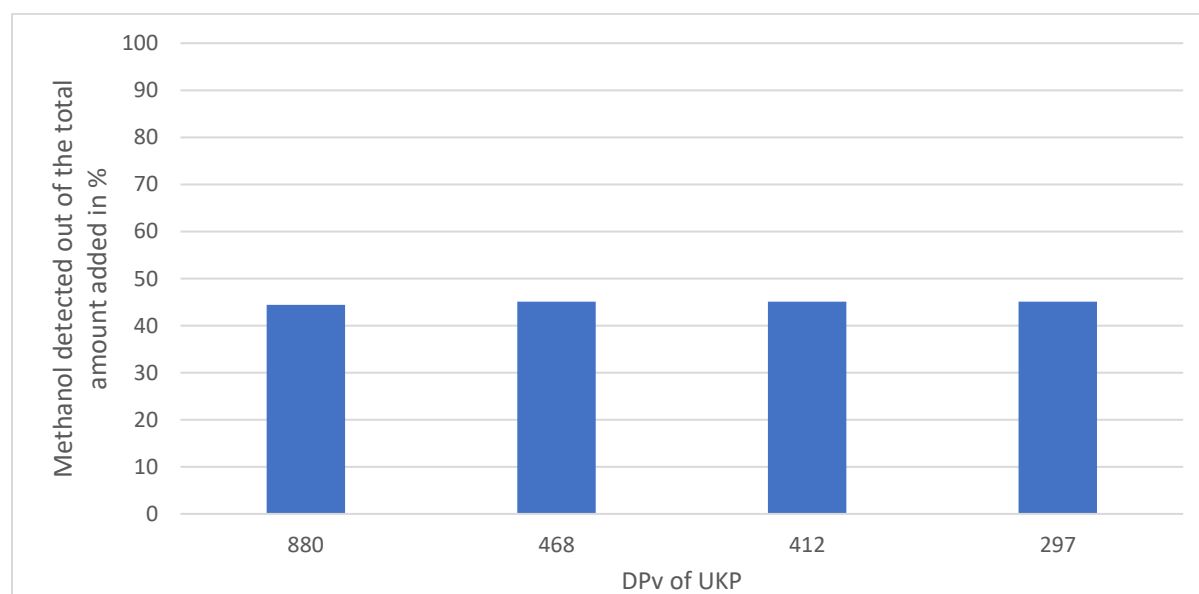


Figure 51: Oil/substrate methanol partition coefficient of UKP, as function of the cellulose DPv after thermal ageing (■). Samples were aged in oil from 2 h to 240 h at 130°C. The measured cellulose DPv is given for each sample. Y scale: represents the amount of methanol that remained in the oil, and therefore did not migrate into paper.

Results show no visible change in the partition coefficient with ageing (Figure 51). Nevertheless, it must be noticed that this experiment does not exactly reflect the state of the paper after ageing, since Soxhlet extraction and subsequent drying removed some components like water and acids created during thermal ageing, that would probably affect the results of the partition coefficient measurements.

iii) Effect of moisture content

Another test consisted in studying the effect of moisture content in paper on the oil/substrate methanol partition coefficient of unaged UKP. Samples were dried in an oven and then removed at selected times to obtain water content between 0.3% to 6.5% by weight. These samples were impregnated in oil, spiked with methanol and sealed. After waiting 48 hours for methanol to homogenize, they were analyzed with HSGC-FID to measure the methanol concentration in the oil. Results of oil/substrate methanol partition coefficient of unaged UKP at different moisture contents are presented in Figure 52.

Important notice: as explained in the method section, the paper drying process starts with a drying in the oven that is then followed by an impregnation with oil. This impregnation is then followed by a degassing where paper samples in oil are put under vacuum to remove any air bubble stuck to the paper. But for this experimental series, this degassing step was omitted from the drying process, since it could interfere and modify the water content in paper.

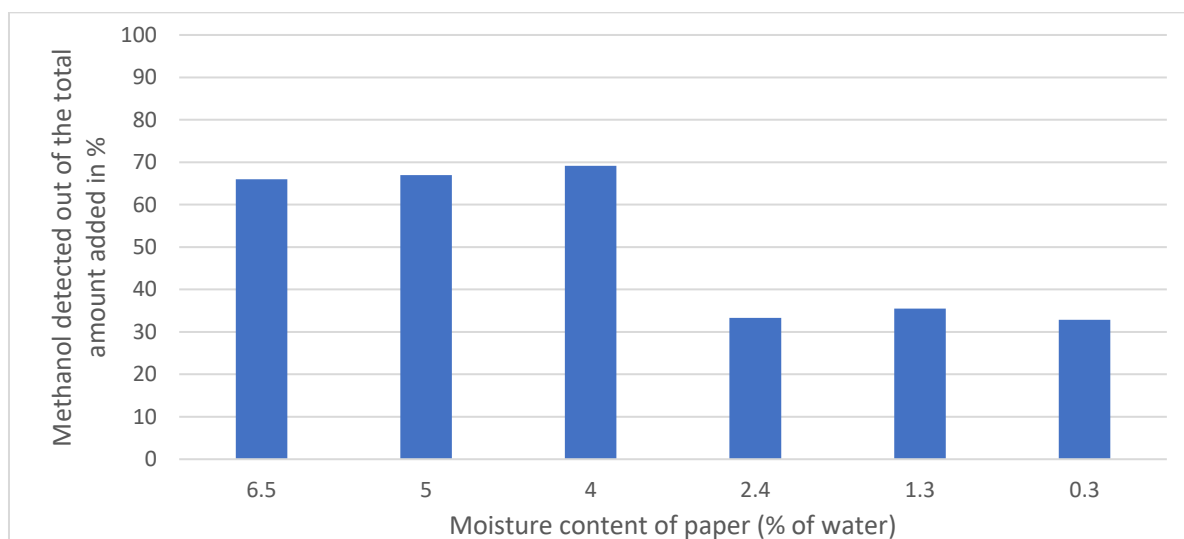


Figure 52: Oil/substrate methanol partition coefficient of unaged UKP at different moisture contents (■).

Results in Figure 52 show that the paper absorbs more methanol when it is dry. When paper is dry (0.3% moisture), 68% of the methanol introduced is absorbed by paper (32% stay in the oil phase) while, when it contains more water (4% moisture for example), the paper absorbs less methanol, around 30% (70% stay in the oil phase). The threshold seems to be when the paper contains 3% of moisture.

iv) Discussion of results

Partition coefficient experiments gave different results. UKP and BKP were shown to have a higher affinity for methanol than CL. Between UKP and BKP only a slight difference of about 3% is observed. Therefore, the main difference in methanol affinity can be explained by the presence of hemicelluloses, rather than lignin. Indeed, compared to lignin, hemicelluloses are of the same alcoholic nature as methanol. Compared to cellulose, hemicelluloses are hydrophilic, disordered and amorphous polymers, and more accessible than cellulose chains inside the microfibrils, since they are located at their surface, like lignin. It can also be noticed that in these laboratory experiments, methanol concentration is much above the concentration found in field transformers.

A comparable study on methanol partition coefficients in literature [14] indicates that around 58% of spiked methanol was not absorbed by UKP. These experiments were done at 40°C while our spiking experiments were done at room temperature. The methanol partition coefficient becomes comparable to our result on UKP (32-33%) when applying a temperature correction factor, as related in [10]: methanol partition coefficient would then drop to 37% for UKP, rather close to our result.

Other comments can be made:

1. Ethanol affinity for paper: It was found that ethanol has a rather poor affinity for paper. Compared to BKP and CL, UKP as a higher affinity for ethanol (about 10% of ethanol absorbed), to be compared with 1% in BKP and CL (Figure 49 and Figure 50). Thus, lignin would play a main role in substrate affinity for ethanol.
2. Effect of paper ageing: no change in the partition coefficient with ageing was found. It must be considered that this experiment did not control all the possible effects of ageing on paper, since a Soxhlet extraction had to be done prior to spiking, removing water and acids created during thermal ageing. It can only be concluded that the changes in the chemical composition of paper after ageing do not affect the partition coefficient (Figure 51).
3. Water and acid content in aged paper should also affect the methanol partition coefficient. It was impossible to control the acid content in paper but the effect of water content has been tested (Figure 52). It seems that there is a plateau at about 3% water content until which the methanol affinity stabilizes, going from 30 % absorption in wet paper to about 70% in dry paper. These results indicate that a higher water content in paper reduces the amount of methanol absorption. During ageing, paper produces significant amounts of water meaning that more methanol would stay in oil when the paper is heavily degraded. Again, it is important to understand that in field transformers, other parameters might play a role that could affect the partition coefficient such as acid content and temperature.

e) Contrasting results with literature

The results obtained in our study can be completed by the literature, in particular the work of Jalbert.

In one of its publication [30], Jalbert shows that the relationship between methanol detection and cellulose depolymerization is valid only before reaching a DP_v value limit. When cellulose DP_v is close to the leveling of DP, *i.e.* close to 200, the methanol detection strongly increased and the validity of the methanol as a tracer starts to come into question. In our study, same behavior is observed when the UKP is aged (Figure 48). Indeed, after the paper reached its end-of life (DP_v around 200), the methanol detection increased a lot suddenly. This behavior is attributed to the accumulation of oxidative products in oil, that may change the partition coefficient.

Other factors may influence the methanol formation, as additives present in the paper. In fact, in another publication [14], Jalbert compared the ageing of two papers, a standard Kraft paper (Clupak HD75) and a thermally upgraded Kraft paper (Manning 220), the ageing trials being carried out in the same oil, with the same operating conditions. The thermally upgraded paper contains a nitrogen-based additive, whereas the standard paper has no additive. Figure 53 presents the results in terms of methanol detection versus the number of cellulose chain-end groups.

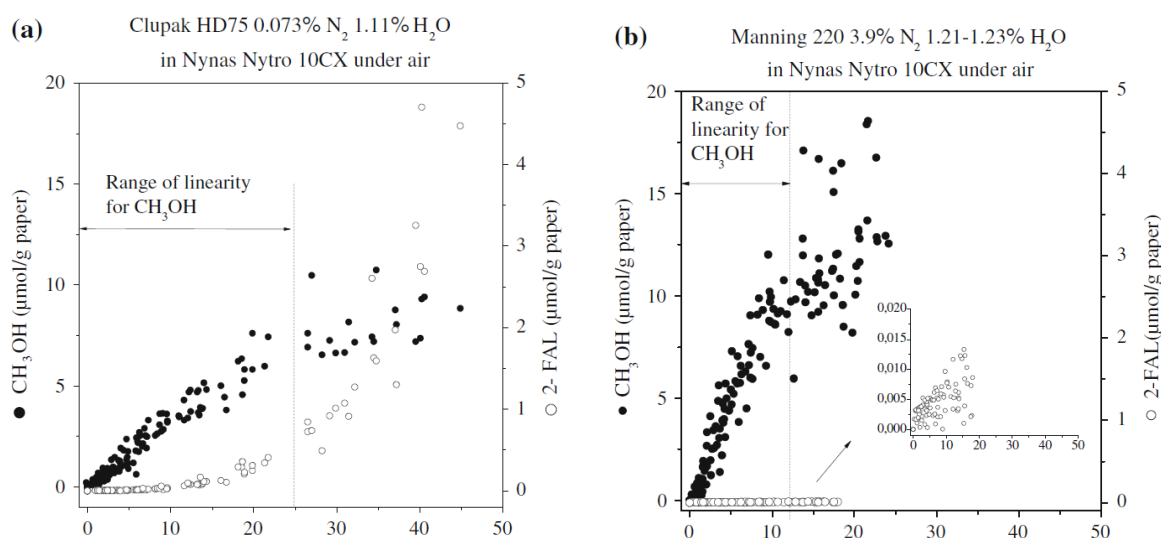


Figure 53: Methanol production as a function of the number of cellulose chain- end groups. Comparison of standard (Clupak HD75) and thermally upgraded (Manning 220) papers. Extracted from Jalbert *et al.* [14].

Figure 53 shows that thermally upgraded Kraft papers (TU paper) produce much more methanol for the same degree of depolymerization than standard Kraft papers (SD). The nitrogen-based additive is known to slow down the release of acidity during ageing which is responsible for the delay of the cellulose depolymerization. Two hypotheses may explain the higher release of methanol with the TU paper. First, with less acidity, methanol production from lignin demethylation is limited compared to methanol production from cellulose, and the reaction of polysaccharides chain-end group with methanol is less important. The limited reaction of methanol with cellulose end groups in TU papers could be responsible for the higher methanol detection. Another explanation may be the following. Because the TU paper will reach the same number of scissions for longer ageing time compared to the SD paper, more methanol can be produced from other sources than cellulose depolymerization (oil ageing for example).

The effect of the nitrogen additive on the methanol formation has been confirmed in another publication of Jalbert [8], where ageing trials have been conducted on Kraft papers containing various amounts of nitrogen-based additive, expressed in nitrogen content (Table 23).

Table 23: Methanol detected in oil and the corresponding amount of methanol calculated following the model of Jalbert – Comparison between papers containing various amount of nitrogen-based additive. Extracted from Jalbert *et al.* [8].

	Munksjö	CE Rotherm	CE Rotherm	Manning 220 Mannitherm D
Nitrogen content in paper (%)	0	0.91	1.15	2.25
Detected amount of methanol (μg)	59.1	72.0	80.1	100.6

It was shown that when the nitrogen content in the paper is increased (increase of the paper protection), more methanol is produced. The relationship between methanol release during ageing and the cellulose DPv is thus varying depending on the paper type.

If the paper composition affects the methanol production during ageing, another parameter should be considered, the oil nature. Indeed, Matharage *et al.* [24] compared the methanol production of standard Kraft papers in mineral (Gemini X) and synthetic ester (MIDEL 7131) oils. They studied the evolution of the acidity and methanol release in the oil all along the ageing. Results are presented in Figure 54 and Figure 55.

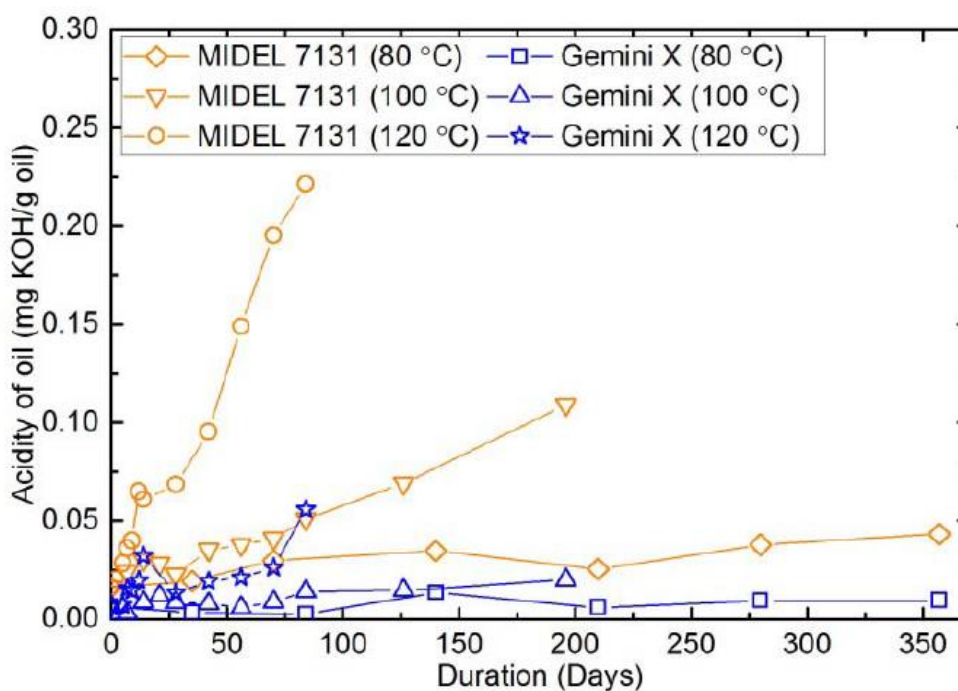


Figure 54: Evolution of the acidity during standard Kraft paper ageing in synthetic ester oil (MIDEL 7131) and mineral oil (Gemini X) for 90 days to 1 year, using temperatures from 80 to 120°C. Extracted from Matharage *et al.* [24].

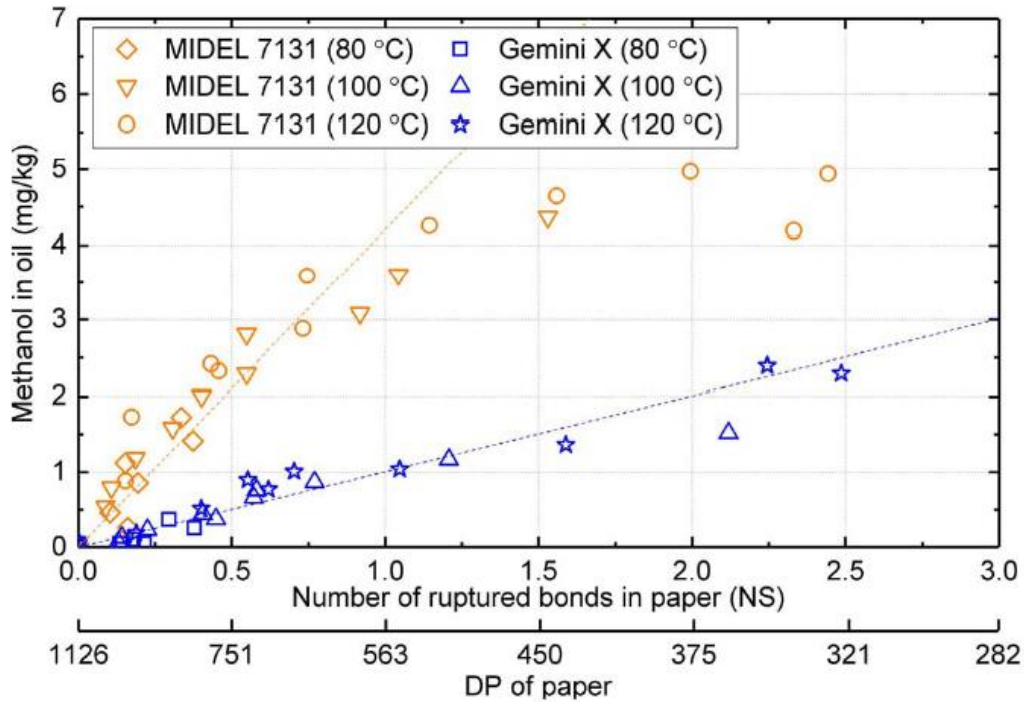


Figure 55: Evolution of the detected methanol during standard Kraft paper ageing in synthetic ester oil (MIDEL 7131) and mineral oil (Gemini X) for 90 days to 1 year, using temperatures from 80 to 120 °C. Extracted from Matharage et al. [24].

Figure 54 shows that acid products are released during ageing in the synthetic ester oil and that the acidity depends on the ageing temperature, whereas in mineral oils, only few acidic by products are liberated. Because this study does not present any blank trial, *i.e.* trial without paper, it is difficult to discriminate acid coming from the paper ageing and acid due to the oil ageing. Moreover, in Figure 55 it can be seen that more methanol is produced when ageing is performed in the synthetic ester oil and that there is a linear relation between methanol detection and cellulose DPv which is not dependent on the acidity (or on the ageing temperature). Finally, this linear relationship stops at the longer ageing time. Even if some trials are missing to conclude on the effect of oil, it is clear that the nature of oil also impacts the methanol release.

Conclusion

The lifetime of electric transformers is sharply linked to the state of its cellulosic insulation. The development of a new tracer is difficult because it requires a global understanding of the ageing process of the cellulosic substrate, while only be able to detect and quantify a limited number of chemicals dissolved in the oil, assumed as representative indicators of the state of cellulosic insulation.

Methanol suitability as an ageing marker in oil has been well established after 15 years of research. Methanol generation is supposed to be linearly related to cellulose depolymerization by acid hydrolysis at high temperature.

The aim of our experiments was to get a more precise understanding of the role of each component of the Kraft paper during the process of methanol generation. Lignocellulosic model compounds were selected and aged in oil under the same conditions as Kraft papers in hot transformers.

To summarize, it was seen in our study that among the three main components of papers, lignin produced about five times more methanol than cellulose and hemicelluloses. In softwood lignin, methanol arises from the demethylation of the guaiacyl units, a phenomenon that is not directly related to the depolymerization of cellulose. Thus, lignin was found to have a significant effect on methanol production and demethylation of lignin plays an ever-increasing role as acidity inside the paper increases with ageing. In polysaccharides, the mechanism of methanol production from cellulose depolymerization is unclear, but it was evidenced that the produced methanol could also react with the chain ends reducing units of carbohydrates. This probably contributes to the relationship between cellulose depolymerization and methanol production. However, this contribution in the initial phase of cellulose depolymerization is rather minor, due to the high cellulose DP_v (and thus, low number of chain ends reducing units) whereas this contribution might increase at lower cellulose DP_v, when the accessibility and the number of chain ends reducing groups is rising. Then methanol consumption increases.

The methanol quantity detected in oil is also dependent on the methanol's partition coefficient between oil and paper. The chemical composition of the paper does not affect this coefficient but water, a by-product of paper ageing, was found to compete with methanol in paper insulation therefore reducing paper's affinity for methanol during ageing.

Given the relatively short time of this study and time-consuming experiments, all parameters that can influence methanol production could not be studied. But in literature, it has been pointed out that the presence of nitrogen-based additive to protect the paper from ageing may also be responsible for higher methanol detection. This is probably linked to the limitation of acid formation in the medium during ageing which leads to decrease the reactivity of carbohydrate chain ends with methanol (methanol is less consumed). The relation between acidity and methanol production would be worth studying in-depth. On the same, other parameters may impact the methanol detection, for example ageing temperature possibly modifies the partition coefficient of methanol.

As a final conclusion, this chapter highlighted that the methanol detected in oil during paper ageing is not only due to cellulose depolymerization. Many other parameters are involved, such

as the paper composition, methanol coefficient partition, acidity in the medium, or even the oil nature should be considered.

References

1. IEEE C57.93-2007, IEEE Guide for Installation of Liquid-Immersed Power Transformers, 2007.
2. IEEE C57.104-2008, IEEE Guide for the Interpretation of Gases Generated in Oil Immersed Transformers, 2008.
3. Bakar N, Abu-Siada A, Islam S. A review of dissolved gas analysis measurement and interpretation techniques, *IEEE Electr Insul Mag*, 2014, 30(3):39–49.
4. Lelekakis N, Martin D, Guo W, Wijaya J. Comparison of dissolved gas-in-oil analysis methods using a dissolved gas-in-oil standard. *IEEE Electr Insul Mag*, 2011, 27(5):29–35.
5. Jalbert, Rodriguez-Celis, Arroyo-Fernández, Duchesne, Morin. Methanol Marker for the Detection of Insulating Paper Degradation in Transformer Insulating Oil. *Energies*, 2019, 18;12(20):3969.
6. Myers, S.D., Kelly, J.J., and Parrish, R.H., *A Guide to Transformer Maintenance*, Transformer Maintenance Institute. Akron, 1981.
7. Cheim L, Platts D, Prevost T, Xu S. Furan analysis for liquid power transformers. *IEEE Electr Insul Mag*, 2011, 27(6):29–42.
8. Jalbert J, Gilbert R, Tétreault P, Morin B, Lessard-Déziel D. Identification of a chemical indicator of the rupture of 1,4- β -glycosidic bonds of cellulose in an oil-impregnated insulating paper system. *Cellulose*, 2007, 16;14(4):295–309.
9. Coulibaly ML, Perrier C, Marugan M, Beroual A. Aging behavior of cellulosic materials in presence of mineral oil and ester liquids under various conditions. *IEEE Trans Dielectr Electr Insul*, 2013, 20(6):1971–6.
10. Jalbert J, Lessard MC, Ryadi M. Cellulose chemical markers in transformer oil insulation Part 1: Temperature correction factors. *IEEE Trans Dielectr Electr Insul*, 2013, 20(6):2287–91.
11. von Steinkirch Souza EMP, Mildemberger L, Akcelrud L, Andreoli MC, dos Santos K, da Silva GC, et al. Evaluation of the chemical stability of methanol generated during paper degradation in power transformers. *IEEE Trans Dielectr Electr Insul*, 2016, 23(5):3209–14.
12. Arroyo-Fernandez OH, Fofana I, Jalbert J, Rodriguez E, Rodriguez LB, Ryadi M. Assessing changes in thermally upgraded papers with different nitrogen contents under accelerated aging. *IEEE Trans Dielectr Electr Insul*, 2017, 24(3):1829–39.
13. Gilbert R, Jalbert J, Tétreault P, Morin B, Denos Y. Kinetics of the production of chain-end groups and methanol from the depolymerization of cellulose during the ageing of paper/oil systems. Part 1: Standard wood kraft insulation. *Cellulose*, 2009, 16(2):327–38.
14. Gilbert R, Jalbert J, Duchesne S, Tétreault P, Morin B, Denos Y. Kinetics of the production of chain-end groups and methanol from the depolymerization of cellulose during the ageing of paper/oil systems. Part 2: Thermally-upgraded insulating papers. *Cellulose*, 2010, 17(2):253–69.

15. Schaut A, Autru S, Eeckhoudt S. Applicability of methanol as new marker for paper degradation in power transformers. *IEEE Trans Dielectr Electr Insul*, 2011, 18(2):533–40.
16. Laurichesse D, Bertrand Y, Tran-Duy C, Murin V. Ageing diagnosis of MV/LV distribution transformers via chemical indicators in oil. In: 2013 IEEE Electrical Insulation Conference. IEEE, 2013, p. 464–8.
17. Arroyo OH, Fofana I, Jalbert J. Relationship between some chemical markers and the mechanical properties of the solid insulation used in power transformers. In: 2014 IEEE Electrical Insulation Conference. IEEE, 2014, p. 348–52.
18. Arroyo OH, Fofana I, Jalbert J, Ryadi M. Relationships between methanol marker and mechanical performance of electrical insulation papers for power transformers under accelerated thermal aging. *IEEE Trans Dielectr Electr Insul*, 2015, 22(6):3625–32.
19. Institute of Electrical and Electronics Engineers, editor. 2015 IEEE 11th International Conference on the Properties and Applications of Dielectric Materials, IEEE, 2015.
20. Rodriguez-Celis EM, Duchesne S, Jalbert J, Ryadi M. Understanding ethanol versus methanol formation from insulating paper in power transformers. *Cellulose*, 2015, 22(5):3225–36.
21. Perrier C, Mamadou-Lamine COULIBALY, Marielle MARUGAN. Methanol as new ageing marker of oil-filled transformer insulation. CIREN, 2015.
22. Matharage SY, Liu Q, Wang ZD. Aging assessment of kraft paper insulation through methanol in oil measurement. *IEEE Trans Dielectr Electr Insul*. 2016, 23(3):1589–96.
23. Fernandez OHA, Fofana I, Jalbert J, Gagnon S, Rodriguez-Celis E, Duchesne S, et al. Aging characterization of electrical insulation papers impregnated with synthetic ester and mineral oil: Correlations between mechanical properties, depolymerization and some chemical markers. *IEEE*, 2018, 25(1):217–27.
24. Matharage SY, Liu Q, Wang ZD, Wilson G, Krause Ch. Aging assessment of synthetic ester impregnated thermally non-upgraded kraft paper through chemical markers in oil. *IEEE*, 2018, 25(2):507–15.
25. Jalbert J, Gilbert R, Denos Y, Gervais P. Methanol: A Novel Approach to Power Transformer Asset Management. *IEEE*, 2012, 27(2):514–20.
26. Ryadi M, Tanguy A, Jalbert J. Methanol marker for the thermal performance qualification of power transformers. In: 2013 IEEE Electrical Insulation Conference. IEEE, 2013, p. 387–91.
27. Institute of Electrical and Electronics Engineers, IEEE Dielectrics and Electrical Insulation Society, editors. 2014 IEEE Electrical Insulation Conference. IEEE, 2014, 496 p.
28. Jalbert J, Lessard MC. Cellulose chemical markers relationship with insulating paper post-mortem investigations. *IEEE*, 2015, 22(6):3550–4.
29. Jalbert J, Rajotte C, Lessard MC, Rodriguez-Celis M. Methanol in oil interpretation model based on transformer post-mortem paper analysis. *IEEE*, 2018, 25(2):568–73.

30. Jalbert J, Rodriguez-Celis E, Duchesne S, Morin B, Ryadi M, Gilbert R. Kinetics of the production of chain-end groups and methanol from the depolymerization of cellulose during the ageing of paper/oil systems. Part 3: extension of the study under temperature conditions over 120 °C. *Cellulose*, 2015, 22(1):829–48.
31. Calvini P. On the meaning of the Emsley, Ding & Wang and Calvini equations applied to the degradation of cellulose. *Cellulose*, 2014, 21(3):1127–34.
32. Calvini P, Gorassini A. On the Rate of Paper Degradation: Lessons From the Past. *Restaurator*. 2006, 27(4).
33. Jalbert J, Duchesne S, Rodriguez-Celis E, Tétreault P, Collin P. Robust and sensitive analysis of methanol and ethanol from cellulose degradation in mineral oils. *J Chromatogr A*. 2012, 1256:240–5.
34. Helferich B, Schäfer W. α -METHYL D-GLUCOSIDE. *Org Synth*. 1926;6:64.

Chapter 3: Characterization of ageing for Kraft insulation oxidation and depolymerization measurements.

Table of content

Introduction	101
1) Dielectric and chemical properties during ageing	102
a) Metallic cations in wood pulps.....	102
i) Role of metallic cations	102
ii) Metal binding to cellulose fibers	104
b) Chemical study of paper ageing	105
i) Depolymerization cellulose and oxidation in paper	105
ii) Oxidation of the cellulose chain	106
iii) Chromatographic and spectroscopic assessment of paper	108
2) Materials and methods	110
a) Materials.....	110
i) Chemical products	110
ii) Instruments used for chemical characterization	110
b) Methods.....	111
i) Method development of ion exchange.....	111
ii) Ion exchange experiments	111
iii) Size exclusion chromatography experiments.....	112
iv) Infrared experiments.....	112
3) Results and discussion	113
a) Ion exchange of paper	113
b) Effect of paper chemical composition on cellulose depolymerization during ageing	115
i) Quantifying the depolymerization of cellulose	115
ii) Effect of pulp polymers composition.....	115
iii) Ion exchange with main metal ions	118
iv) Ion exchange with transition metal ions	120
c) Effect of paper chemical composition on polymers oxidation during ageing.....	121
i) Oxidation of the cellulose chain	121
ii) Effect of pulp composition	122
iii) Ion exchange with main metal ions.....	126
iv) Ion exchange with transition metal ions	128
v) Synthesis on depolymerization and oxidation results.....	129
Conclusion.....	134

References 136

Introduction

The conventional test to evaluate the state of degradation of insulation Kraft paper during ageing in transformers is the measurement of the degree of polymerization of cellulose (DP_v test). However, assessing paper oxidation could also add relevant information. It is assumed that the loss of mechanical properties only comes from the loss of entanglement resulting for the shortening of cellulose chains. Paper degradation is governed by two main type of reactions; hydrolysis and oxidation. While acid hydrolysis is considered to be the main factor for cellulose depolymerization, it is also related to carbohydrates oxidation. Oxidation of Kraft insulation in power transformers in the presence of oil, which is also involved in the process, is a complex subject, that is not fully understood at the present time.

This study aims to combine a classical evaluation of the depolymerization of cellulose with a spectroscopic study of the pulp, to assess its oxidation state. To follow cellulose depolymerization, not only the conventional DP_v test (viscosity-average degree of polymerization), but also size-exclusion chromatography of the dissolved substrate, were used. Substrate oxidation was followed by FTIR spectroscopy. Samples used in the study were chosen to represent the main components of paper. Virgin paper is composed of a combination of organic matter (cellulose, hemicelluloses and lignin) and inorganic components (residual metals ions and their related anions) that come from the wood and from the pulping process (Ca, Na, Mg and Fe). During ageing in transformers, copper ions, other metal ions and inorganic components penetrate in the paper in contact with metal parts, for example paper wrapped around copper wiring. Aged oil is also a vector, since it contains a variety of dissolved ions associated with organic components.

The aim of these chapters is to analyze the individual impact of each paper component on the insulation properties during the ageing process. This is done by analyzing paper samples of multiple compositions (unbleached Kraft pulp (UKP), bleached Kraft pulp (BKP) and Cotton linters bleached pulp). Chemically modified UKP samples that only contain one type of metal ion were also studied. The main metal ions in paper are Ca, Na and Mg. Na comes from the Kraft process chemicals; Ca and Mg are introduced during the full washing steps of the pulp, by ion-exchange process with sodium, which is supposed to be almost totally removed from the final dielectric paper. This is also the case for transition metal ions (Fe and Cu) that are known to impact Kraft insulation in transformers.

1) Dielectric and chemical properties during ageing

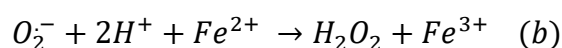
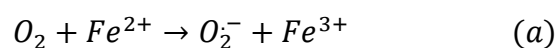
- a) Metal ions in wood pulps
 - i) Role of metal ions

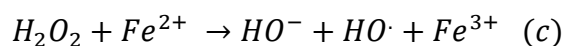
Metal ions management in paper industry is a diverse and complex subject. In practice most research in this field is related to peroxide bleaching where metal ions interfere with the bleaching chemistry, promoting the formation of strong oxidizing radicals, and affect the brightness of the paper. Ionic Fe, Cu and Mn species increase the decomposition rate of hydrogen peroxide [1], and they also promote cellulose oxidation and depolymerization. Ca^{2+} and Mg^{2+} are normally absent in the fiberline of the Kraft process, since they make organic matter precipitates, responsible for fouling and scaling phenomena in reactors and pipelines. Metal ions can cause discoloration, precipitation, and emulsion instability and pollution in waste waters [2]. Multiple studies were done about the effect of iron in paper degradation because of the use of iron rich inks, called gall inks, commonly used in the 5th to 19th century [3]. Most publication focus on paper degradation in atmospheric conditions where oxidative degradation is the main degradation pathway for cellulose. In non-oxidative conditions (found in transformers), the main contributor to cellulose depolymerization is an autocatalytic cycle of acid hydrolysis. The acidity level to start this cycle appears after a slow release of organic acids coming from β -alkoxy elimination reactions generated on polysaccharides end chains, leading to the formation saccharinic acids. Impurities in the pulp lead to the formation of strong oxygenated oxidants (hydroxyl radicals), peroxide and superoxide anions in the presence of oxygen and water, with metal ions (Cu, Fe, Mn) having a catalytic role. Pulps are purposely made with a slightly alkaline pH to prevent acid hydrolysis. Of all the impurities, residual metals are the only one that can be controlled during manufacture of the pulps.

The metal ions content of electrotechnical grade paper is followed closely to ensure it is as small as possible. Metal cations act as charge carriers that greatly decreases dielectric properties of paper, namely they raise the dielectric loss factor ($\tan \delta$) – defined in Chapter 4 of this thesis. Metal cations are removed after Kraft pulping by acid washing (pH 2, 90°C for 2 hours), the use of chelating agents, and Na substitution by Ca or Mg with successive washes. In practice it is impossible to completely remove metal ions without a significant deterioration of cellulose in strong and prolonged acidic conditions [4]. With regards to ions, the literature survey shows that the main concern of electrotechnical grade pulp manufacture is the loss of dielectric properties. Few studies look at the effect that they might have on thermal ageing properties, in the context of electrotechnical grade pulps.

There are two types of metal ions present in the pulp, transition and main metals.

Transition metals (Fe, Cu) mainly come from contamination during wood pulp manufacturing or from the transformer corrosion (acids can dissolve the copper of the transformer winding). Iron and copper ions can be easily absorbed and complexed to lignin or cellulosic moieties, so they are hard to remove. They have a catalytic role in the formation of reactive oxygen species through Fenton reactions, as detailed below:





The initial reaction between O_2 and a reducing metal ion (Fe^{2+} , for instance) removes one electron from O_2 to form the superoxide radical anion ($O_2^{\cdot-}$) (a). The presence of superoxide has been proved by chemiluminescence studies during oxidation in humid atmosphere [5]. Superoxide is a long-life radical species in the cellulose matrix, not able of electron abstraction from simple saccharides or cellulose [6]. Instead superoxide is extremely reactive with water, which leads to the formation of hydrogen peroxide (b). Hydrogen peroxide further reacts through the well-known Fenton reaction, from which (c) is the first step, to create HO° radicals that can oxidize cellulose.

The Fenton mechanism (step c) starts when the transition metal ions are in a reduced form (Cu^+ or Fe^{2+}). In the full mechanism involving Fe as a catalyst (not presented here), Fe^{2+} is regenerated from Fe^{3+} reduction by HO_2° , which makes a cyclic catalytic cycle.

Copper ions (Cu^{2+}) and some other transition metal ions are known to be catalytically active in the Fenton reaction. In paper, the most probable reducer for Cu^{2+} would be the aldehyde group present on the reducing end groups (REGs) of cellulose and hemicelluloses chains. The rest of the depolymerization process is explained in the first part of this study.

The most common main metals in pulps are Na, Ca and Mg. They are generally inactive in normal writing paper, but their possible involvement in the depolymerization of cellulose during paper ageing in transformers is not known. The concern for electrotechnical paper manufacturers is the increase of $\tan \delta$ that is directly traceable to the amount of Na in paper. For this reason, washing steps are intended to replace as much Na^+ by Ca^{2+} and Mg^{2+} ions in the final product. Several literature references also suggest a protective effect of Mg during pulp bleaching processes. It is well known that cellulose during alkaline oxygen bleaching or hydrogen peroxide bleaching can be protected from depolymerization by small addition of $MgSO_4$ in the pulp.

The work of Selih *et al.* in 2007 [3] tried to correlate the production of hydroxyl radicals with the rate of chain scission in pure cellulose (Whatman No. 1 filter paper). Paper samples were aged in oxidative conditions at $80^\circ C$ and 65% RH, and cellulose degradation was measured by the DPv. $CaCO_3$ and $MgCO_3$ were added by submersing papers in $Ca(HCO_3)_2$ and $Mg(HCO_3)_2$ solutions. Iron and copper ions were also added to the pulps. The pH was 8 for calcium papers and 9.4 for magnesium papers. The following figure describes the results and Table 24 shows the amount of metal cation present in the pulp during ageing.

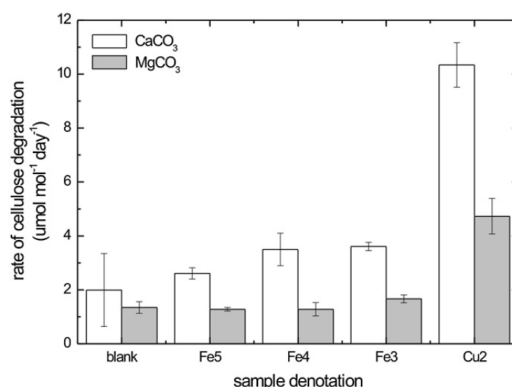


Figure 56: Rate of degradation of paper samples with multiple ion contents. Extracted from Selih *et al.* [3].

Table 24: Iron and copper content in samples immersed into differently concentrate solutions of their respective chlorides. Data extracted from Selih et al. [3].

Sample	Ion content (ppm)	
	CaCO ₃ -containing samples	MgCO ₃ -containing samples
Fe3	3.1 ±0.7	2.0 ±0.4
Fe4	0.79 ±0.02	0.56 ±0.06
Fe5	<0.2	0.6 ±0.1
Cu2	0.87 ±0.02	1.37 ±0.01

MgCO₃ papers exhibited a slower rate of degradation, meaning a decrease in the catalytic activity of Fe and Cu compared to CaCO₃ papers. The catalytic action of Cu is greater than that of Fe. It is suggested that the higher pH of magnesium pulps compared to calcium pulp is involved, or a possible co-precipitation of transition metals with Mg-compounds that form stable coordination compounds. These results also show that variations in the range of low, catalytic contents of iron (μmol/g) didn't significantly change the rate of degradation. It should be noted that this samples contain a vast alkaline reserve and that this is was not the case at higher concentrations of iron or copper.

ii) Metal binding to cellulose fibers

Ion exchange experiments allow to change the amount and type of metals found in cellulosic fibers. Pulp is immersed in an ionic solution where metal binding is dictated by a concentration balance between the solution and cellulosic fibers. The strength of the metal complexes formed can also play a role in the equilibrium [7]. Inside the cellulosic matrix, the main groups binding to metal ions are carboxylic acids, present at a rate of 50–200 meq/kg in the original wood pulp [8], an amount which can vary with the pulping process. Hexenuronic acids, not initially present in wood, are generated during Kraft pulping. They have an important affinity with transition metal ions [9]. In unbleached Kraft pulps, phenolic groups and catechols also bind to metal ions. Other forms in which metals are salts of low solubility such as hydroxides, oxalates, sulfates, and phosphates at alkaline pH.

After ion exchange, there is a difference of ionic concentration between the inside and the outside of the fibers. The trapped ions inside the fibers lead to a charge buildup at fiber surface. Cellulose fibers in Kraft pulps trap positive cations, leading to a net negative charge at fiber surface and the presence of a cation counter layer in the near solution. Fibers can collect metal cations regardless of the potential binding potential of acidic groups in fibers.

The question then becomes how well these metals will bond to the pulp. It is complicated to evaluate this since it is impossible to separate free cations from bound cations during an ion exchange. The bonding equilibrium constant between cations and acidic groups inside fibers cannot be directly evaluated because of the impossibility to measure the concentration of free cations inside fibers, since their distribution is not uniform, and also because cellulosic fibers swell and therefore, there is a change of the overall volume of the solution by unpredictable amounts. The most common model used is the Donnan theory. It is based on the residual charge that emerges from the accumulation of cations in fibers, called the Donnan potential [10]. Ions separate between those bound in the fiber and those free in the solution according to a partition

coefficient that is determined experimentally for a given ion. Then, the Donnan theory predicts that all other cations will have the same distribution. This model has two main limitations: (1) particular types of chemical bonding in the fibers tends to reduce the accuracy of this model, and (2) the partition constant can vary greatly, according to experimental determination. In wood pulps, metal-acidic groups bonds superimpose to the electrostatic Donnan equilibrium. In general, wood pulp is known for its ability to absorb metal ions, a property which can be used in the recovery of metals from industrial waste water [11].

b) Chemical study of paper ageing

i) Depolymerization cellulose and oxidation in paper

Cellulose depolymerization followed by the viscometric DP_v test is used as a reference characterization to follow the state of degradation of cellulosic fibers. The evolution of mechanical properties is much harder to evaluate because they vary with temperature and water content. The effect of ageing on dielectric properties will be discussed in the chapter 4 of this thesis.

For mechanical properties, it is generally accepted that a loss of entanglement between cellulose chains is the main factor explaining the global loss of fiber wall resistance. Cellulose chains are bonded together by hydrogen bonds and the movement of one chain is impeded by other chains. A loss of DP_v means less interaction between chains and more free volume, thus making a stiffer and more brittle material. Other factors, not directly related to cellulose chain length can affect mechanical properties.

In parallel to depolymerization, chemical degradation modifies the chemical structure of the main pulp components (cellulose, hemicelluloses and lignin) and creates by-products (oligo and monosaccharides, acids, water).

Chemical oxidation of the cellulose chain can affect mechanical properties in two main ways: chain cohesion, crosslinking. Oxidation is known to appear in parallel chemical pathways leading to the formation of different types of carbonyl groups [12,13]. The latter disrupt the hydrogen bonding network due the modification of the natural geometry of glucopyranose units, but also strong hydrogen bonds can be formed between hydroxyls and the new carbonyl groups [14]. After oxidative damage, rearrangement of sugar units during acid β -alkoxy elimination, acid hydrolysis and pyrolysis also contribute to further damages of cellulose chains. Oxidation and acid hydrolysis, acting together, often lead to saccharinic acid type rearrangement leading to the formation of acid groups. The latter can give rise to crosslinks with polysaccharides through esterification reactions. Other reactions involving acids yield degradation byproducts. Loss of hydrogen bonding inevitably contributes to a loss of mechanical properties. Any type of crosslinking has the consequence of making a material stiffer and more brittle. Although no study has proven this, analogy to known polymer chemistry suggest that some byproducts could also make hydrogen bonds with cellulose chains and therefore act like plasticizers in synthetic polymers. Plasticizers decrease the mechanical strength of a polymer by reducing chain interaction.

Oxidation of hemicelluloses has been less studied. The cause is mainly that residual hemicelluloses in pulps have a variety of structure depending on the wood source and pulping conditions. It is generally assumed that most degradation reactions are similar to those on

cellulose, since both materials are structurally similar. Chemical oxidations that affect lignins in the context of Kraft paper aging in transformers are known but have not been extensively studied.

ii) Oxidation of the cellulose chain

In the context of cellulose chains, carbon atoms making more than one bond with oxygen atoms are considered oxidized. This is the case for carboxylic acids, carbonyls and their corresponding tautomeric form [15]. The only naturally present carbonyl functionality in cellulose is the aldehyde group at the reducing chain end (Reducing End Group - REG). All other oxidized carbons are formed during pulp manufacturing and cellulose degradation. In the figure below (Figure 57), the REG can be seen in the aldehyde forms. The vast majority of REGs are present as hemiacetals in pyranose units but a small fraction of them exists as aldehydes and aldehyde hydrates. It should be noted that REGs are the starting points of the well know peeling reactions of cellulose. This peeling reactions are favored by alkaline conditions and therefore not considered kinetically determinant in PT aging conditions.

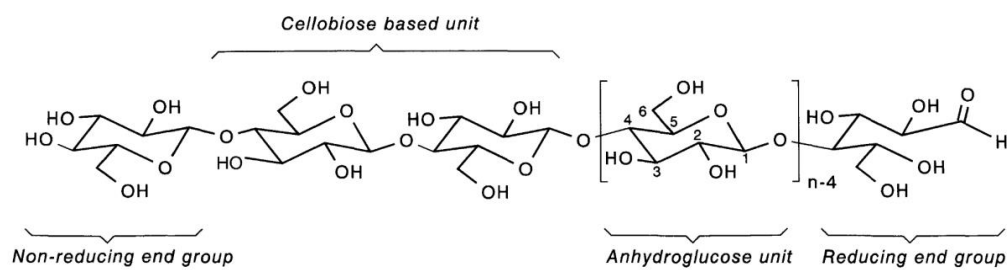
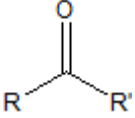
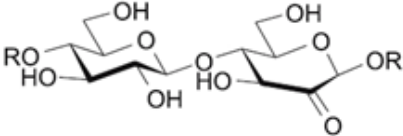


Figure 57: Schematic representation of the cellulose chain. Extracted from Potthast et al. [15].

As discussed previously, unaged cellulose present in PT will always have an initial oxidative damage already present in the ($\mu\text{mol/g}$) range. Oxidation of cellulose has been mostly described outside the field of PT, and most literature derives from the field of pulping and bleaching processes applied to wood pulps, annual plants and textiles. Selective oxidation of C2, C3 (Malaprade reaction) and C6 (TEMPO oxidation) carbons are reported for specialty applications [15]. Studies on the ageing of historical documents also look into cellulose oxidation but, unlike electrotechnical papers in PT, historical documents age in atmospheric conditions where oxidation plays an important role.

The main types of oxidations affecting cellulose is listed in the following table:

Table 25: Functional groups found in the cellulose chain and their associated characteristics. The numbers for the concerned carbon are based on those found on the figure above [15].

Functional groups	Concerned carbons	Types	Schematic representation
Carbonyl 	C1	REGs	See Figure 57
	C2, C3 ²	Keto groups	

	C6	6-aldehyde structures	
Carboxylic acid ¹ 	C1	Gluconic acid	
	C6	Glucuronic acid	
Ester 	C2 or C3 and C1 in another chain	Lactone entities	

¹ While carboxylic acid groups are not naturally present in cellulose, hemicelluloses naturally contain carboxylic acid groups and can therefore potentially form ester bonds.

² Malaprade reaction can form 2,3-dialdehyde structures but their ageing will only create oxidations on C2 or C3.

It should also be noted that a significant part of carbonyl groups exists in alternative forms [16] (Figure 58). For unaged paper, NMR experiments have shown that only about 62 % of keto groups exist in the conventional doubled-bonded form and about 38 % exist in a tautomeric form. Around 0.01% of carbonyls also exist in open cycles, with 0.0059% of carbonyls and 0.0040% of carbonyls hydrates. The reasons behind hydration of carbonyls is uncertain, but seems to vary with the water content of the pulps indicating a potential stabilization of tautomeric forms with hydrogen bonds of water molecules.

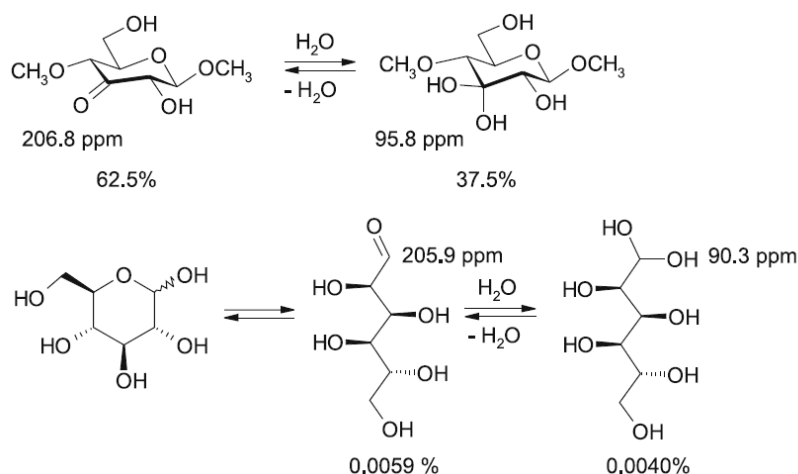


Figure 58: Schematic view of the equilibrium of tautomeric forms of carbonyl functions in cellulose. Extracted from Potthast et al. [16].

iii) Combined chromatographic and spectroscopic assessment of paper (Bagniuik et al. 2019)

Quantification of oxidized groups in paper can be done by a variety of methods focusing on carbonyl groups, carboxylic acid groups and lactones. The Copper number test, a well-known standard testing method applied in the industry, focuses on all types of carbonyl groups in pulp. It is used for specialty pulp applications. Since the REGs of polysaccharides are also quantified by this test, it is also sensitive to the size of cellulose and hemicelluloses chains, and their degradation during aging.

For more detailed analysis, two levels of quantification can be envisaged:

- Total amount of chemical groups regardless of their location in cellulose. They mostly rely on direct titrations of oxidized groups in pulps, as in Copper number test, NaBH₄ reduction of carbonyl groups, carboxyl group determination by cation-exchange methods or by the methylene blue sorption, red-dye titration of REGs (TTC photometric titration) [17].
- Functional group quantification for a given subgroup defined by its molecular weight or chemical characteristics. This can be done by selective labeling of given functional groups in cellulose with a chemical marker, and the use of size-exclusion chromatography (SEC) to separate different cellulose fractions by size. Typically, on cellulose, UV or fluorescent labelling can be applied, like the CCOA and “FDAM” methods for carbonyl and carboxyl groups analysis, respectively [18].

In the field of PT, only global analytical methods have been generally applied in the industrial cases. They only give a rough idea of pulp oxidation while the second level analysis is mostly used in research, to differentiate different types of oxidations. The latter methods are slow and expensive. In a promising new study [19], tried to correlate cellulose depolymerization, followed by SEC, with the corresponding cellulose oxidation followed by FTIR. The added spectroscopic measurement allows tracking both hydrolysis and oxidation. It is claimed that a field application might be envisaged, but the publication does not detail how FTIR measurement would be technically possible with an added sensor inside a PT. This new method was used to evaluate model paper samples made of almost pure cellulose (99.5% cellulose - P1 samples). Kraft insulation samples were also analyzed, unaged smooth and crimped variants (designated TS0 and TC0, respectively). Aged samples of the same type were taken from 50-year-old transformer: smooth samples (TS1 and TS2) from upper and lower voltage winding, and a crimped sample (TC1) from lower voltage outings braid. The article states that samples were lignin-free, implying that they were made of fully-bleached pulp, or bleached before the analysis, which is not representative of normal Kraft pulps analyzed in PT.

Aging took place in a dry atmosphere (0% humidity level) at 90 °C and 150 °C for ageing times from 0 to 48 days. 90°C represents the minimal temperature available to have accelerated aging and transformer-like conditions while 150°C was used as the maximum temperature possible before pyrolysis becomes the dominant degradation pathway. After toluene extraction, samples were analyzed by transmission FTIR in which paper samples were scratched until sufficient transmission was detected. The degree of polymerization was followed by SEC with a DRI and MALS detector. Prior to chromatography, cellulose was derivatized into cellulose tricarbonyl (CTC) and solubilized in tetrahydrofuran (THF).

The results of this analysis can be seen below in Figure 59:

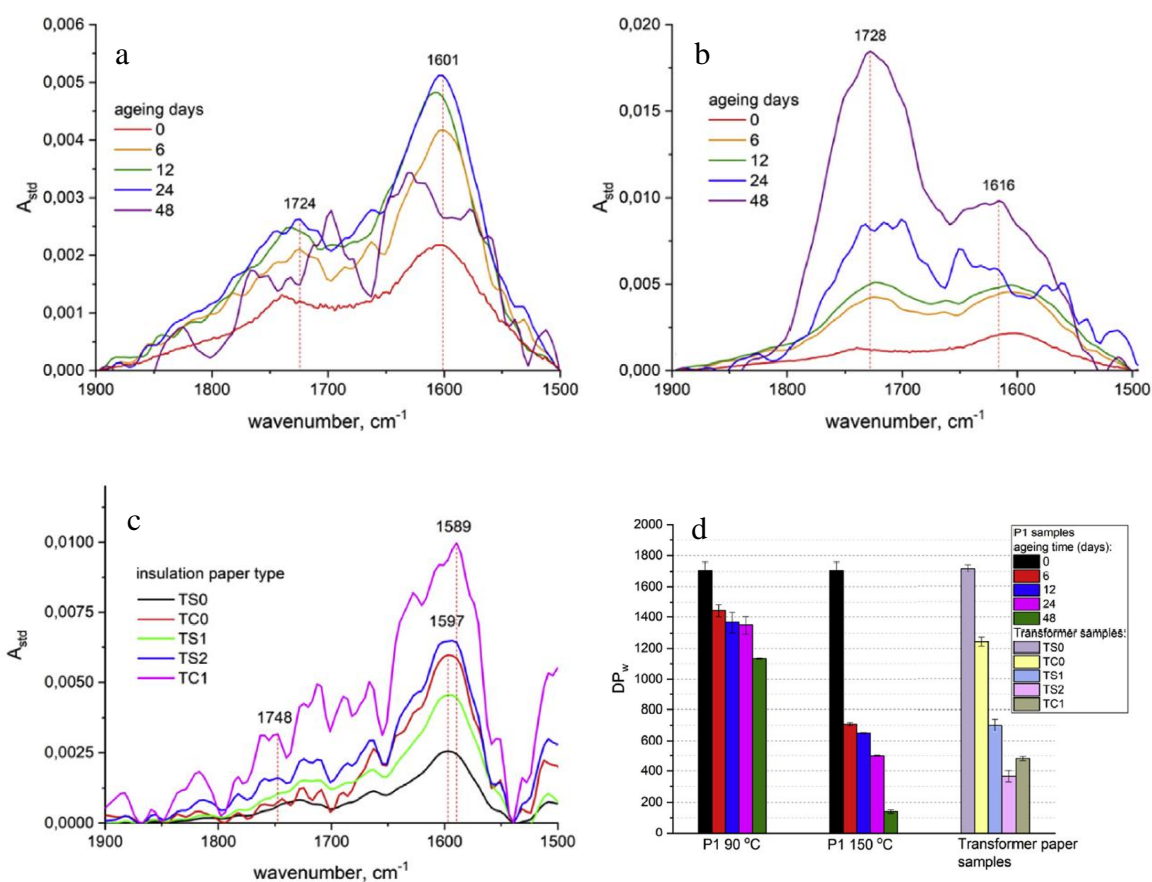


Figure 59: FTIR spectra for pure cellulose samples aged at 90 °C (a) and 150 °C (b) and samples taken from a PT (c). Weight-average degree of polymerization (DP_w) of the corresponding samples measured with SEC (d). Extracted from Bagniuik et al. [19].

Figure 59d clearly shows that paper completely degrades during the experiment. Results for pure cellulose (P1) at 90°C and 150°C are in accordance with general data in the literature. Transformer paper samples showed that the degraded paper has not reached its end of life DP value (LODP of about 200).

In Figure 59a, b, and c carbonyl groups spectral bands appear in the range from 1900 to 1500 cm⁻¹. The two main bands at 1740 and 1620 cm⁻¹ are visible, they were assigned to carbonyl groups and highly conjugated ketones, respectively [20]. For pure cellulose samples (Figure 59 a and b) both signals increased with ageing. It can be seen that ageing at higher temperature (150°C) produces more oxidized products, *i.e.* aldehydes and carboxylic acids (1740 cm⁻¹) than conjugated ketones (1620 cm⁻¹). For transformer samples (Figure 59c), the oxidation behavior was similar to reference samples aged at the lower temperature of 90°C, *i.e.* ageing in that case produced higher amounts of conjugated ketones. Despite the publication stated that the samples were “lignin-free”, it is possible to see the characteristic signal of lignin at 1520 cm⁻¹ for transformer samples [21] (Figure 59c). Therefore, two distinct behaviors arise, higher temperature favors a higher proportion of aldehyde and carboxylic acids, while at lower temperatures generation of conjugated ketones dominates.

2) Materials and methods

a) Materials

i) Chemical products

Oil: NYTRO Taurus oil (uninhibited transformer mineral oil) supplied by NYNAS Co.

Kraft and cotton linters pulps: Unbleached Kraft Pulp (**UKP**) and Bleached Kraft Pulp (**BKP**) from ASPA mill in Sweden (Munksjo Co.). Cotton linters (**CL**) from CELSUR in Spain. TAPPI handsheets were made with a grammage of 130 g.m² from these raw pulps using deionized water (180 µm thickness, 14 cm diameter).

Chemicals: calcium chloride (98%) and sulfuric acid (99%) were purchased from Fluka. Sodium chloride (99%), iron chloride (99%), copper chloride (98%), dimethylsulfoxide (DMSO) and magnesium chloride (98%) were purchased from Merck. Acetone, phenyl isocyanate, copper-ethylenediamine (CuED) and tetrahydrofuran (THF) were purchased from Sigma-Aldrich. Hydranal Coulomat E (Mettler) was used for Karl Fischer titration of oil.

ii) Instruments used for chemical characterization

Size Exclusion Chromatography (SEC): dry cellulosic samples were derivatized into cellulose tricarbonyl (CTCs), to make them soluble in THF used as chromatographic eluent. The chromatographic apparatus consisted in an injector system (GPC MAX VE2001) and set of coupled detectors (Viscotek TDA 302 system, included DRI, LALS, RALS and Intrinsic Viscosity detectors and a column oven, all working at 35°C). The column set included three PLGEL 10 µm mixed B columns (75x300) preceded by a PLGEL precolumn (Agilent), working at a solvent flow rate of 1 mL/min.

Viscosity-average degree of polymerization (DP_v): pulps were grinded (using a Forplex hammer grinder) and dissolved in a standard CuED solution (0.5 M in Cu, 1 M in ethylene diamine). After degassing with nitrogen, the cellulose solutions were measured for their viscosity using a Ubbelohde-type capillary viscosimeter. Intrinsic viscosity and DP_v values were calculated using the standard formula given in the (IEC 60450).

Fourier Transformed InfraRed spectroscopy (FTIR): The apparatus used was a Perkin Elmer Spectrum 65. Spectra were recorded in transmission mode. Each paper sample was analyzed in a dry atmosphere under a nitrogen gas flow in the sample chamber. Once dried in an oven, the samples were immediately taken from the oven to the spectrometer.

Karl-Fischer analysis: water determination in oil and in impregnated paper was carried out by Karl-Fischer analysis coupled to thermal desorption of the sample (oven temperature 140°C), under dry air flow. Water content analysis was analyzed by coulometry (Metrohm 831 KF coulometer coupled to Metrohm 832 Thermoprep oven).

b) Methods

i) Method development of ion exchange

There are widely available ion exchanges protocols for paper pulps. The two main methods used to remove metal ions in pulps are acid washing and chelation. Acid washing, as described by Bouchard *et al.* [4], was chosen for its simplicity and superior ability to indiscriminately remove all types of ions. After acid wash, the pulp was poured in deionized water to wash off the excess acid. A solution of sulfuric acid was used to lower the pH to 1.5. The solution was kept at this pH for 30 min then washed with deionized water until the pH came back to its initial value of 6-7. It was experimentally determined by Bouchard *et al.* that, at pH 1.5, full removal of metal cations from the pulp takes place. They also showed that the type of acid used had no influence on the efficiency of ion removal. Although the acid wash is short, there was a concern about possible cellulose depolymerization, but a test showed no depolymerization of the pulp after the treatment. Once the original metal ions were removed, the pulps were added to a solution containing dissolved metal chlorides (such as CaCl_2), following the procedure described Yantasee *et al.* [22].

ii) Ion exchange experiments

The first step was to remove the original metal cations from the pulp and the second step was to re-introduce selected ions in the pulp. Only UKP was used for ion exchange experiments, 60 g were solubilized in 3 L of distilled water to obtain a suspension at 2% consistency by weight. Then, the pH was set to 1.5 by using sulfuric acid (2 M) addition under stirring. The solution was then heated at 50°C for 30 minutes. After heating, the pulp suspension was washed on a sintered glass crucible with deionized water, until the initial pH of 6-7 was regained. To confirm none of the original ions remained in the pulp, a titration was performed on the last water used during washing and showed that there were no detectable amounts of calcium or magnesium. Once the original ions were removed, the pulp was re-suspended in a solution containing selected metal cations: main metals (Ca, Na, Mg) and transition metals (Fe and Cu). Based on literature reports, the chosen ion concentration in the solution used for pulp impregnation was 0.03 mol/L. Pulps was left under stirring at room temperature, then a new wash using deionized water on a sintered glass crucible removed unbounded ions to the pulp. The last water used during washing was also titrated and showed that there were no detectable main metals. Since iron and copper colored their respective solution, the end of the wash was indicated by the loss of color. Then, TAPPI handsheets were made with the pulps, to be used in ageing experiments. The TAPPI handsheets used deionized water to prevent new ions introduction in pulps. Mass used are visible in the table below:

Table 26: Compounds used and their corresponding mass during ion exchange experiments.

Sample	Compound used for ions exchange	Mass of compound dissolved (g)
Calcium	CaCl_2	10.1
Sodium	NaCl	5.3
Magnesium	MgCl_2	8.6
Iron	FeCl_2	11.5
Copper	CuCl_2	12.2

To assess the result of ion exchange, the ash content, after calcination at 525°C (TAPPI T211), was dissolved in acid and titrated using EDTA and conductivity titrations. Calcium, Sodium and Magnesium content was titrated using a combination of EDTA (to titrate Ca and Mg) and conductometric titrations (to titrate all the ions). Due to time-consumption, titrations were only applied to confirm the efficiency of the initial phase of ion-exchange experiments (cation removal). Metal ions quantifications of the final paper samples used for ageing were done by external analysis in Institut des Sciences Analytiques de Lyon (CNRS UMR 5280), by ICP/MS. One sample used as a reference was left without added ions after acid demineralization followed by deionized water wash. It is referred here as the demineralized sample.

iii) Size exclusion chromatography experiments

UKP, BKP and CL handsheets were tested. Each sample was aged for up to a week and compared to a reference unaged sample (Table 27). Paper was first dried at 93°C for 24 hours and was impregnated with Nynas Taurus oil. Then, ageing experiments were done at 130°C. Oil and paper were put in an open glass container that was inside a closed airtight steel bottle. Before ageing, each bottle was degassed with nitrogen to obtain a non-oxidative atmosphere (removal of oxygen). After ageing, oil was removed from paper using Soxhlet extraction with hexane. Samples were then tricarbanilated to dissolve cellulose in the chromatographic eluent (THF), then analyzed by SEC with a multidetector.

Table 27: Sample type and ageing times for samples analyzed by SEC.

Sample type	Ageing time (days)			
UKP	0	2	5	7
BKP				
Cotton				

iv) FTIR spectroscopy

Samples analyzed by FTIR spectroscopy included the main UKP, BKP and CL reference samples, as well as all the samples obtained after ion exchange. Each sample was dried and aged in the same manner than for SEC experiments. The ageing time is shown in the table below:

Table 28: Sample types and ageing times for samples analyzed by FTIR spectroscopy.

Sample type	Ageing time (days)				
UKP	0	6	16	35	46
BKP					
Cotton					
Calcium					
Sodium					
Magnesium					
Iron					
Copper					
Demineralized					

After ageing, oil was removed using Soxhlet extraction. Samples were then grinded using a Forplex grinder, the resulting fibers were used to make KBr discs. The pulps and the fibers were mixed together at a concentration of 1 mg of pulp for 100 mg of KBr powder. The mixture was put under 10 tons of pressure to make KBr discs of 1 cm diameter. Each disc was dried at 105°C for 16 hours. Then, samples were removed from the oven and directly put in the spectrometer. FTIR spectral acquisition was done in transmission mode under Nitrogen flow, each spectrum used a resolution 4 cm⁻¹ with 128 scans in a wavelength range of 1500 to 3000 cm⁻¹. Paper oxidation progress was followed by observing spectral changes in a range of 1500 - 1850 cm⁻¹ where the carbonyl groups bands develop.

3) Results and discussion

a) Ion exchange of paper

Ion exchange experiments followed the purpose of changing the metal ions profile of papers, feeding one particular metal ion in the pulp and releasing the other ones.

Identical pulps were subjected to the same concentrations of metal chlorides while changing the metal counter ion. Therefore, differences in metal concentration in the final pulp can only be attributed to differences in pulp affinity for each metal.

Event tough electrotechnical paper is purified to contain very few metal ions (especially Fe and Cu) compared to normal Kraft papers, there are still traceable amounts of iron (and very few copper), but the main cations are Mg²⁺ and Ca²⁺, introduced by ion-exchange during the last washing steps of the pulp using filtrated environmental waters.

The first sample tested was the **reference UKP**.

This sample showed the expected ionic concentration for electrotechnical grade pulps (Table 29).

Table 29: Sample types and their corresponding ion content measured by (ICP/MS).

Samples	Ca ²⁺ (ppm)	±	Na ⁺ (ppm)	±	Mg ²⁺ (ppm)	±	Fe ²⁺ (ppm)	±	Cu ²⁺ (ppm)	±
Reference (UKP)	720	22	49	22	113	13	45	6	11	6
Demineralized	none		none		none		none		none	
Calcium	641	22								
Sodium	59	4	228	22						
Magnesium	42	4			359	13				
Iron	102	4					1463	6		
Copper	48	4							1435	6

In electrotechnical papers, a high calcium content is generally associated with a low sodium content, since pulp manufacturers wash their pulps at the end of the Kraft process with purified local water (from lakes, groundwater and rivers), to reduce as much as possible the Na content in papers, known to increase the dielectric losses (tan δ value). Iron and copper are present in

minimal amounts. Their total removal is impossible by acid washing, without the risk of an important degradation of cellulose, as shown by multiple studies [11]. For the demineralized pulps, without further ion re-introduction by ion-exchange, no ash was found after calcination.

Metal cations could be successfully removed and replaced, as shown by the results (Table 29) in the different papers denoted “calcium”, “sodium”, “magnesium”, “iron” and “copper”. In parallel to target metal quantification, residual calcium was measured made in each sample. The observed decrease in calcium concentration shows that the initial ions in UKP were successfully removed during the first demineralization step. It is also clearly shown that main metals (Ca, Mg) have much less affinity with the pulp than transition metals.

It can be noted that the “reference UKP” used in our study for ion exchange has a metal ion profile normally expected for electrotechnical papers. In Table 30 below, it can be seen that it is rather comparable to another electrotechnical-grade UKP. Both of them have a much lower main metal ion content (especially sodium) than the so-called “standard UKP” for papermaking usage. In the latter, calcium and sodium content are multiplied by two folds, and magnesium content is multiplied by four.

Table 30: Ion content for multiple types of UKP. Reference UKP denotes the samples used in this study. Electrotechnical grade UKP values are extracted from the thesis of Barnett et al. [23]. Standard UKP values are extracted from the thesis of Yantasee et al. [24].

Samples	Ca ²⁺ (ppm)	±	Na ⁺ (ppm)	±	Mg ²⁺ (ppm)	±	Fe ²⁺ (ppm)	±	Cu ²⁺ (ppm)	±
Reference UKP	720	22	49	22	113	13	45	6	11	6
Electrotechnical grade UKP	850	--	108	--	111	--	15	--	--	--
Standard UKP	1562	3	220	23	410	9	14	2	--	--

Values of ion content in electrotechnical-grade papers are dependent on many process parameters. Our reference UKP is a pure pulp, and not paper or pressboard. Iron and copper are still present in int trace amounts, meaning that strong linkages remain between transition metals and some target organic functions in pulp, mainly uronic acids in hemicelluloses (including hexenuronic acids formed during Kraft cooking), and phenolic and quinonic groups in lignin.

A few tests were carried out with more concentrated solutions of calcium, at 0.05 M. They showed insignificant differences in calcium absorption.

Results found in the literature are consistent with those found in these tests. Sodium binds consistently less than magnesium and calcium [22]. Literature studies report about competitive ion-exchange, putting together different metal ions that can bind to the pulp with more or less strength (there were no competitive ion exchanges in this study). When there is a competition between divalent ions (Mg²⁺ and Ca²⁺) and monovalent ion (Na⁺), the monovalent: divalent ion exchange ratio tends to a value of 2:1. This supports the theory that ions bind to the same functional groups (monovalent ligands), but divalent cations can bind to two ligands while monovalent cations to only one ligand, resulting in a doubled binding strength in the latter case.

Transition metals show a completely different behavior. Again, literature emphasizes that Fe²⁺ and Cu²⁺ have a very strong affinity towards fibers, and this is visible in our results with a concentration around 1450 ppm for each one. Similar concentrations mean they possibly have

the same bonding sites and similar affinities for those bonding sites. It is impossible to know if they have exactly the same bonding sites than main metal ions (Ca, Mg, Na), or just have a stronger binding strength with them. At least in the case of hexenuronic acids in Kraft pulps, it was established that metal ion binding was much stronger for transition metals than for main metals [11].

b) Effect of metal ions and chemical composition on cellulose depolymerization during ageing

Papers samples were aged in oil up to 46 days in order to reach complete degradation of the samples. At high temperature, our study confirmed the general observation that the DP_v falls rather quickly and stabilizes around the LODP value, after which a very slow decay is observed, while the oxidation of the organic matter continues. The first week of ageing, before the LODP is reached, was analyzed in more detail by using size-exclusion chromatography (SEC), in order to determine the evolution of the molar mass distribution (MMD) of cellulose. This study was only done for UKP, BKP and CL. For all the other samples, only the DP_v was used to follow depolymerization. To follow the oxidation period that takes place after the initial DP_v fall, all the samples that had aged at least one week were analyzed by FTIR spectroscopy.

Ageing was performed at 130°C in non-oxidative conditions (without air) meant to correspond as best as possible to PT working under a nitrogen atmosphere. The ageing time lasted 46 days to reach similar conditions as the ones used by Bagniuik *et al.* [19].

i) Quantifying the depolymerization of the cellulose chain

From the molar mass distribution curves, different molar mass averages can be calculated:

- number-average molar mass (M_n), defined as:
$$M_n = \frac{\sum M_i N_i}{\sum N_i} \quad (9)$$

- weight average molar mass (M_w), defined as:
$$M_w = \frac{\sum M_i^2 N_i}{\sum M_i N_i} \quad (10)$$

Corresponding DP-average values (DP_x) can be deduced by dividing M_n and M_w by M₀ (519 g/mol), the molar mass of the tricarbonylated anhydroglucose unit:
$$DP_x = \frac{M_x}{M_0} \quad (11)$$

The viscosity-average degree of polymerization (DP_v) was measured with the conventional CuED standard method.

The dispersity index (Đ_M) is used to assess the width of the molar mass distribution. It is expressed as the ratio of (M_w) and (M_n) values:

$$\text{Đ}_M = \frac{M_w}{M_n} \quad (4)$$

ii) Effect of paper composition on depolymerization rate of cellulose

UKP is represented by 3 main polymeric components (lignin, hemicelluloses and cellulose), while BKP is represented by only two components (hemicelluloses and cellulose), and CL contains a single component, cellulose.

All the samples were aged under the same conditions for all the experiments. The evolution of the average DP, calculated from the SEC experiments, are displayed in the following figure:

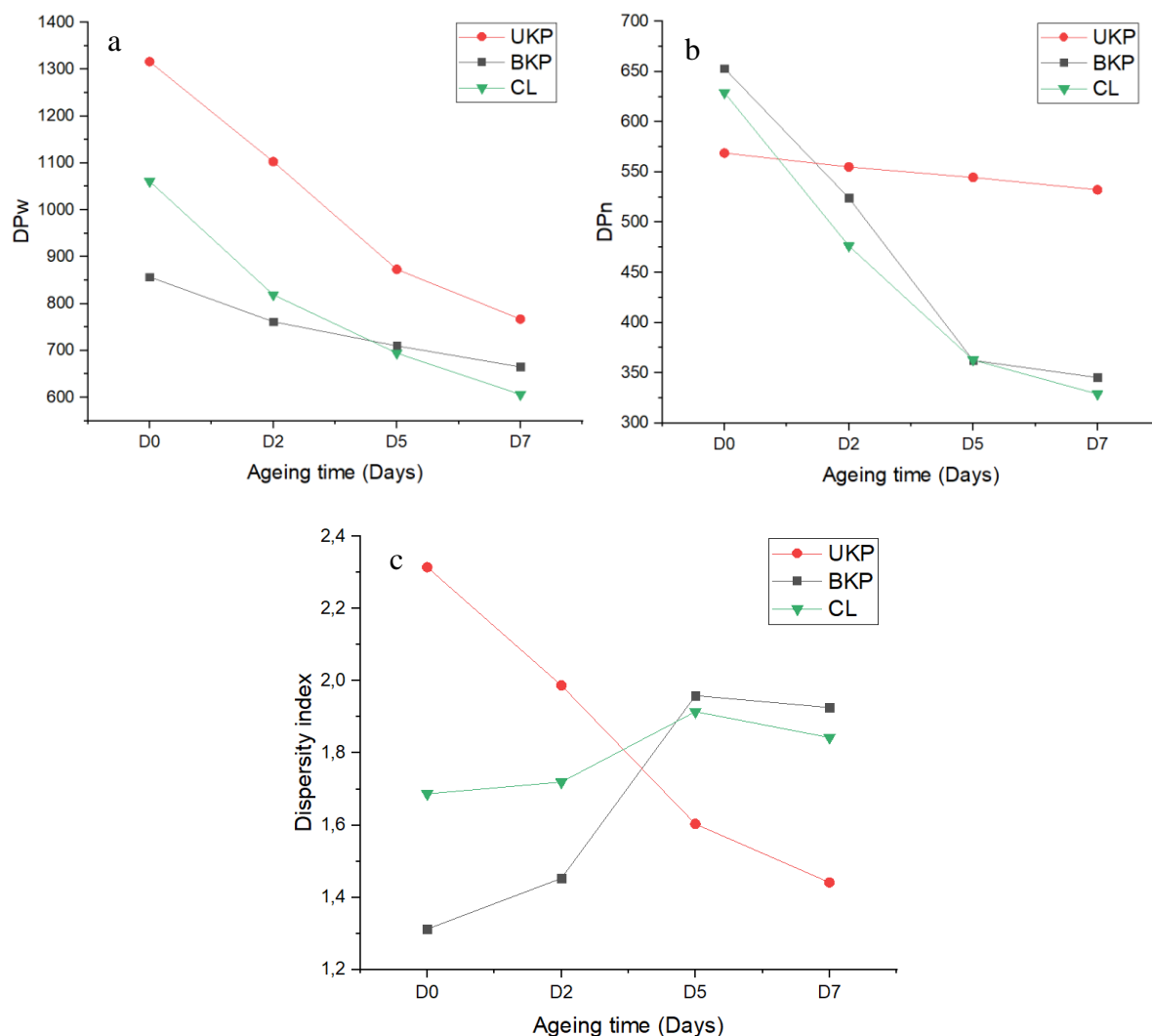


Figure 60: Evolution of the DPw (graph a), DPn (graph b) and the dispersity index (\mathfrak{D}_M) (graph c) for the first 7 days of ageing. Measurements were done by SEC after tricarbanylation.

The above figures show that there is an important contrast between the samples with and without lignin. BKP and CL, which do not contain lignin, exhibit an important DPn drop, while it remains much more stable for the lignin-containing pulp, UKP. Contrary to that, the DPw drop follows a rather similar pattern for all the samples (although the drop is slightly more pronounced for UKP).

Each behavior should be analyzed independently.

For UKP, both the DPw and DPv drop down importantly while the DPn varies much less. Therefore, it seems that ageing affects much more the longest chain of cellulose, which mainly contribute to the high initial values of DPw and DPv. In contrary, the slow decrease of DPn indicates that short chains are less affected by ageing, without an important production of new smaller chains. As a result, the dispersity index decreases significantly, meaning that the width of the chain length distribution is reduced.

Contrary to the above described behavior, BKP and CL exhibit simultaneous drops of DP_w and DP_n (although it can be noticed that the DP_w drop is less for BKP than for CL). As for UKP, long cellulose chains are degraded into smaller chains (DP_w drop), but also the smaller chains are degraded and a significant number of new chains are produced (DP_n drop). Since the loss of DP_w is slower than the loss of DP_n, there is an increase in the dispersity index, meaning a broader distribution.

Cellulose has a unique polymer composition, and the other polysaccharides, hemicelluloses, are likely to be similar in a bleached or unbleached Kraft pulp produced in the same Swedish mill, with the same wood species (a Scandinavian mix of northern softwoods in the present case). Therefore, the role played by lignin is important. It seems that the presence of lignin may protect the shorter chains from depolymerization, but not the longest chains. Some oligosaccharides might be produced for samples without lignin which brings some protective effect. These results also show that the ratio between the DP_w and DP_n is not constant. This feature has not been reported in the most recent publications, in which a constant correction factor has been used to switch from DP_v measurements to DP_n values, in order to calculate a so-called chain scission number. Such an error in the conversions between DP_w and DP_n may lead to errors in the mathematical models that were built, involving the rate of scission at different temperatures for different types of paper.

The measured DP_v variation (in CuED) during long-time degradation at 130°C is displayed in the graph below (Figure 61):

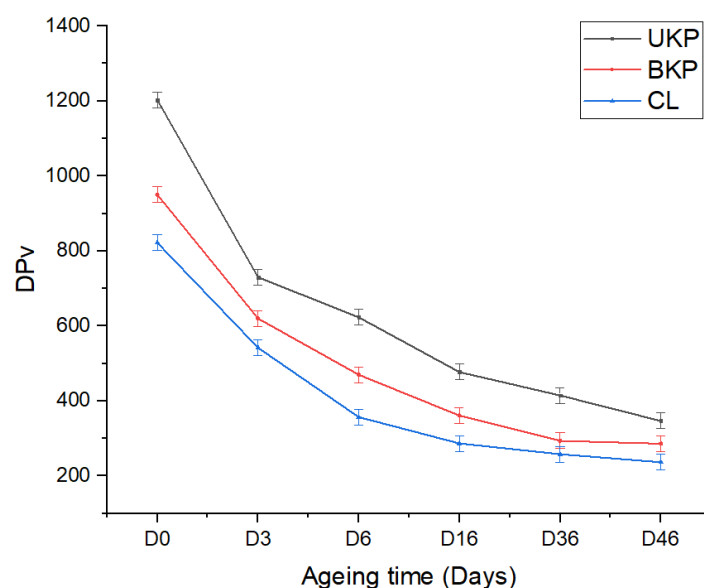


Figure 61: Evolution of the viscosity-average degree of polymerization measured in CuED (DP_v) during 46 days of ageing for unmodified UKP, BKP and CL paper samples.

The evolution of the DP_v in CuED follows the expected trend, reported in many former publications: an initial fast decay until a plateau, denoted LODP (levelling-off DP_v). Since DP_v curves are parallel, it appears that the rate of DP_v decay is rather similar for the 3 pulps; but the LODP is more rapidly attained for the CL and BKP, because of their smaller initial DP_v. According to these viscometric measurements in CuED, the rate of depolymerization does not seem to be significantly affected by the presence of lignin and the difference in the time for complete depolymerization is due to differences in the starting DP_v. In general, DP_v values are

rather close to DP_w values, since a few populations of large molecules can greatly influence the viscosity of polymer solutions. Indeed, in the present case, DP_v values measured in CuED are much closer to DP_w values measured by SEC than to DP_n values measured by SEC.

iii) Effect of (Ca²⁺, Mg²⁺, Na⁺) on cellulose depolymerization rate

It is known that sorbed calcium and magnesium ions in pulps play a role in the acidification observed during paper ageing, thus influencing the rate of cellulose depolymerization. In the present study, it was interesting to see how a pulp enriched after acid demineralization with one predominant cation behaves in comparison to the reference UKP sample.

The DP_v evolutions for UKP samples enriched with either Ca, Mg or Na are displayed in the graph below (Figure 62).

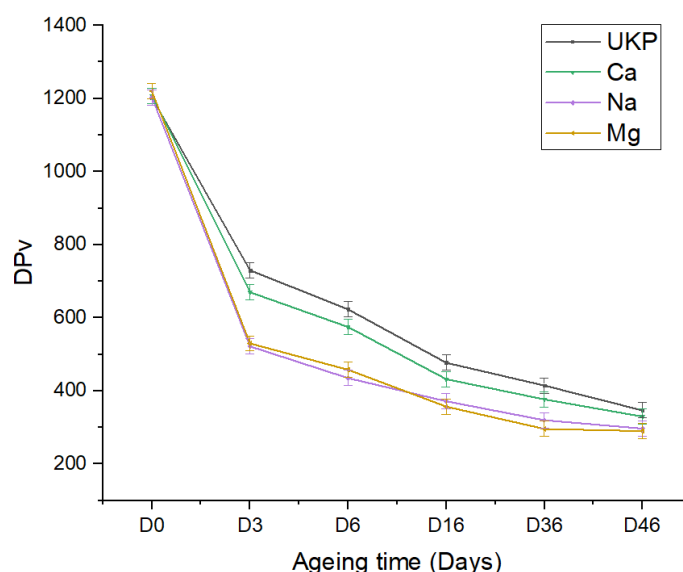


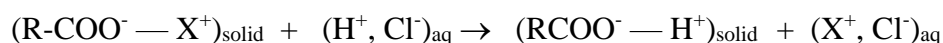
Figure 62: DP evolution during 46 days of ageing. All the samples are made with UKP. UKP was taken as a reference sample, while the other samples were submitted to demineralization followed by ion-exchange with Ca, Na or Mg.

Clearly, it can be seen that the fall of DP_v is accentuated for all the sample that underwent an ion-exchange treatment. Compared to UKP, the Ca paper seems to be the less degraded sample, the closest one to the reference UKP. It can be noticed that UKP and Ca samples have rather close calcium content. With the margin of error for DP_v measurement (about +/- 20 units), Na and Mg samples tend to behave in the same manner.

In literature, calcium is considered to have an alkaline activity that prevents an acid buildup, unlike sodium or magnesium. Moreover, the literature reports different behavior for Mg: MgCO₃ enriched paper has an alkaline reserve that the MgCl₂ used in the ion exchange does not have.

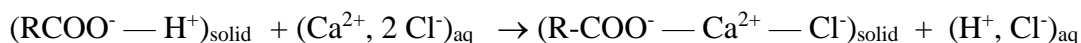
Our observations with calcium lead to the following interpretations.

During the demineralization step with HCl, all carboxyl groups in the pulp are protonated:



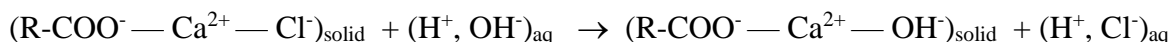
where X^+ stands for a cation initially attached to carboxyl groups in the reference pulp.

Then, because of the high affinity of Ca^{2+} with substrate carboxyl groups, introducing $CaCl_2$ in the pulp suspension gives rise to the following exchange:



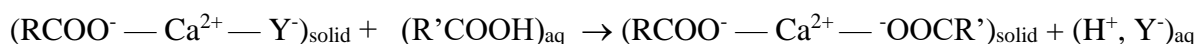
During this step, aqueous HCl is finally washed out from the pulp by pure water.

Possibly, depending on the end pH of pulp washing, a little part of the chloride ions binded to carboxyls might be replaced by hydroxyl ions, providing an alkaline reserve inside the pulp:



The presence of an alkaline reserve inside the pulp can be understood in the following way.

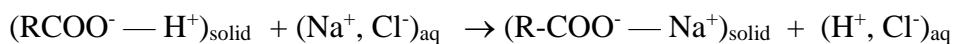
During pulp ageing, cellulose degradation releases small organic acids (denoted $R'COOH$, which are mainly acetic and formic acid). These small molecules are mobile in the liquid phase and can attach to the calcium ions attached to the substrate, giving rise to a double attachment of the kind:



where Y^- stands for Cl^- or OH^- . In the former case (calcium initially binded to Cl^-), free HCl is released in the liquid which contributes to strong catalysis of cellulose depolymerization. But if calcium is initially attached to OH^- (existence of an alkaline reserve in this case), H_2O is released and cellulose depolymerization is much less catalyzed.

In this context, the difference between the reference pulp can be explained by the fact that the reference pulp, originating from the alkaline Kraft process, contains a higher alkaline reserve (hydroxylated Ca) than the remineralized Ca pulp sample (which was remineralized by $CaCl_2$, and not $CaOH$). A probable improvement would have been obtained by carrying out a final washing of the Ca pulp by a dilute solution of NaOH or KOH, followed by careful washing with pure water to eliminate the excess sodium or potassium. Such a final Cl^-/OH^- anion exchange would have helped to create the necessary alkaline reserve to prevent cellulose depolymerization.

The case of NaCl ion exchange is different, since Na^+ is a monovalent ion which, once binded to carboxyl groups on the substrate, cannot bind to free hydroxyls (which would constitute an alkaline reserve). The exchange with NaCl can be written as follows:



The $(R-COO^- - Na^+)_{solid}$ cannot give rise to further reaction with the generated organic acids during pulp ageing. Therefore, the alkaline reserve is null in this case.

The case of $MgCl_2$ ion exchange is still a different one. It is known that Mg^{2+} has much less specific affinity than Ca^{2+} towards carboxyl groups in the pulp. In the pulp bleaching science, the case of $MgSO_4$ has been studied extensively. Mg^{2+} introduced at neutral or acidic pH can spread in the pulp without specific attachment to particular hydroxyl groups. But as soon as the pH is shifted to alkaline, colloidal $Mg(OH)_2$ precipitates are generated near to surfaces of cellulose molecules, inhibiting the action of the oxidizing radicals present (such as the short-life hydroxyl radical HO°), and possibly capturing transition metal ions. $MgSO_4$ was thus

discovered as a major protecting agent towards the oxidation of cellulose in the chemical bleaching stage involving oxygenated agents (O_2 , H_2O_2).

Therefore, in the present experiments, the rather low affinity of Mg^{2+} towards carboxyl groups of the pulp, lower than Ca^{2+} affinity (which, used as $CaCl_2$, provided a rather poor protection) makes $MgCl_2$ a very poor protective agent to inhibit cellulose depolymerization during ageing.

Finally, it can be concluded that neutral washing by $CaCl_2$, $MgCl_2$ or $NaCl$ cannot bring any better protection to the reference pulp, which was observed experimentally. In the case of calcium, and possibly magnesium, it could be interesting to generate an alkaline reserve in the pulp by further washing with a dilute alkaline solution of $NaOH$ or KOH .

iv) Effect of ion exchange with transition metal ions (Fe, Cu) on depolymerization

DPv measurements for ion exchange samples with transition metals are visible in Figure 63:

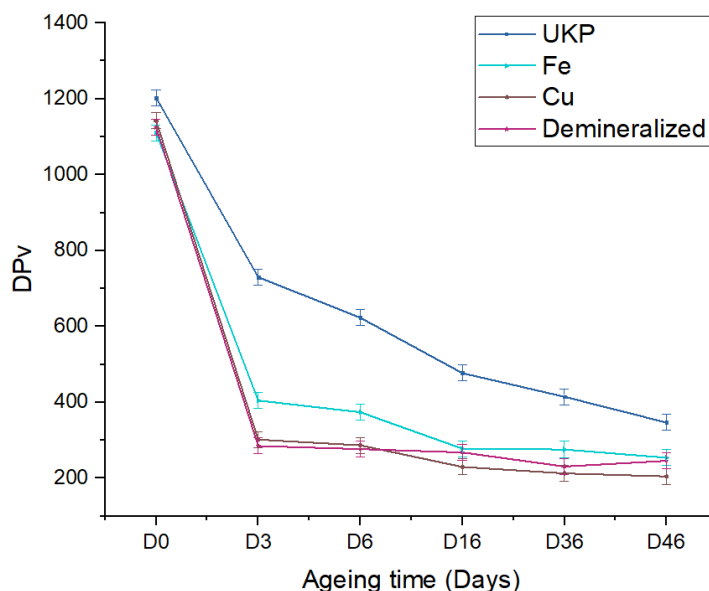


Figure 63: DPv evolution during 46 days of ageing. All the samples are made with UKP, taken as a reference. For the other pulps, UKP was first demineralized, and then submitted to ion-exchange with transition metals (Fe and Cu).

Transition metals are known to strongly catalyze the formation of oxygenated radicals, such as the hydroxyl (HO°) and superoxide ($O_2^{\circ-}$) anion radicals. It is therefore expected that they should affect the rate of cellulose depolymerization in the context of cellulose ageing in PT conditions. Indeed, compared to the behavior of the reference UKP pulp, it is immediately visible that transition metals, although in small amounts, accelerate very much the drop of DPv. Cu paper reaches the LOPD value in about 3 days. Fe paper (in which Fe^{2+} and Fe^{3+} are more hydroxylated than Cu^{2+}) gives rise to a little slower cellulose depolymerization. Cu^{2+} and Cu^+ are known to have a stronger catalytic effect in the Fenton reaction than Fe ions.

It is interesting to notice that the demineralized pulp, in which the acidity was not neutralized after the ion exchange, degrades as fast as the Cu pulp. Reaching the LOPD means that the amorphous phase in the cellulose chains is fully degraded by acid hydrolysis, which occurs in

a very little time at this temperature. It is thus important, after demineralization, to re-cationize the pulp and if possible, to create an alkaline reserve in it.

c) Effect of chemical composition on paper oxidation during ageing

i) Oxidation of the cellulose chain

Paper ageing is traditionally followed by cellulose depolymerization. In this process, acid hydrolysis plays a major role, but cellulose oxidation is also involved. Moreover, it plays a role in the loss of macroscopic mechanical properties. Although they are distinct processes, acid hydrolysis and oxidation of the cellulose chains can exert a catalytic or synergetic effect on each another, because oxidation results in the formation of weak carboxylic acids which promote acid hydrolysis. The latter leads to the formation of new reducing end groups on cellulose chains, which are substrates for oxidation. Additionally, oxidation produces water and acids that are responsible for an increase of hydrolysis and consequently, water production. Water supplies protons for hydrolysis and active oxygen for oxidation.

In this study, it was therefore decided to follow pulp oxidation at the same time as cellulose depolymerization.

Oxidation can be followed by FTIR spectroscopy in the range of 1500 to 1800 cm^{-1} where the carbonyl bands appear. As previously explained, there are many types of oxidations that can happen inside insulation paper. The two visible bands at 1740 and 1620 cm^{-1} were assigned to aldehyde groups, (-CHO), carboxylic acids (-COOH) and highly conjugated ketones (-C=O). These are the only type of oxidized groups detectable by this technique, with no way to discriminate where the oxidations are located on the cellulose chains. It should be noted that unlike the reference study done by Bagniuk *et al.* [19], samples were analyzed with the KBr disc method and not by mechanical thinning of paper. Using KBr disc does not change the transmission values of the signals, in both studies, comparable Cotton reference samples had similar ageing behavior and absorbance values in the same order of magnitude from 0.001 to 0.020. A noise effect was not observed for highly degraded samples since, this method doesn't rely on the mechanical properties of paper (the pulp is grinded).

A first observation was that surprisingly, the acid wash treatment had an effect on the unaged pulps. It increased the amounts of aldehyde and carboxyl groups. Prior to this observation, only the DP_v had been used to evaluate whether the acid wash had caused any damage to the pulp. Without any change of DP_v, it had been concluded that the acid wash created no damage to the pulp.

Following the finding that some oxidation damage was brought to the pulp by acid washing, all the remineralized samples were analyzed by FTIR before ageing. It was found that despite no change of DP_v, pulp oxidation occurs. Characteristic bands for aldehydes and carboxylic acids (1720 cm^{-1}) increased significantly, while conjugated ketones (1620 cm^{-1}) remained very close to their original value. As an example, the signal for demineralized pulps and the reference UKP is shown in the following Figure 64:

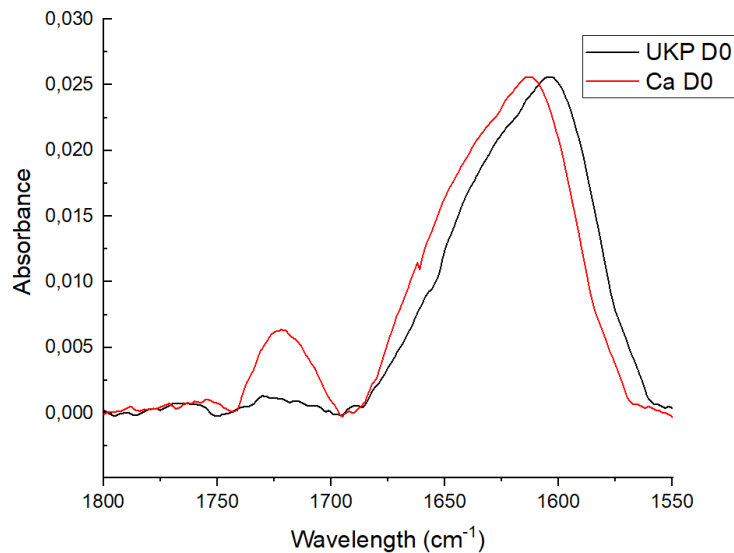


Figure 64: FTIR spectra of the untreated reference UKP and Ca paper. Both samples were unaged. Characteristic bands arising at 1720 cm^{-1} correspond to aldehyde and carboxylic acids signals. The peak for conjugated ketones around $1600\text{-}1620\text{ cm}^{-1}$ barely changed.

Such an increase either comes from the C6 oxidation (aldehyde formation) or from carboxylic acids formation. It should be noted that lignin oxidation could also play a role in this increase. It can also be noted that for the Ca paper, the signal for conjugated ketones at 1620 cm^{-1} is slightly shifted to the left; this is a known interference from calcium, but a similar shift was observed for other ions.

ii) Effect of the pulp's composition on the oxidation of paper

The effect of the main polymer composition in the pulp was studied by comparing unaged UKP, BKP and CL samples. Demineralized samples are also compared to the unmodified UKP.

The obtained FTIR spectra are displayed below in Figure 65:

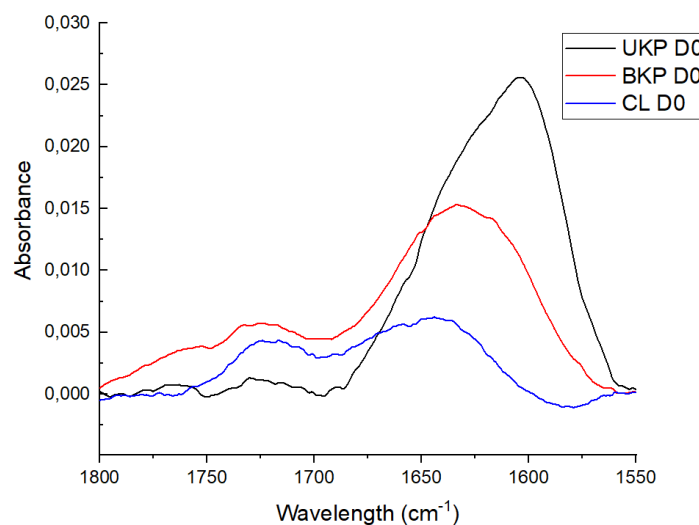


Figure 65: FTIR spectra of unaged UKP, BKP and CL samples.

There is a strong contrast in the initial oxidation state of UKP, BKP and CL. The conjugated ketones band at 1620 cm^{-1} is much higher in UKP, thus attributed to the presence of lignin. Aldehydes and carboxylic acids at 1740 cm^{-1} are almost undetectable in UKP. Aldehydes from reducing end groups (REGs) of polysaccharides barely contribute to this signal, which is also reported in the literature [19]. It is considered that there are too few REGs and their presence is drowned by the other signals. BKP, and to a lesser extent CL, have similar numbers of REGs as UKP (since their DP_v are of the same order). Peaks at 1740 cm^{-1} were observed in BKP and CL but not in UKP. They must come from oxidation damages during bleaching of BKP and CL, since both of them have been subjected to oxygenated bleaching agents (especially hydrogen peroxide) in the bleaching sequence. Indeed, UKP and BKP come from the same factory, but UKP was not subjected to a bleaching sequence. It should be noted that in Bagniuk's study [19], the P1 samples (containing 99.5% cellulose) showed a similar signal as BKP and CL in our study. This is coherent since their samples was purified from lignin.

Ageing of the Cotton Linters pulp sample:

Ageing of the CL sample was followed during 46 days. Figure 66 shown below depicts the evolution of the FTIR spectra:

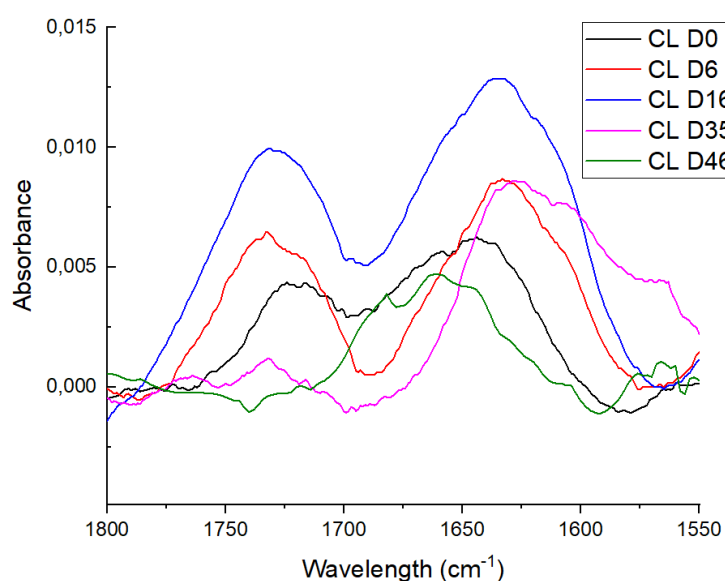


Figure 66: Evolution of the absorbance value for CL samples during 46 days of ageing.

It is shown a graduate increase of the aldehydes and carboxylic acids signal at 1740 cm^{-1} , and correspondingly, a slower increase of the conjugated ketones signal (1620 cm^{-1}). Both peaks reach their highest value after 16 days (D16). When the ageing time is prolonged, signals at 1740 and 1620 cm^{-1} tend to decrease. After 46 days, the two signals have almost completely vanished, but a large signal around 1650 cm^{-1} has arisen.

A similar behavior was observed in the study of Bagniuk [19]; the CL sample in our study is of similar composition as the P1 pure cellulose sample aged at 150°C in Bagniuk's study. Their study also exhibited a disproportional increase of the signal of aldehydes and carboxylic acids, compared to that of conjugated ketones.

Ageing of the BKP sample:

The obtained FTIR spectra are shown in the Figure 67 below:

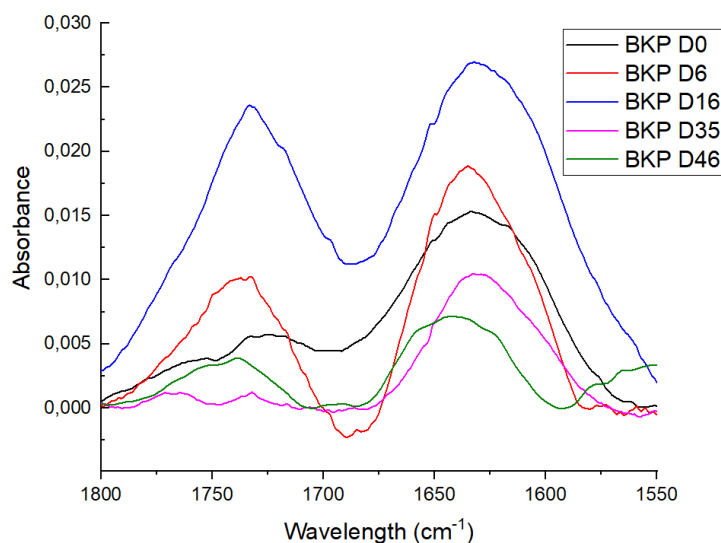


Figure 67: Evolution of the absorbance value for BKP samples during 46 days of ageing.

A rather similar ageing behavior can be observed for the BKP sample. This looks coherent since there is an important molecular similarity between cellulose and hemicelluloses. The only notable difference is that the ratio between the signal at 1740 cm^{-1} over that at 1620 cm^{-1} is higher, indicating that there is a higher proportion of acid groups over ketones. It can also be seen that signal intensities for BKP are higher than that for CL. Hemicelluloses are likely to be more prone to oxidation. Samples used in Bagniak's study do not match our observed signals for the BKP.

Ageing of the UKP sample:

The obtained FTIR spectra are shown in the Figure 68 below:

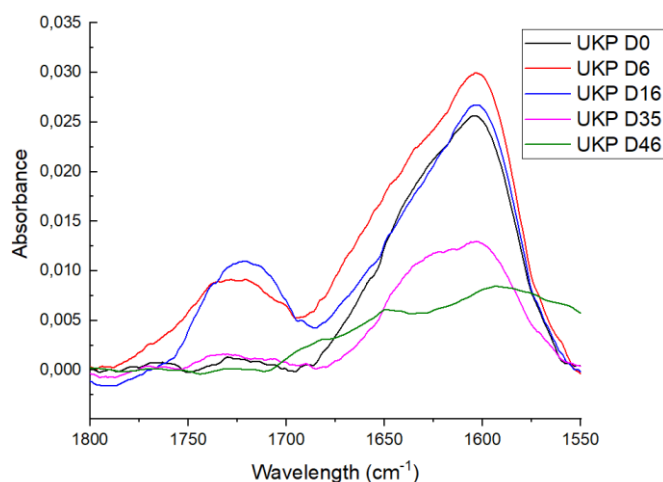


Figure 68: Evolution of the absorbance value for UKP samples during 46 days of ageing.

For UKP, a similar behavior is globally observed but with different intensities. The buildup in aldehydes and carboxylic acids signal at 1740 cm^{-1}) is less pronounced than that of BKP. The conjugated ketones signal at 1620 cm^{-1} is much higher since the beginning of ageing, and it increases only slightly. There is less oxidation than for BKP or CL, and the ratio between the signals shows that oxidation produces comparatively less acids. These results were expected since lignin is known to have an antiradical activity that hinders extended oxidation, yielding acid formation. A comparison with the UKP used in Bagniuik's study shows similar tendencies with no aldehydes and carboxylic acids (1740 cm^{-1}) buildup, like for the transformer samples used in his study.

This study leads to conclude that the presence of lignin in the sample introduces a main difference of ageing behavior of the pulps. UKP is clearly much less oxidized than lignin-free pulps, especially with much less formation of conjugated ketones. The results from Bagniuik also support this observation, since transformer samples also behave in this way. The claim in this study is that the analyzed samples are lignin-free, but this is probably a mistake, since PT normally use UKP and not BKP (nor CL). Also, in their PT samples, there is a clear FTIR signal at 1520 cm^{-1} , which is characteristic of lignin. Our study clearly shows that lignin protects the pulp and inhibits partly the formation of oxidized groups during ageing, compared to the BKP with the same chemical composition, except that it is lignin-free.

Ion exchange samples:

The potential effect of the treatment should be examined. There are two factors that could influence results. The first is a possible acid damage to the pulps. However, all pulps were submitted to the same demineralization treatment and therefore have comparable acid damage. The second factor is that some pulps might have retained more protons than others since ions have different affinities with the pulp.

The demineralized pulp contains the maximum number of bonded protons. The ageing behavior of the demineralized pulp is shown in Figure 69 below:

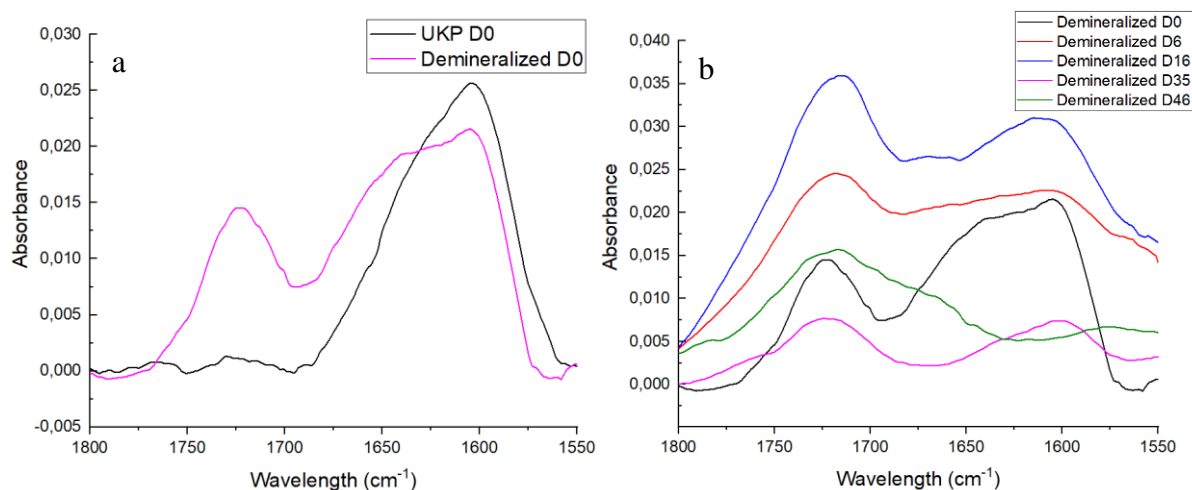


Figure 69: Oxidation behavior of demineralized pulp. a: Comparison of the unaged UKP (reference sample) with the demineralized UKP at initial time (D0). b: Evolution of the absorbance spectra of the demineralized pulp during 46 days of ageing.

The demineralized pulp is strongly oxidized since it exhibits the highest oxidation peaks. Residual acids themselves could participate in the signal. Compared to the ageing of UKP (Figure 68), there is an important increase of the aldehyde and carboxylic acids signal at 1740 cm^{-1} , but a smaller increase of conjugated ketones at 1620 cm^{-1} . Ageing of the demineralized pulp clearly produced more acidity than for the reference UKP.

iii) Ageing of Ca, Mg and Na pulps; effect on oxidation

Ageing of Ca, Na and Mg pulps can be compared to the reference UKP.

First, the different spectra at initial time (D0) are shown in Figure 70 below:

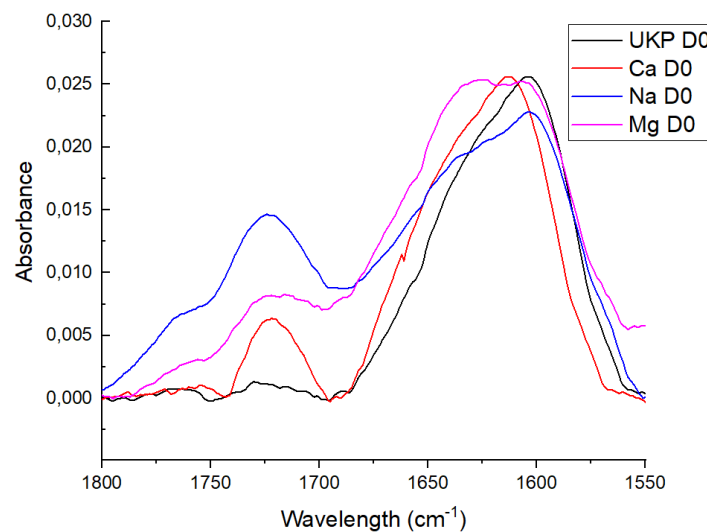


Figure 70: Spectra comparison of unaged UKP with unaged Ca, Na and Mg pulps.

Two differences with the reference UKP pulp can be seen. First, the signal for conjugated ketones at 1620 cm^{-1} is slightly shifted to the left, which can be attributed to the interference brought by the ions bonded to the functional groups. The second difference is visible at 1740 cm^{-1} . As already observed on the demineralized pulp, the acid wash leads to a growth of the signal at 1740 cm^{-1} , which was attributed to aldehydes and carboxylic acids formation during this acidic step. This is visible in all the samples that underwent an acid wash and were later remineralized. This effect appears to be the strongest one with the Na pulp, even though this pulp had the lowest ion content after ion-exchange. For some samples, there seems to be a small peak growth around 1640 cm^{-1} , especially visible in the Mg sample. This is the peak of water, as some samples had a small water contamination. Any significant amount of water can overshadow the signals of conjugated ketones.

Ageing curves during 46 days are displayed for each pulp in the graphs below (Figure 71):

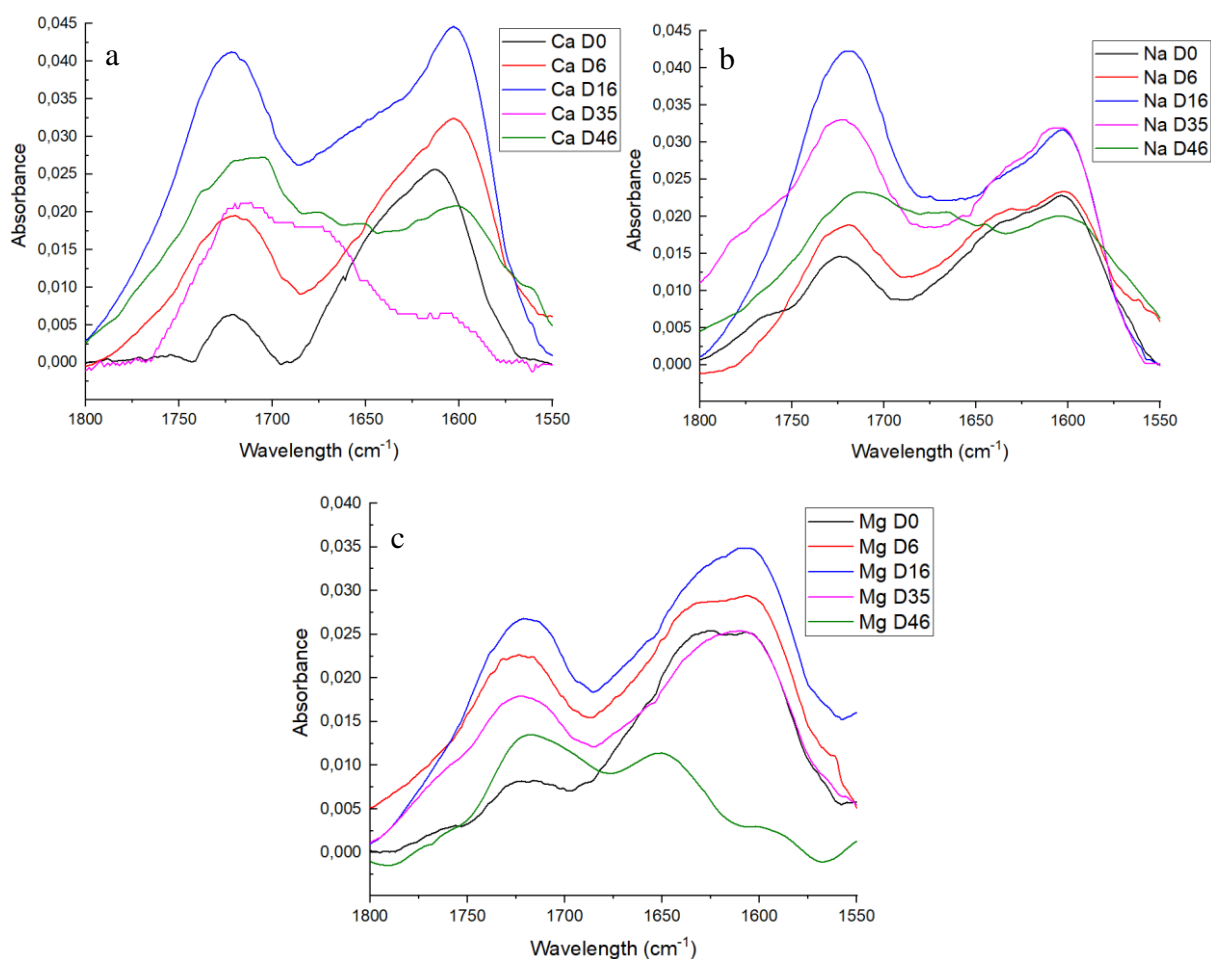


Figure 71: FTIR absorbance spectra for the Ca (a), Na (b) and Mg (c) sample during 46 days of ageing.

Calcium samples ageing showed a behavior that is reminiscent of lignin free samples. Oxidation increased and the signal ratio between aldehydes and carboxylic acids at 1740 cm^{-1} and conjugated ketones at 1620 cm^{-1} attained almost one at D16, where the highest oxidation is observed. Ageing produced more acids than before ion exchange.

Na samples ageing showed an important increase in the signal ratio between aldehydes and carboxylic acids at 1740 cm^{-1} and conjugated ketones at 1620 cm^{-1} , with acids overtaking ketone for the most degraded samples. Ageing produced much more acids than before the ion exchange.

Finally, the overall oxidation for Mg samples keeps slightly below that of Ca and Na samples. The peak ratio evolution was rather similar to that of Ca samples.

When comparing all the main metals, it is seen that the oxidation behavior of calcium and magnesium samples looks rather similar to that of the demineralized pulp samples, showing these ions had little or possibly no contribution to oxidation. Conversely, Na samples showed a significant increase in acids formation compared to the reference UKP and demineralized samples. This change can be rightfully attributed to the specific effect of sodium ions, especially since they are present in small quantities (228 ppm).

iv) Effect of ion exchange with transition metals on the oxidation of paper

Transition metals (Fe, Cu) exchanged pulps can be compared to the reference UKP before ageing, as shown by the graphs of Figure 72 below:

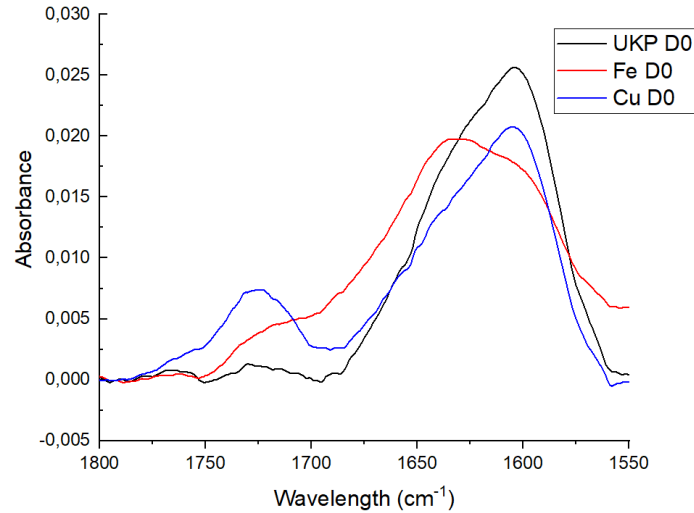


Figure 72: FTIR spectra of Fe and Cu pulps, compared to the reference UKP.

Result for unaged samples are similar to those already seen for Ca, Na and Mg pulps: the increase in the peak of aldehydes and carboxylic acids at 1740 cm^{-1} is visible on all the ion-exchanged pulps. Some of the samples also had water contamination at 1650 cm^{-1} (caused by some humidity re-absorption during sample cooling at the exit of the oven).

The ageing behavior of each transition-metal sample can be seen below in Figure 73 and Figure 74:

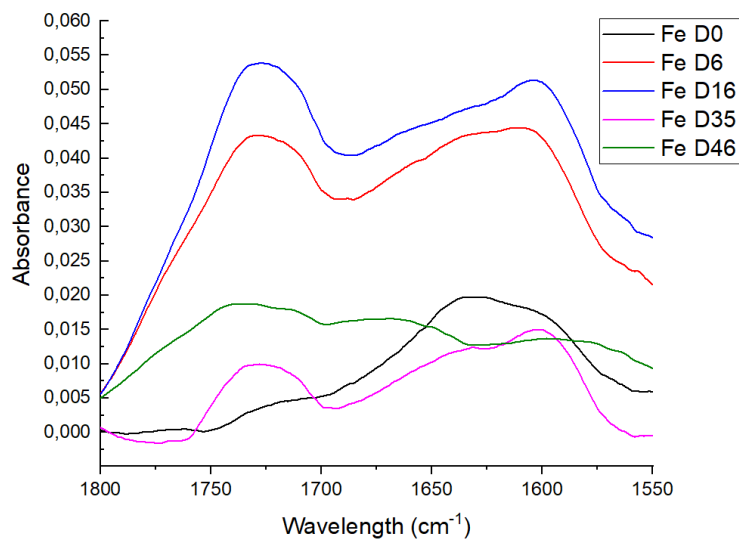


Figure 73: Evolution of FTIR absorbance spectra for Fe samples, during 46 days of ageing.

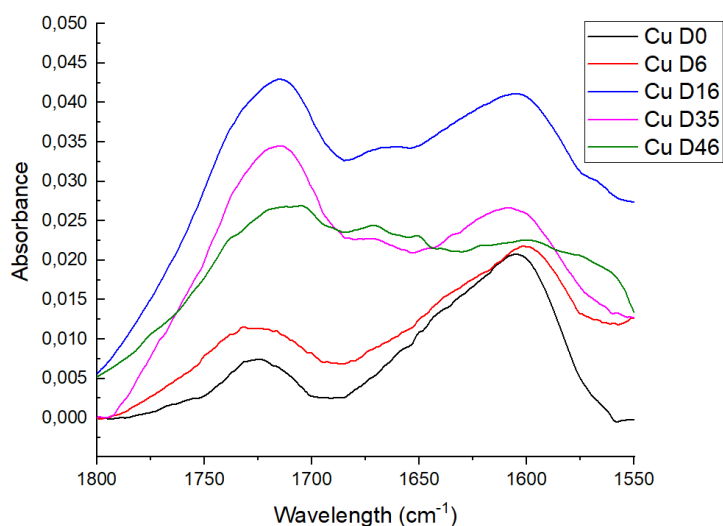


Figure 74: Evolution of FTIR absorbance spectra for Cu samples, during 46 days of ageing.

Samples with transition metals, both iron and copper, show an important increase for both aldehydes and carboxylic acids peak at 1740 cm^{-1} and conjugated ketones peak at 1620 cm^{-1} . The balance between both signals is stable with a slight advantage for the peak at 1740 cm^{-1} .

When comparing results, copper ions lead to less oxidative damage than iron ions. The reference UKP at D16 is far below the peak intensity observed with transition metal pulps. This is also the case of the demineralized pulp, for which the peak at D16 is almost multiplied by 3 for iron and 2 for copper. Again, since pulps were thoroughly washed to remove the excess acid, such differences are attributed to the specific effect of the transition metal ion on oxidation, and not simply to the acidity remained after demineralization.

v) Synthesis of the depolymerization and oxidation results

An examination of the overall behavior of the samples should be taken by combining all the known evolutions detectable by depolymerization and oxidation. Through oxidation, it was possible to see that degradation doesn't constitute a straightforward path to an increase in the oxidation and that this oxidation is not necessarily proportional to the depolymerization.

A behavior that was observed on all the samples was an increase and then a decrease of the total oxidation values during ageing. Unlike depolymerization, that followed a straight path down, oxidation of the pulps increased to a maximum after 16 days of ageing on all the samples (except UKP that reached their maximum after 6 days) and then decreased again after 35 days, with some of them having another increase after 46 days. To explain this behavior the chemistry of oxidation, it should be noted that paper is not isolated during ageing; it interacts and exchanges byproducts of ageing with the oil and indirectly with the gas layer inside the ageing vessel (or gas layer of PT in real life applications), these interfaces constantly exchange byproducts that can therefore exit or enter the Kraft insulation. Oxidized products, can decompose or rearrange in the paper to produce oligosaccharides that are small enough to be dissolved in oil (*i.e.* methanol), eventually some of them can turn into well-known gases that even escape into the gas phase, and in free breathing reactors: the atmosphere. All these byproducts were once part of paper and therefore of the overall oxidation signal detected by FTIR. It can be postulated that at the start of ageing, acid hydrolysis and oxidation increase the

overall oxidation of the pulp. Yet, once a chemical function is oxidized it can go into a further downwards path that eventually leads to an ever-simpler molecule that in high temperatures can change, for example, from complex molecules such as glucose or guaiacyl units into smaller molecules such as methanol. To further examine this change, one of the curves was analyzed at a lower range down to 1500 cm^{-1} ; it is known that in FTIR spectroscopy, it is possible to see the signal of aromatic lignin groups at 1520 cm^{-1} , the results are visible in Figure 75 below:

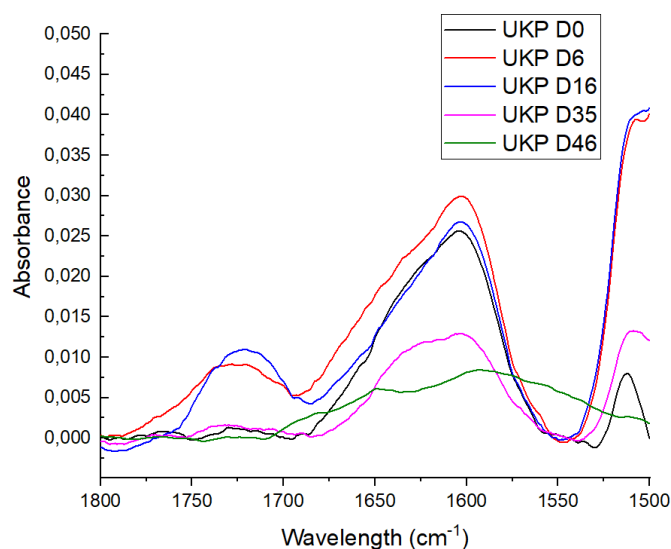


Figure 75: Evolution of the absorbance value for UKP samples during 46 days of ageing. This figure includes the values going from 1800 to 1500 cm^{-1} to show the degradation of lignin visible at 1520 cm^{-1} .

Above, the overall value of oxidation is shown to increase up to the 16 days and then decrease after. At the same time, a clear pattern emerges since the peak of aromatic lignin (1520 cm^{-1}) decreases after 16 days of ageing. This shows lignin is being degraded during ageing and since matter doesn't just disappear, it is safe to assume a part of lignin is degraded into simple chemical compounds that could exit the paper through the paper-oil interface. In the reference study, this zig zag behavior is also observed for P1 samples aged at 90°C and the transformer samples.

A further look at how the oxidation behavior of each type of sample compares to the depolymerization is visible below. For this, the integral value of the oxidation of each signal was integrated following the method developed by Bagniuk *et al.* [19]. The signal OI_{FTIR} represents the integral value for the oxidation going from 1800 to 1500 cm^{-1} . A comparison to the reference study is limited because they did not use the same ageing temperatures (90 and 150°C) although the integrated oxidation values were in the same order of magnitude for both studies, between 1 at 4. It should be noted OI_{FTIR} is the overall oxidation value for both the aldehydes and carboxylic acids peak (1740 cm^{-1}) and the conjugated ketones peak (1620 cm^{-1}); this signal doesn't discriminate how much each peak contributes to the overall value. Therefore, the oxidation ratio between both peaks was calculated for each sample. Below are the oxidation and depolymerization values of all samples present in this chapter (Figure 76) and the corresponding ratio between both peaks (Figure 77):

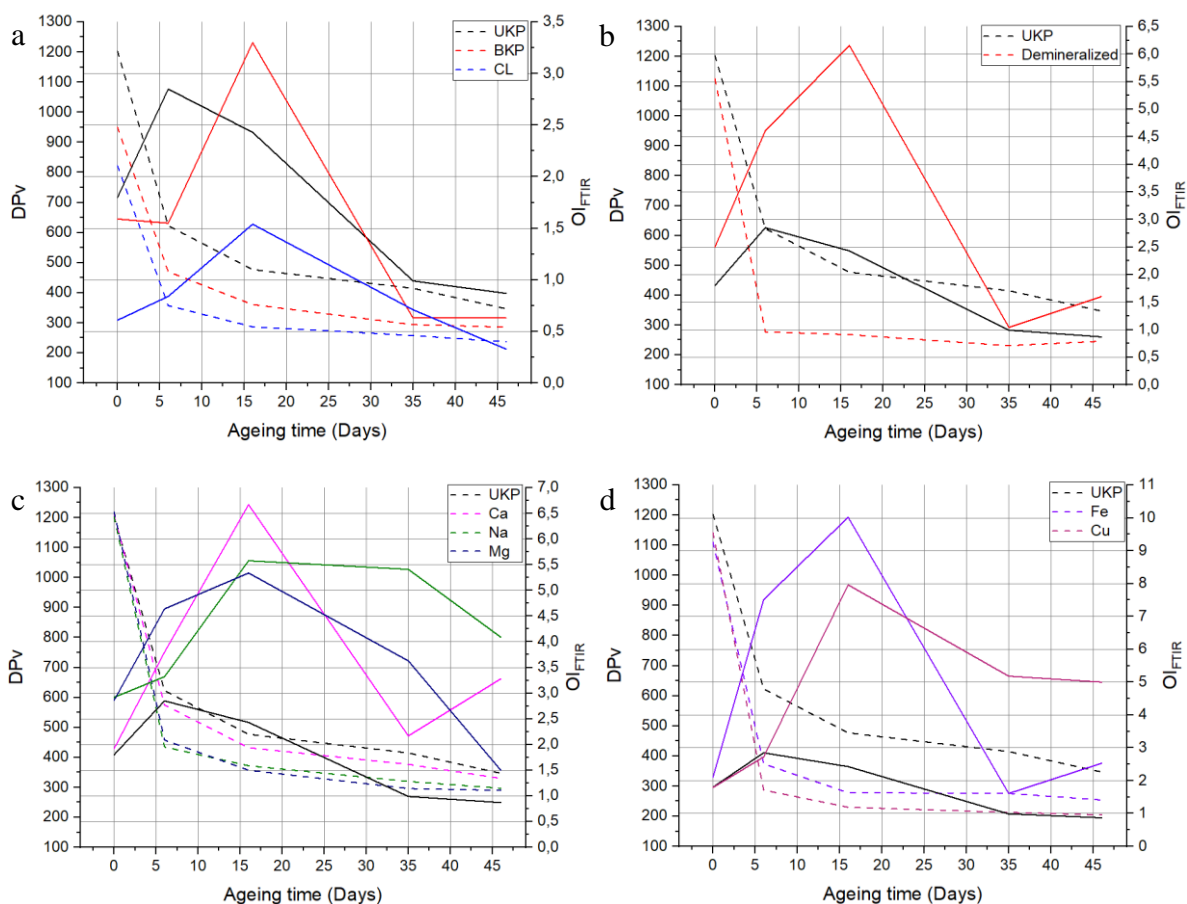


Figure 76: Evolution of the absorbance and depolymerization value for ion exchange during 46 days of ageing for samples of multiple compositions (a), demineralized samples (b), ion exchange samples with main (c) and transition (d) metals. Dash lines represent DPV while straight lines represent OIFTIR.

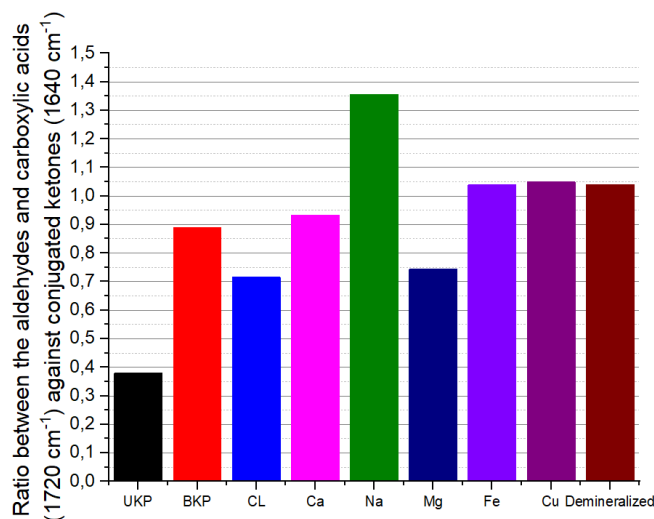


Figure 77: Evolution of the peak ratio between aldehydes, carboxylic acids (1740 cm^{-1}) and conjugated ketones (1620 cm^{-1}) for the samples with the highest oxidation levels. All the samples reached their highest oxidation value after 16 days except for UKP that reached their highest oxidation value at the 6 day of ageing.

A general outlook into depolymerization and oxidation shows an increase in the OI_{FTIR} signal around the time each sample is reaching the LODP and then a decrease in the oxidation value. It could be speculated that an important part of the initial increase is the result of by-products of the initial acid hydrolysis of weak glycosidic bonds in the amorphous phase of cellulose. These byproducts can then further degrade and dissociate from the pulp. Most of the signals seem to bounce back at D46, it is unlikely this behavior is the reflection of another increase in the oxidation and could better be attributed to the flattening of the FTIR signals that makes integrations prone to errors. Nevertheless, all the samples did not behave in the same manner, the organic and metallic composition drastically altered their ageing behavior. For UKP, an analysis of the neutralization value with KOH was done for the oil samples used during ageing, this analysis quantifies the amount of dissolved acids present in the oil by doing a titration of the dissolved acids with OH^- . Results can be seen in Figure 78 below:

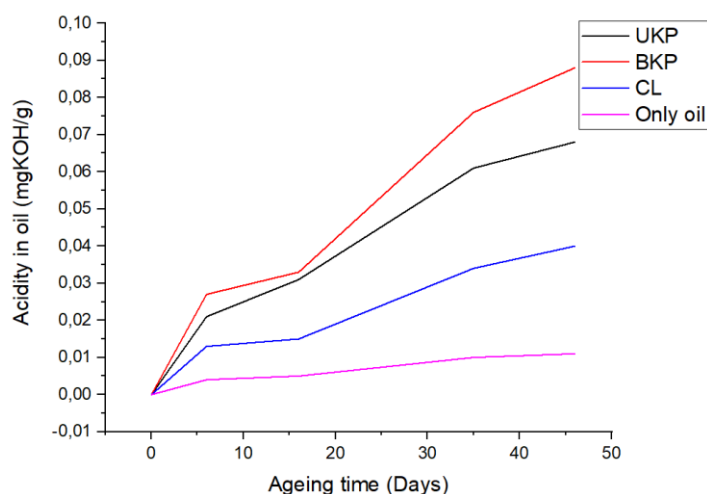


Figure 78: Evolution of the acidity level of oil during ageing for UKP, BKP and CL. An additional result is shown for oil aged without paper, called “Only oil”. Results shown are for the amount in mg of neutralized KOH for each g of oil.

When examining the acidity of each oil, a clear trend appears; the amount of acids dissolved in oil quickly increases after a plateau around the sixth day, this increased seems to be delayed for UKP and CL to the sixtieth day. Meanwhile, oil without paper only shows a small increase in acidity. From these results, two main interpretations can be drawn. First, the increase in the acid content corresponds with the loss in the oxidation value OI_{FTIR} . For the other samples, the acids certainly come from the paper samples. The increase in acid content seems to have plateau that correlates to the OI_{FTIR} peak, it can clearly be seen that the acidity takes off only after D16 for BKP and CL while it increases much sooner for UKP.

Results for UKP, BKP and CL were coherent with the chemistry of their components. Before ageing, OI_{FTIR} does not represent the same chemical function for all the samples; for each sample it represents the oxidative damage of its components; UKP (cellulose, hemicellulose and lignin), BKP (cellulose, hemicellulose) and CL (cellulose). BKP and CL start with a higher proportion of aldehydes and carboxylic acids (1740 cm^{-1}) that certainly come from the bleaching process since UKP doesn't show this peak. UKP shows signal for aldehydes and carboxylic acids peak (1740 cm^{-1}). Given their similarities (DPv, wood source, origin) the difference in the OI_{FTIR} of UKP and BKP is minimal, showing a small signal from lignin. CL is harder to compare since there are more chemical differences between the signal but the lower

initial value is coherent since unaged cellulose should have less oxidized groups than hemicellulose or lignin.

During ageing, it is interesting to observe the behavior of pure cellulose; the actual depolymerization speed of CL is slower than BKP while the oxidation is higher. Given its chemical structure, hemicellulose is inherently more susceptible to oxidation than cellulose; BKP therefore shows a higher OI_{FTIR} than CL. UKP shows the smallest increase in the OI_{FTIR} signal, it should be noted that given this small oxidation ratio (0.4), most of the increase represents conjugated ketones and not acids like BKP and CL. Only unmodified UKP reached its peak OI_{FTIR} after 6 days, lignin antiradical's role is fully apparent with an almost total disappearance of the signal, the change in the delay most probably comes from the lower amount of acids.

Before examining ion exchange samples, a look into demineralized samples is warranted. It should be remembered that the potential effect of the ion exchange experiments can come from two sources, besides the ions, they are the oxidative damage in the pulp and residual acids. Demineralized samples showed an increase in acid production compared to the reference UKP, this is the maximal potential impact coming from the residual acids. The oxidative damage will be equal between pulps and therefore can be dismissed when comparing ion exchange samples. Before ageing, all the ion exchange samples have almost the same degree of oxidation, slight variations seem to be derived from small amount of water contaminations.

During ageing, ion exchange samples should be first compared to both the reference UKP sample and the demineralized samples. When observing the oxidation ratio, it can clearly be seen there are acid lead oxidation with a high oxidation ratio for Fe, Cu and demineralized samples while Ca and Mg have a ketone lead oxidation. Samples with acid lead oxidation behavior also showed the highest oxidation OI_{FTIR} values. More importantly, acid lead oxidation had a complete drop of DP_v after 6 days while oxidation lead samples took around 40 days. In the case of Na, there is a high oxidation ratio but the overall OI_{FTIR} value remains similar to the other main metals, the slow depolymerization behavior also correspond to the other main metals. In practice, the additional acidity from sodium doesn't affect the depolymerization rate of cellulose.

Conclusion

Cellulose ageing in oil is a heterogeneous process that leads to changes in paper physical and chemical properties and loss of cellulose DPv. Degradation of paper in oil may not follow a uniform behavior. Oxidation affects chemical groups in paper. Small molecules that results from the oxidation or from the acid hydrolysis can either be released from paper by diffusion in oil, or stay in paper and further degrade into smaller molecules. The degradation process of cellulose interacts with the environment around the paper, *i.e.* the oil and the gas phase inside the ageing vessel used at laboratory.

During ageing, an acid build-up was observed at the time kinetics of depolymerization were transition to a first order kinetics. It can be said that, during ageing, paper submerged in oil produces important amounts of acid byproducts that come from the initial easy zero order degradation kinetics of the amorphous phase, this acid production is slowed once a transition to a first order kinetics is reached. These byproducts are highly oxidized forms of cellulose, hemicelluloses and lignin that are even more vulnerable to degradation than the untouched components, it is therefore logical that without at new supply of acids, their degradation will entail a progressive decrease in size of this molecules. Given enough degradation, each byproduct can reach a stage where it can migrate to oil. Then, depending on the properties of the acids (hydrophilic, lipophilic) it will solubilize or dissolve in oil. An equilibrium will start to appear between the concentration of the acid in oil, paper and gas, this equilibrium is called the partition coefficient. It is known that many byproducts end in the oil and gas phase (Chapter 2), but it should be noted since they come from paper, their appearance in the oil means they are no longer in paper, therefore lowering the oxidation state of paper.

The ageing behavior of the samples of this study showed the organic and mineral composition of paper can play a critical role during ageing. Early results showed the polydispersity index of UKP changed during ageing, this information should be considered for the mathematical models used to model ageing. A further demonstration of lignin's role against an acid build up was visible, because UKP samples produced significantly less acid oxidation than lignin free samples (BKP, CL). Hemicellulose were also shown to be more vulnerable to acid degradation than cellulose. Regarding metallic composition, it is visible that even a small metallic contamination (in the order of ppms) can drastically change the depolymerization and oxidation during ageing. Oxidation and hydrolysis showed intertwined ageing behaviors. Oxidation, and especially acid oxidation, showed to correlate with the depolymerization speed of cellulose. Calcium, magnesium, and to a lesser extent sodium, showed a lower proportion of acid lead oxidation that correlates to slower kinetics of depolymerization while iron and copper showed an important acid oxidation that correlate to an immediate drop of the DPv to LODP levels.

It is hoped this study shade some light on the ageing of Kraft insulation and that eventually it will contribute to a more accurate assessment of the state of Kraft insulation that goes beyond the degree of polymerization. A further interesting fact, that will be develop on the next chapter, is that the oxidation state of cellulose correlates to changes in the dielectric properties. This study was limited by the available time and constraint resulting from the coronavirus pandemic, a study of the relation between the amount of paper and the available volume of oil and gas could be coupled to a chromatographic study to match dissolved compounds with known degradation pathway in order to map which molecules are responsible

for these changes in oxidation. An analysis technique that could better discriminate between the oxidation damages, such as CCOA labelling, could also further map the exact nature of the byproducts of degradation.

References

1. Axega°rd, P.; Carey, J.; Folke, J.; Gleadow, P.; Glullichsen, J.; Pryke, D.C.; Reeve, D.W.; Swan, B.; Uloth, V. Minimum Impact Mills: Issues and Challenges. Proceedings of the 1997 TAPPI Minimum Effluent Mills Symposium. TAPPI, 1997, 9–21.
2. Brooks, T.R.; Edwards, L.L.; Nepote, J.C.; Caldwell, M.R. Bleach Plant Closeup and Conversion to TCF: A Case Study Using Mill Data and Computer Simulation. TAPPI, 1994, 77(11), 83.
3. Šelih VS, Strlič M, Kolar J, Pihlar B. The role of transition metals in oxidative degradation of cellulose. *Polym Degrad Stab.* 2007, 92(8):1476–81.
4. Luc Lapierre, Michael Paleologou, Richard Berry and Jean Bouchard. Limits of Metal Removal from Kraft Pulp by Acid Treatment. International Pulp Bleaching Conference Proceedings. 1997, 539–42.
5. Ko_car D, Strlic M, Kolar J, Rychly´ J, Matisova´-Rychla´ L, Pihlar B. Ageing and stabilisation of polymers. 2005, p.88–407.
6. Schuchmann MN, Von Sonntag C. Hydroxyl radical-induced oxidation of diethyl ether in oxygenated aqueous solution. A product and pulse radiolysis study. *J Phys Chem*, 1982, 86(11):1995–2000.
7. Helfferich, F. Ion Exchange. Dover Publications, 1995, Vol 7, p.267.
8. Katz, S.; Beatson, R.; Scallon, A. The determination of strong and weak acid groups in sulfite pulps. *Svensk Papperstidn*, 1984, R48–53.
9. Buchert, J., Teleman, A., Harjunpää, V., Tenkanen, M., Viikari, L., and Vuorinen, T. Effect of cooking and bleaching on the structure of xylan in conventional pine kraft pulp. TAPPI, 1995, p.125–30.
10. Rudie AW, Ball A, Patel N. Ion Exchange of H⁺, Na⁺, Mg²⁺, Ca²⁺, Mn²⁺, and Ba²⁺ on Wood Pulp. *J Wood Chem Technol*, 2006, 26(3):259–72.
11. Kim Granholm, Leo Harju, and Ari Ivaska. Desorption of metal ions from kraft pulps. Part 1. Chelation of hardwood and softwood kraft pulp with EDTA. *Bioresources*, 2010, p.206–26.
12. Łojewska J, Miśkowiec P, Łojewski T, Proniewicz LM. Cellulose oxidative and hydrolytic degradation: In situ FTIR approach. *Polym Degrad Stab*, 2005, 88(3):512–20.
13. Łojewska J, Lubańska A, Miśkowiec P, Łojewski T, Proniewicz LM. FTIR in situ transmission studies on the kinetics of paper degradation via hydrolytic and oxidative reaction paths. *Appl Phys*, 2006, 83(4):597–603.
14. Kato KL, Cameron RE. A review of the relationship between thermally accelerated ageing of paper and hornification. *Cellulose*, 1999, 6(1):23–40.
15. Potthast A, Rosenau T, Kosma P. Analysis of Oxidized Functionalities in Cellulose. In: Klemm D, editor. *Polysaccharides II*. Springer Berlin Heidelberg, 2006, p.1–48.

16. Zhu Y, Zajicek J, Serianni AS. Acyclic Forms of [^{13}C]Aldohexoses in Aqueous Solution: Quantitation by ^{13}C NMR and Deuterium Isotope Effects on Tautomeric Equilibria. *J Org Chem*, 2001, 1;66(19):6244–51.
17. Klemm D. *Polysaccharides II*. Berlin New York. Springer, 2006. p.8–15.
18. Potthast A, Rosenau T, Kosma P, Saariaho AM, Vuorinen T. On the Nature of Carbonyl Groups in Cellulosic Pulps. *Cellulose*, 2005, 12(1):43–50.
19. Bagniuk J, Pawcenis D, Conte AM, Pulci O, Aksamit-Koperska M, Missori M, et al. How to estimate cellulose condition in insulation transformers papers? Combined chromatographic and spectroscopic study. *Polym Degrad Stab*, 2019, 168:108951.
20. Calvini P, Gorassini A. FTIR – Deconvolution Spectra of Paper Documents. 2002, 23(1).
21. Y.Lin S, Carlton W. Dence. *Methods in Lignin Chemistry*. Springer Verlag, 1993, Chapter 4, p.92.
22. Yantasee W, Rorrer GL. Comparison of ion exchange and donnan equilibrium models for the ph-dependent adsorption of sodium and calcium ions onto kraft wood pulp fibers. *J Wood Chem Technol*, 2002, 12;22(2–3):157–85.
23. Axelle Barnet. *Compréhension des phénomènes de vieillissement des papiers électrotechniques dans les transformateurs de puissance et recherche de solutions industrielles*. Université Grenoble Alpes, 2020.
24. Wassana Yantasee. *Kinetic and Equilibrium Analysis of Metal Ion Adsorption onto Bleached and Unbleached Kraft Pulps*. Oregon State University, 2001.

Chapter 4: Characterization of ageing for Kraft insulation via dielectric spectroscopy and breakdown measurements.

Table of content

Introduction	143
1) Bibliographic study: dielectric study of paper ageing	144
a) Dielectric properties of an insulator: main characteristic parameters	144
i) General considerations	144
ii) Resistivity	144
iii) Permittivity.....	145
iv) Loss angle.....	146
v) Dielectric strength.....	148
b) Previous measurements and analyses of dielectric spectroscopy of Oil - Paper systems 148	
i) A cautionary statement about FDS results	148
ii) Xie et al.; Physical Model for Frequency Domain Spectroscopy of Oil–Paper Insulation in a Wide Temperature Range by a Novel Analysis Approach (2020).....	149
iv) Jadav et al.; Understanding the Impact of Moisture and Ageing of Transformer Insulation on Frequency Domain Spectroscopy (2014).....	154
v) Xia et al.; A New Method for Evaluating Moisture Content and Aging Degree of Transformer Oil-Paper Insulation Based on Frequency Domain Spectroscopy (2017). 156	
2) Materials, experimental methods, and experiments carried out.....	157
a) Materials and experimental methods.....	157
i) Chemical products	157
ii) Sample preparation and chemical characterizations	157
iii) Instruments used for chemical characterization	158
iv) Instruments used for dielectric spectroscopy.....	158
v) Instruments used for breakdown measurements	159
b) Measurements carried out	160
i) Dielectric spectroscopy experiments in oil.....	160
ii) Dielectric breakdown experiments	161
3) Influence of paper chemical and residual metal composition on dielectric properties during ageing	161
a) Objectives.....	161
b) Preliminary results.....	162
i) Calibration of measurements	162
ii) Dielectric properties of oil and non-impregnated UKP paper.....	162
iii) Dielectric properties of unaged impregnated UKP	163

iv) Influence of water content	168
c) Dielectric properties of impregnated UKP during ageing.....	171
i) Influence of ageing during 46 days	171
ii) Evolution of permittivity and water content during ageing.....	172
iii) Characterization of aged oil and aged UKP paper alone	175
iv) Discussion of results.....	176
d) Influence of paper composition on ageing	178
i) Effect of paper composition on unaged samples	178
ii) Effect of paper composition on aged samples	179
e) Effect of ion exchange during ageing	179
i) Effect of ion exchange on unaged samples	180
ii) Effect of ion exchange on aged samples	181
f) Dielectric breakdown	182
i) Dielectric strength of paper of different compositions (UKP, BKP and CL).....	183
ii) Dielectric strength of paper after ion exchanges	183
Conclusion.....	185
References	187

Introduction

The ageing of Power transformer's Kraft insulation is usually quantified by measuring depolymerization of cellulose. Operators are mainly concerned with the mechanical properties of Kraft insulation that will ultimately decide the life expectancy of Power Transformers. Evolution of dielectric properties during ageing is seldom studied: most of time authors suggest that water production induced by ageing should be exclusively responsible for the degradation of dielectric properties (e.g. dielectric losses and breakdown voltage).

An analysis of Kraft insulation was performed, with the aim to see how much does the oxidation and depolymerization of the pulp affect dielectric properties. The samples used in the study were the same as those of the previous chapters. They are meant to represent the diversity of organic matter (cellulose, hemicelluloses and lignin) and inorganic residual metals (main and transition metals) that can be found in electrotechnical paper. The aim of this chapter is to analyze individual components of the paper in order to investigate the effect each component can have on key dielectric properties.

This is done by analyzing paper samples of multiple compositions (UKP, BKP and Cotton) as well as chemically modified UKP samples that contain only one type of metal; we selected main metals (Ca, Na, Mg) and transition metals (Fe and Cu) known to have an impact on paper ageing and present in field conditions. The purpose is to develop fundamental understanding of their role on the dielectric response before and during ageing. Field Dielectric Spectroscopy (FDS) is mainly used as an assessment method to study ageing of Power Transformer insulation. Compared to standard permittivity and $\tan\delta$ measurements at a fixed frequency (usually 50 Hz), FDS may provide more insight regarding the impact of variations in material composition. This method is also interesting for utility operators, because it can be applied on a full-scale transformer, and could provide a non-intrusive and quick method to estimate the moisture content and ageing of a Power Transformer insulation. Chemical investigations on a real transformer are restricted to the analysis of oil, that may provide indirect information about paper ageing, but taking paper samples is usually impossible without stopping, opening, and dismantling the transformer. In the followings, we will first expose the basis of dielectric properties and measurement methods, and then present the results obtained.

1) Bibliographic study: dielectric study of paper ageing

- a) Dielectric properties of an insulator: main characteristic parameters
 - i) General considerations

Before looking into any relevant literature, a survey of main basic dielectric properties and relevant parameters is presented. Electricity is a form of energy resulting from the existence of charged particles (such as electrons or protons), either static (*i.e.* a local accumulation of charges) or dynamic (*i.e.* moving charges, producing a conduction current). There are many types of charge carriers involved in currents, common examples are electrons found in metals or ions found in ionic liquid solutions. When a dielectric material is placed in an electric field, most of electric charges present in the material cannot flow through the material (as they do in an electrical conductor) but instead only slightly shift from their average equilibrium positions (dielectric polarization), inducing a current related to such phenomena. However, all dielectric materials do contain a very small amount of electric charges able to flow, inducing a conduction current superposed to the polarization current. It should be noted the difference between a “dielectric material” and an “insulator”, since both terms are frequently used. An insulator is defined as a substance with a conductivity low enough to be used in practical systems to separate electrical pieces at different potentials, while a dielectric material simply means a material that is polarizable by an electrical field. Because they are quite similar, both terms tend to be used interchangeably. The main parameters that will be useful in this study are resistivity, permittivity, loss angle, and dielectric strength, they are listed below.

ii) Resistivity

Electrical resistivity is a fundamental property that quantifies how strongly a material resists to the flow of an electric current. Its inverse, called electrical conductivity, quantifies how well a material conducts electricity. Every material has its own characteristic resistivity, it is defined by the equation below (illustrated by the capacitance visible below):

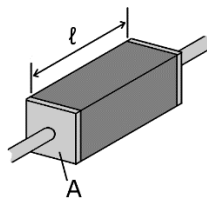


Figure 79: Schematic representation of an insulator between two electrodes, constituting a capacitance. Extracted from the Transformer oil handbook [1].

$$\rho = R \frac{A}{l}$$

Here, ρ represents the resistivity ($\Omega \cdot m$) while R represents the measured resistance (in Ω), A the cross-section surface (m^2), and l the length (m) of the specimen. A good insulator usually gets a very high resistivity from 10^{10} to 10^{20} $\Omega \cdot m$ while a conductor has a resistivity between 10^{-2} to 10^{-12} $\Omega \cdot m$. The resistivity both depend on the density of mobile charge carriers, and of their ability to move (mobility), that may considerably vary (by more than 10 decades) between conducting and insulating materials. The very low conductivity of insulators usually results

both from the low number of available charge carriers, and from their low mobility (*i.e.* ions moving through a solid material).

iii) Permittivity

Permittivity ϵ (F/m) is a measure of the electric polarizability of a dielectric material. When immobile charges are placed under an electric field \vec{E} , a coulomb force is exerted on the charges, that leads to the appearance of a polarization. Figure 80 shows an example of electronic polarization, but polarization of many other types also exists.

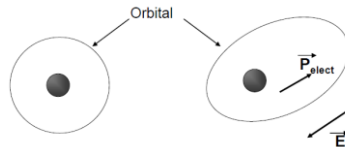


Figure 80: Schematic representation of electronic polarization.

$$\vec{P}_{elect} = \epsilon_0 \alpha \vec{E} \quad \epsilon = \epsilon_0 \times \epsilon_r$$

The resulting polarization \vec{P} (\vec{P}_{elect} in fig) will be proportional to the electrical field \vec{E} and depend on the polarizability α of the species. The absolute permittivity ϵ (F/m) is derived from the product of vacuum permittivity ϵ_0 (F/m) by the relative permittivity ϵ_r (dimensionless). It can be seen in Figure 81 that multiple polarization mechanisms are possible in a material. Some of them require a very short time to appear (such as electronic or atomic polarization: about 10^{-15} s), while others require much longer times (such as interfacial polarization $\gg 1$ s).

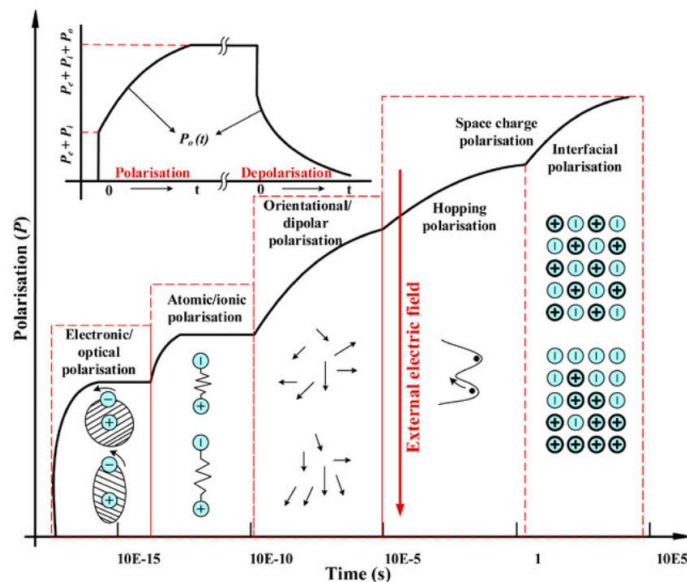


Figure 81: Polarization times necessary for multiple types of relaxations. Extracted from *physics of insulators* [2].

Under alternative field, the frequency constitutes a parameter of major influence on polarization phenomena. If the polarization and depolarization cycle have enough time to follow the changes in the electric field, no energy is lost by the system. On the contrary, if depolarization is not complete before a reversed field is applied, energy will be lost correcting the residual

polarization in the material. Permittivity and the corresponding dissipated energy will therefore be dependent on the frequency. Permittivity is also affected by chemical structure, presence of defects, temperature, pressure, and sometimes value of the applied field.

As mentioned previously, conduction and polarization are the two phenomena that influence dielectric properties, that will vary with frequency. Conduction losses (*i.e.* Joule dissipation) are predominantly found at low frequencies. Relaxation losses coming from a large range of polarization phenomena, with widely distributed typical times, occur over a wide range of frequencies. Therefore, a complete study of permittivity and losses carried out versus frequency (*i.e.* Dielectric Spectroscopy) provides much more insight into these phenomena, as compared to measurements at a single frequency such as in standard test methods. Such standard tests (measurements of permittivity and losses at 50 Hz) only intend to verify the practical suitability of a material for the application, and to compare materials using a fixed standard protocol.

Pulsation (ω in $\text{rad}\cdot\text{s}^{-1}$) is used to represent frequency, with $\omega=2\pi f$ (with f the frequency in Hz), for sinusoidal voltage wave. Measurements at various frequency makes it possible to describe the complex permittivity:

$$\varepsilon^* = \varepsilon_\sigma^* + \varepsilon_r^*$$

The behavior of the complex permittivity (ε^*) is defined as the sum of complex permittivity's conduction (ε_σ^*) and relaxation (ε_r^*) component. Each component can be further defined:

- Permittivity's conduction component ε_σ^* :

$$\varepsilon_\sigma^*(\omega) = \frac{\sigma_0}{i\omega\varepsilon_0}$$

Here, σ_0 represents the conductivity of the dielectric material while ε_0 refers to the reference permittivity of vacuum. These relaxations can be identified in a spectrum because conductive losses follow a linear slope of -1.

- The complex permittivity's relaxation component ε_r^* :

$$\varepsilon_r^*(\omega) = \varepsilon_\infty + \frac{\varepsilon_s - \varepsilon_\infty}{1 + i\omega\tau}$$

Here, ε_s and ε_∞ are the static dielectric constant and optical-frequency dielectric constant for a single relaxation process, with τ is the polarization time. The complex permittivity has a real and imaginary parts.

iv) Loss angle

Loss angle δ can be obtained from precise phase measurement between applied field and measured current, and allows calculating the loss tangent $\tan \delta$, which provides a dimensionless parameter that quantifies the ratio between dissipated “active” energy, and non-dissipating “reactive” energy involved in the material. When a sinusoidal voltage is applied to a dielectric material modelled as a parallel RC circuit (Figure 82), the total current flowing through the material is the sum of two components, one resistive I_p in phase with voltage that induces energy losses, and the other capacitive I_c with a phase shift of 90° with voltage that induces no losses (Figure 83).

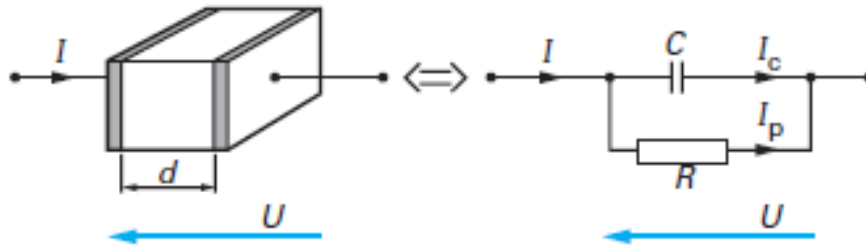


Figure 82: Real capacitor as a schematic representation of an ideal capacitor (C) and a resistance (R) in parallel. Extracted from physics of insulators [2].

$$\underline{I} = \underline{I}_C + \underline{I}_P$$

With:

$$\underline{I}_C = j\omega C \underline{U} \quad \text{and} \quad \underline{I}_P = \frac{\underline{U}}{R}$$

Together, they make the complex current \underline{I} showing a phase shift $\theta = (\pi/2) - \delta$ with applied voltage:

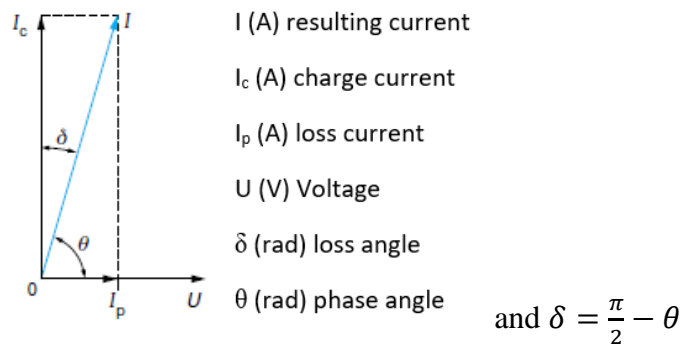


Figure 83: Visual representation of the $\tan \delta$ angle of dielectric loss. Extracted from physics of insulators [2].

The losses factor $\tan \delta$ can be calculated as the ratio of the loss current and the charge current, in practice it is simplified by the ratio of the complex (ϵ'') and real (ϵ') permittivity:

$$\tan(\delta) = \frac{|I_p|}{|I_c|} = \frac{\epsilon''}{\epsilon'}$$

$\tan \delta$ has a simple physical meaning: it represents the ratio of active (dissipating) power to the reactive (non-dissipating) power. By convention, $\tan \delta$ is usually quoted in percent. Excellent dielectric materials (*i.e.* PTFE, TeflonTM) may show very low $\tan \delta$ down to 10^{-5} , whereas it may raise up to 10^{-1} (at 50 Hz) in oil-impregnated paper. This illustrates the fact that impregnated paper insulation, although acceptable and well adapted to power transformers, would be unacceptable for other applications such as capacitors, where a very low $\tan \delta$ constitutes a mandatory acceptance criterion. One reason for this comes from the fact that in a transformer, energy losses due to dielectric materials are negligible when compared to other losses coming from magnetic materials and copper wires. Measurements of $\tan \delta$ in transformers is however of great interest, since abnormal high values constitute a very useful

indication that problems (e.g. presence of water or poor quality of materials) exist in the insulation.

v) Dielectric strength

As seen previously, a dielectric material placed in a moderate electric field becomes polarized and conducts extremely small amounts of electricity. At very high fields, ionization of the matter may eventually occur, and lead to the appearance of an electric arc (usually called “electrical breakdown”) leading to strong currents, very high temperatures (several 1000 K), and irreversible destruction of materials. No simple theory of electrical breakdown in dielectric solids do exist, and such phenomena remains rather unpredictable. The voltage at which breakdown occurs is known as the “dielectric strength”, and this voltage is usually normalized by the thickness of the sample to obtain the “breakdown field” quoted in V/m:

$$E = \frac{U}{e}$$

Electrical breakdown only happens in fraction of seconds and the actual breakdown mechanism is specific to each material, therefore dielectric breakdown strength is only used as a qualitative and comparative indicator. For high voltage applications, the dielectric strength of materials is carefully considered during the equipment design. Since dielectric breakdown is highly dependent on the presence of defects or impurities, the measurement of breakdown voltage constitutes a very useful way to check the quality of a material.

b) Previous measurements and analyses of dielectric spectroscopy of Oil - Paper systems

i) A cautionary statement about FDS results

Before analyzing the scarce available experimental results of FDS for paper and oil systems, it should be noted that in the current time there is no theoretical model that fully explains and predicts how a highly heterogeneous material, such as paper impregnated by oil, behaves. It is not well understood how much of the FDS measurements comes from oil, and how much comes from the paper. A qualitative answer will be attempted in this study. When Kraft insulation is impregnated with oil, the free space between cellulose fibers is filled with oil, and the amount of oil will depend on the density of fibers. Therefore, the final permittivity of impregnated paper will depend on its density: a low-density paper will contain a higher proportion of oil. This can be observed in known permittivity measurements of various types of impregnated Kraft insulation: low density pressboard shows a lower permittivity compared to high-density pressboard, that correspondingly absorbs less oil. Indeed, permittivity of oil (2.2) is lower than that of cellulose (> 4.5). The permittivity of each component is visible in the table below:

Table 31: Permittivity of Kraft pressboard impregnated with mineral oil at 50 Hz and at different temperatures. Extracted from the Transformer oil handbook [1].

Material	Temperature		
	25°C	90°C	130°C
Mineral Oil	2.4	2.3	2.2
Low density pressboard	3.9	3.9	4.1

High density pressboard	4.5	4.7	4.9
-------------------------	-----	-----	-----

In addition to this, it appears that experimental errors also probably affect several published data of FDS measurements in impregnated paper. Most values found in the literature show a permittivity that varies between 2 and 3 at medium and high frequencies (10^2 to 10^6 Hz and 25°C), *i.e.* rather low values compared to known values obtained in standard measurements, that should lie between 3 and 5 (at 25°C and 50Hz). In the paper presented below, an interesting analysis of FDS is carried out, but the real permittivity measured is around 2 at 25°C and 50Hz, which is obviously too low and casts doubts on the interpretation provided. One possible interpretation of this wide scatter of results could be linked to the practical problem of establishing a good “contact” between electrodes and the impregnated paper. The paper cannot be metallized, and the random arrangement of cellulose fibers may provide an irregular interface between the paper and the electrode, depending on the actual paper shape.

The aim of the literature survey was to find suitable data and interpretations derived from previous FDS measurements in impregnated paper. Considering the uncertainties in several published measurements, and the limited number of available studies, this objective is not fully addressed. We will however summarize several results extracted from available literature.

ii) Xie et al.; Physical Model for Frequency Domain Spectroscopy of Oil–Paper Insulation in a Wide Temperature Range by a Novel Analysis Approach (2020)

In the past 30 years, progress in dielectric spectrometer technology has allowed Field Dielectric Spectroscopy (FDS) to be widely available. As was discussed before, the response of a material comes from multiple interaction that happen simultaneously. It is known they originate from conduction and all the possible types of relaxations, but identifying each interaction by FDS remains challenging, especially in heterogeneous systems, such as oil-paper insulation. Only one recent publication [3] attempts to explain the dielectric behavior of paper/oil insulation, using the analysis tools developed for homogenous single dielectric materials. Despite this basic limitation, this publication provides some insight about the FDS of oil-paper insulation.

The analysis rely on the two different origins of the dielectric response:

- Conduction should be clearly identifiable in spectra because it will make a linear curve with a slope value of -1. Another phenomena is commonly observed at very low frequency, called Low Frequency Dispersion (LFD):

$$\varepsilon_{LFD'}(\omega) \propto \varepsilon_{LFD''}(\omega) \propto \omega^{-\gamma}$$

Here, the range of slope coefficient γ goes from 0 to 1, this slope is calculated from experimental data. The LFD process becomes usually more dominant with increased temperatures. The origin of this phenomena is unknown, it is speculated that it is a form of conduction that originates from charge dispersion at low frequencies.

- Polarization is harder to identify since there exists many types of possible polarization. The most common models used to describe a single relaxation process are Debye [4],

Cole–Cole [5] and Havriliak–Negami (H-N) models [6]. The example given is a HN model:

$$\varepsilon_{HN}^*(\omega) = \varepsilon_{\infty} + \frac{\varepsilon_s - \varepsilon_{\infty}}{(1 + (i\omega\tau)^{\alpha})^{\beta}}$$

Here, parameters α and β are calculated from experimental data, and are considered to be related to a material's structure.

In this paper, FDS experiments were carried out with unaged 2 mm thick cellulose pressboards impregnated in mineral oil. The frequency domains ranged from 10^{-3} to 10^5 Hz. All experiments were done within three groups of temperatures denoted low temperature (-40 to 20°C), medium temperature (20 to 40°C) and high temperature (80 to 100°C). The results are presented in Figure 84:

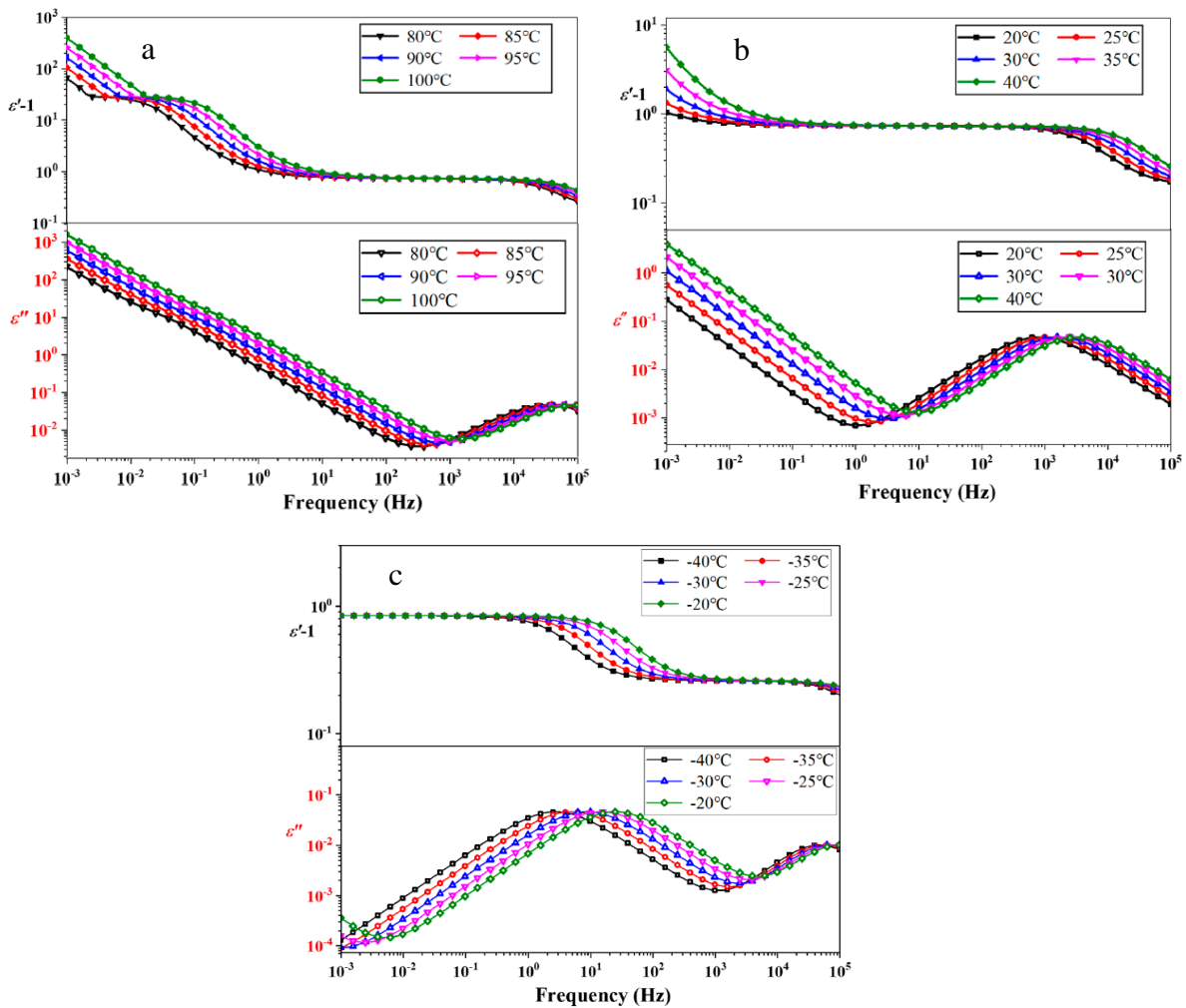


Figure 84: Real (ε') and imaginary (ε'') permittivity for UKP samples at high (a), medium (b) and low (c) temperatures. Extracted from Xie et al. [3].

FDS curves represent multiple independent physical processes, and some of them happen simultaneously. The strength, or even existence, of each physical process depends on the temperature. Some physical process only induce a response visible on the complex permittivity and therefore don't appear on the signal of real permittivity. Measurements at high temperatures are shown in Figure 85 (80 to 100°C).

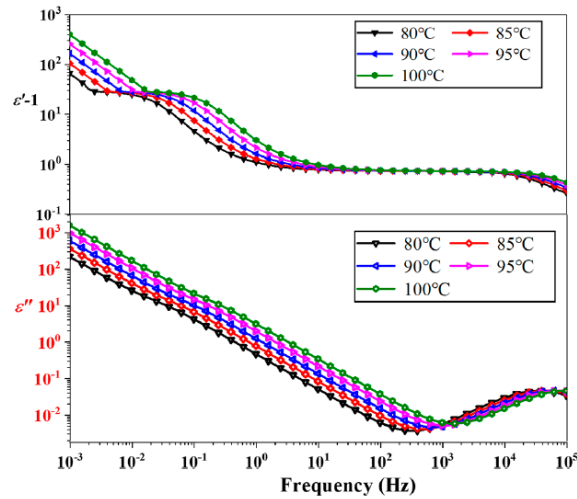


Figure 85: Real (ϵ') and imaginary (ϵ'') permittivity for UKP samples at high temperatures (80, 85, 90, 95 and 100°C). Extracted from Xie et al. [3].

These signals show a decrease of ϵ'' in the low frequency ranges that is consistent with conductivity. ϵ' shows a flat section associated to an extremely weak variation of ϵ'' , attributable to an electrode polarization phenomenon. The corresponding polarization time should depend on the distance between anode and cathode. Results obtained with different paper thicknesses are presented in Figure 86. A correlation between the sample's thickness and the appearance of the electrode polarization phenomena is seen.

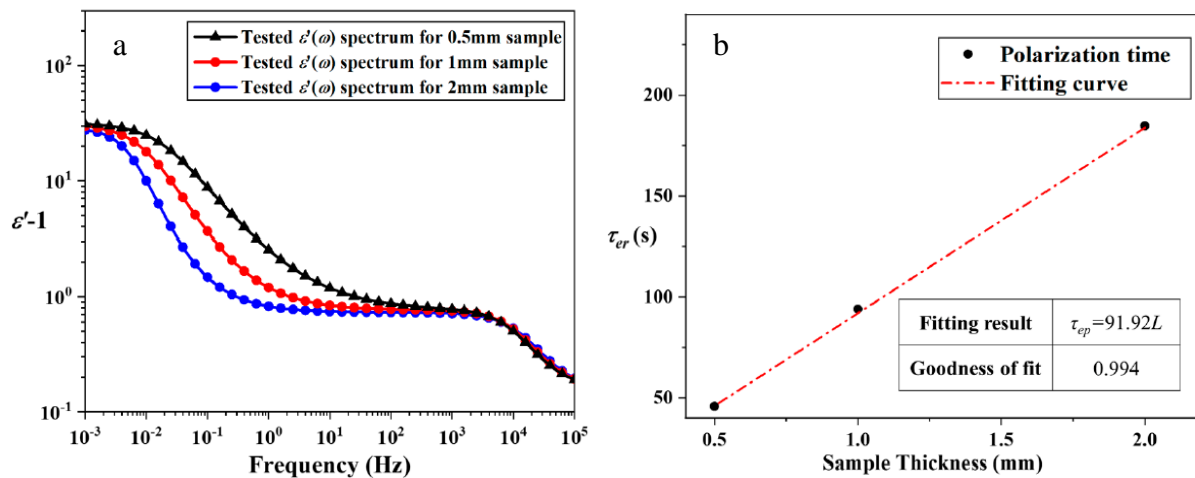


Figure 86: a: Real (ϵ') permittivity of UKP samples with different thicknesses (2, 1 and 0.5 mm). b: Correlation curve between the polarization time and the sample thickness. Extracted from Xie et al. [3].

For higher frequencies, another polarization is visible from 10^2 to 10^3 Hz. Previous literature suggests this polarization is a type of interfacial relaxation between the oil and paper, with an accumulation of charges at the contact surface between them. To confirm this, an experiment (Figure 87) was conducted to compare the spectra between paper alone and paper impregnated with oil. These results indeed show the polarization signal disappears when there is no oil in the system.

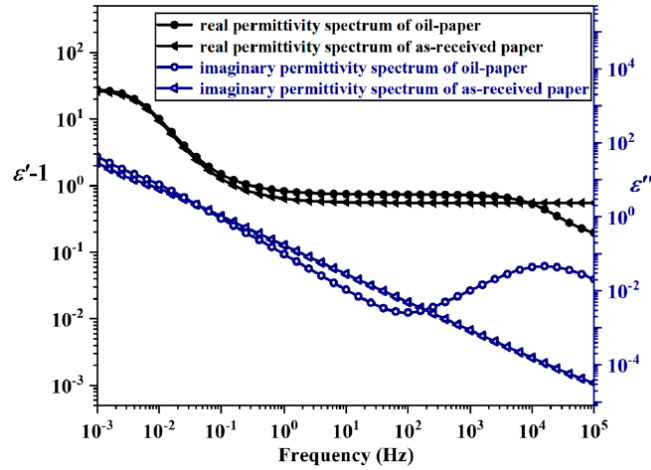


Figure 87: Real (ϵ') and imaginary (ϵ'') permittivity for UKP samples as an oil-paper system and with paper only. Extracted from Xie et al. [3].

Several facts however cast doubts on these measurements:

- The permittivity ϵ' (about 2 from 10^0 to 10^3 Hz) is obviously too low for impregnated paper (it should be around 3.5 – 4.5 for 2 mm pressboard).
- It even drops below 2 above 10^4 Hz, which has no physical meaning for condensed matter.
- Almost no difference in ϵ' is seen between paper without oil and impregnated, contrary to other measurements.

A summary of the analysis at medium and low temperatures is presented in Figure 88 and Figure 89:

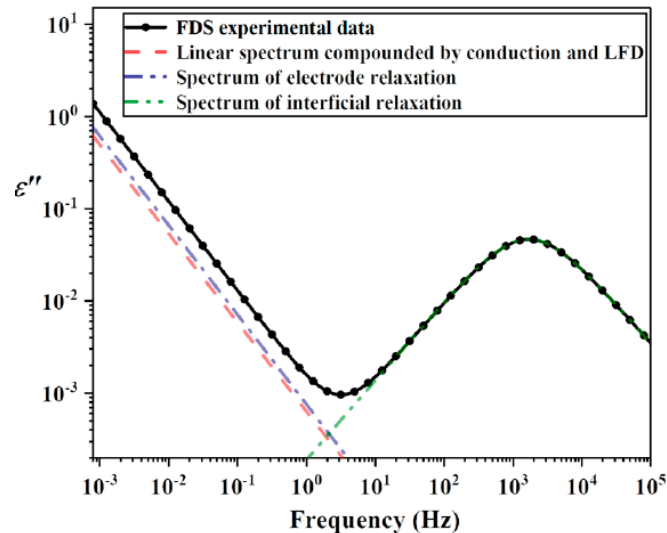


Figure 88: Physical interpretation of the imaginary (ϵ'') permittivity signal for UKP samples at medium temperatures (30°C). Extracted from Xie et al. [3].

For medium temperatures, FDS shows that conductivity losses significantly decrease as well as electrode polarization, while interfacial polarization remains unchanged. All polarization signals are shifted to lower frequencies since lower temperatures increase polarization and

depolarization times. Conductions is also reduced since charge carriers density and mobility decrease.

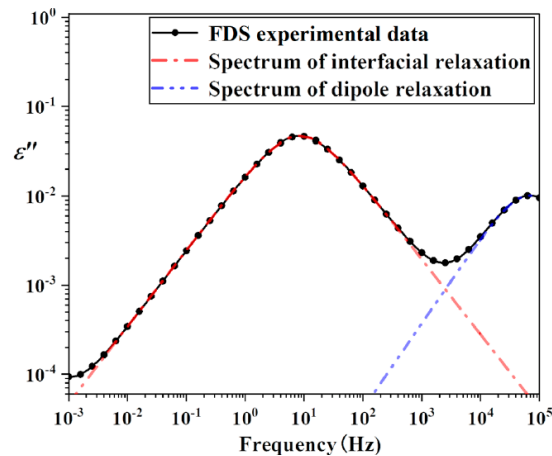


Figure 89: Physical interpretation of the imaginary (ϵ'') permittivity signal for UKP samples at low temperatures (-30°C). Extracted from Xie et al. [3].

At low temperatures ($< 0^{\circ}\text{C}$) conductivity and FDS losses totally disappear. Electrode polarization is not any more observed (polarisation times becomes too long), and interfacial polarization keeps the same intensity but is now visible over the entire spectrum.

Although doubts exist on the values of ϵ' obtained in this paper, pieces of analysis (especially dealing with conduction) will be used in the interpretation of our results.

iii) Evaluating changes of dielectric properties during ageing

In the available literature, the cause behind the loss of dielectric properties during ageing is attributed to two main components: moisture and ageing. The moisture comes from the water formed in paper by the ageing process. For ageing, the definition is more complex since there exists multiple reasons to explain why the length of cellulose chains and its degradation could affect dielectric properties:

- More chain mobility resulting from a loss of entanglement, and loss of hydrogen bonds resulting from cellulose oxidation;
- Oxidation of cellulose chains could add new types of polarization along the fibers;
- By-products of oxidation, such as acids, could act as mobile charge carriers.
- Formation of new chemical groups in the oil and paper that could modify water and charge equilibrium of the electrical double layer in the oil-paper interface.

Technically, water is also a by-product of ageing, but its conductivity is much larger than that of organic acids produced by degradation, therefore it is classified in its own separate category. Only a few recent publications on FDS of oil-paper systems during ageing exist. Some recent publications trying to analyze the role of each component are summarized below.

iv) Jadav et al.; Understanding the Impact of Moisture and Ageing of Transformer Insulation on Frequency Domain Spectroscopy (2014)

One of the most complete studies was published in 2014 by Jadav *et al.* [7]. The main aim was to separate the effect of moisture from that of ageing. To explore the effect of moisture, paper with different moisture contents were impregnated with oil. The aged papers were compared before and after they were cleaned from the by-products of ageing (removal of water and acids). An analysis of the ageing of oil was also performed, including other measurements such as Furan quantification (by DGA), not relevant to this study.

Samples were made of pressboard of two density levels called Low Density (LD with 1 g.mm³ and 1 mm of thickness) and High Density (HD with 1.24 g.mm³ and 1.5 mm of thickness), dried in vacuum at 80°C and impregnated at 60°C for a week. Moisture was controlled via different air humidity levels before impregnation. Ageing was done at 105°C in sealed non-oxidative conditions for up to 81 days.

Some FDS experiments used the aged oil, while others were made with washed samples and impregnating them with new mineral oil. For washing, paper was removed from the oil and submerged for 3 days in water to extract water soluble acids. Then, samples were submerged 3 days in acetone to extract moisture and oil. The study states that this procedure does not changes dielectric properties. Paper was finally washed for 3 days in hexane to extract any remaining oil, then dried and impregnated with new oil. Out of the results obtained in this publication, the study of the role of the moisture, ageing of paper, and ageing of oil are presented below.

Real (ϵ') and imaginary (ϵ'') permittivity's for unaged pressboard samples with different moisture content is presented in the Figure 90. Samples with moisture contents of 0.4% and 5.5% were made with low density pressboards (LD) while samples with 0.3, 2.2 and 4.5% moisture contents were made with high density pressboards (HD).

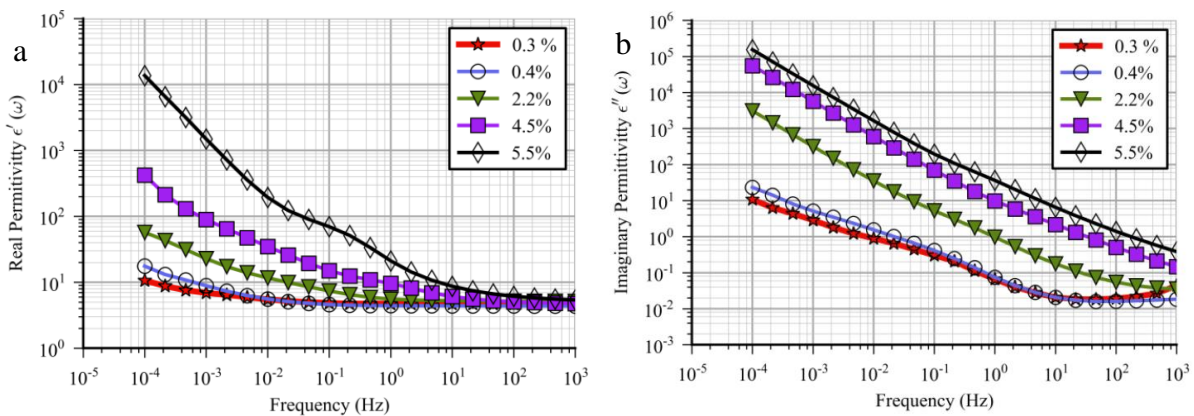


Figure 90: Real (a/ ϵ') and imaginary (b/ ϵ'') permittivity signal for unaged UKP pressboards samples with multiple moisture contents visible in the captions. Density of pressboards: filled symbols: HD, unfilled symbols: LD. Measurements were carried out at 55°C. Extracted from Jadav *et al.* [7].

Unaged samples showed a marked rise in both ϵ' and ϵ'' attributed to conduction and LFD losses induced by water. Some signal from an electrode polarization is visible at 10⁻¹ Hz at low moisture content, but it is drowned by the conductivity at higher moisture contents.

Then, changes in the imaginary (ϵ'') permittivity of pressboard during ageing were tested. In these experiments, the moisture and ageing parameters are quantified together (because the samples were not dried after ageing) (Figure 91).

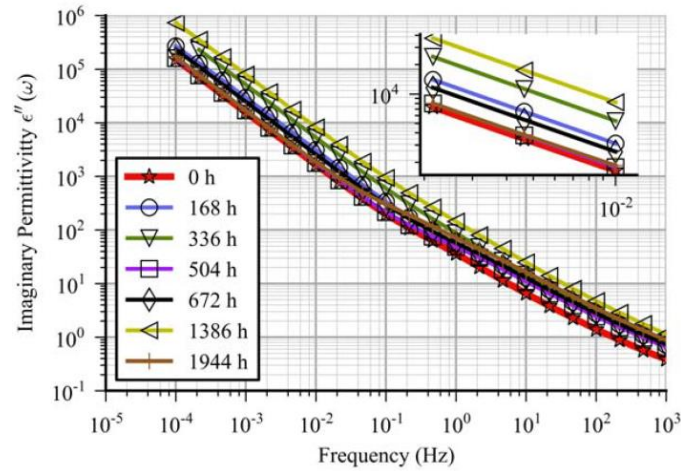


Figure 91: Imaginary (ϵ'') permittivity signal for unaged low density UKP pressboards samples with multiple ageing times visible in the captions. Measurements were carried out at 55°C. Extracted from Jadav et al. [7].

The results shown are for HD density pressboard, LD pressboards gave similar results. It is interesting to observe that the change in ϵ'' is not constant: it increases up to 336 hours (14 days), then decreases until 504 hours (21 days), increases again up to 1286 hours (53 days), to again decrease in the last measurement at 1944 hours (81 days). Both the moisture and the ageing play a role in the variations of ϵ'' . Similar changing effects were found in other publications [8–10]. Similar results will be found in the next part of this chapter, and correlated to variations of water content. Changes in ϵ'' for moist and dry pressboard samples are visible in Figure 92:

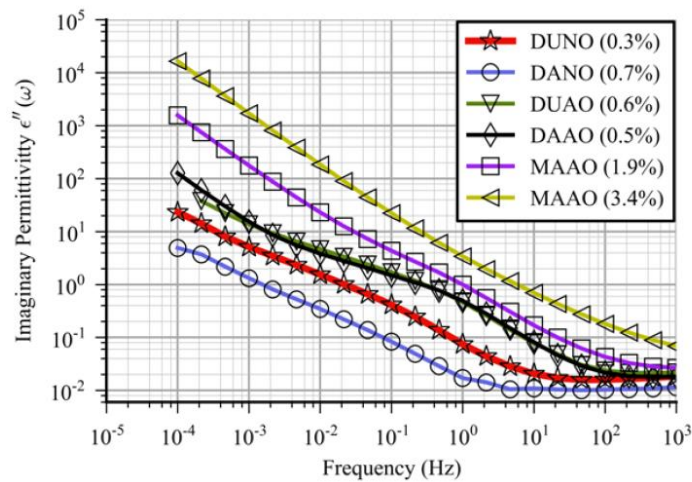


Figure 92: Imaginary (ϵ'') permittivity signal for unaged low density UKP with **Dry Unaged paper in New Oil (DUNO)**, **Dry Aged paper in New Oil (DANO)**, **Dry Unaged paper in Aged Oil (DUAO)**, **Dry Aged paper in Aged Oil (DAAO)** and **Moist Aged paper in Aged Oil (MAAO)**. In the legend; moisture is present in parenthesis. Measurements were carried out at 55°C. Extracted from Jadav et al. [7].

Multiple variables are analyzed in this figure, corresponding to LD pressboards aged for 1944 hours. Some aged and unaged paper samples were dried and impregnated with new or aged oil, they are called dry samples. Other aged paper samples were dried and conditioned to obtained a moisture content of 1.9 and 3.4 % before being impregnated again with aged oil, they are called moist samples. A drop in ϵ'' between unaged and aged paper samples in new oil (DUNO and DANO) is visible here. In aged oil, there was no difference between dry aged and unaged paper (DUAO and DAAO) with almost identical moisture contents, leading the authors to conclude that the moisture is the main factor behind the increase in permittivity. To further assess this conclusion, moist aged samples showed an important increase in conduction losses when compared to their dry counterparts (DAAO and MAAO), showing that in this situation the difference almost exclusively comes from moisture.

The general conclusion of this paper shows that dielectric properties were mostly influenced by moisture, while the impact from changes in the chemistry of paper and acid byproducts was deemed much smaller. Similar ideas were further explored a few years later in the publication [11] presented below.

v) Xia et al.; A New Method for Evaluating Moisture Content and Aging Degree of Transformer Oil-Paper Insulation Based on Frequency Domain Spectroscopy (2017)

Some of the methods and techniques used in this study are not precisely defined, for example it is said that the Degree of Polymerization (DP) is measured but not specified what method is used to quantify the DP. Nevertheless, this study provides valuable insight that helps better understanding the relative influences of moisture and ageing. Samples were made of 1mm thick “cardboard” in naphthenic mineral oil. Ageing was conducted at 120°C in oxidative conditions, in an open bottle, for 0, 14, 35, 55 and 80 days. After ageing, paper was dried at 110°C for 24 hours until a moisture content of 0.21% was obtained. The oil was placed in controlled humidity levels in order to obtain multiple moisture contents. Moisture contents were measured with changes in mass during drying. These methods contain some intrinsic errors since the mass measured includes some oil: changes in mass don't only come from water evaporation. Nevertheless, there certainly exists differences in moisture content between samples. No wash was done before FDS experiments done at 30°C. The study uses $\tan \delta$ plots instead of ϵ'' because it is more relevant to the direct assessment of transformers.

Tan δ for unaged (0 days - DP 1250) and aged (80 days - DP 402) samples with different moisture content was analyzed (Figure 93):

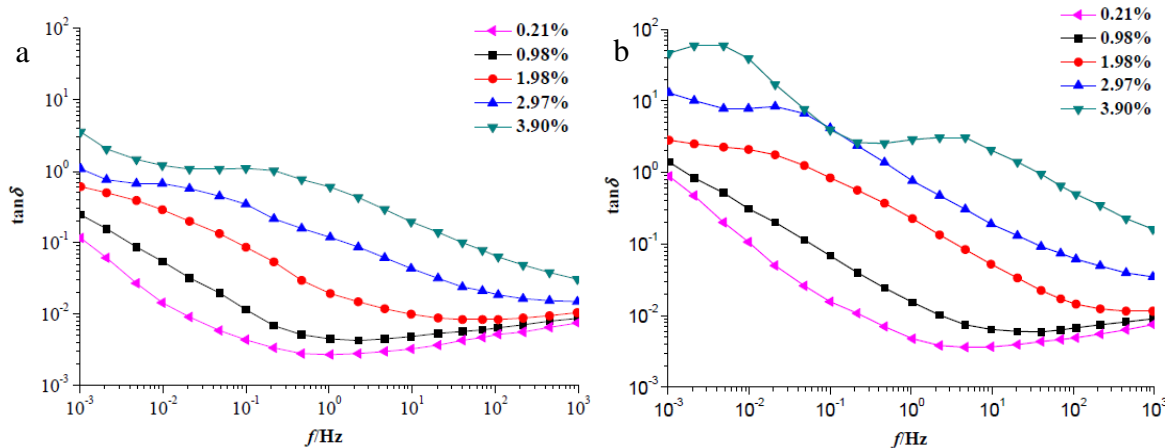


Figure 93: a: $\tan \delta$ signal for unaged samples (DP 1250). b: $\tan \delta$ signal for unaged samples (DP 402). Moisture content for each sample is visible in the captions. Measurements were carried out at 30°C. Extracted from Xia et al. [11].

A comparison between the dry (0.21%) aged and unaged paper shows an increase in conduction at low frequencies (10^{-3} to 10^0 Hz): $\tan \delta$ increases from 0.1 to 1 at 10^{-3} Hz for example. The increase in water content doesn't affect aged and unaged paper in the same manner: with 3.98 % moisture, $\tan \delta$ (10^{-3} Hz) increases to around 50 for aged paper but only to 5 for unaged paper. The paper suggests that the moisture and the ageing don't contribute independently to $\tan \delta$, since ageing amplifies the influence of moisture. In the paper the authors state that ageing mainly affects $\tan \delta$ at low frequency ranges (10^{-3} to 10^0 Hz), and moisture affects $\tan \delta$ at higher frequency ranges (10^1 to 10^3 Hz).

Below a moisture content of 2%, the ageing doesn't seem to affect the dielectric response, but above 2% the ageing starts to significantly influence $\tan \delta$, arguably by amplifying the influence of moisture. This suggests a clear interference between the two.

2) Materials, experimental methods, and experiments carried out

a) Materials and experimental methods

i) Chemical products

Oil: NYTRO Taurus oils, supplied by NYNAS Company.

Paper pulps: Unbleached Kraft Pulp (**UKP**) and Bleached Kraft Pulp (**BKP**) originate from ASPA™ mill in Sweden. Cotton linters (**CL**) were obtained from CELSUR™ in Spain. TAPPI (Technical Association of the Pulp and Paper Industry) handsheets were made with a grammage of 130 g/m² from these raw pulps using deionized water (180 μm thickness, 14 cm diameter).

ii) Sample preparation and chemical characterizations

All samples used in this chapter are the same as those used in the previous chapter (Chapter 3), therefore all the methods used to modify the ion content as well as the chemical analysis of the samples contained in this chapter can be found there.

iii) Instruments used for chemical characterization

Karl-Fischer analysis: water content measurement in oil and in impregnated paper was carried out by Karl-Fischer analysis, coupled to thermal desorption of the sample (oven temperature 140°C) under dry air flow, and water content analysis by coulometric titration (Metrohm™ 831 KF coulometer coupled to Metrohm™ 832 thermoprep oven).

iv) Instruments used for dielectric spectroscopy

The analysis of dielectric properties according to frequency was done through Frequency Dielectric Spectroscopy (FDS), using a Novocontrol™ analyzer. Because water greatly affects dielectric properties of paper, a special airtight test cell was built at G2Elab laboratory for this project, in which paper samples could be first dried, and then impregnated with dry oil without opening the test cell. The test cell was placed in a climatic chamber for temperature control.

The main difficulty associated with measuring the dielectric properties of paper is that under atmospheric conditions, paper contains around 5% of water (by mass). To obtain good dielectric properties, it must be dried well below 1% water content. Paper is made of very hydrophilic hydroxyl groups, and rapidly absorbs water from ambient air. In typical atmospheric conditions, dry paper absorbs more than 1% of water content in less than a minute. Any attempt to dry the paper, and then transfer it via ambient air to the test cell incurs a high risk of water contamination. To solve this issue, drying and impregnation by oil must be done inside the measurement test cell, without contact with air.

For FDS measurements, airtight custom test cells were built, following a classical arrangement made of parallel plane electrodes (34 mm in diameter), containing the paper sheet (34 mm disks). A guard ring surrounds the lower electrode used for current measurement (Figure 94). To ensure a good contact between electrodes and paper, the lower electrode is pushed by a spring that controls the overall pressure applied to the paper. In these hermetically closed steel cells, the upper electrode can be moved up and down from the outside. With the electrode moved up, the paper is free to move. The cell is then heated (93°C) while vacuum (10^{-2} Pa) is applied to properly dry the paper during 2 hours. After drying, a valve is opened to insert dry oil within the cell, and impregnate the paper. The oil was previously degassed and dried, with a water content tested at 2-5 ppm by Karl-Fischer analysis. Because small air bubbles may occur after impregnation, a vacuum is then applied for 1 hour, to remove any remaining bubbles, and further dry and impregnate paper. Once drying and impregnation are completed, the upper electrode is moved down and pressed on the paper for dielectric characterization. The test cell was then placed in a regulated oven for measurements. Tests showed that 2 hours were needed to obtain a stable and uniform temperature within the cell.

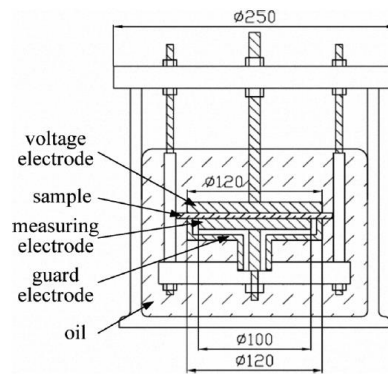


Figure 94: Schematic view of a dielectric test cell, the represented lengths are in mm. Extracted from Wang et al. [12].

Two test cells were built, one for measurements on the paper alone, and the other for measurements on paper in oil (Figure 95). The main difference is the nature of electrodes used: for dry tests without liquid they were made of conducting silicon rubber to ensure a good contact with the uneven paper surface, while they were made of metal (stainless steel) for tests in oil. The cell's volume was also smaller (around 150 ml for oil versus 500ml for dry cells) to reduce oil consumption for each experiment. The dry cell was equipped with Dew Point, temperature, and pressure sensors to precisely monitor the surrounding gas during drying of the paper, and provide an indirect measure of the paper water content, via the known equilibrium between paper water content, and surrounding gas water content. This test cell could not be heated above 50°C to protect sensors. The oil test cell was only equipped with a temperature sensor and an external vacuum sensor, and could be heated up to more than 100°C.



Figure 95: Photographs of the dielectric tests cell used during this study. left: interior part of oil-paper dielectric test cell. Right: complete oil-air dielectric test cell.

v) Instruments used for breakdown measurements

A custom breakdown test cell was built (Figure 96), in which the impregnated paper was placed on a flat electrode connected to ground. A 4 mm sphere connected to high voltage was placed on the paper, producing a sphere-plane electrode geometry. High AC voltage was applied to the sphere, and raised at constant rate (1kV/s) up to breakdown. Once breakdown occurred, the voltage was monitored (breakdown voltage) and the voltage was stopped. On each paper

sample, a series of 20 breakdown voltages was measured at different locations on the paper sheet, in order to obtain a good statistical meaning of the measurement.

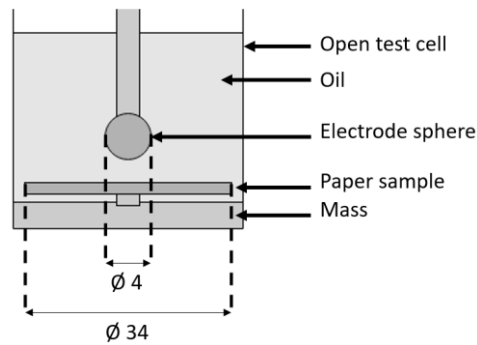


Figure 96: Schematic view of the breakdown test cell, the represented lengths are in mm.

Samples were conditioned (2 hours, 93°C under vacuum), and directly transferred to the dielectric breakdown test cell, the paper was kept submerged in the oil during the transfer. Because the experiments were short (around 1 hour) and done at room temperature (21°C), the test cell was exposed to open air without any impact on the results (no significant water uptake by the oil).

b) Measurements carried out

i) Dielectric spectroscopy experiments in oil

Samples analyzed in dielectric spectroscopy were from the same batch as those used in the previous chapter (Chapter 3). A view of the analyzed samples and the temperature ranges used can be seen below (Table 32). In addition, measurements could be made with new or aged oil. Several measurements were done over a wide temperature range, starting with the coldest (-30°C) to the warmest (90°C). Because of technical limitations and some equipment failure, all samples were not tested over this complete temperature range.

All FDS measurements of new paper samples were done with unaged oil. Aged samples were investigated using 3 different protocols:

- Type 1: aged oil. Samples were analyzed in the oil in which they aged;
- Type 2: new oil. After ageing, aged oil was replaced by new oil before measurements;
- Type 3: new oil. After paper had a soxhlet extraction (Using pentane in 2-hour cycles). Aged paper samples were cleaned via a soxhlet extraction, that removed all the oil and residues induced by ageing. In previous studies [7], moisture and acids were removed by leaving samples in water, acetone and hexane for up to 3 days at 55°C. These studies used thicker samples (up to 1.5mm) that probably required more time than the 140 µm samples of this study.

Table 32: List of samples used for FDS measurements with their ageing times and the different temperatures used in the experiment.

Samples	Ageing time (days) and analysis type				Temperature tested (°C)
UKP	D0	D6	D16	D35	-30/-20/-10/10/20/30/70/80/90
		1/2/3	1/2/3	1/2/3	

BKP	D0	D46 1/2/3	-30/-20/-10/10/20/30/70/80/90
Cotton	D0		-30/-20/-10/10/20/30/70/80/90
Calcium	D0	D46 1/2	90
Sodium	D0		90
Magnesium	D0		90
Iron	D0		90
Copper	D0		90
Demineralized	D0		90

ii) Dielectric breakdown experiments

Samples analyzed in dielectric spectroscopy were then used for dielectric breakdown experiments. Dielectric breakdown tests were performed for the samples listed in the table below:

Table 33: List of samples used for dielectric breakdown experiments with their ageing times.

Samples	Ageing time (days) and analysis type	
UKP	D0	D46
BKP		
Cotton		
Calcium		
Sodium		
Magnesium		
Iron		
Copper		
Demineralized		

3) Influence of paper chemical and residual metal composition on dielectric properties during ageing

a) Objectives

As explained in the first part of this chapter, there is no clear consensus on the mechanisms leading to the modification of dielectric properties with ageing. The only consensus commonly cited in literature is that water is mostly responsible for the loss of dielectric properties of paper, while acids and other ageing by-products play a minor role in these changes. Another postulated explanation is the increase in polar content from the pulp itself, that would in turn increase the possibility of charge carriers and therefore conductive losses.

In our study, we will further investigate the question of ageing by doing FDS experiments aiming at comparing paper of different composition, and measuring the impact of different ion content during ageing. This study is made possible thanks to the chemical methods and analyses developed from the previous chapters.

Samples studied are the same as those of the previous chapter, namely UKP, BKP, Cotton Linters and the ion exchange experiment samples. FDS measurements were time consuming, so only UKP was analyzed at all temperatures and various degree of ageing. Unaged samples

were dried, impregnated, and tested with new mineral oil. For aged samples, most were tested in the oil in which they aged but UKP, BKP and Cotton were tested with the three Types described previously. The objective was to try to identify the relative influence of several phenomena occurring during ageing: ageing of oil, ageing of paper, presence of ageing by-products (mainly moisture).

Before starting these investigations, several preliminary experiments were carried out with the objective to validate the experimental system with a reference material (PTFE), and provide some results illustrating the complexity induced by the heterogeneous nature of impregnated paper.

b) Preliminary results

i) Calibration of measurements

Before analyzing paper-oil systems it was important to check the correct response of the dielectric test cells developed. The reference material used was PTFE (Teflon™) because of its excellent dielectric properties, and their indifference to external environmental conditions (negligible water uptake). The test showed a permittivity around 2.1 and a loss angle around 0.0002, both at 21°C and 50 Hz, in line with well-known results for this material.

ii) Dielectric properties of oil and non-impregnated UKP paper.

A first set of experiments was conducted on unaged samples of UKP paper and oil separately, analyzed at multiple temperatures. The Dielectric response for UKP and oil can be found in Figure 97:

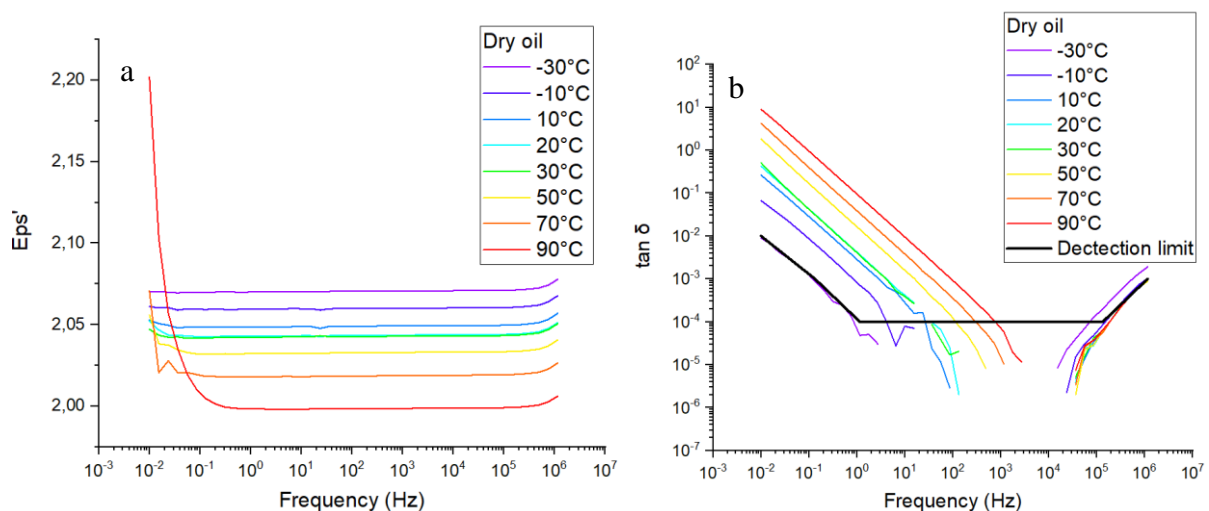


Figure 97: Real permittivity (a / ϵ') and $\tan \delta$ (b) at multiple temperatures going from -30°C to 90°C for unaged (D0) oils samples without paper. The water content of the samples is 6 ppm. The detection limit of the spectrometer is shown.

In mineral transformer oil, the typical behavior of non-polar liquids previously reported in other studies [13] is observed. $\tan \delta$ shows a variation proportional to $1/\omega$ over a wide frequency range, that is typical of conductivity losses coming from ions present in the liquid. Since conductivity depends on ion mobility, which is inversely proportional to viscosity, a large

increase of conductivity with temperature is observed (viscosity decreases when temperature is raised). Above some frequency, $\tan \delta$ drops below the detection limit of the spectrometer, indicated on figures. Below this limit, the erratic values provided by the spectrometer have no meaning. At frequencies above 10^5 Hz, the measurements are also limited by the response of the spectrometer. At the lowest temperature investigated (-30°C), the losses of the liquid are so low that they cannot be measured over the complete frequency range.

The permittivity ϵ' is very stable, and slightly decreases with temperature (about -3%), which is due to the decrease of liquid density when temperature is raised [13]. Almost no dielectric losses resulting from polarization phenomena can be seen in this non-polar and highly insulating liquid. At the highest temperature (90°C) and lowest frequency (10^{-2} Hz) investigated, a small increase of permittivity ϵ' is recorded (+ 10%), probably attributable to electrode polarization. Previous studies in mineral transformer oil also concluded that the very low water content that can be dissolved in mineral oil (saturation level about 30 ppm at room temperature) has almost no influence on permittivity and losses. Results for dry unaged oil samples are visible below in Figure 98:

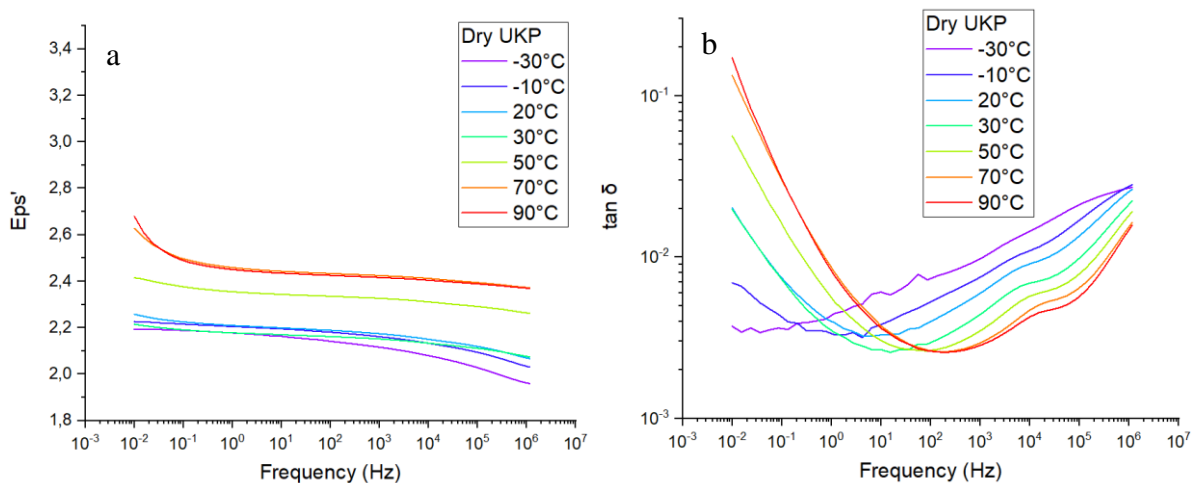


Figure 98: Real permittivity (a / ϵ') and $\tan \delta$ (b) at multiple temperatures going from -30°C to 90°C for unaged dry **UKP samples without oil**. The water content of the samples is 0,3%.

Non-impregnated UKP paper exhibits a rather different pattern with interfacial polarization likely occurring at high frequencies, and losses at low frequencies that do not vary as $1/\omega$, meaning that some polarization phenomena are mixed with conduction losses. At low frequency, losses due to conduction are clearly observed and dominate at high temperature (90°C), whereas only losses due to polarization are seen at low temperature (-30°C). Opposite to mineral oil, a small increase of permittivity ϵ' is seen when temperature is raised. The rather low value of permittivity ϵ' recorded (from 2.2 to 2.5) is due to non-homogeneous structure of paper, constituted by solid fibers that represent about 60% of the volume (see next chapter), with air between them that represents about 40% of volume. This heterogeneous structure greatly complicates the interpretation of FDS measurements, as compared to dense homogeneous solids.

iii) Dielectric properties of unaged impregnated UKP

A comparison was first made at fixed temperature (21 °C) between the dry UKP paper in air and impregnated with oil. Both UKP samples came from the same source, and were initially dried (0.3 % water content). A comparison between the two experiments is visible below in Figure 99:

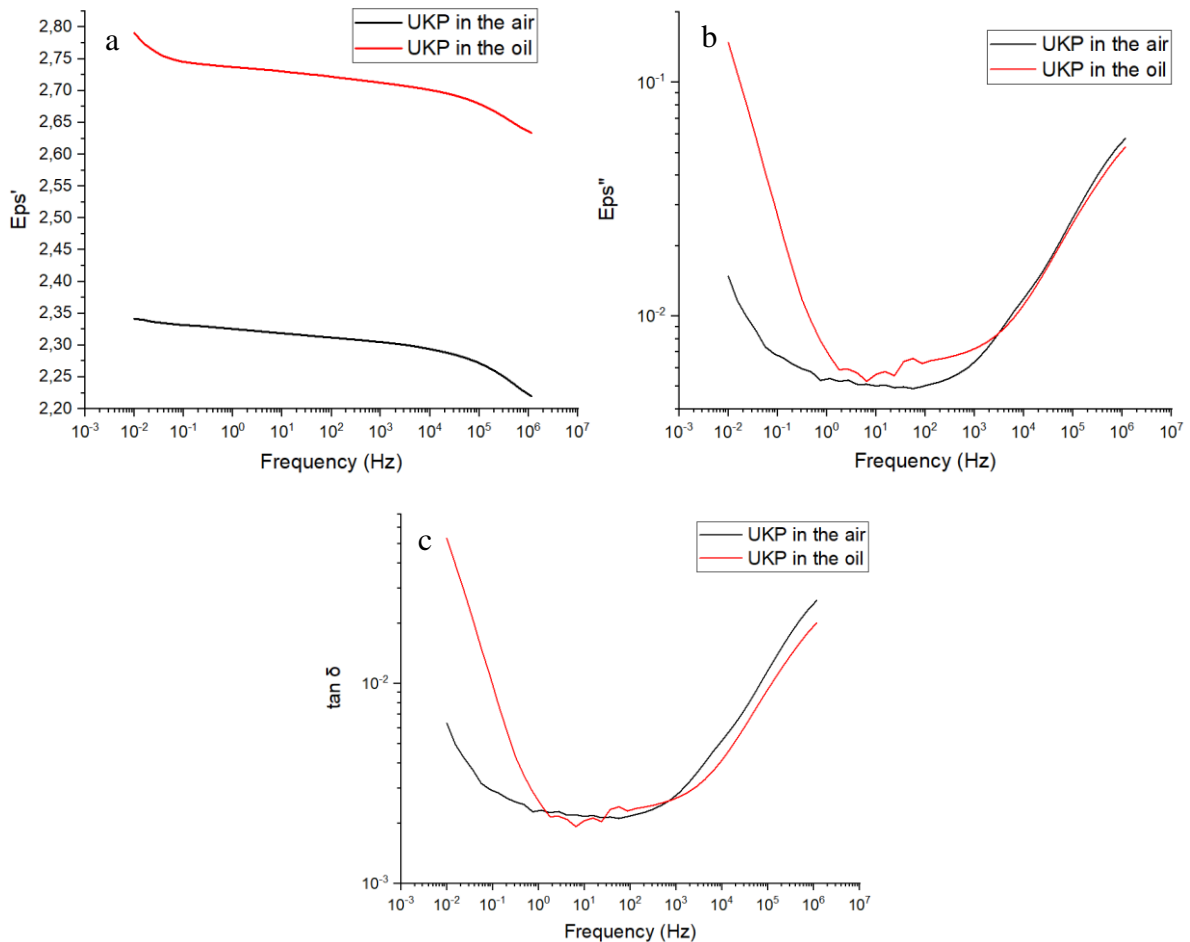


Figure 99: Real (a / ϵ') and imaginary (b / ϵ'') permittivity and $\tan \delta$ (c) at 21°C for the same unaged dried UKP (0.3% water content), either impregnated with oil (red), or in air (black).

At 50 Hz, the permittivity ϵ' in the air was 2.31 while it was 2.72 in the oil. This influence is coherent, since the available free space is now filled with oil of higher permittivity compared to air ($\epsilon_r = 1$). $\tan \delta$ at low frequency also increases a lot (about 1 decade), which is also consistent with the fact that losses of the liquid at room temperature ($\tan \delta \approx 5 \times 10^{-1}$, see Figure 97) are much greater than in the paper alone. It is interesting to evaluate the amount of oil actually present in the paper. For these calculations, we will assume that the free space (void volume) inside paper doesn't change when paper is impregnated with oil. To calculate the void volume, the following parameters will be used:

- Sheet grammage (kg/m^2): $G = w/A$
- Sheet apparent density: $\rho_{\text{app}} = w/V = w/(A \cdot e) = G/e$
- Lignocellulosic matter density: $\rho_{\text{cell}} = w/V'$

where:

- w: sheet weight (kg)

- V: sheet volume (m³)
- V': dense matter volume (m³)
- A: sheet area (m²)
- e: sheet thickness (m)

The Voidage (also called porosity) is given by the formula: $\text{Voidage} = 1 - \rho_{\text{app}}/\rho_{\text{cell}}$

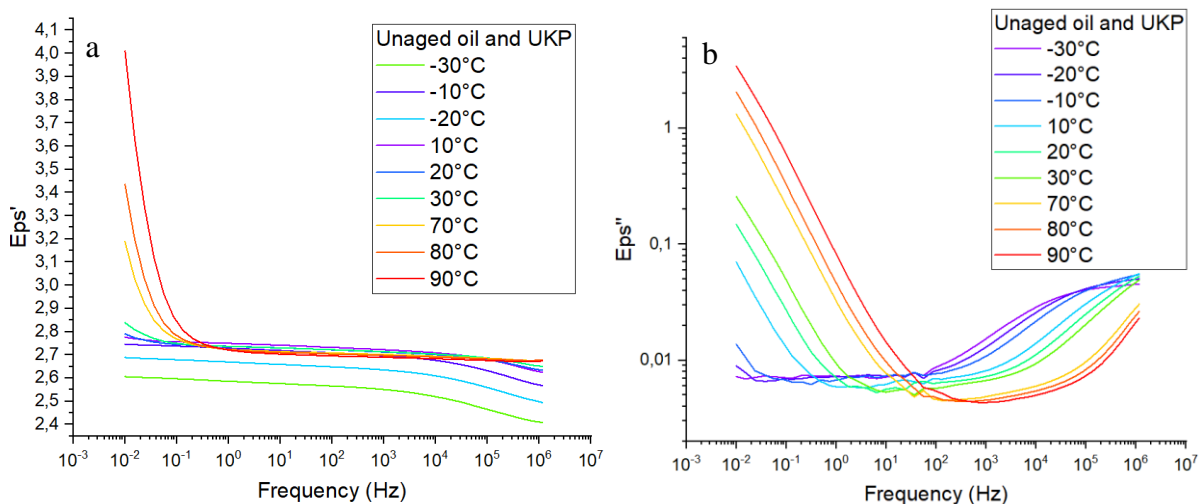
To calculate the voidage in the reference UKP samples, we use:

$G = 0.130 \text{ kg/m}^2$; $e = 1.40 \times 10^{-4} \text{ m}$; $\rho_{\text{cellulose}} = 1540 \text{ kg/m}^3 \Rightarrow \rho_{\text{app}} = 928.6 \text{ kg/m}^3$; $\text{Voidage} = 0.397$

The Voidage found for the UKP paper samples is 39.7% ($\approx 40\%$), and the volume occupied by the dense matter is 60.3% ($\approx 60\%$). Impregnated paper thus contains 40% of oil (in volume). Therefore, it is clear that the permittivity and losses of impregnated paper partly reflects that of cellulose fibers and oil. The permittivity of the solid material constituting fibers is not well known, and should be much higher than the value ($\epsilon' = 2.5$) measured for dry paper containing 60% of fibers in air. In the case of denser pressboard, values of 4.5 are reported (Table 31), and up to 8.4 in the case of even more dense very thin layers of cellulose. Calculating the equivalent permittivity and losses of a heterogeneous two-phase material is a very complex question, since it strongly depends on the shapes of both phases, and also on possible interactions between them.

In the study of Xie *et al.* [3] almost no change was recorded between samples impregnated or not, which again casts doubt on the experimental results obtained in this study.

The FDS analysis for the reference unaged UKP impregnated with new oil over a large temperature range is presented in Figure 100:



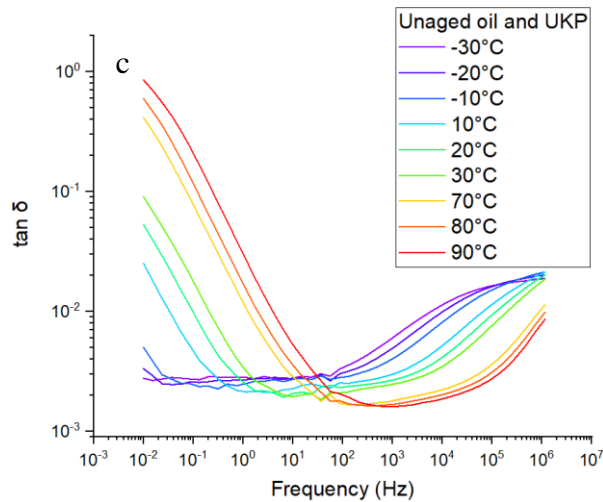


Figure 100: Real (a / ϵ'), imaginary (b / ϵ'') permittivity and $\tan \delta$ (c) at multiple temperatures going from -30°C to 90°C for unaged UKP paper samples impregnated with oil. The water content of the samples is 0.3%.

Experiments over a large temperature range (-30 to 90°C) basically show a very large increase of losses $\tan \delta$ at temperatures above 10°C and low frequency, and a moderate increase of permittivity ϵ' at low frequency and temperatures above 30°C . At the practical frequency of 50 Hz, almost negligible variations of ϵ' , ϵ'' , and $\tan \delta$ are seen, showing the good stability of such insulating material for transformers. Permittivity $\epsilon' \approx 2.8$ is measured, in line with previously available data for impregnated low-density paper of comparable thickness [7], and lower than values corresponding to thicker and denser pressboard ($\epsilon' > 4$). A $\tan \delta$ of 0.13 is measured at 50 Hz and 20°C , this measurement is in line with literature: a value of $\tan \delta$ below 0.5% is used to verify an insulation is properly dried [1].

Although ϵ' values were abnormally low in Xie *et al.* paper [3], most of trends were similar between both studies. In their measurements, a decrease of losses versus frequency is also visible at high temperature and low frequency, attributed to LFD and conduction. Interfacial polarization is seen in both studies, but is better observed in our measurements carried out up to 10^6 Hz (instead of 10^5 Hz). The dipole polarization visible at -30°C for Xie *et al.* [3] is not visible above, it is consistent with the fact that the entire spectra is shifted to the left. Regarding changes at low temperatures, they are not visible in the other studies while it is visible on all FDS measurements with UKP, BKP and CL.

In order to better identify the origin of losses in the impregnated paper, it is interesting to compare $\tan \delta$ measured in oil alone, paper alone, and impregnated paper at different temperatures (90 , 20 , and -30°C), see Figure 101.

At 90°C , $\tan \delta$ of oil and paper are identical at 30 Hz, and $\tan \delta$ of impregnated paper is also logically identical at that frequency. Below and above 30 Hz, the impregnated paper shows a $\tan \delta$ intermediate between that of paper and oil:

- Below 30 Hz, $\tan \delta$ reflects mostly the losses of oil (due to conduction).
- Above 30 Hz, $\tan \delta$ reflects mostly the losses of paper (due to polarization).

At 20°C , the situation is similar, with a lower “transition” frequency (about 1 Hz).

At low temperature (-30°C) the losses of oil become negligible compared to that of paper, and losses of impregnated paper mostly reflects those of the paper.

The global plot of $\tan \delta$ of impregnated paper at different temperatures (Figure 101) clearly shows two typical zones, below and above a “transition” frequency about 30 Hz:

- Below 30 Hz, losses are mainly due to conduction in oil, and increase a lot when temperature is raised.
- Above 30 Hz, losses are mainly due to polarization in the paper, and decrease when temperature is raised.

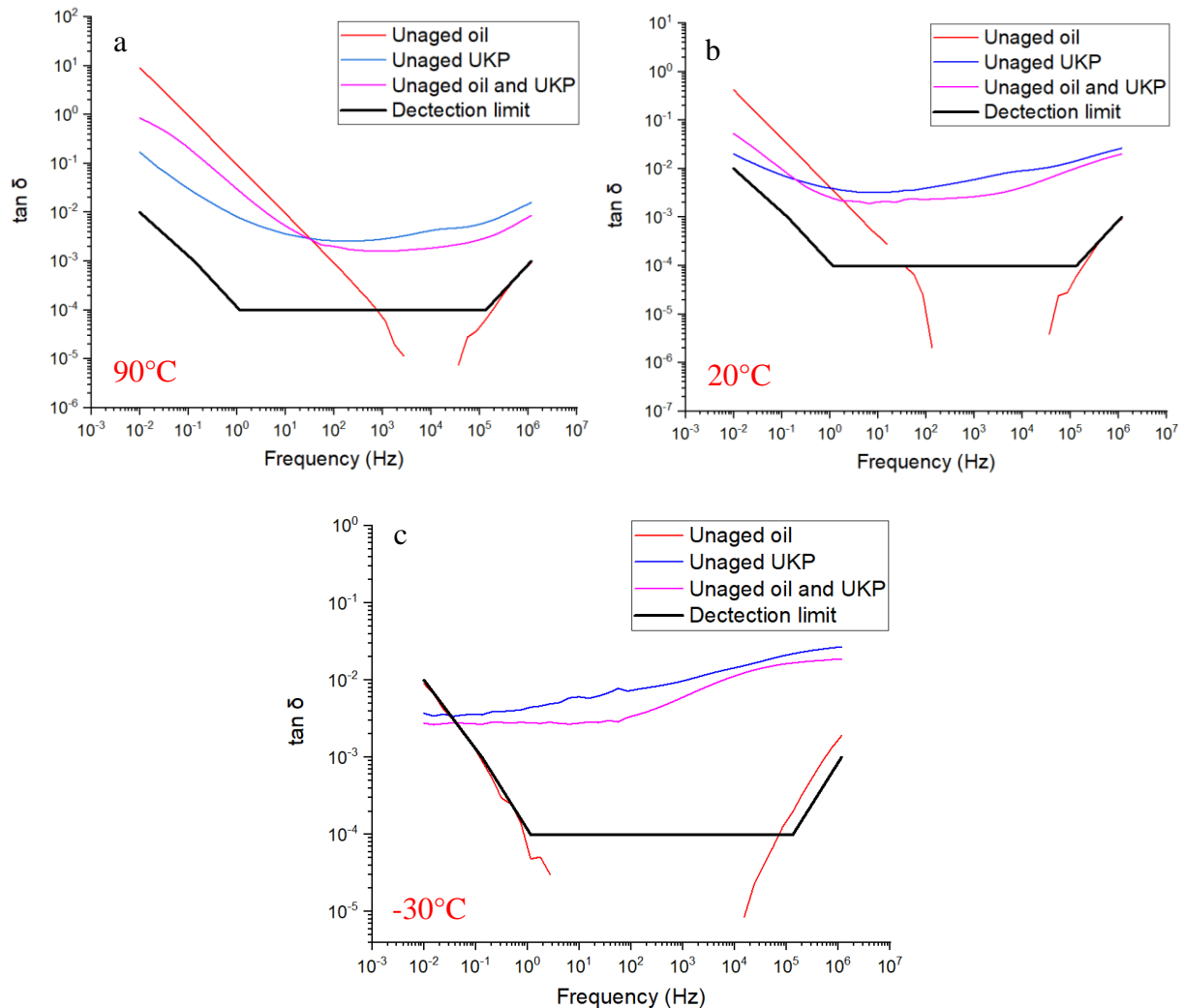


Figure 101: $\tan \delta$ of unaged oil, UKP paper and impregnated UKP samples at high (a / 90°C), medium (b / 20°C) and low (c / -30°C). The moisture content of both UKP samples was 0.3%, this moisture was measured at 21°C . The detection limit of the spectrometer is shown.

It is however not possible to consider that impregnated paper simply results from the “sum” of contributions of oil and paper, as two independent capacitors in parallel would do. Interaction between these two materials also exists. At low frequency and high temperature, a large electrode polarization takes place in impregnated paper, inducing a significant increase of permittivity ϵ' (from 2.8 to 4 at 90°C , 10^{-2} Hz). This effect is much more marked than in oil alone (almost no electrode polarization occurs in paper alone), and evidence the interaction between the materials.

A well known interaction between transformer paper and mineral oil is constituted by the electrical “double layer” that establishes at their interface [14]. This interaction induces two parallel layers of charge. In the first layer, positive charges from impurities in the oil are adsorbed onto the Kraft insulation due to chemical interactions. The second layer is composed of ions attracted by the surface charge via the Coulomb force, electrically screening a negative charge in response to the first layer. This interaction plays a key role in a phenomenon called “flow electrification” that leads to a buildup of charges in Kraft insulation following the flow of oil. Such charge buildup can lead to high local potential and electric field, that can eventually cause partial discharges or breakdown [14]. These studies focused on measuring the charges and potential of different types of paper and oils, but almost no study was dedicated to evaluate its role on dielectric spectroscopy measurements. Conditions existing at the interface between cellulose and oil within the paper are certainly very different from a standard macroscopic paper / oil interface: distances are much smaller, and the charge equilibrium is probably different, and rather difficult to predict. However, we may suppose that the presence of charges at the interface, resulting from chemical interaction between oil and cellulose, may influence FDS measurements of impregnated paper.

The electrode polarization in impregnated paper is less prominent in our study than in comparable studies of Xie *et al.* [3]. This certainly comes from the lower thickness of our samples (140 μm) compared to 2 mm in the reference study [3] (real power transformer’s paper is around 100 μm thick). In their experiments with thinner samples, the signal from electrode polarization became less pronounced. An experiment done here with thicker UKP paper (2.16 mm) showed a similar trend in Figure 102: electrode polarization is more pronounced at lower thicknesses.

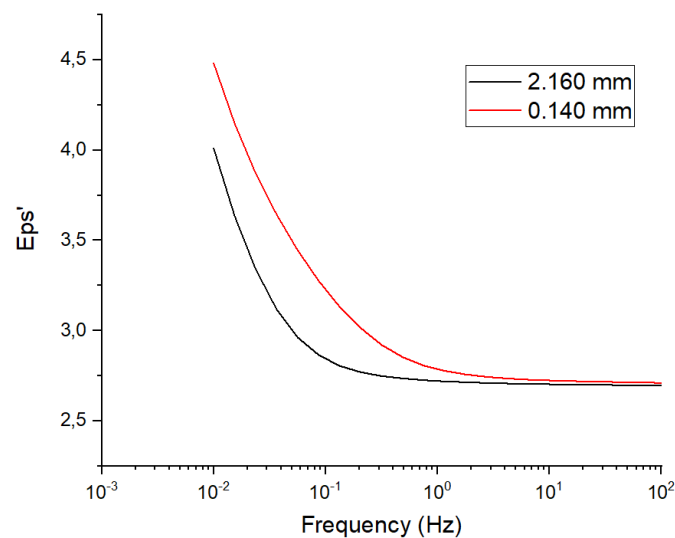


Figure 102: Real permittivity of unaged **UKP paper samples in oil** with a thickness of 0.140 and 2.160 mm. All the FDS measurements were done at 21°C and the moisture content of the samples is 0.3%.

iv) Influence of water content

The influence of water constitutes a parameter with a huge impact for the properties of both new and aged impregnated paper, and further complicates the interpretation of FDS

measurements. In atmospheric conditions around 5% of the weight of paper is due to water absorbed from the environment. Water conductivity and permittivity (80 F/m) are very high, which means that even a small amount of water would greatly increase the permittivity and losses of paper, as previously reported in other hygroscopic materials such as epoxy resins.

FDS experiments were conducted on paper samples without oil. Starting with humid paper containing 4.8% water, the aim was to progressively dry each sample in order to investigate FDS measurements with different paper water contents W_p (expressed in % of mass). Since samples are thin (140 μm) drying under vacuum was very fast, and hard to graduate. It was also impossible to measure the actual W_p during drying. However, values of the surrounding atmosphere water content provided by the Dew Point sensor were used to estimate W_p from the known equilibrium plots. The Dew Point was used instead of relative humidity because it is independent of temperature. After the paper was dried under vacuum to a given degree, the exchange between the water in the surrounding air and in the paper took up to 12 hours before reaching an equilibrium, evidenced by the fact that the Dew Point in the surrounding air became then stable. FDS measurements were done after equilibrium was reached. The spectra obtained are visible in Figure 103.

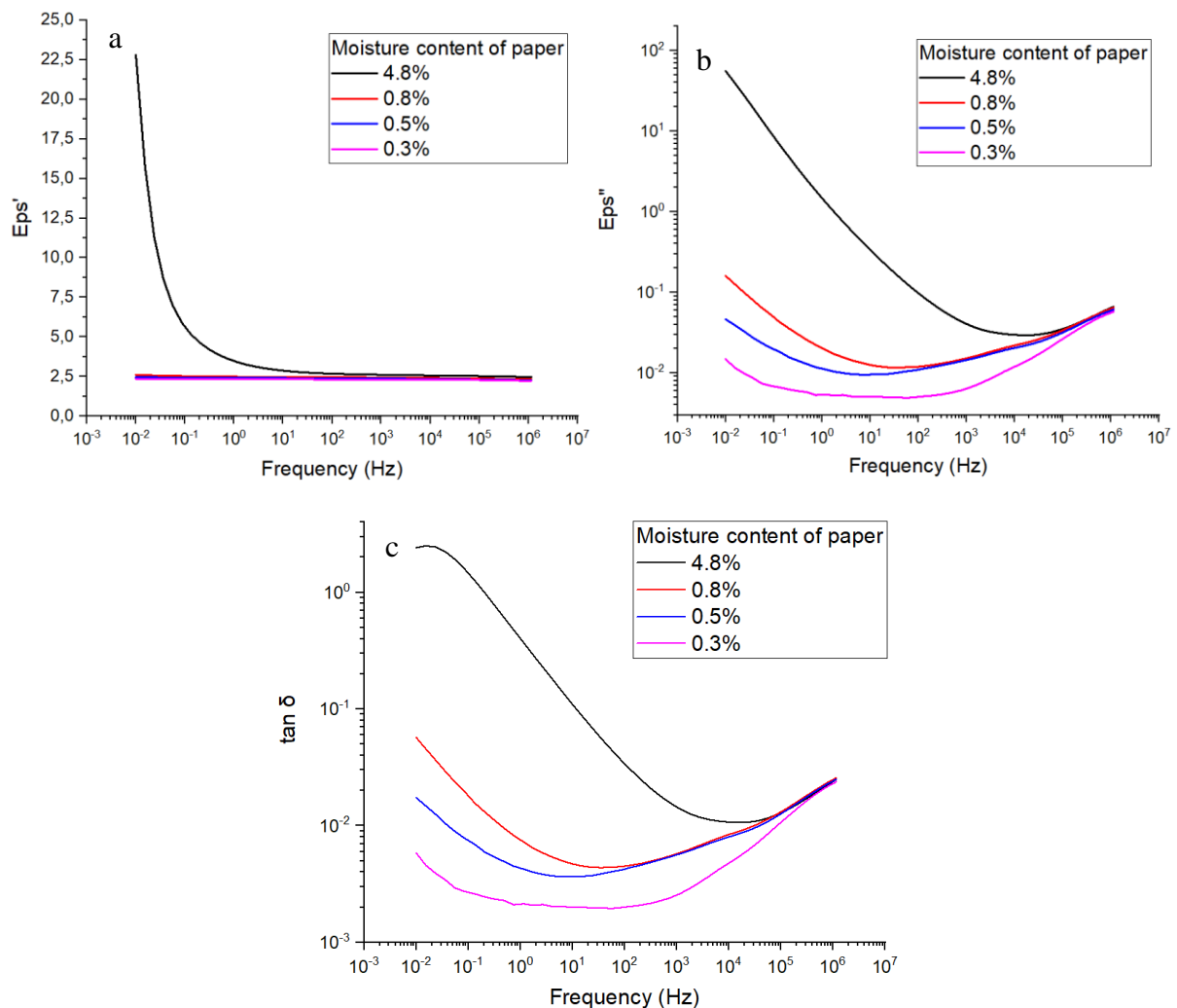


Figure 103: Real (a / ϵ') and imaginary (b / ϵ'') permittivity and $\tan \delta$ (c) at 21°C during drying with the corresponding moisture content W_p in UKP samples.

As expected, ϵ'' and $\tan \delta$ considerably increase with W_p (more than two decades), while ϵ' shows a marked increase only at the maximum water content and at low frequency. ϵ' remains remarkably stable with $W_p < 1\%$, while ϵ'' shows a large increase from the lowest water content achieved (0.3%). It is possible that smaller W_p would lead to even lower losses. The losses at low frequency and high-water content are attributable to conduction.

The behavior of wet paper impregnated with oil at different temperatures is shown on Figure 104. In this experiment paper was first conditioned in air (20 °C, 50 % relative humidity) before impregnation, and its moisture content can be estimated to 7.2% from equilibrium plots.

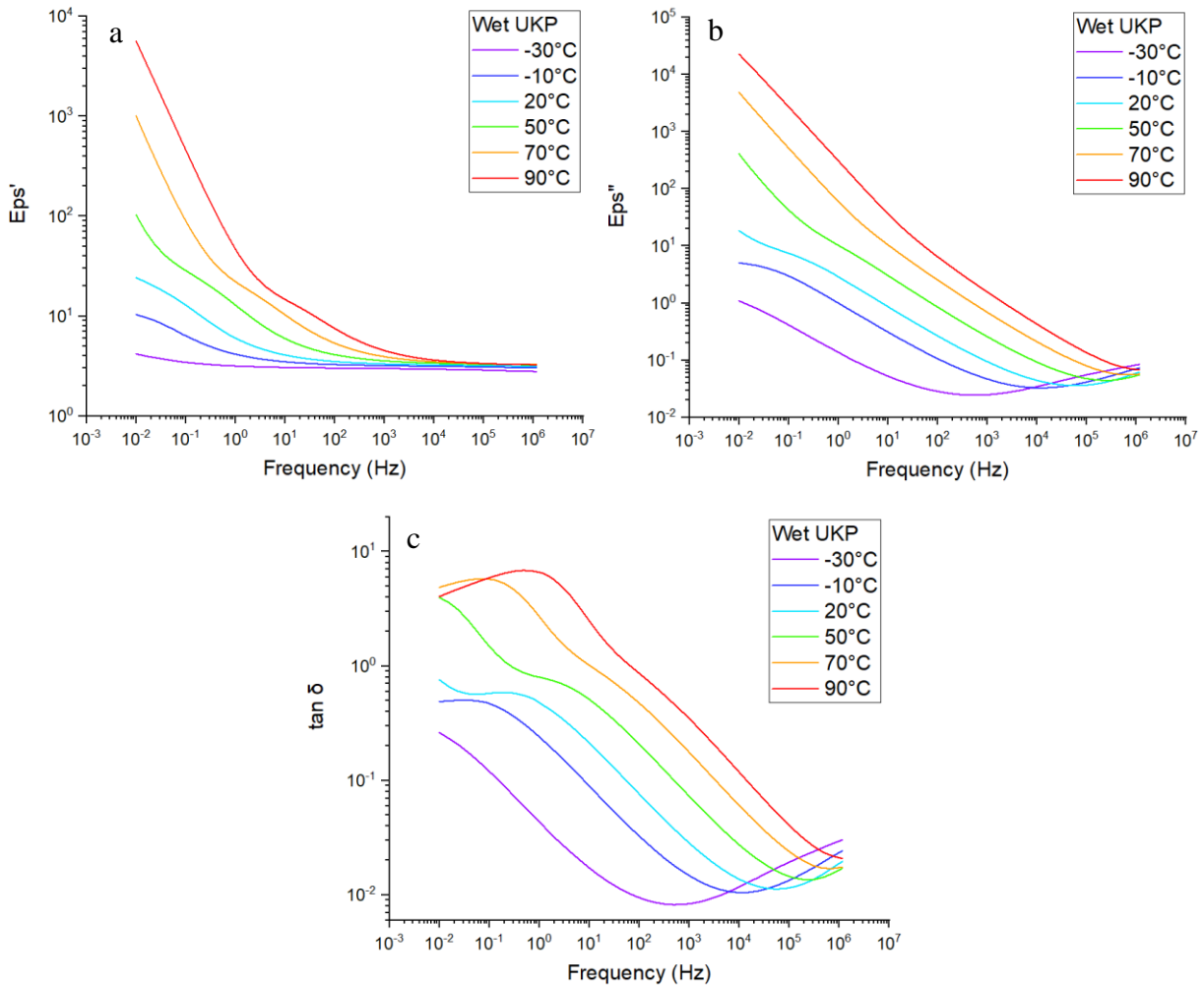


Figure 104: Real (a / ϵ') and imaginary (b / ϵ'') permittivity and $\tan \delta$ (c) for wet UKP samples in oil. The moisture content of UKP samples was 7.2%, this moisture was measured at 21°C.

Such high water content has a huge effect on the dielectric response of impregnated paper. The maximum $\tan \delta$ recorded (at 90°C, 1 Hz) raises up to ≈ 10 , whereas it was about 10^{-1} in paper with $W_p = 0.3\%$. At low frequency, a very large electrode polarization occurs, with ϵ' raising up to 5500. Even at the reference frequency of 50 Hz, ϵ' is not any more stable, and increases up to 10 at 90°C. Clearly, at such high-water content, the impregnated paper cannot be used in transformers. Losses at 50 Hz become dominated by conduction, even at low temperatures.

From oil/paper equilibrium plots, the actual amount of water in oil may raise up to several 100 ppm at high temperatures. Since losses of mineral oil are almost independent on its water

content, and since measured $\tan \delta$ are now well above those measured in oil alone at different temperatures, one may conclude that losses are now dominated by the contribution of wet paper. The plot of $\tan \delta$ at 20°C compares with that of paper with $W_p = 4.8\%$ without oil (Figure 103).

c) Dielectric properties of impregnated UKP during ageing

In this part, the evolution of impregnated UKP during ageing will be tentatively analyzed by FDS measurements, as well as the potential effect of degradation by-products. The overall objective is to determine whether or not FDS constitutes a proper way to detect and quantify ageing.

i) Influence of ageing during 46 days

The objective was to compare unaged UKP with the same sample aged for 46 days. FDS measurements after ageing were carried out in either aged oil (Type 1 protocol), new oil (Type 2), and after a soxhlet extraction and new oil (Type 3). The results are visible on Figure 105; showing FDS performed at high, medium and low temperatures, respectively at 90, 30 and -30°C.

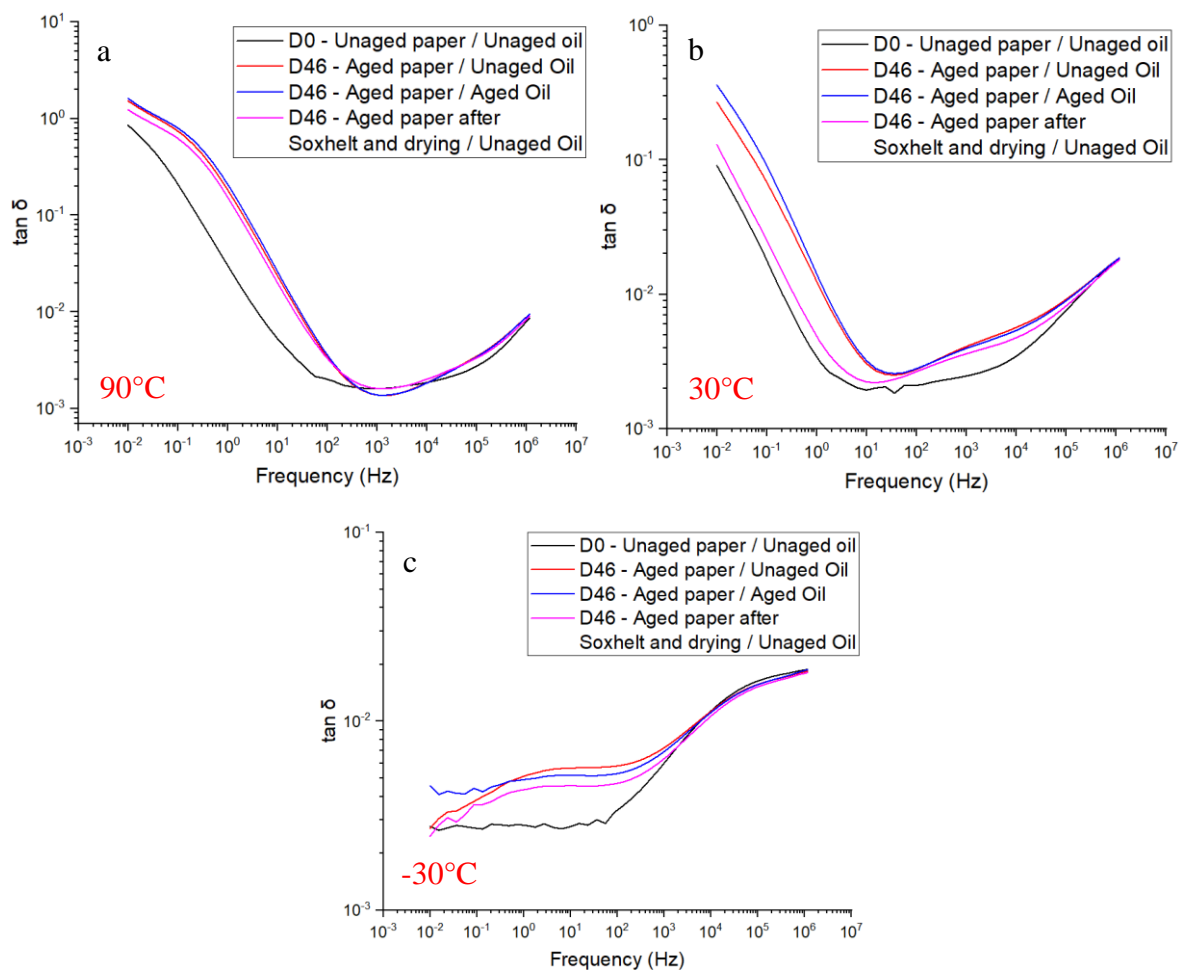


Figure 105: $\tan \delta$ of UKP samples at high (a / 90°C), medium (b / 30°C) and low (c / -30°C) temperatures aged for 46 days. The moisture content of samples was 0.3% at D0 and 1.5% at D46, this moisture was measured at 21°C.

The comparison between unaged sample and aged sample with aged oil show a moderate change in the dielectric response due to ageing. Moreover, changing the oil after aging (Type 2 measurement), and after Soxhlet extraction and drying (Type 3) has almost no influence (excepted at 30°C where a slight decrease of losses is seen in Type 3). It should be noted that this behavior was observed in repeated similar measurements with UKP, and was also visible in BKP and CL (figures that represent these trends are shown in the annex). No simple interpretation can be provided for these results.

The results at 90°C show a significant increase of losses at low frequency. Since such losses are mostly influenced by the conduction of the liquid when the paper water content is low, a first hypothesis would be that liquid ageing could be responsible for such increase. However, changing the liquid (Type 2 measurement) provides no change. Another possibility would be that losses of the aged solid now dominate at low frequency, either due to some degradation of the paper, or to some increase of its water content. Removing ageing by-products and water (Type 3) produces no change, indicating that an increase of aged paper losses could be the main factor, while presence of water has a negligible influence.

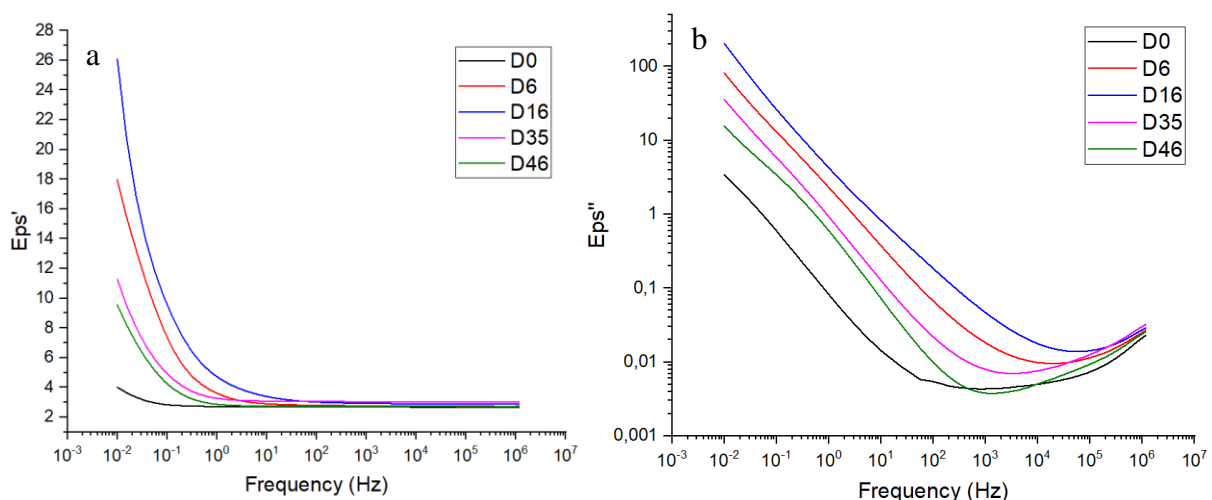
Results at 30°C provides a slightly different conclusion, since Type 3 treatment now induces some reduction of losses, indicating that water or ageing by-products could constitute the main reason for increase of losses.

At -30°C, the influence of liquid on losses should be nearly absent, and FDS is expected to provide information mainly related to the paper. The results showing some increase of losses suggest that losses of the paper increased, presumably due to paper ageing or increased water content.

Since the presence of water may constitute a parameter of great influence, experiments were carried out to follow the evolution of water content during ageing, correlated to FDS measurements.

ii) Evolution of permittivity and water content during ageing

Dielectric properties were measured during ageing, with FDS measurements carried out at regular intervals at a fixed temperature of 90°C, without changing the oil. The results are visible in Figure 106.



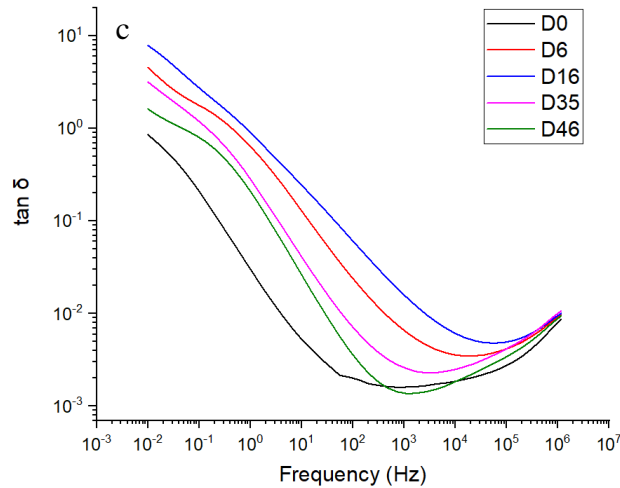


Figure 106: Real (a / ϵ') and imaginary (b / ϵ'') permittivity and $\tan \delta$ (c) of UKP samples in oil for unaged and aged samples at up to 46 days. All the FDS measurements were done at 90°C. The water content of the samples is visible below in Figure 107.

Interesting data are obtained from these measurements. The evolution of dielectric properties versus time was not progressive: conduction losses first increased from D0 to D16, and then decreases at D35 and D46. An identical variation during ageing was also observed for BKP and Cotton. Since these results were somewhat contra intuitive, another series of 46-day ageing under identical conditions were done, and showed the same results. Ageing at D16 and D46 was also performed twice to verify there was no experimental errors, but they gave the same results.

A similar phenomenon was actually observed several times in previous literature [8–10]. The actual duration after which ϵ'' decreases is not identical in different papers, since samples are of different types, and aged under different conditions. In other studies, with even longer durations, multiple inversions were sometimes reported. The main explanation postulated is that the non-uniform trend in the dielectric response are correlated with the variations in moisture content in the oil. In these studies, FDS measurement were done at fixed temperature (55°C or lower).

It was thus interesting to estimate the water content in oil and paper during ageing. Unfortunately, it was not possible to obtain a direct measurement of these data. Samples of oil were taken at days 6, 16, 35, and their moisture content was measured at room temperature. Although the water equilibrium between paper and oil considerably changes between room temperature and ageing temperature (Figure 108), water content in oil during ageing can be used to estimate the moisture content of paper from equilibrium plots. For this calculation, it was considered that the equilibrium did not change with ageing. Figure 107 shows that during ageing, the paper water content first increases, goes through a maximum about 2.5 % after about 15 days, and then decreases. The final water content at D = 46 days is larger than the initial one (0.3%), and reaches about 1.5 %, which in turn should induce significant variations of FDS measurements.

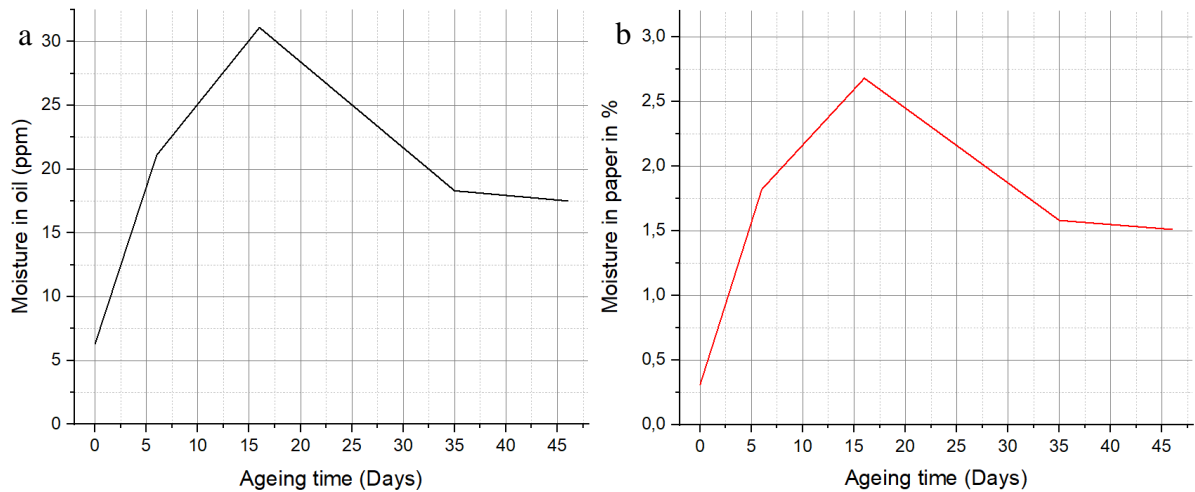


Figure 107: Evolution of the moisture content at 20°C in oil (a) and paper UKP samples (b) during ageing at 130°C in non-oxidative conditions. The moisture content for paper is represented as the mass ratio of water divided by the mass ratio of paper, shown in percentage. For oil, the moisture content of water is shown in ppm.

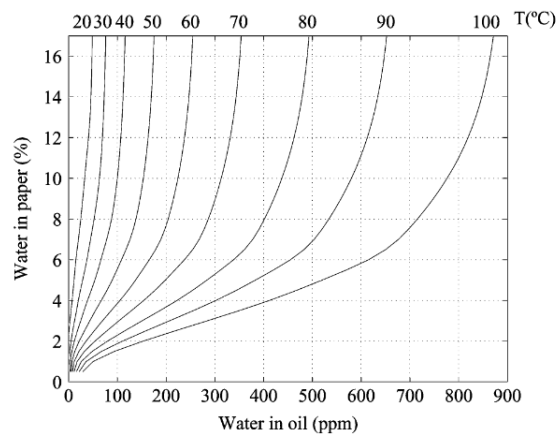


Figure 108: Range of paper-oil moisture equilibrium curves at multiple temperatures. Extracted from Garcia et al. [15].

The correlation between paper water content during ageing and dielectric losses is rather obvious, and strongly suggests that variations of FDS are primarily attributable to the increase of water content. With a much larger water content (estimated to 7.2 %) the measurements of Figure 104 showed that the losses of impregnated paper become entirely dominated by those of paper, even at low frequency. Although the paper water content induced by ageing is lower (1.5 % after 46 days), some of the features observed in Figure 104 with 7.2% can be also observed on Figure 106 after 46 days:

- A large electrode polarization at low frequency is observed when the water content is maximum, inducing a large increase of ϵ' up to 26 at 90°C at day 16, *i.e.* about 8 times the normal permittivity of paper. Such increase cannot be explained if the losses due to the liquid still dominate.
- Losses increase a lot even at high frequency, where the contribution of paper dominates.

To obtain further insight in phenomena occurring during ageing, FDS characterizations were also carried out in aged oil alone, and in non-impregnated aged paper.

iii) Characterization of aged oil and aged UKP paper alone

Dielectric properties were measured for paper and oil separately, after 46 days of ageing. After ageing, the paper was cleaned from oil and by-products by Soxhlet extraction, and then dried down to 0.3% water content before measurements without oil. The results are visible in Figure 109 and Figure 110:

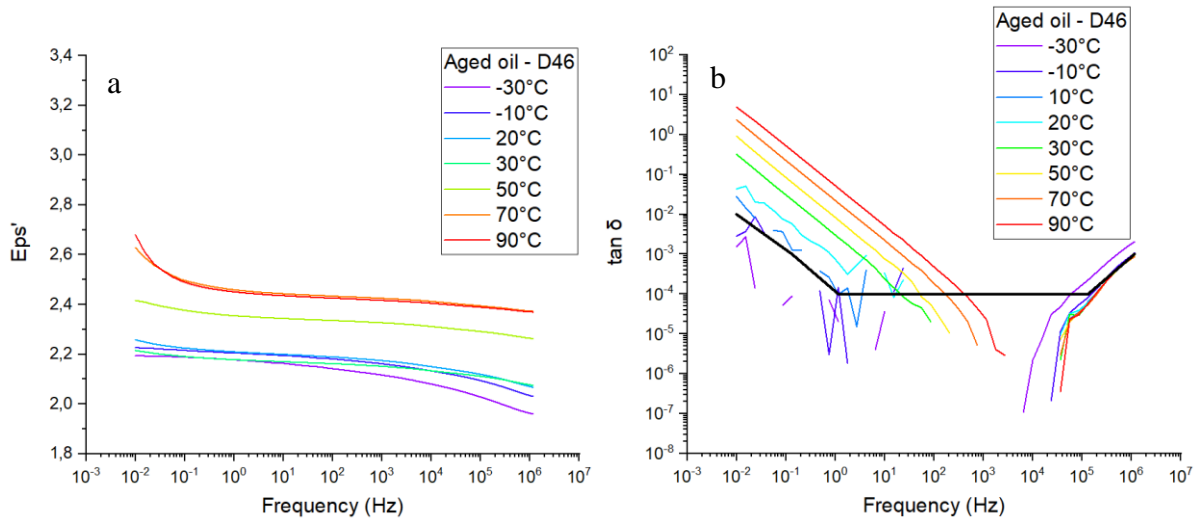


Figure 109: Real permittivity (a / ϵ') and $\tan \delta$ (b) at multiple temperatures going from -30°C to 90°C for aged oil for 46 days. The water content of the samples 17 ppm.

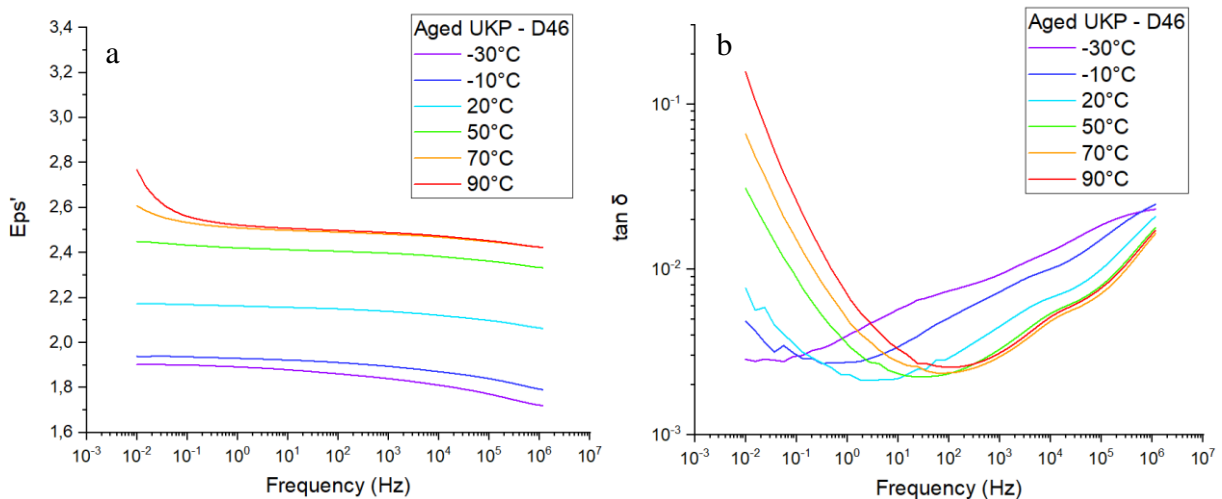


Figure 110: Real permittivity (a / ϵ') and $\tan \delta$ (b) at multiple temperatures going from -30°C to 90°C for aged paper for (D46) without oil. The water content of the samples 0.3%.

Since aged UKP samples were dried before measurements, water does not play a major role in these results and mostly the chemical modification of paper should change the dielectric response. These figures show that there was no significant change in the dielectric response of aged oil and aged UKP samples when compared to unaged samples. These results suggest that the dielectric response of aged impregnated UKP does not reflect modifications of the materials (oil, paper), and are mostly influenced by the change of water content, and also presumably by modifications of the interaction between oil and paper.

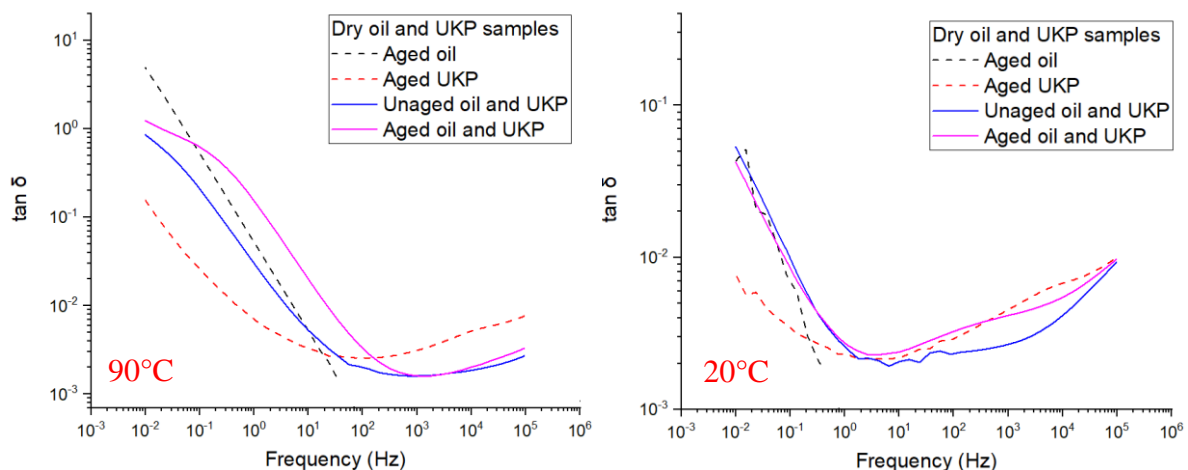
iv) Discussion of results

Most studies [7,11] clearly state that the moisture variations during ageing is the main contributor to changes in dielectric properties. An ageing component to this response is hinted at in one study [7], and is attributed to a drop in the molecular weight of the pressboard. However, most studies point out that no obvious correlation between the ageing, measured by the degree of polymerization, and the dielectric response can be established [16]. In a more recent study [11], it was concluded that moisture and influence of materials ageing interact with each other, with moisture significantly increasing the influence of ageing once a threshold of 2% moisture content is reached.

From our measurements, no simple and unique answer emerges regarding the relative influences of paper ageing and water.

- The obvious correlation between variations of the water content during ageing and dielectric losses supports the conclusion that water constitutes a primary parameter to explain variations of FDS measurements.
- The fact that changing the oil, removing by-products and water (Soxhlet treatment) has almost no influence suggests an opposite conclusion: paper ageing seems to constitute the dominant parameter.
- The fact that dried aged paper shows almost no enhancement of losses seems to contradict this conclusion.

Figure 111 below shows a comparison of the dielectric response of the aged components (aged oil, dried aged UKP), with unaged dry impregnated UKP, and aged impregnated UKP.



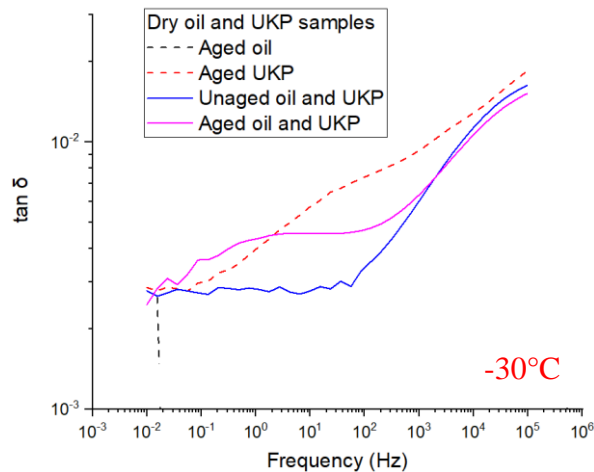


Figure 111: *Tan δ of oil, UKP and oil-UKP samples at high (a / 90°C), medium (b / 30°C) and low (c / -30°C) temperatures unaged and aged samples for 46 days. The moisture content of UKP samples was 0.3% this moisture was measured at 21°C. The water content of the oil samples 17 ppm.*

At 20°C and low frequencies, no influence of ageing on losses of impregnated UKP is seen. Losses are dominated by those of oil. At frequencies above 100 Hz, losses of impregnated paper slightly increase, and this increase is correlated to an increase of losses of the paper. This is consistent with the fact that at such frequency the influence of oil becomes negligible.

At -30°C, a similar observation is done: the influence of oil is negligible, and some increase of losses of aged impregnated paper occurs compared to new impregnated paper.

At 90 °C, the low frequency losses of aged impregnated paper are not any more intermediate between those of oil and paper (as in the case of new impregnated paper), but now higher than those of oil alone. This suggests the presence of a moderate quantity of water.

All together, it appears that the influence of ageing on FDS measurements probably results from a complex and rather unpredictable combination of the influences of paper ageing, increased water content, and also possibly modified interactions between oil, paper, and water that also may influence FDS measurements. Such modified interactions could involve for instance the charged layer existing between cellulose and oil, or the equilibrium of water between oil and paper versus temperature.

Regarding the results of this FDS study and their correlation with other measurements carried out during ageing, it appears that no relationship can be established between the degree of polymerization and the moderate changes in FDS measurements recorded. This agrees with previous conclusions present in the literature. Based on this conclusion, FDS does not constitute an efficient tool to detect and quantify paper ageing. Yet, during aging changes in losses correlated to variations in water content are correlated to changes in oxidation recorded via FTIR spectroscopy. It was observed in the previous chapter that there exists a decrease in the overall oxidation of the pulp at D35 and D46. These observations provide some support to the claim that chemical modifications in the paper's composition can be correlated to changes in dielectric properties.

d) Influence of paper composition on ageing

Ageing experiments were carried out to compare the dielectric response of UKP with BKP and Cotton Linters (CL). For unaged samples, this could elucidate if some typical paper components influence the dielectric response in a significant manner (*i.e.* cellulose, hemicellulose, and lignin). For aged samples, it could help to show if lignin could play a potential role in preserving the dielectric properties and the role of oxidation.

i) Effect of paper composition on unaged samples

The results obtained in impregnated unaged samples of UKP, BKP and CL at 90 °C are visible in Figure 112. All samples were prepared, dried, and impregnated with dry oil following the same protocol, therefore, any changes in the results should come from differences in the paper's composition.

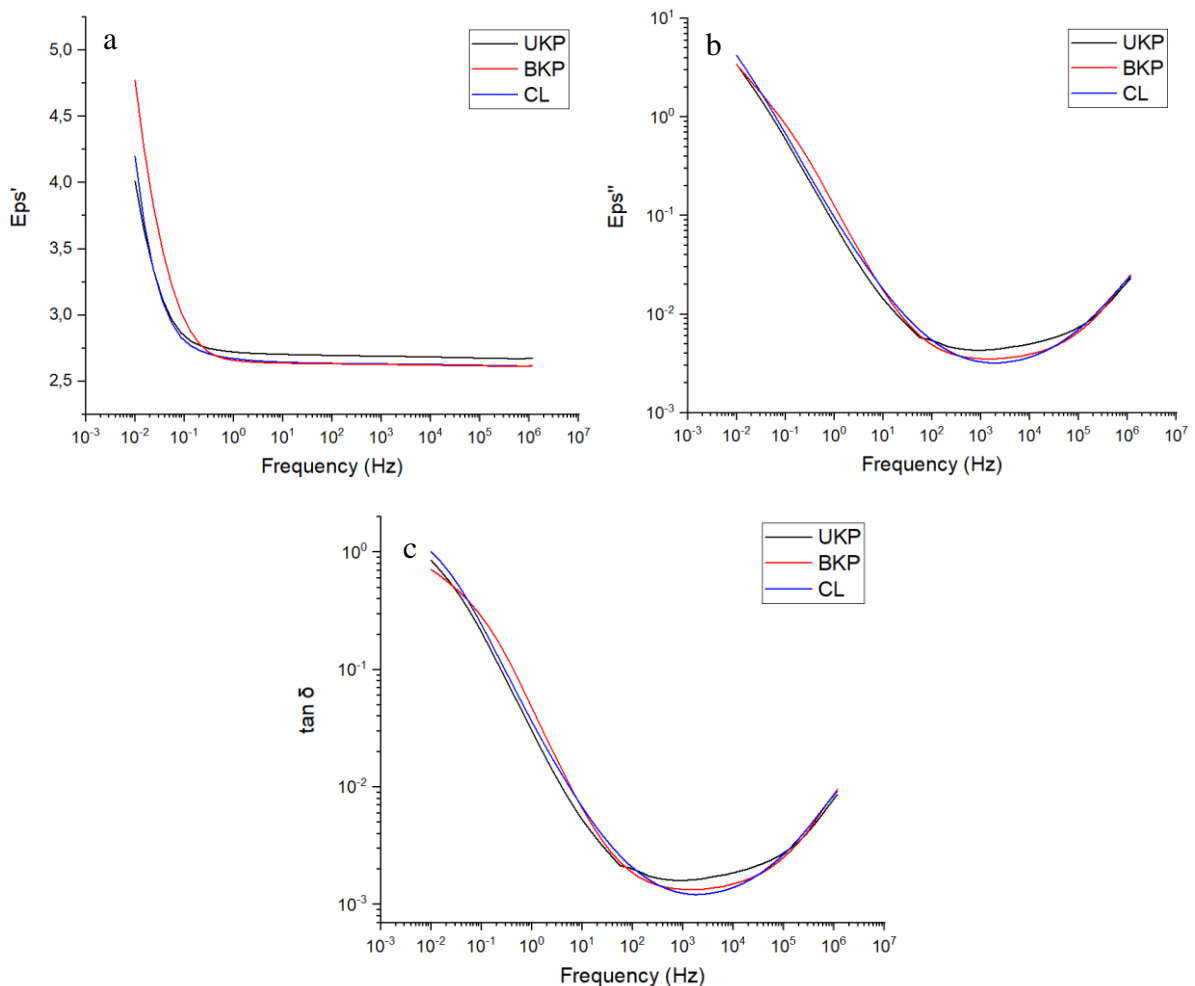


Figure 112: Real (a / ϵ') and imaginary (b / ϵ'') permittivity and $\tan \delta$ (c) comparison between the imaginary permittivity ϵ'' of unaged UKP, BKP and CL samples. All the FDS measurements were done at 90°C and the moisture content of the samples is 0.3%.

The paper composition plays almost no role in unaged samples. Chemically, UKP contains lignin while BKP and CL only contain carbohydrate-based polymers (Cellulose and

Hemicellulose). This shows that for unaged samples lignin doesn't play a role in dielectric properties for unaged samples.

ii) Effect of paper composition on aged samples

The same samples were analyzed after they were aged for 46 days. The results are visible on Figure 113:

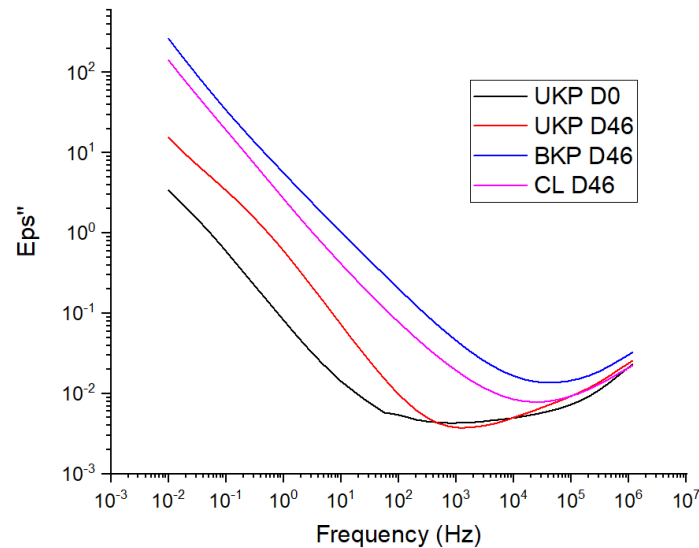


Figure 113: Comparison between the imaginary permittivity ϵ'' of UKP, BKP and CL samples after 46 days of ageing and an unaged UKP sample. All the FDS measurements were done at 90°C.

The paper's composition did play a significant role in the evolution of dielectric properties. The increase in conduction losses is larger in samples free of lignin. These results correlate with FTIR spectroscopy results, where BKP and CL showed significantly higher increases in oxidative damage than UKP. Conduction losses are highest for BKP, a logical result provided hemicellulose of BKP is more vulnerable to oxidation than the pure cellulose of Cotton. The electrode polarization is masked by the increase in conduction of BKP and Cotton but is visible in UKP. The overall trend indicates lignin's anti-radical activity efficiently protects UKP from oxidation damage, and consequently from the conductivity increase associated with it.

e) Effect of ion exchange during ageing

Experiments were carried out to compare the dielectric response of UKP samples after an ion exchange with main metals (Ca, Na, Mg), transition metals (Fe, Cu), and demineralized samples. For unaged samples, the purpose is to identify the effect metals could have on the dielectric properties. For aged samples, the aim is to examine the potential effect they could have on ageing.

i) Effect of ion exchange on unaged samples

Figure 114 shows the results for main metals, transition metals, and demineralized samples:

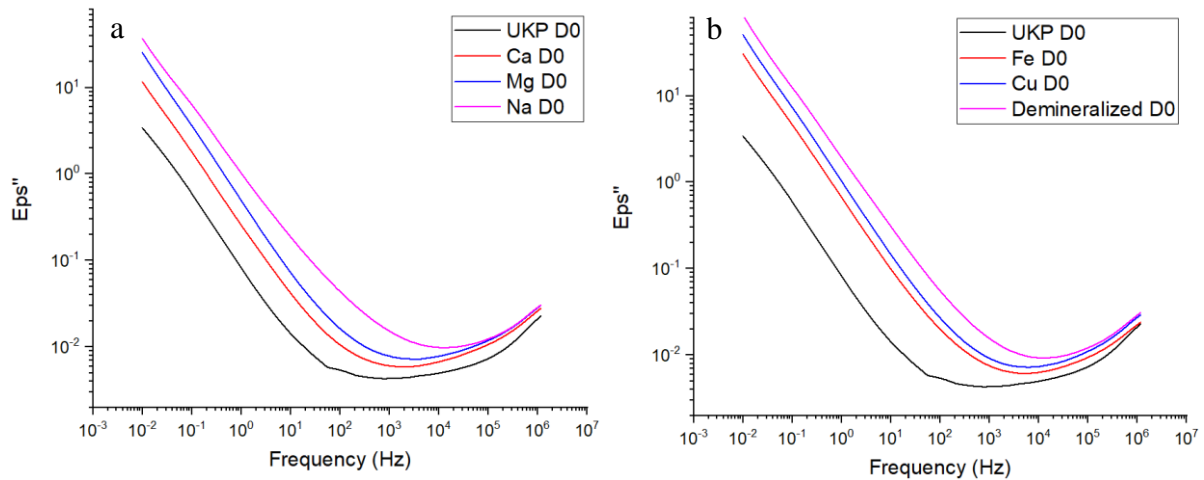


Figure 114: Comparison between the imaginary permittivity ϵ'' of unaged **UKP** and **main (a) and transition (b) metal** samples. All the FDS measurements were done at 90°C and the moisture content of the samples is 0.3%.

All samples were subjected to the same acid treatment but neither showed a difference in DP_v, and only a small change in oxidation before ageing. Given there is no difference in moisture content or oxidation damage, it can be assumed that the small even a very small amount (a few ppm) of ions was enough to significant changes of ϵ'' are visible at low frequency, corresponding to changes in conduction. The most likely explanation is that the presence of ions altered the electrical double layer equilibrium that increased the positive charges of oil in the surface that could enhance conduction losses. Regarding demineralized samples, the sample contains acids, evidencing their influence on conduction.

For main metals, samples with sodium shows the highest conduction losses. This coincides with the fact that paper producers pay special attention to remove sodium from pulps devoted to electrotechnical applications. The large influence of sodium is further supported by the fact that elemental analysis shows there is significantly less sodium present in the sample (228 ppm), as compared to calcium (641 ppm) or magnesium (359 ppm). Measurements with Calcium are the closest to the original UKP sample, despite the concentration of Calcium was the largest. Samples with the with an oxidation that had an important acid component (Sodium, transition metals and demineralized samples) showed an important increase in permittivity unlike magnesium and calcium, this seems to indicate that the acids produced by oxidation act as charge carriers that increase permittivity and conjugated ketones have a comparatively smaller impact, the actual oxidation of the samples is visible in the Chapter 3 of this thesis. For transition metals (iron and copper), a large increase is visible for all samples. The demineralized sample shows even higher conduction losses attributable to mineral acids, this samples is full of residual acids from the acid treatment that could act as charge carriers. Unfortunately, it was not possible to quantify the amount of acid present in the demineralized paper.

ii) Effect of ion exchange on aged samples

The ageing of ion exchanged samples was compared to the reference UKP aged in the same conditions. The results are visible on Figure 115:

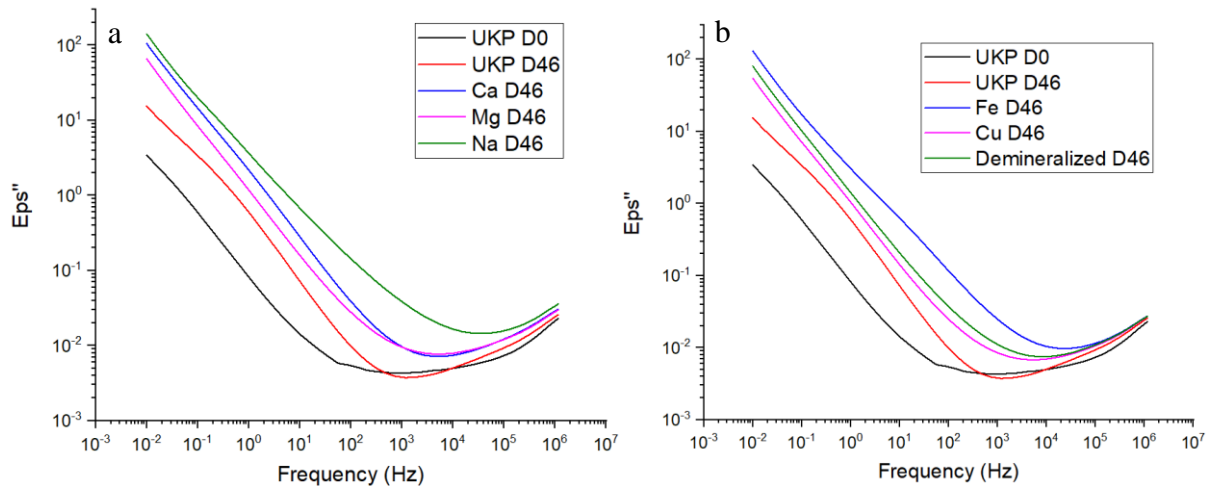
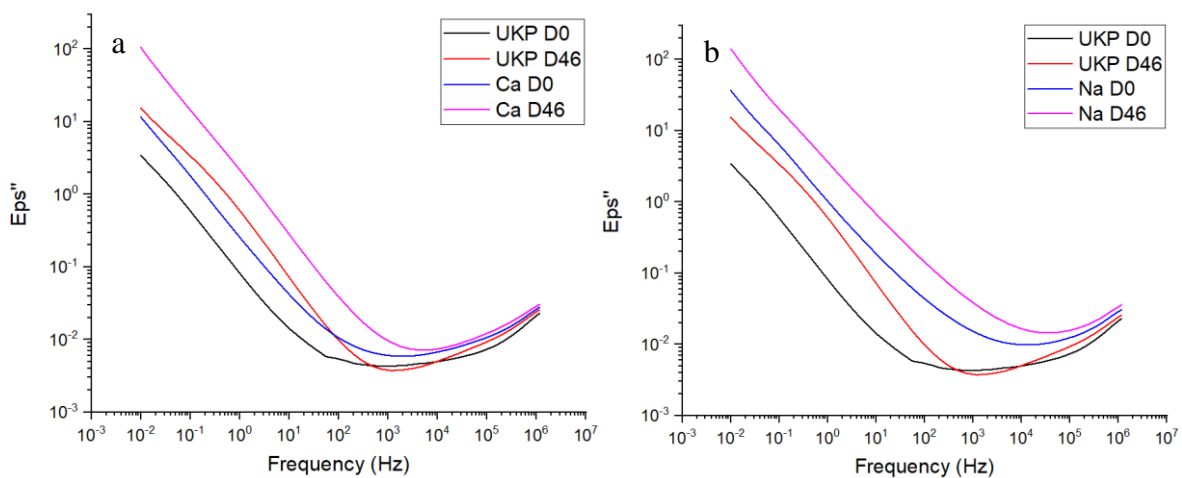


Figure 115: Comparison between the imaginary permittivity ϵ'' of UKP and samples with main (a) or transition (b) metals after 46 days of ageing and an unaged UKP sample. All the FDS measurements were done at 90°C .

After ageing (Figure 116), samples were aged under the same condition but, unlike samples of different composition, they did not have a similar dielectric response before ageing. Conductivity is the only type of loss that significantly increases with ageing. Once again, the increase in conduction correlates with increases in the oxidation results while no correlation with the sample's DPV is shown.



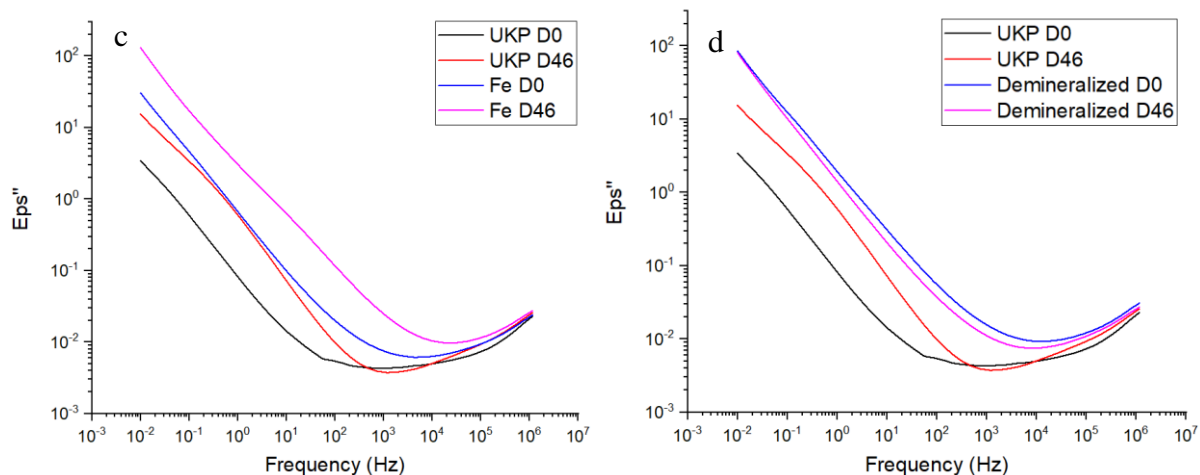


Figure 116: Comparison between the imaginary permittivity ϵ'' of UKP samples after calcium (a), sodium (b), iron (c) ion exchange samples and demineralized (d) samples for unaged and aged (46 days) samples. All the figures include an UKP reference sample. All the FDS measurements were done at 90°C, the moisture content of unaged samples was measured at 0.3%.

For main metals, sodium takes an important role in the dielectric properties, also to note the sodium samples were those with the most oxidative damage (among main metals) showing that sodium itself increases conduction losses but it's known catalytic effect in the acid formation and therefore oxidation of the pulps also significantly increases the dielectric responses to the similar levels as transition metals even though there is around 6.5 times less sodium than copper or iron. Demineralized samples showed almost no change in dielectrical properties as the residual acids from the ion exchange experiments already contained organic acids similar to those produced during ageing. For transition metals, iron overtook copper and demineralized samples, a result that again correlates with the oxidation damage. These results point to a direct correlation between the oxidation of the pulp and the increase in permittivity and therefore dielectric losses.

f) Dielectric breakdown

The dielectric strength of samples was measured before and after ageing. It should be noted that the dielectric strength of paper is influenced by the paper density, but no samples with the same density as our samples was found in the literature. Similar experiment showed a dielectric strength around 120 kV/mm for a paper thickness of 148 μm and a density of 0.82 g/cm³. In our study, UKP paper showed a significantly higher dielectric strength of 211 kV/mm for a paper thickness of 140 μm and a density of 1.3 g/cm³. The dielectric strength of aged samples was tested in comparison with unaged samples. The samples were aged the same way as in previous experiments (ageing at 130°C in non-oxidative conditions). During the dielectric strength tests, unaged oil was used for unaged samples. For aged samples, tests were performed in the same oil in which they aged.

i) Dielectric strength of paper of different compositions (UKP, BKP and CL)

Dielectric strength experiments were performed on unaged samples of UKP, BKP and CL and then after 46 days of ageing. The results are visible in Figure 117:

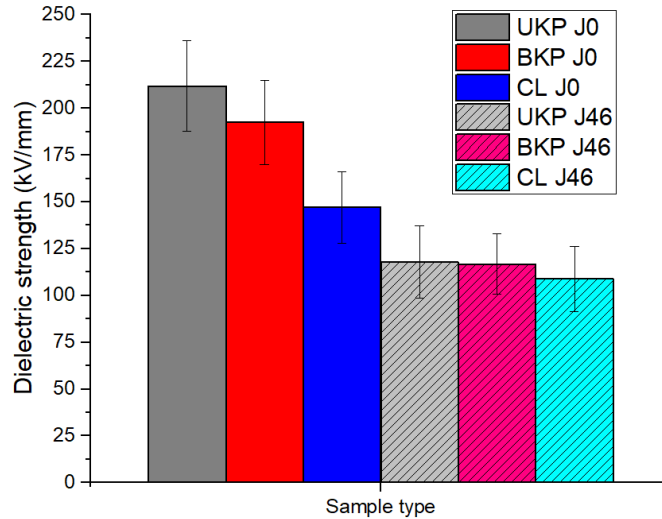


Figure 117: Dielectric strength of unaged UKP, BKP and CL samples and aged paper samples after 46 days. Measurements were performed at 21°C.

Unaged samples show a marked difference in dielectric strength, with Kraft samples showing a significant advantage over Cotton linters. However, after ageing, a large drop of dielectric strength occurred for Kraft samples (-45%), and less for Cotton (-27%). Nearly identical values were then recorded after ageing for all samples. The loss of dielectric strength due to ageing is known to be correlated to the mechanical properties of paper. When comparing to DPv, visible in chapter 3, it is possible to see that samples the dielectric strength correlates to the DPv at D0. After 46 days all the samples have degraded to the point they all have similar mechanical properties with a DPv in the low 200, this resulted in similar dielectric breakdown strength. These results show mechanical properties are the main factor behind changes in the dielectric breakdown strength and not the chemical composition of paper.

ii) Dielectric strength of paper after ion exchanges

Samples obtained after ion exchange experiments were compared to the reference unmodified UKP sample. The results are visible in Figure 118:

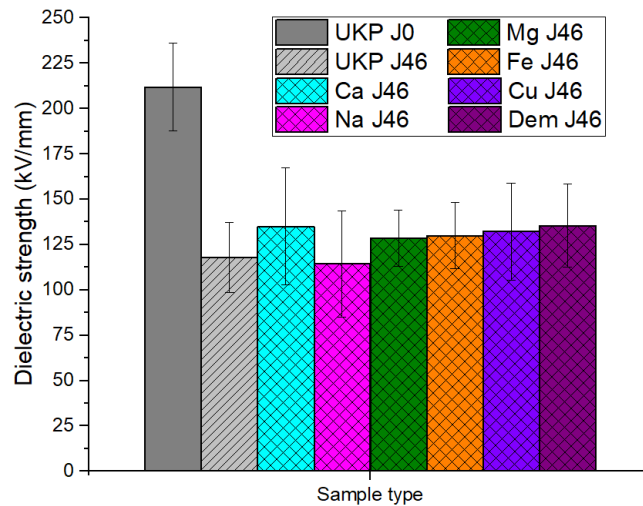


Figure 118: Dielectric strength of unaged samples, aged unmodified UKP and aged samples that with main and transition metals after 46 days of ageing. Measurements were done at 21°C.

These results show the ion exchange had almost no influence on the dielectric strength after aging. It was shown in this study that these samples differ in ion content as well as in dielectric properties. In the previous chapter it was also shown that the oxidation of each sample is widely different. One may conclude that differences in oxidation and dielectric properties play no role in the mechanisms that determine dielectric strength of paper.

Conclusion

Kraft insulation impregnated with oil constitutes a quite complex non-homogeneous insulating material. In turn, it shows a dielectric response difficult to analyze. There are different components contributing to this response: the oil, the paper and the interactions between the oil and the paper. Since paper is highly hygroscopic (contrary to oil), the water content of the paper also has a very large influence on losses. In addition, the equilibrium of water between the oil and the paper widely changes with temperature.

In unaged dry samples it was showed that the dielectric response of the oil and paper insulation was dominated at low frequencies by the conduction losses of oil, and at high frequencies by interfacial polarization. The conduction losses were shown to increase with temperature. Experiments showed that the dielectric response change with ageing of Kraft insulation and oil together, although paper and oil taken separately surprisingly show no large modification. This suggests two main factors for the change in the dielectric response due to ageing: the increasing moisture content, and also a change of the interactions between materials present in the system: paper, oil, and water. Such interactions are far from being identified and understood. A typical example of interaction is the electrical double layer existing between oil and paper that could influence FDS measurements, although in an unpredictable way. Since chemical analysis obviously shows chemical modifications of the paper (oxidation, degree of polymerization, generation of by-products), one may suppose that such interactions could also change.

When comparing the results obtained with the literature, it is difficult to give a universal answer to which parameter affects the dielectric response during ageing, because few studies have been done using FDS analysis on this subject, and also because all of them were carried out with different parameters. Changes in the measurement method such as temperature or equilibration time can significantly change the dielectric response. Furthermore, the ageing method can also significantly modify the manner in which paper and oil age and therefore the contribution of their ageing. Even in fixed and well-defined conditions, experiments may lead to somewhat different conclusions, e.g. the dominant influence of either paper ageing or water content. In contrast, oil ageing in non-oxidative conditions induces only minor variations of its properties.

As seen in literature and in this study, the dielectric response of paper-oil insulation doesn't correlate to the degree of polymerization of Kraft insulation. This is the most common method used to assess the state of degradation and further shows that using a single parameter to quantify the state of paper is misleading since not all properties are correlated to DPv. At the same time, this study showed the oxidation parameter of paper consistently correlate with the dielectric response at all temperatures. This was true for all the results found in all the sample of this study. As for moisture, it is evident that some of the contradictions found in literature stem from different analysis temperature and hopefully further studies could improve in their interpretations by doing their analysis at multiple temperatures. In any case, this study further demonstrates that water isn't the only factor behind changes in the dielectric response and this is particularly true in the case of the high temperatures found in Power Transformers. For example, some of the conclusions found in literature [11], such as a 2% threshold where ageing and moisture start to interact, are only valid at certain temperatures.

The role of Kraft insulation constituent's (lignin, hemicellulose, cellulose) in the dielectric response was also evaluated. For unaged samples, lignin is shown to have a minimal role in

dielectric properties, but, as the ageing progresses, the antiradical activity of lignin consistently showed that it protected the pulp from oxidation and therefore from a further increase of the dielectric response. Also, hemicellulose could constitute a weak link with regards to oxidation, as shown with the increased response of BKP compared to CL.

Ion exchange experiments showed that even in unaged samples, small changes in the metal content of paper, in the ppm range, can have an important impact in the dielectric response. Of particular effect are sodium, copper and iron; this is consistent with the fact that most manufactures of electrotechnical grade pulps particularly targets these specific metals during the pulping process. Their effect is not restricted to unaged samples either, they are known to accentuate oxidation and depolymerization of cellulose, with copper and iron having a stronger effect. This probably comes from an important capacity to produce super oxides and to catalyze hydrolysis. They increase both hydrolysis and oxidations that result in further conduction losses. Sodium, is shown to have similar worse effect on the pulps than even transition metals even though its concentration was six times lower.

The measurement of breakdown strength is sensitively affected by ageing, and therefore constitutes a relevant tool to characterize the paper. In contrast, the metallic composition played no role in the dielectric breakdown strength of paper. After ageing samples with multiple oxidations levels showed no difference in their breakdown strength, suggesting this parameter is independent from oxidation.

It is hoped that this study can give insights for the potential development of FDS as an assessment method of transformers oil-paper insulation. This study was limited by technical and practical limitation brought by the COVID pandemic. The oxidation assessment method (FTIR spectroscopy) only gave a broad idea of the state of paper but other techniques (such as CCOA labelling) could give a more precise picture of the oxidation of cellulose in comparison to the dielectric response. A more complete quantification of water content, including the direct measurement of water within the paper, and its relation to temperature could further contribute toward a better understanding of the temperature's role on FDS.

References

1. Harlow JH. Electric power transformer engineering. 3rd ed. Boca Raton. CRC Press, 2012.
2. Wintle HJ. Basic physics of insulators. IEEE, 1990, 25(1):27–44.
3. Xie J, Dong M, Yu B, Hu Y, Yang K, Xia C. Physical Model for Frequency Domain Spectroscopy of Oil–Paper Insulation in a Wide Temperature Range by a Novel Analysis Approach. *Energies*, 2020, 1;13(17):4530.
4. Baral A, Chakravorti S. Condition assessment of cellulosic part in power transformer insulation using transfer function zero of modified debye model. IEEE, 2014, 21(5):2028–36.
5. Wolny S, Adamowicz A, Lepich M. Influence of Temperature and Moisture Level in Paper-Oil Insulation on the Parameters of the Cole-Cole Model. IEEE, 2014, 29(1):246–50.
6. Hadjadj Y, Meghnefi F, Fofana I, Ezzaidi H. On the Feasibility of Using Poles Computed from Frequency Domain Spectroscopy to Assess Oil Impregnated Paper Insulation Conditions. *Energies*, 2013, 18;6(4):2204–20.
7. Jadav R, Ekanayake C, Saha T. Understanding the impact of moisture and ageing of transformer insulation on frequency domain spectroscopy. IEEE, 2014, 21(1):369–79.
8. Linhjell D, Lundgaard L, Gafvert U. Dielectric response of mineral oil impregnated cellulose and the impact of aging. IEEE, 2007, 14(1):156–69.
9. Jian Hao, Ruijin Liao, Chen G, Zhiqin Ma, Lijun Yang. Quantitative analysis ageing status of natural ester-paper insulation and mineral oil-paper insulation by polarization/depolarization current. IEEE, 2012, 19(1):188–99.
10. Jadav R, Ekanayake C, Saha T. Understanding the impact of moisture and ageing of transformer insulation on frequency domain spectroscopy. IEEE, 2014, 21(1):369–79.
11. Xia G, Wu G, Gao B, Yin H, Yang F. A New Method for Evaluating Moisture Content and Aging Degree of Transformer Oil-Paper Insulation Based on Frequency Domain Spectroscopy. *Energies*, 2017, 12;10(8):1195.
12. Institute of Electrical and Electronics Engineers, IEEE Dielectrics and Electrical Insulation Society, Ha’erbin-Ligong-Daxue, editors. IEEE 9th International Conference on the Properties and Applications of Dielectric Materials, 2009.
13. Chau TRAN DUY. Propriétés diélectriques de liquides isolants d’origine végétale pour applications en haute tension. 2009.
14. Audrey Bourgeois. Study of flow electrification phenomena on high power transformers pressboards. 2007.
15. Garcia B, Burgos JC, Alonso AM, Sanz J. A Moisture-in-Oil Model for Power Transformer Monitoring—Part I: Theoretical Foundation. IEEE, 2005, 20(2):1417–22.
16. Betie A, Meghnefi F, Fofana I, Yeo Z. On the impacts of ageing and moisture on dielectric response of oil impregnated paper insulation systems. Annual Report Conference on Electrical Insulation and Dielectric Phenomena. IEEE, 2012, p.219–22.

General conclusion

The ageing process involved in the degradation of power transformer insulation is a subject that, despite several decades of research, is still too complex to be fully understood. This thesis aims to further investigate this complex subject via novel studies on analytical techniques used to evaluate paper ageing. Understanding how paper ages can be used to further improve the ageing assessment of Kraft insulation, an ultimately be used to more accurately predict the lifetime of Power Transformers.

In the first chapter, an overview of existing literature that allow to understand the purpose and structure of Power Transformers (PT) and its Kraft insulation is provided. PT constitute strategic components that play a key role in power grids. They are custom made machines, according to specific requirements. In normal working conditions, degradation of the Kraft insulation of a PT constitutes the main process that will ultimately decide its end of life; it is therefore important to constantly monitor its state. There exists no unique formula able to predict its end of life. Mathematical models that describe the remaining life expectancy however exist, and are coupled to experimental known cellulose degradation indicators, in order to predict the end of life of the insulation.

In the second chapter, a bibliographic study introduced the last 15 years of research regarding the suitability of methanol in oil as an ageing marker. Methanol generation is supposed to be linearly related to cellulose depolymerization by acid hydrolysis. The aim was to evaluate the postulated role of lignin regarding methanol production, and its origin. The main purpose of these experiments is to investigate the origin of methanol production. At the reduced scale of paper samples, experiments that compared paper with and without lignin showed that there is an important contribution of lignin to methanol production. Experiments demonstrate that most of the contribution from lignin comes from the demethylation of the guaiacyl units, independently of cellulose depolymerization, for polysaccharides-based polymers (cellulose and hemicellulose). It was evidenced that the produced methanol could also react with the end-chain reducing units of carbohydrates. Partition coefficient experiments were carried out and showed that water, a by-product of paper ageing, could interfere with the affinity of paper to methanol while changes in its chemical composition did not play any important role. This chapter demonstrated that lignin is a significant contributor to methanol production, this information should be useful for grid utilities that want to normalize methanol as a tracer for DGA. There was a significant lack of understanding with regards to the origin of methanol production. Hopefully, the results obtained here could guide more research on the subject.

For the third and fourth chapter, the same paper samples were built and used. These samples included materials of multiple compositions (UKP, BKP and CL), and samples that had undergone ion exchange experiments with metals (Ca, Na, Mg, Fe and Cu). The results from the ion exchange experiments showed results consistent with literature, the number of ions retained by the pulp were very similar to previous comparable experiments.

In both chapters it was possible to monitor an increase, and then a decrease of the oxidation and dielectric losses during ageing. The increase corresponded to the initial fall of DP_v that happens during the acid hydrolysis of the amorphous phase of cellulose, while the decrease was observed when the depolymerization rate dropped. An explanation of this behavior is proposed: the initial depolymerization process produces a byproduct build-up. These initial byproducts are not

stable and proceed to decompose yet, since depolymerization slowed, and are not replaced as fast as they appeared. Out of all acid byproducts produced during degradation, the lipophilic acids will migrate into the oil. Therefore, as byproducts degrade in paper, there is an important increase in the total acid content of oil. Water content in oil did not follow this behavior. The origin and properties of water can explain this difference since, unlike lipophilic acids, water doesn't have any affinity to oil (especially when it cools down) so the amount of water that was lost when the sample was cooled and opened is unknown. The final result is that the overall oxidation and dielectric loss decreases as soon as the depolymerization rate slows down.

Concerning dielectric spectroscopy (FDS) as a tool able to monitor paper ageing, different conclusions were obtained. To explain variations recorded by FDS during ageing, no unique mechanism can be invoked: several results point that changes in the paper chemical composition (appearance of oxidation damage and oxidation byproducts) are responsible for the change in losses, but water also has a large influence. It was also concluded that FDS is not able to track paper depolymerization efficiently, and shows a small sensitivity to paper composition and ion content. On the other hand, it is very sensitive to the presence of water. This provides indications and guidelines about the practical interest of FDS that can be expected for the diagnostic of transformers.

A better understanding of dielectric spectroscopy measurements would be necessary to improve the diagnostic of insulation. Several aspects such as the interactions between oil, paper, and water should be better characterized. The postulated influence of the electrical double layer at the cellulose / oil interface could be investigated by doing FDS experiments on layers of paper and oil in series. Since this phenomenon is highly dependent on material chemical nature, experiments with various materials (papers, oils) where the double layer is already characterized could be helpful. About the influence of water, it would be necessary to carry out experiments in situations where the equilibrium is reached. Experiments done here at different temperatures were done without opening the measuring gap, and it is difficult to ascertain that such equilibrium was reached.

The ageing behavior also shows that the polydispersity index of UKP is not stable, this is not considered by the mathematical models used for ageing. Regarding paper composition, unaged samples with lignin proved to have similar oxidation value with samples without lignin. A small amount of acid oxidation was detected lignin-less samples, this damage seems to come from the bleaching step. Once ageing starts, lignin protects the pulp from oxidation, not only by reducing overall value of the oxidative damage but also the proportion of acid components in the oxidation. This correlated with permittivity and depolymerization, in both cases, samples with an acid lead oxidation corresponded to the fastest depolymerization and loss of dielectric properties. Main metals (even in ppms concentration) showed to have an important effect on depolymerization and oxidation. Calcium, magnesium, and to a lesser extent sodium, showed a lower proportion of acid lead oxidation that correlates to slower kinetics of depolymerization while iron and copper showed an important acid oxidation that correlate to fast depolymerization kinetics.

Annex

Annex

1) SEC Results.....	193
a) Samples List	193
b) Results per samples	194
i) UKP.....	194
(1) UKP D0.....	194
(2) UKP D2.....	196
(3) UKP D5.....	197
(4) UKP D7.....	199
ii) BKP.....	200
(1) BKP D0.....	200
(2) BKP D2.....	202
(3) BKP D5.....	203
(4) BKP D7.....	205
iii) CL.....	206
(1) CL D0.....	206
(2) CL D2.....	208
(3) CL D5.....	209
(4) CL D7.....	211
2) Analysis technique	212
a) Head Space Gas Chromatography with a Flame Ionization Detector.....	212
b) Size Exclusion Chromatography (SEC).....	215
c) Viscometric degree of polymerization	216
d) Karl Fischer titration	217
e) Soxhlet extraction.....	218
References	218

1) SEC Results

a) Samples List

Samples tested through SEC (Size Exclusion Chromatography) after carbanilation of cellulose:

Table 34: List of the samples that were analyzed through SEC:

Sample type	Ageing time (hours)	Sample name
Unbleached Kraft Pulp (UKP)	0	UKP D0
	48	UKP D2
	120	UKP D5
	168	UKP D7
Bleach Kraft Pulp (BKP)	0	BKP D0
	48	BKP D2
	120	BKP D5
	168	BKP D7
Cotton Linters (CL)	0	CL D0
	48	CL D2
	120	CL D5
	168	CL D7

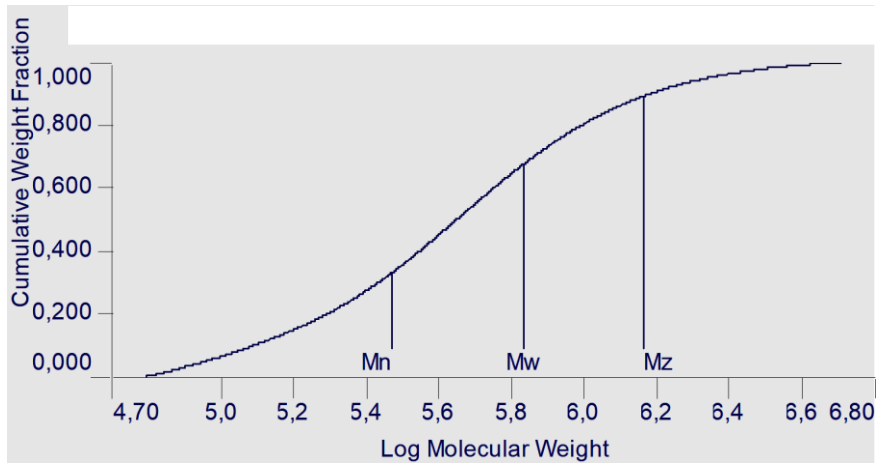
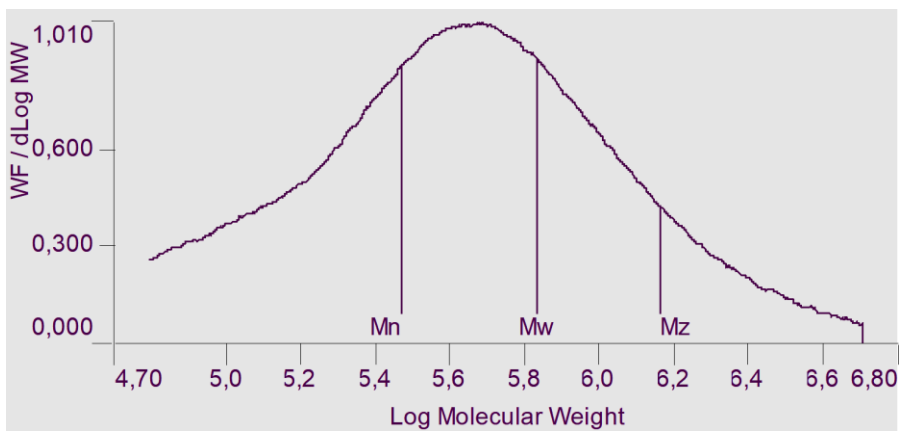
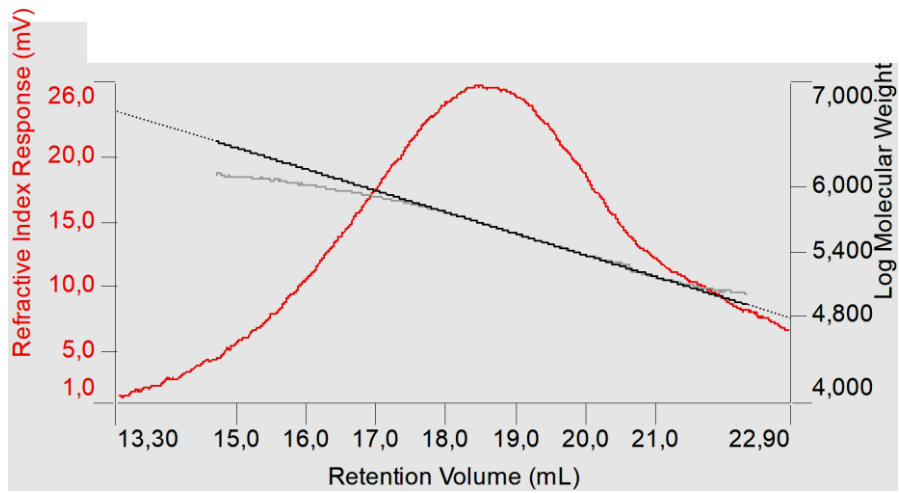
b) Results per samples

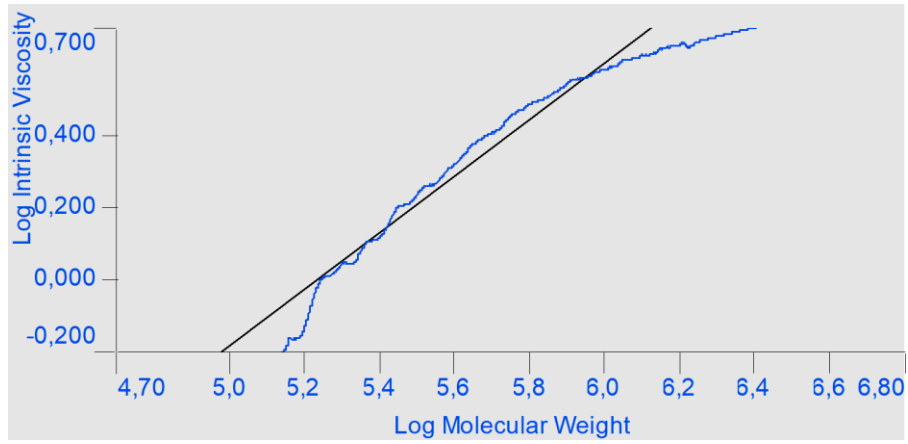
The different results are listed below. The significance of the data is given in the following table:

Size exclusion chromatographic (SEC) data		
Analysis	Units	Comments
Peak RV	ml	Retention volume at the peak of concentration (DRI peak)
Mn	Daltons	Number average molecular mass
Mw	Daltons	Weight average molecular mass
Mw / Mn	ad.	Dispersity
IV	dl/g	Weight average intrinsic viscosity
Rh	nm	Weight average hydrodynamic radius
Rg	nm	Weight average gyration radius
Wt Fr	ad.	Peak weight fraction (DRI chromatogram)
Mark-Houwink a	ad.	MHS law exponent factor
Mark-Houwink logK	dl/g	MHS law pre-exponent factor

i) UKP (1) UKP D0

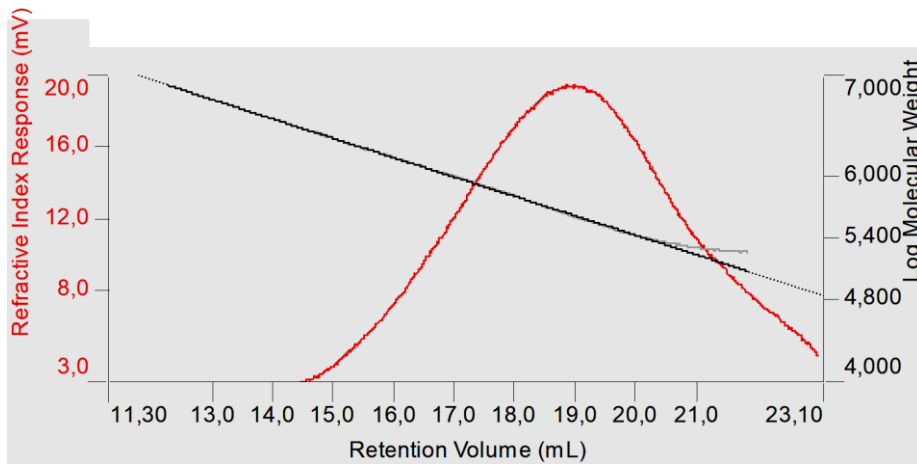
SEC Results	
Peak RV – (ml)	18,463
Mn – (Daltons)	295 198
Mw – (Daltons)	683 196
Mw / Mn	2,314
IV – (dl/g)	2,4284
Rh – (nm)	26,035
Rg – (nm)	40,651
Wt Fr (Peak)	1,000
Mark-Houwink a	0,787
Mark-Houwink logK	-4,119

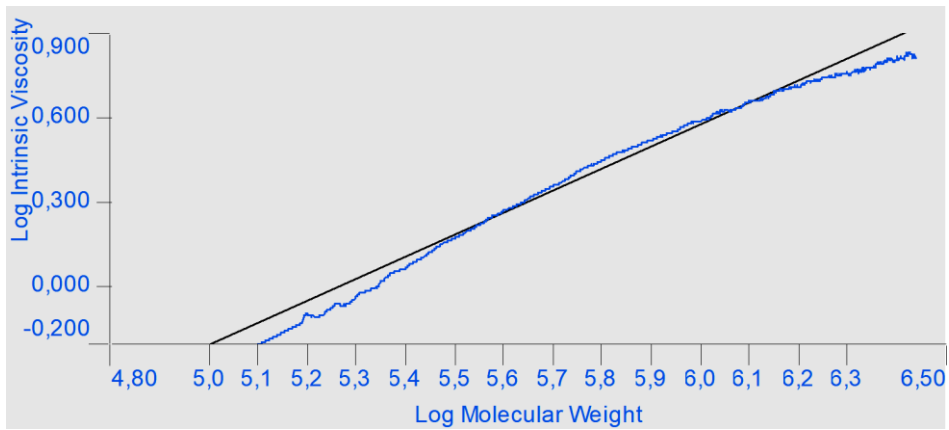
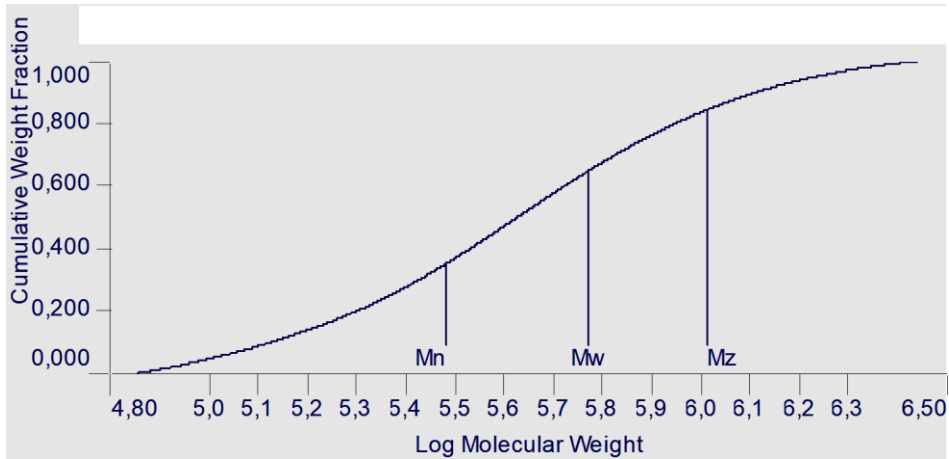
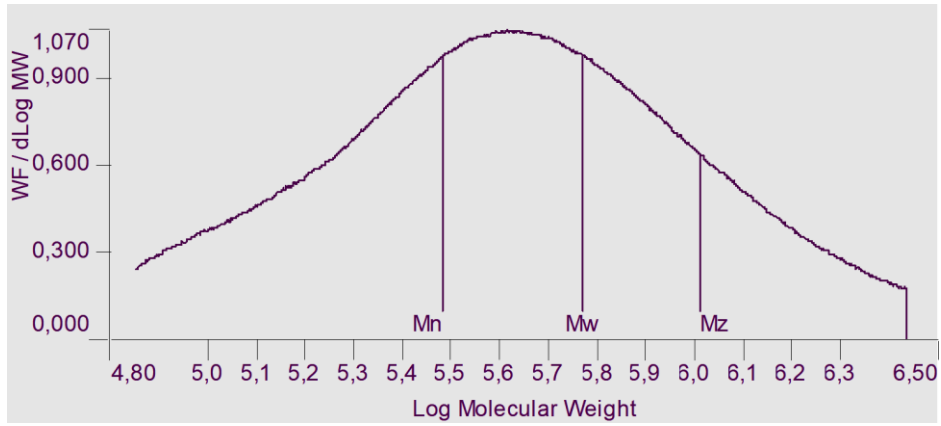




(2) UKP D2

SEC results	
Peak RV - (ml)	19,000
Mn - (Daltons)	303 085
Mw - (Daltons)	589 891
Mw / Mn	1,946
IV - (dl/g)	2,3079
Rh - (nm)	26,463
Rg - (nm)	43,877
Wt Fr (Peak)	1,000
Mark-Houwink a	0,778
Mark-Houwink logK	-4,093

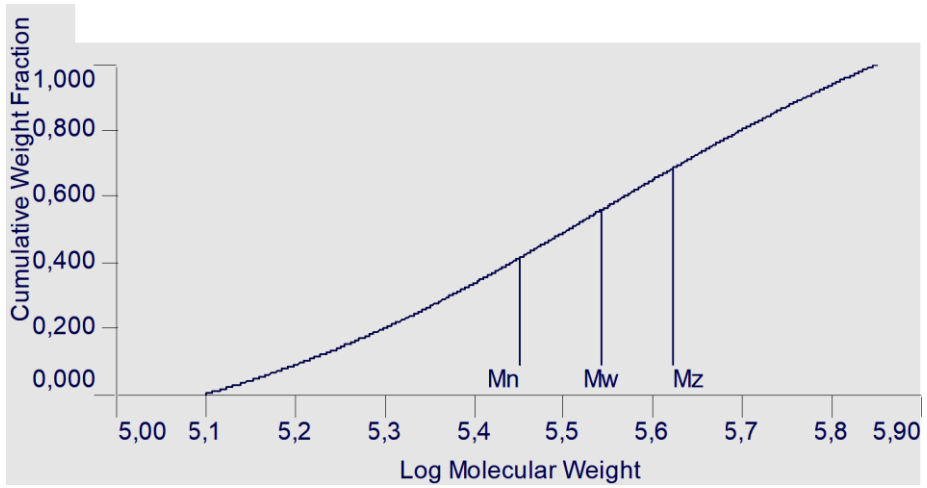
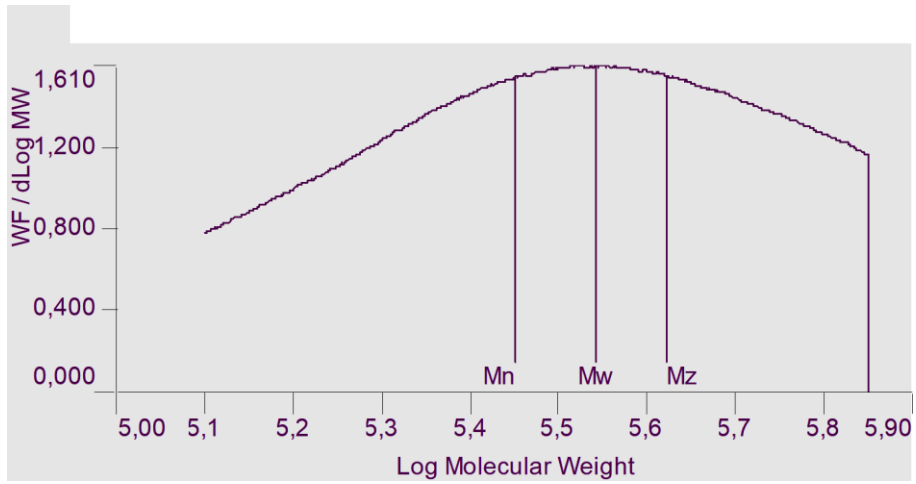
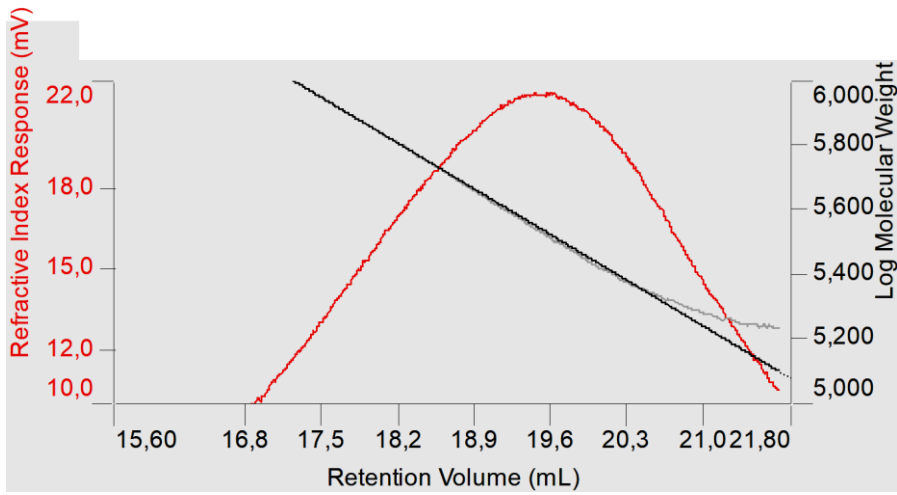


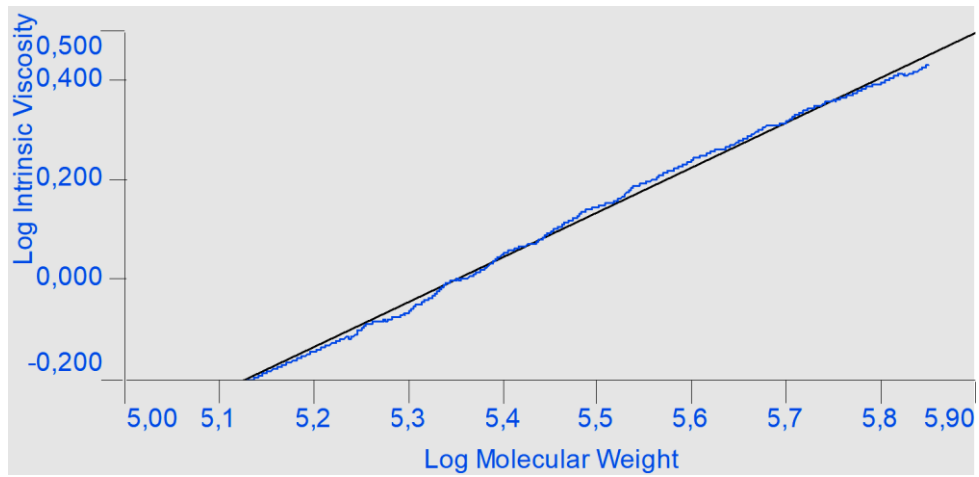


(3) UKP D5

SEC results	
Peak RV - (ml)	19,597
Mn - (Daltons)	282 621
Mw - (Daltons)	454 721
Mw / Mn	1,603
IV - (dl/g)	1,4763
Rh - (nm)	19,774
Rg - (nm)	34,895
Wt Fr (Peak)	1,000
Mark-Houwink a	0,898

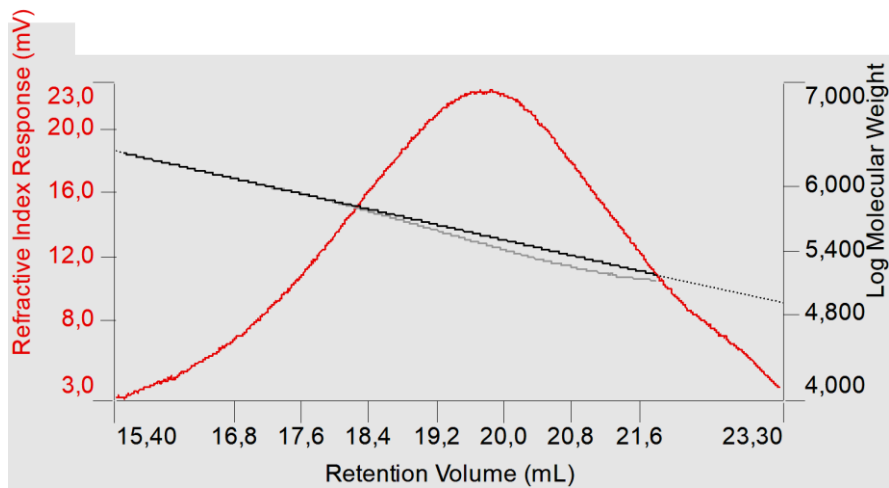
Mark-Houwink logK | -4,805

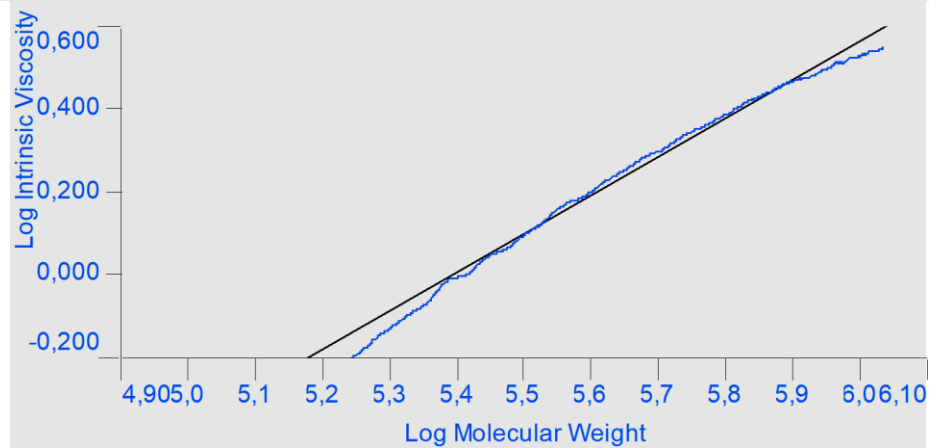
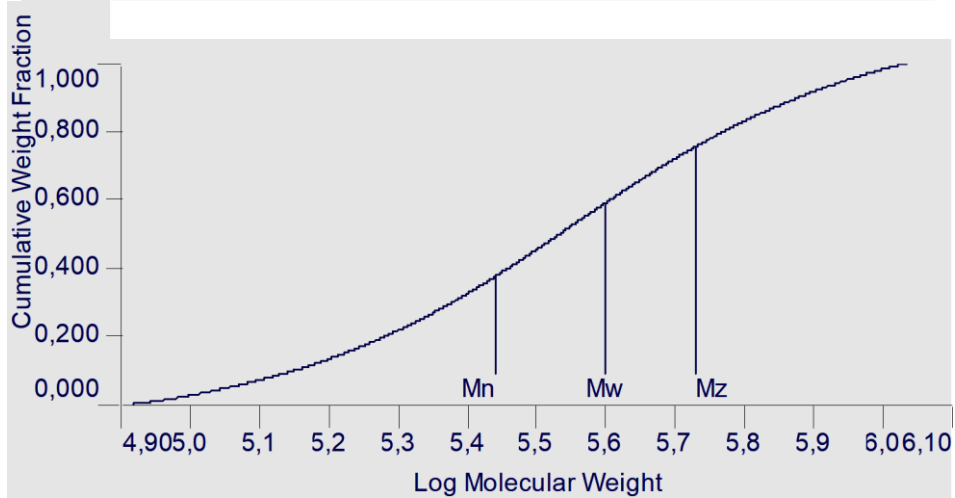
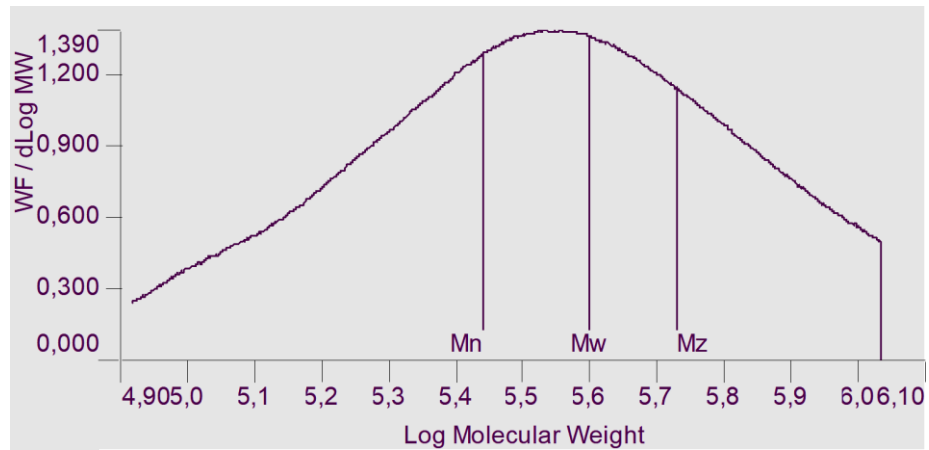




(4) UKP D7

SEC results	
Peak RV - (ml)	19,723
Mn - (Daltons)	276 238
Mw - (Daltons)	398 138
Mw / Mn	1,441
IV - (dl/g)	1,5044
Rh - (nm)	19,603
Rg - (nm)	28,711
Wt Fr (Peak)	1,000
Mark-Houwink a	0,931
Mark-Houwink logK	-5,023

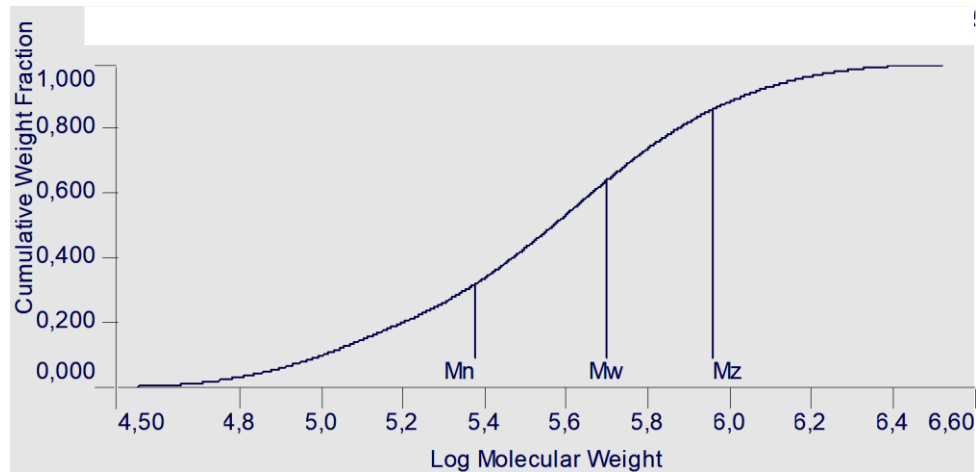
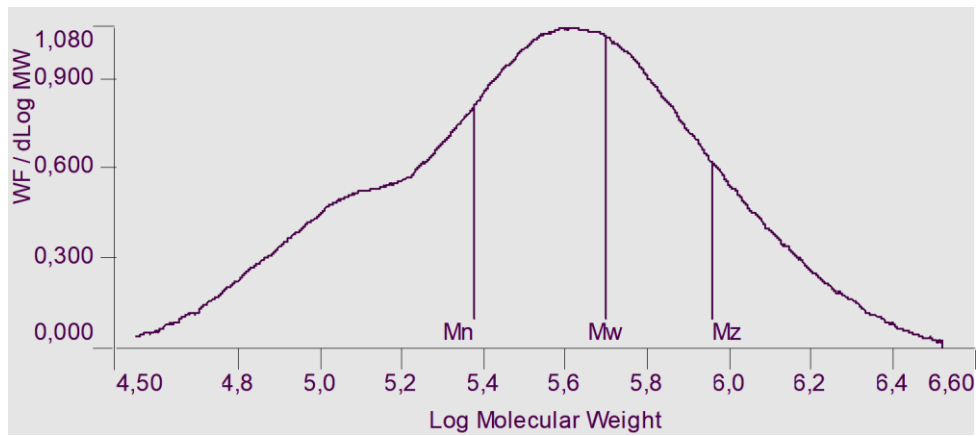
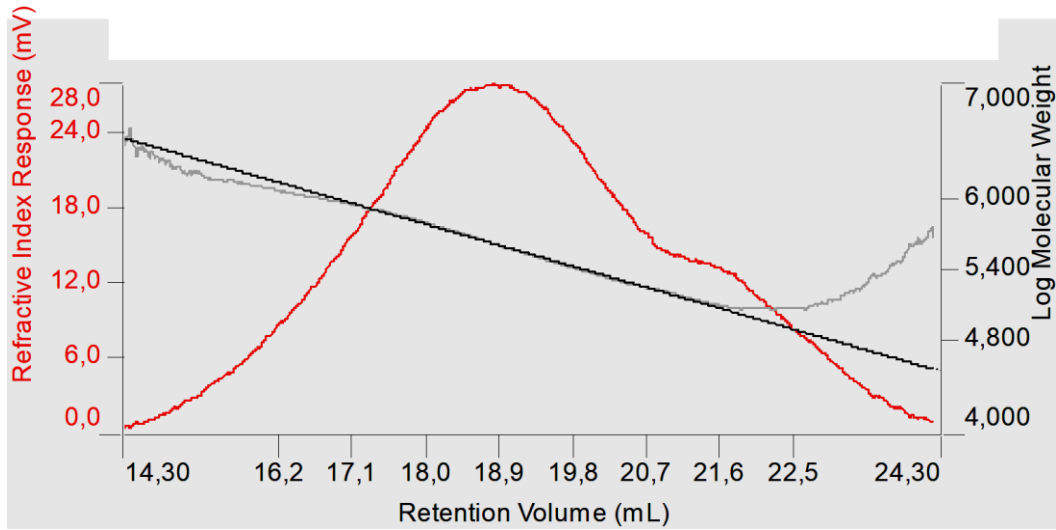


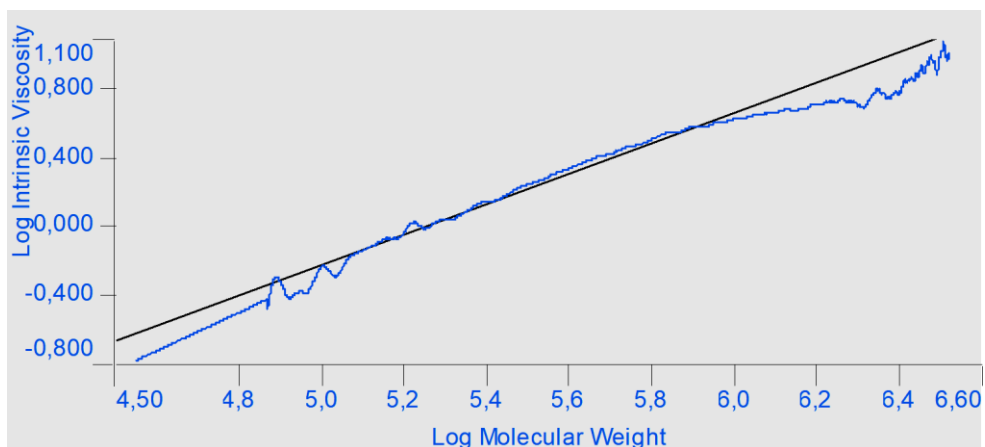


- ii) BKP
- (1) BKP DO

SEC results	
Peak RV - (ml)	18,827
Mn - (Daltons)	338 990
Mw - (Daltons)	444 850
Mw / Mn	1,312
IV - (dl/g)	2,2830
Rh - (nm)	24,509
Rg - (nm)	39,683

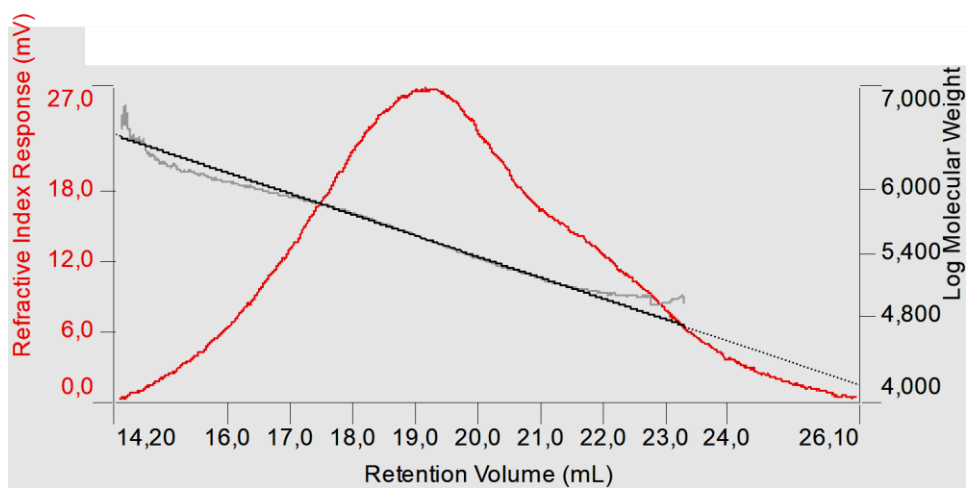
Wt Fr (Peak)	1,000
Mark-Houwink a	0,887
Mark-Houwink logK	-4,663

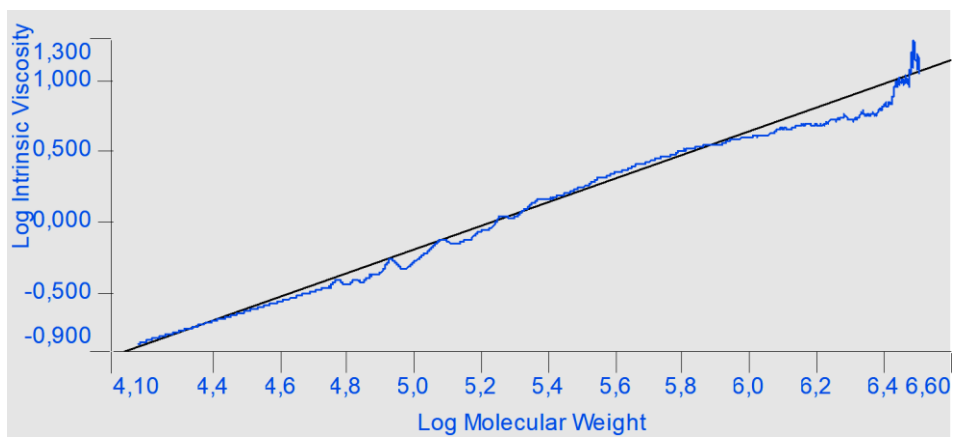
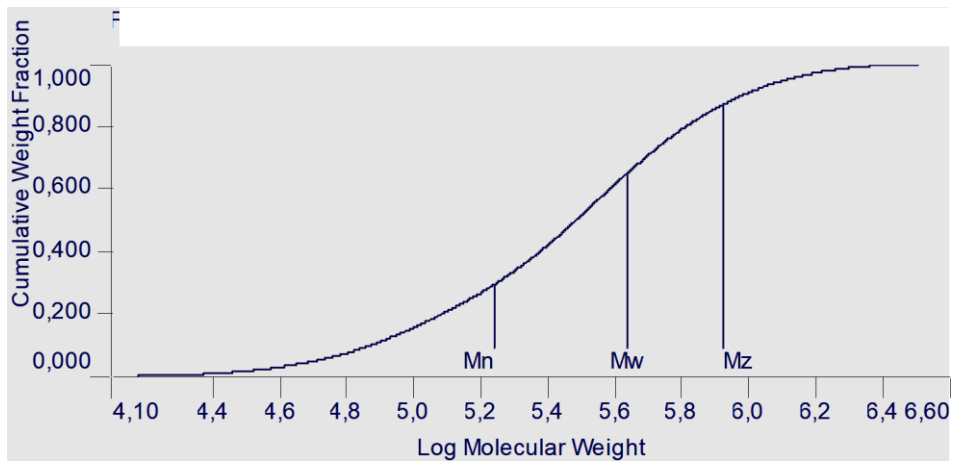
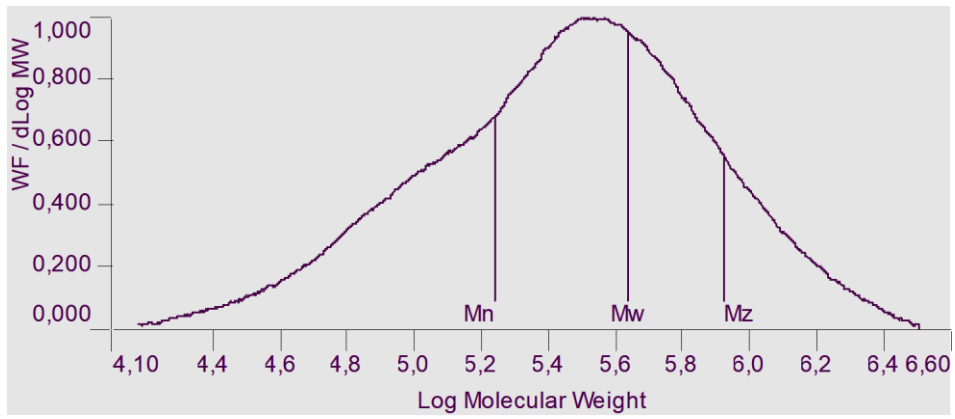




(2) BKP D2

SEC results	
Peak RV - (ml)	19,183
Mn - (Daltons)	272 093
Mw - (Daltons)	395 313
Mw / Mn	1,452
IV - (dl/g)	2,0079
Rh - (nm)	22,153
Rg - (nm)	36,448
Wt Fr (Peak)	1,000
Mark-Houwink a	0,833
Mark-Houwink logK	-4,354

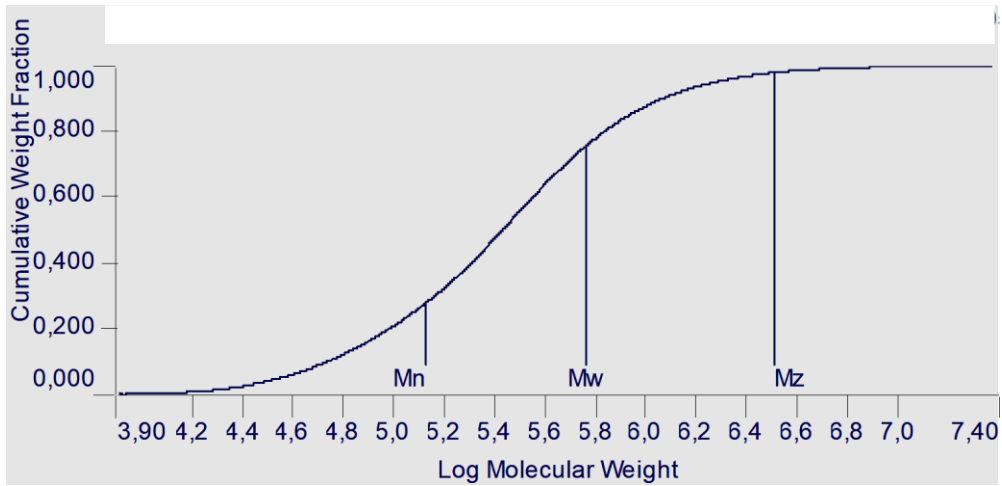
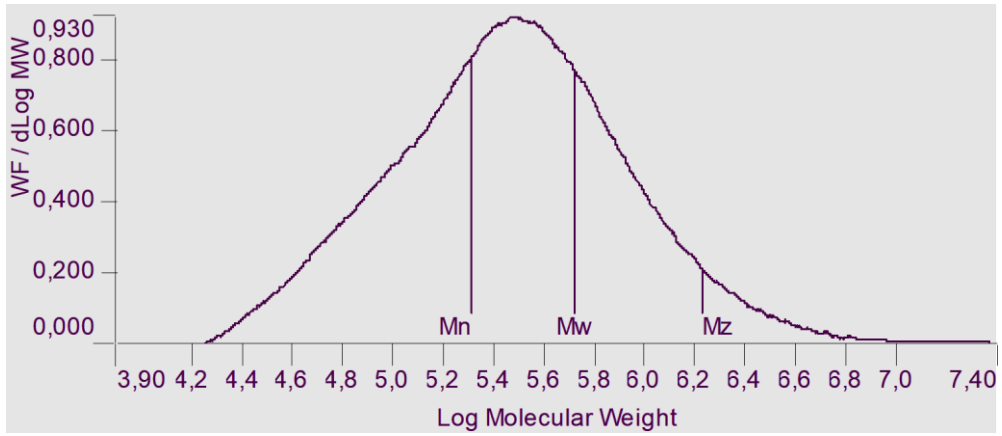
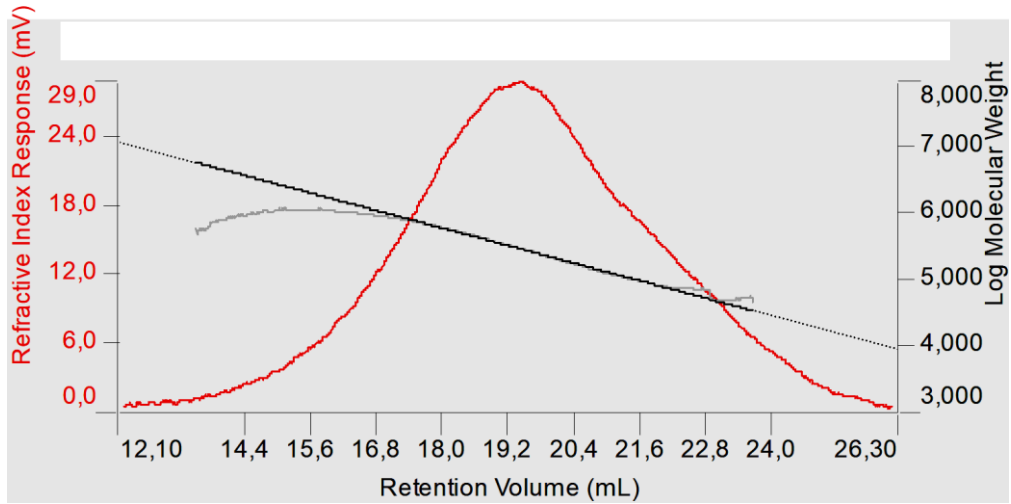


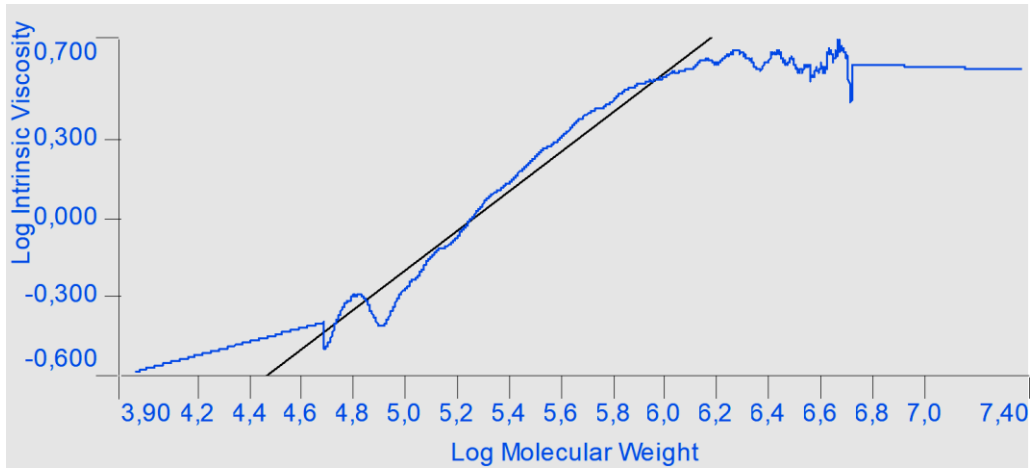


(3) BKP D5

SEC results	
Peak RV - (ml)	19,437
Mn - (Daltons)	188 137
Mw - (Daltons)	368 571
Mw / Mn	1,959
IV - (dl/g)	1,6550
Rh - (nm)	19,957
Rg - (nm)	39,515
Wt Fr (Peak)	1,000

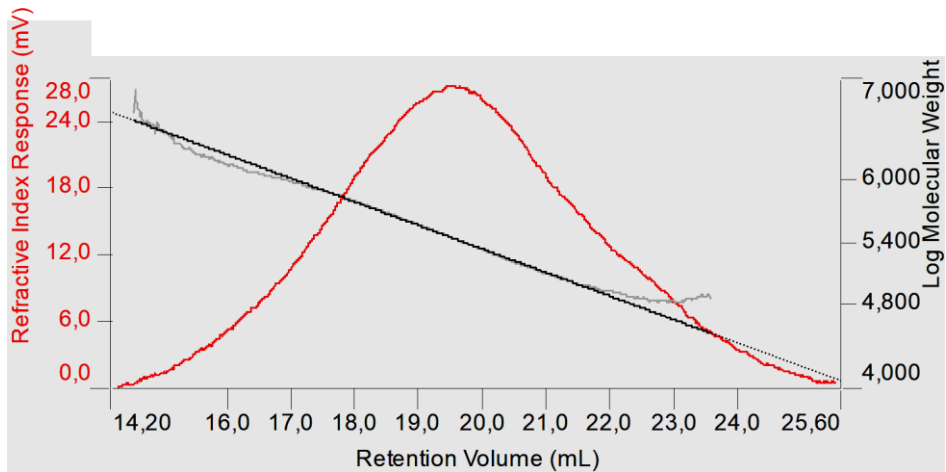
Mark-Houwink a	0,741
Mark-Houwink logK	-3,899

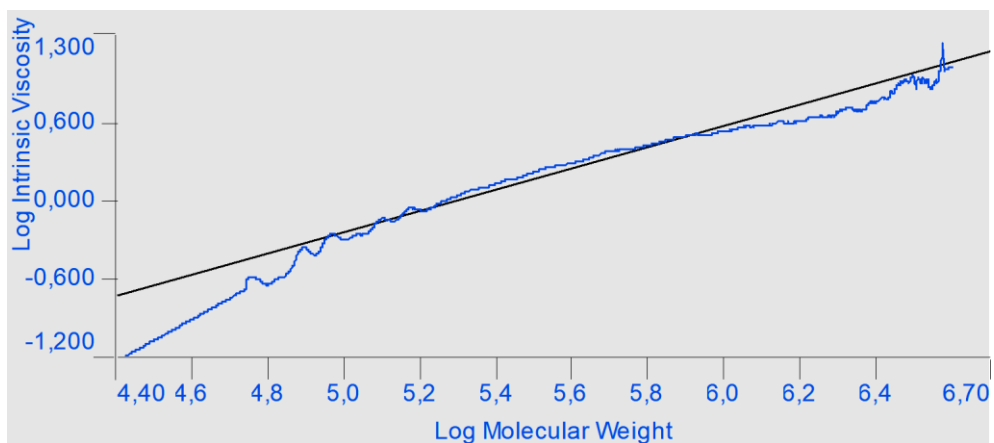
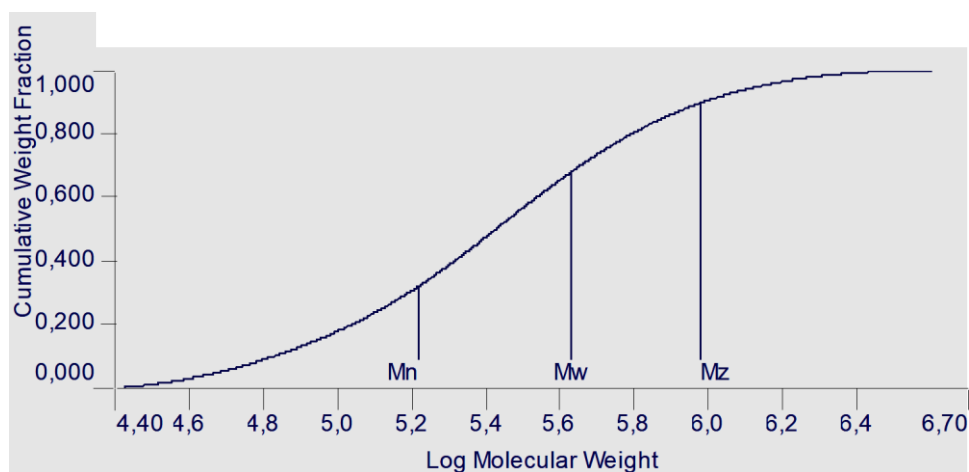
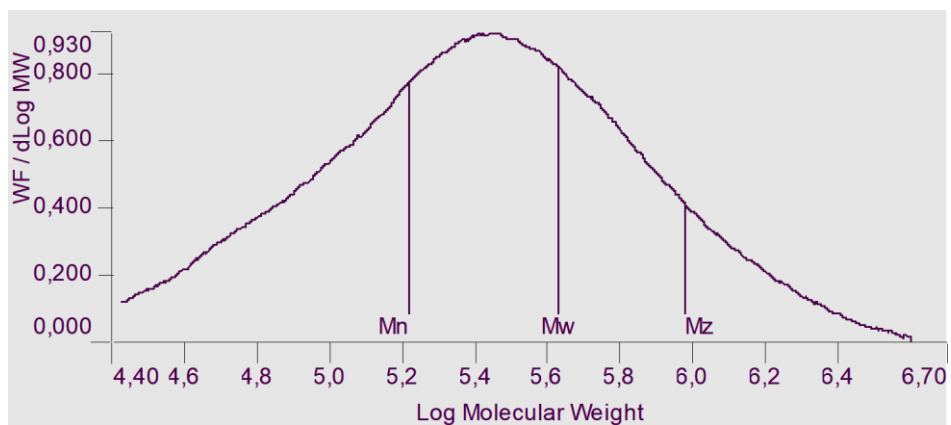




(4) BKP D7

SEC results	
Peak RV - (ml)	19,517
Mn - (Daltons)	179 267
Mw - (Daltons)	345 249
Mw / Mn	1,927
IV - (dl/g)	1,6980
Rh - (nm)	20,507
Rg - (nm)	25,446
Wt Fr (Peak)	1,000
Mark-Houwink a	0,821
Mark-Houwink logK	-4,339

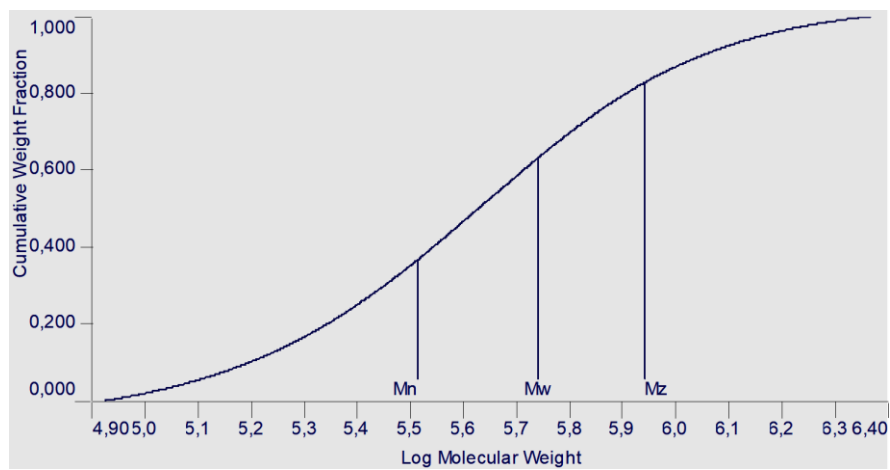
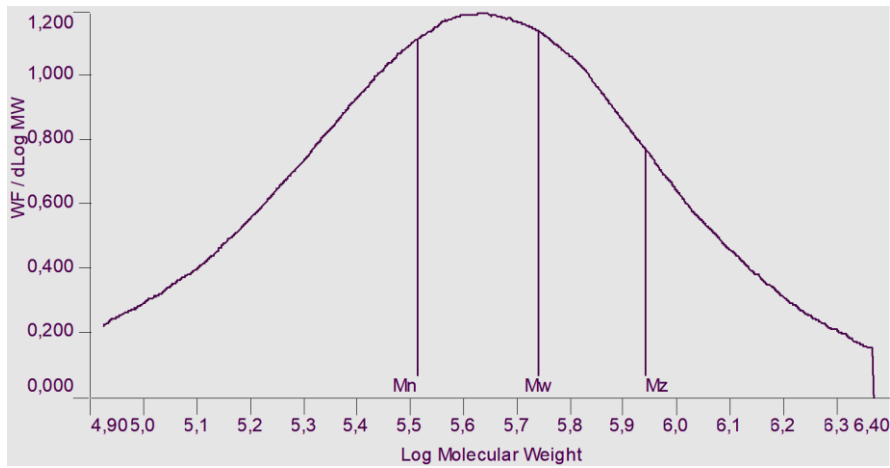
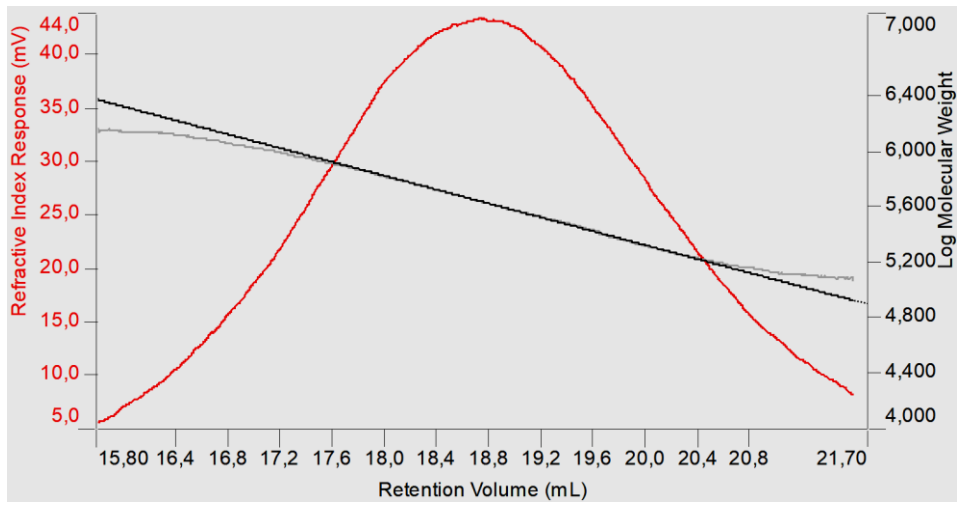


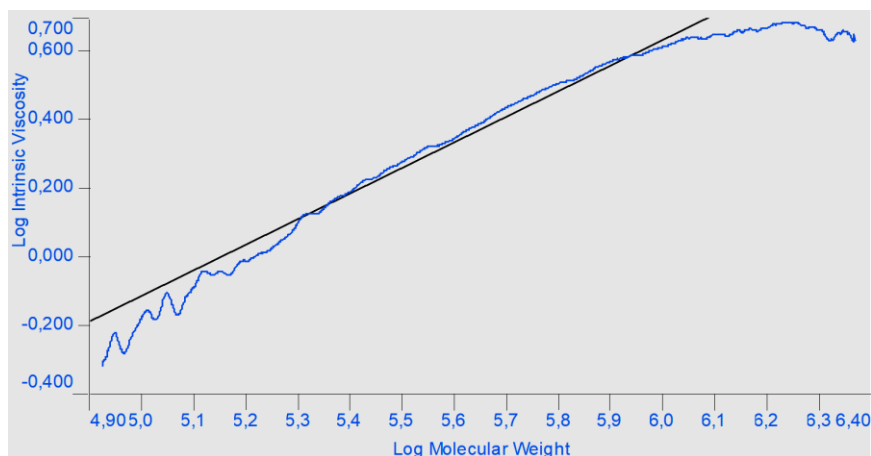


iii) CL
(1) CL D0

SEC results	
Peak RV - (ml)	18,737
Mn - (Daltons)	326 453
Mw - (Daltons)	550 674
Mw / Mn	1,687
IV - (dl/g)	2,5114
Rh - (nm)	26,344
Rg - (nm)	36,108

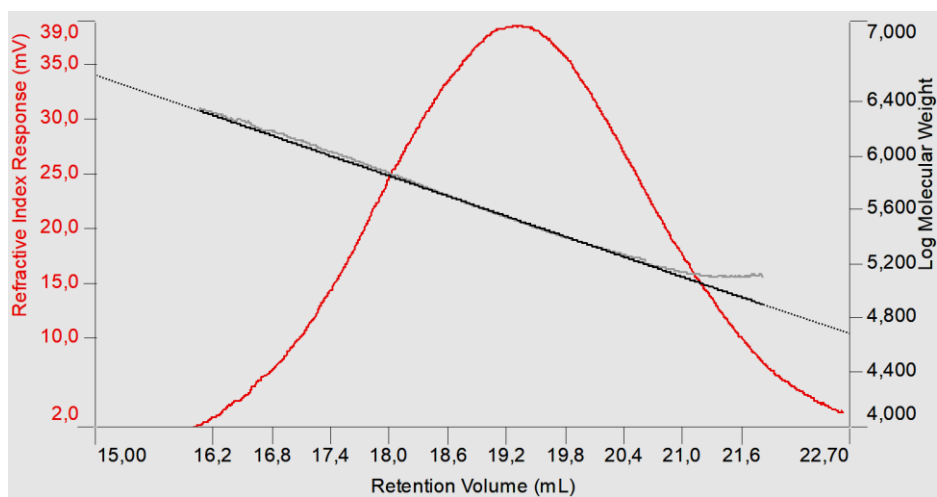
Wt Fr (Peak)	1,000
Mark-Houwink a	0,751
Mark-Houwink logK	-3,872

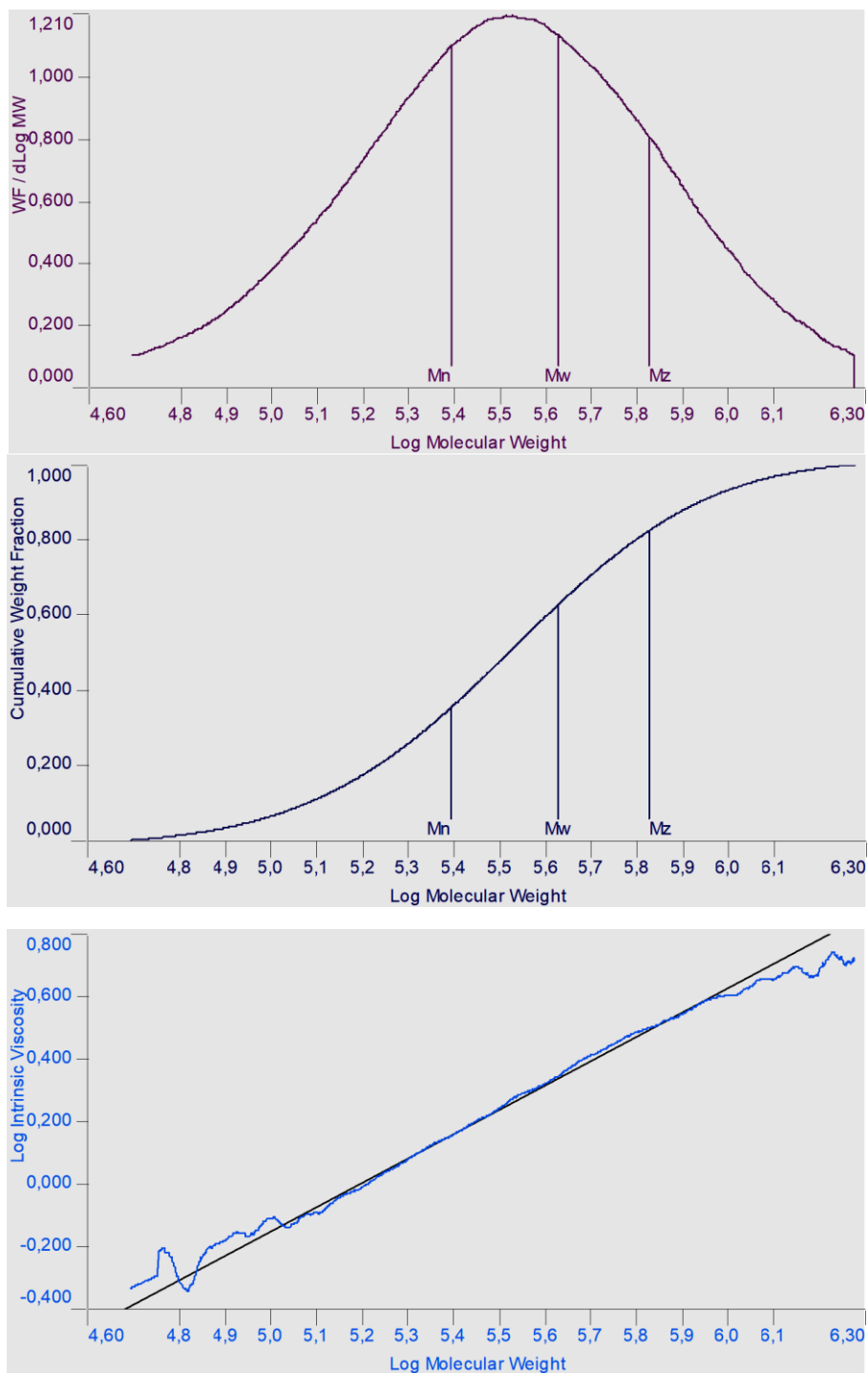




(2) CL D2

SEC results	
Peak RV - (ml)	19,313
Mn - (Daltons)	247 287
Mw - (Daltons)	425 193
Mw / Mn	1,719
IV - (dl/g)	2,0528
Rh - (nm)	23,216
Rg - (nm)	32,645
Wt Fr (Peak)	1,000
Mark-Houwink a	0,780
Mark-Houwink logK	-4,053

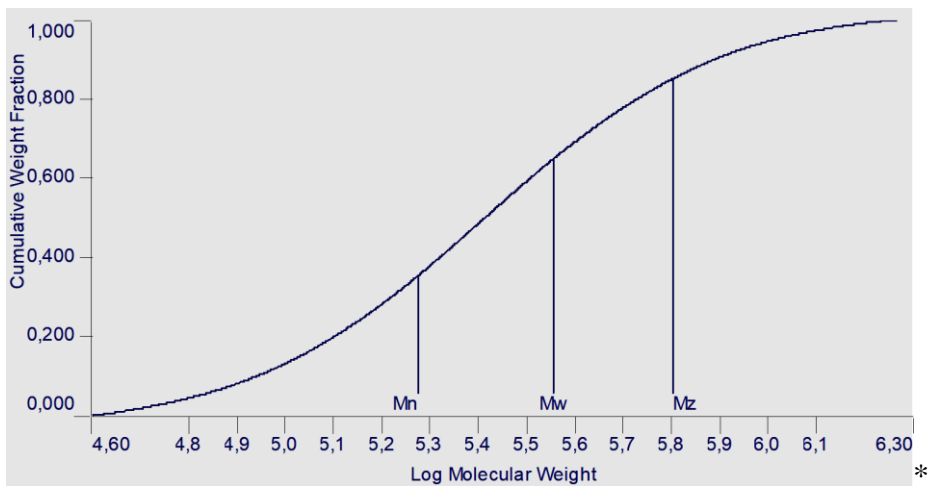
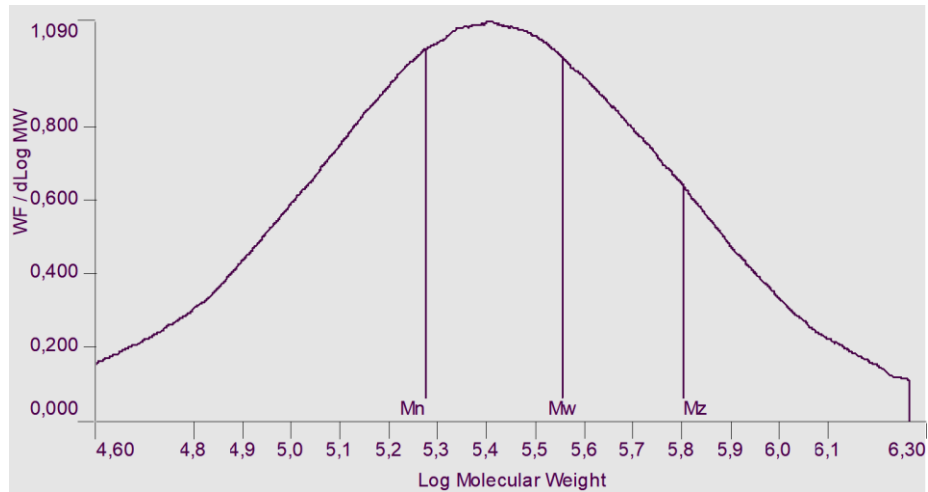
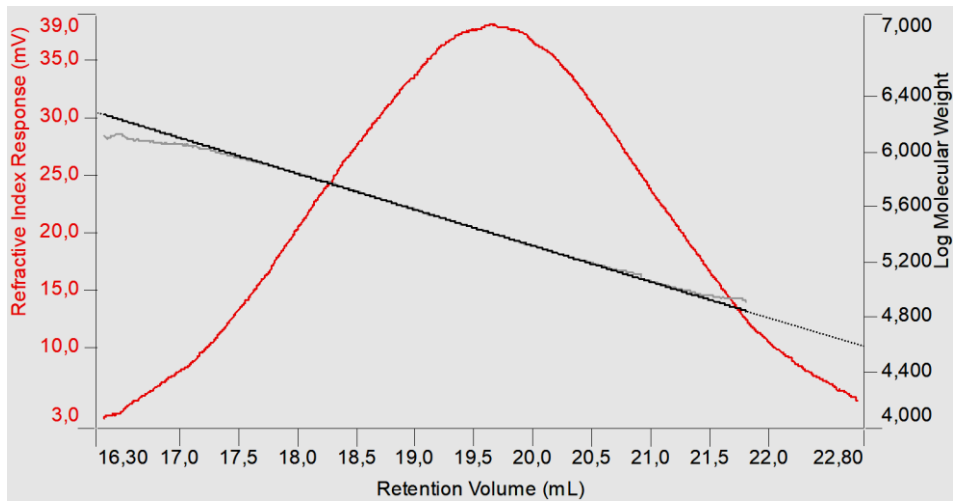


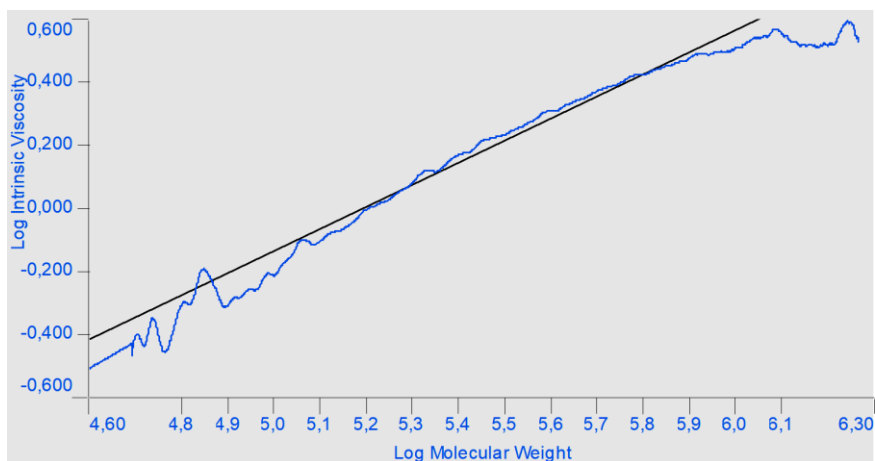


(3) CL D5

SEC results	
Peak RV - (ml)	19,643
Mn - (Daltons)	188 357
Mw - (Daltons)	360 626
Mw / Mn	1,915
IV - (dl/g)	1,6181
Rh - (nm)	19,793
Rg - (nm)	29,303

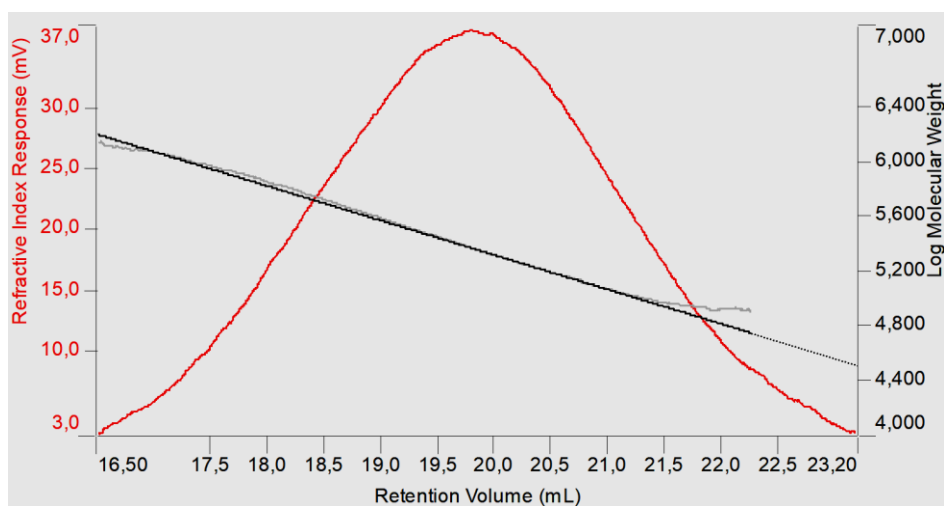
Wt Fr (Peak)	1,000
Mark-Houwink a	0,703
Mark-Houwink logK	-3,649

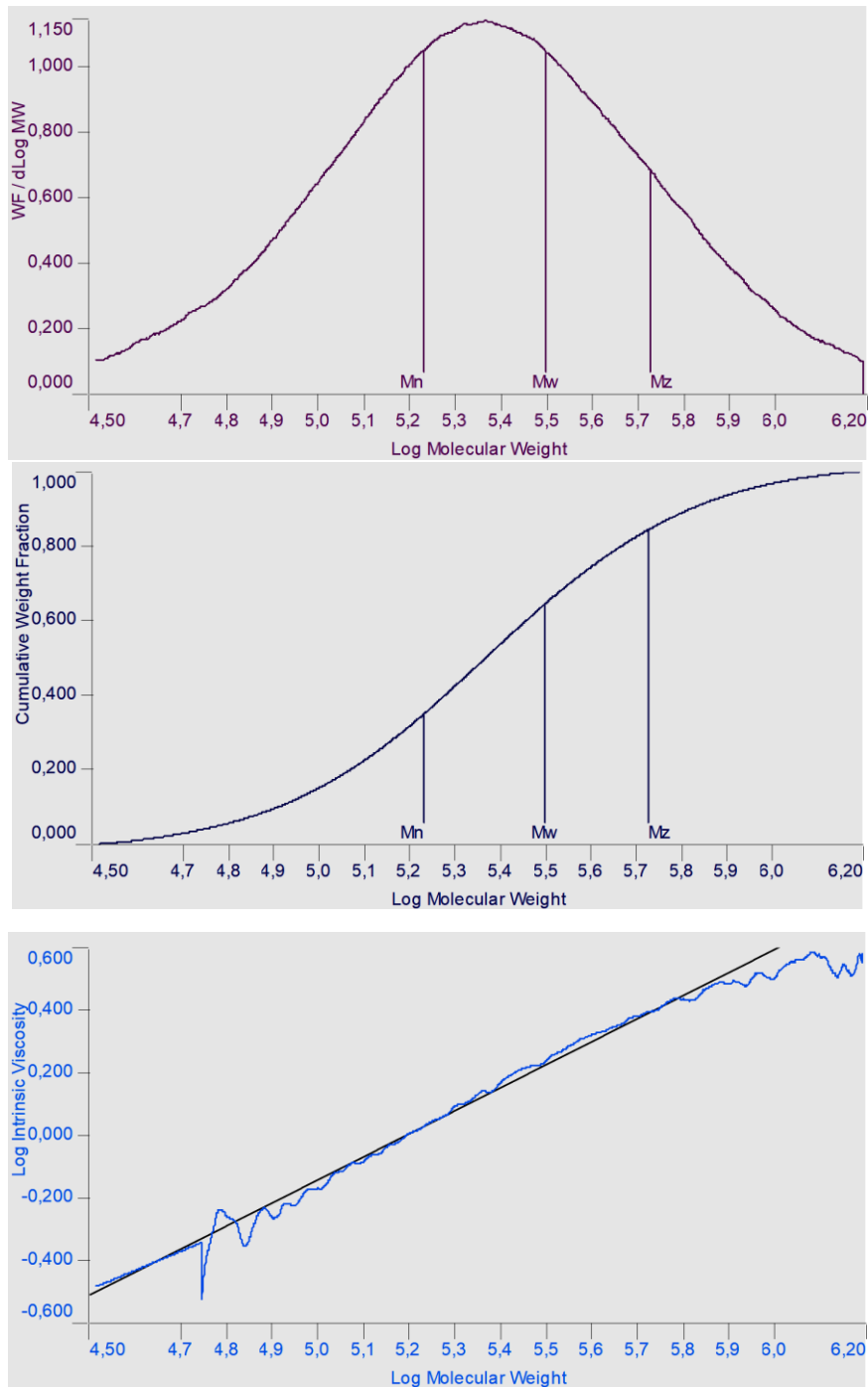




(4) CL D7

SEC results	
Peak RV - (ml)	19,793
Mn - (Daltons)	170 752
Mw - (Daltons)	314 679
Mw / Mn	1,843
IV - (dl/g)	1,5414
Rh - (nm)	18,971
Rg - (nm)	26,135
Wt Fr (Peak)	1,000
Mark-Houwink a	0,740
Mark-Houwink logK	-3,841





2) Analysis technique

a) Head Space Gas Chromatography with a Flame Ionization Detector

A Headspace Sampler (HS, Perkin-Elmer, TurboMatrix HS 16) equipped with a 1 mL sample loop was connected to a split/splitless injector of a Gas Chromatograph (GC, Perkin-Elmer,

Clarus 690), equipped with a Flame Ionization Detector (FID). The method used was taken from Jalbert *et al.* (2012) publication [1]. The exact conditions used in the analysis are visible below:

Headspace sampler parameters		
Temperature	Sample	90 °C
	Transfer line	110 °C
Pressure	Gas sampling valve and injection loop	120 °C
	Vial over-pressure	20 psi
Times	Equilibration at 90 °C with shaking	40 min
	Pressurization	0.2 min
	Loop fill	0.12 min
	Loop equilibration	0.25 min
	Injection	6 min
	Power	Maximum level
Gas chromatograph parameters		
He carrier gas flow		0.5 mL.min ⁻¹ for 38 min 0.5 to 0.8 mL at 0.1 mL.min ⁻¹
Injector split/splitless		250 °C, 35 psi
Split ratio		30:1
Oven		40 °C for 10 min
		40–110 °C at 5 °C min ⁻¹
		110–290 °C at 20 °C min ⁻¹ 290 °C for 11.5 min

Figure 119: Analysis conditions used during HSGC-FID. Extracted Jalbert *et al.* [1].

The analysis is divided into three steps:

1. **Sampling step:** this step takes a sample of gas phase of the vial and transfers it to the GC column. In the present study, 10 mL oil is contained in a 20 mL vial that is heated (and shaken) in a vial- oven. Then, a needle pierces the septum of the vial and pressurizes it at a stable pressure. A valve opens and leaves the gas escape to the GC. At a given temperature, the amount of gas leaving the vial is always the same, giving the method a very good repeatability.
2. **GC separation:** methanol separation is operated under the following operating conditions: column type, inlet pressure, nature of carrier gas (helium), gas flow rate, heating program (heat-up, plateau and cool-down, temperature and duration of each phase), total time of analysis.
3. **Detection step:** Flame ionization detectors (Helium flow, hydrogen flow).



Figure 120: Photo of HSGC-MS, from the right to the left there is: Head Space, Gas Chromatogram and Mass Spectrometer. Most of the GC come with an included Flame Ionization detector.

Calibration for methanol analysis: GC was calibrated by injecting a series of dilutions prepared from a stock solution of methanol and ethanol in oil. All volumetric measurements were recorded. The stock solution was prepared by diluting 4 μ l of methanol and ethanol in 40 mL of oil to obtain a concentration of around 80 μ g/g of each alcohol. The prepared stock solution was used to spike it directly inside the 20 mL HS vials containing 10 mL of blank oil. All vials were crimped with aluminum caps equipped with silicon/Teflon septum using a standard crimper head. Calibration standards with concentrations ranging from 0 to 1800 ng/g were prepared and analyzed. The concentrations used in calibration curves were chosen based on the amount of methanol produced during the experiments. This range of concentration was chosen based on the observed concentration of analytes present in power transformer oil.

Table 35: Stock solutions used to spike methanol in partition coefficient experiments.

Concentration of methanol and ethanol (ng/g)	
0	960
240	1360
400	1760
640	

The calibration curve for the model compounds experiments are visible below:

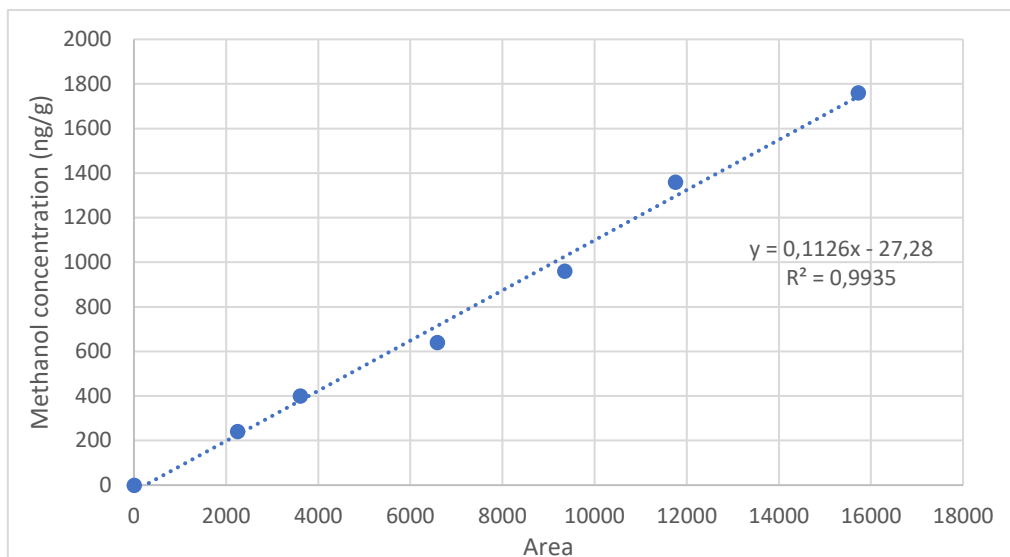


Figure 121: Calibration curve used for lignin model compound experiments X-scale: the area corresponds to the calculated area of methanol's signal detected by a Flame Ionization Detector. Y-scale: the concentration the spiked methanol in the oil.

b) Size Exclusion Chromatography (SEC)

To do SEC, samples of 125 mg were prepared. Before SEC, cellulose must be dissolved in a solvent, here called eluent but natural cellulose is not soluble in the eluent used (THF), therefore a chemical modification of cellulose must be performed to make it less polar, and ultimately, soluble in THF, this is called a derivatization of cellulose. The pulp was first grinded using a Forplex and then solubilized in DMSO, the solution was heated at 70°C and phenyl isocyanate was added to the mixture. The reaction lasted for 48 hours until a phenyl isocyanate group was grafted to all the hydroxyl groups of cellulose. The reaction can be seen below (Figure 122), it is stopped with the addition of acetone and the resulting cellulose is washed with THF and prepared for chromatography.

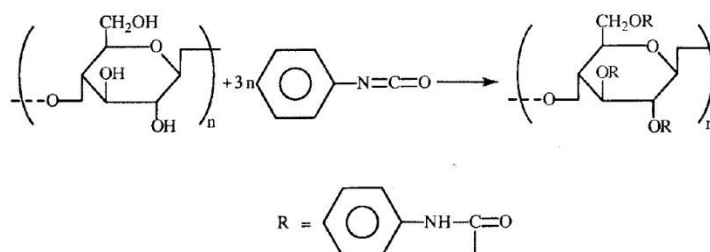


Figure 122: Schematic representation of the carbanilation on cellulose.

Then, cellulose was dissolved in THF to be analyzed by SEC. The chromatography system (GPC MAX VE2001) uses a pump system coupled with a manual purge valve and automatic sample changer. The detection apparatus (Viscotek TDA 302) was made of 3 detectors types; a refractive index detector (RI), light scattering detector (LS) and viscosity detector (Intrinsic Viscosity Differential Pressure IV-DP) coupled with a column oven. In the final injection, only about 1,6 mg of derivatized cellulose is injected into the column. Columns used are the PLgel

MIXED, 7.5 x 50 mm, 10 μ m, guard column and 3 Agilent PLgel MIXED-B LS 7.5 x 300 mm, 10 μ m, HPLC column. The exact conditions used in the analysis are visible below:

Table 36: Conditions used in size exclusion chromatography experiments.

Parameter	Conditions used
Eluant	THF
Acquisition time	60 minutes
Rate of flow	1 mL/min
Injection volume	100 μ L
Column Temperature	35°C
Refractometer Temperature	35°C

c) Viscometric degree of polymerization

Not all the viscometric degrees of polymerization were done with the same method. In the second methanol chapter, a holocellulose experiment was performed on all the paper samples before been grinded in a commercial blender. For the third and fourth chapter, all the presented DP_v were done with without a prior holocellulose experiment and the grinding was done using a Forplex instead. All the other steps in the DP_v measurement were done using the same protocol. The reason behind this change is that the second chapter was meant to be compared to a previous experiment [2] that used the holocellulose method. The third and fourth chapter were to be compared to literature and therefore followed IEC standards (IEC 60450).

Holocellulose

Holocellulose is a standard method to remove lignin from a Kraft pulp. It was applied on paper to compare samples with and without lignin. Then, the viscosity of the paper was measured in copper-ethylenediamine (CuED) to determine the viscosity-average degree of polymerization of cellulose (DP_v).

2 g of paper were disintegrated in 1 L of distilled water with a blender for 2 min. Fiber suspension was filtered on a sintered glass funnel (porosity index of 2) and recovered. In a separate beaker, 25 g of sodium chlorite were dissolved in 250 mL distilled water. 5 mL of concentrated acetic acid were then added to this solution. 100 ml of the final solution was added into the fibers placed in a bottle. Then, the bottle was tight up and placed in the dark for 16 hours. After that time, the mixture was filtered on the same kind of sintered-glass funnel and washed with distilled water until the yellowish color of fibers became stable. Finally, the fibers were laid on a screen and air-dried.

DP_v measurement

A small amount of air-dried fibers (the weight amount is tabulated according to the DP_v value of the sample) were weight for the viscosity test.

For the second chapter the air-dried fibers were disintegrated using a commercially available blender (after a holocellulose treatment) while the samples from third and fourth chapter were disintegrated using a Forplex (without having a holocellulose treatment).

The sample was placed in bottles with a tight cap, then 25 ml distilled water was added and the flask was shaken for 1 hour. Thereafter, 25 mL of CuED was added to the mixture. The vials were then degassed with a flow of nitrogen, closed and covered with an aluminum foil, then shaken for 2 hours. The cellulose solutions were measured for their viscosity using Ubelhodge-type capillary viscosimeters, kept in a water bath at 20 ± 0.5 °C. The viscosimeter is washed before each analysis. Then, it is filled to a calibrated level. A water-pump is used to fill another reservoir to the top. Then the flow-time through the capillary column is recorded. This measurement was done twice and each measurement should not deviate from the previous one by more than one second. Intrinsic viscosity is derived from the flow-time and sample concentration, and a standard relationship allows to calculate the DP_v from the intrinsic viscosity value.

Table 37: Amount of paper weight for DP_v analysis, corresponding to different stages of ageing.

Paper condition	Average expected DP _v	Approximate mass to be weighted
new	1000 to 2000	0.025< 0.05 <0.075
good	650 to 1000	0.040< 0.0825 <0.125
average	350 to 650	0.075< 0.15 <0.225
aged	< 350	0.125< 0.2625 <0.400

d) Karl Fischer titration

A coulometric Karl-Fischer titration was used to measure the water content in paper and oil samples. Each sample was put inside an 8 mL vial that was sealed with an airtight silicon/PTFE cap. Paper samples were analyzed in sample vials and analyzed through a thermal extraction while oil was analyzed through the use of a direct titration. The mass of sample that was chosen based on the expected water content, as seen below:

SAMPLE WATER CONTENT	COULOMETRIC SAMPLE SIZE
100%	NOT RECOMMENDED
50%	0.01 g
10% (100,000 PPM)	0.01 to 0.05 g
5% (50,000 PPM)	0.05 to 0.10 g
1% (10,000 PPM)	0.10 to 0.50 g
0.5% (5,000 PPM)	0.20 to 1.00 g
0.1% (1,000 PPM)	1.00 to 2.00 g
0.01% (100 PPM)	2.00 to 5.00 g
0.001 (10 PPM)	5.00 to 10.0 g
0.0001% (1 PPM)	10.0 g OR MORE

Figure 123: Mass of sample to be introduced according to the expected water content (Metrohm recommendations)

For paper samples, the sealed vials with paper were inserted in an Metrohm 832 thermoprep oven that heated each sample at 140°C. The aim is to desorb any water contained inside the

paper. A double walled syringe pierces the cap and introduced a dry air flow to pass through the vial and extract the vapor, a flow rate of 20 - 60 ml/min of dry air was used. The extracted gas was then bubbled in the titration cell of a Metrohm 831 KF using Coulomat E. For oil samples, 2.5 ml were directly injected in the titration cell using Coulomat oil. Analysis started once derivation was below 20 $\mu\text{g}/\text{min}$ of water and 3 blanks were used for paper samples. Coulometric detection and titration of water was made with electrodes.

e) Soxhlet extraction

Paper samples cannot be analyzed for DPv without removing the oil first. Soxhlet extraction was performed on all the oil-impregnated paper samples before analysis. The first step is a gross precleaning where paper samples are submerged in pentane and all the excess oil is removed. Then the soxhlet extractor was used: the paper sample is laced in a cellulose cartridge, then 200 mL of pentane is added into the 250 mL balloon, glass beads are added in the balloon to ensure homogeneous heating (Figure 124). The balloon is heated at 36°C to distillate pentane. Each cycle consists of pentane evaporating from the balloon and then condensing in the refrigeration column, from where it goes back to the soxhlet cartridge. When the cartridge is full, a syphon takes back the pentane in the balloon and the cycle starts again. Each cycle should last 22 min and a total of 5 cycles is needed for cleaning the paper from oil. Finally, paper is removed from the cartridge and dried under nitrogen.

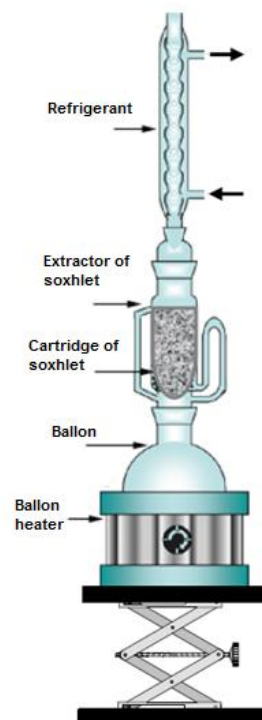


Figure 124: Schematic of soxhlet extraction

References

1. Jalbert J, Duchesne S, Rodriguez-Celis E, Tétreault P, Collin P. Robust and sensitive analysis of methanol and ethanol from cellulose degradation in mineral oils. *Journal of Chromatography A*, 2012, 1256:240–5.
2. Axelle Barnet. Compréhension des phénomènes de vieillissement des papiers électrotechniques dans les transformateurs de puissance et recherche de solutions industrielles. Université Grenoble Alpes, 2020.

Résumé en Français

Table des matières

Introduction générale.....	2
1) Origine de la production de méthanol lors du vieillissement du papier Kraft dans les transformateurs de puissance	4
a) Contexte	4
i) L'analyse des gaz dissous.....	4
ii) Le méthanol comme indicateur de vieillissement.....	5
b) Résultats et discussion	5
i) Comprendre l'approche expérimentale	5
ii) Origine du méthanol – Composés modèles.....	6
iii) Origine du méthanol – Echantillons de papier.....	9
c) Conclusion.....	11
2) Caractérisation du vieillissement pour les mesures d'oxydation et de dépolymérisation des isolants Kraft	11
a) Contexte	11
b) Résultats et discussions	12
i) Echange d'ions	12
ii) Effet de la composition du papier dans la cinétique de la dégradation de la cellulose	13
iii) Dépolymérisation et oxydation de la cellulose pendant un vieillissement thermique accéléré.....	15
c) Conclusion.....	19
3) Caractérisation du vieillissement des isolants Kraft par spectroscopie diélectrique et mesures de claquage.....	20
a) Contexte	20
b) Résultats et discussions	20
i) Contexte.....	20
ii) Propriété diélectrique de la pâte écrue et de l'huile neuve	21
iii) Changement des propriétés diélectriques de la pâte écrue lors d'un vieillissement thermique accéléré.....	23
iv) Effet de la composition du papier sur ses propriétés diélectriques	25
c) Conclusion.....	25
Conclusion générale	27



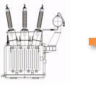


Introduction générale

Répandue depuis la fin du 19^e siècle, l'électricité est désormais considérée comme une nécessité quotidienne. Dès l'origine, la difficulté à transporter efficacement l'électricité a été l'un des principaux obstacles à la démocratisation de l'électricité. Le principal problème dans le transport de l'électricité est que la tension utilisée par la plupart des appareils (100-220 V) est si faible que la dissipation de chaleur rendrait inefficace le transport de l'électricité sur de longues distances. Par conséquent, les lignes électriques longue-distance opèrent à une tension plus élevée et à un courant plus faible pour transporter de l'électricité avec des pertes minimales. Des centrales électriques massives ont été construites pouvant produire de l'électricité à moindre coût grâce à des économies d'échelle. Les transformateurs sont au cœur des réseaux de transport du courant alternatif, ils permettent de changer de tension de manière simple et très efficace. Ils ont d'abord concurrencé les solutions mécaniques impliquant des moteurs et des alternateurs, mais ont finalement triomphé grâce à leur meilleure simplicité, fiabilité et efficacité énergétique (> 98 %).

Au début du 20^e siècle, les lignes électriques reliaient une seule centrale électrique à une ville ou à une usine, mais avec le temps, les lignes se sont interconnectées et ont donné naissance à des réseaux électriques à l'échelle du pays. Après la seconde guerre mondiale, une augmentation massive de la consommation électrique s'est produite chez les particuliers et dans l'industrie. Un pic de croissance d'installation de réseaux a eu lieu à partir des années 1970 dans les pays occidentaux. Les réseaux sont divisés en trois parties : la production, le réseau de transport haute tension sur de longues distances et le réseau de distribution moyenne tension aux consommateurs, donnant lieu à différents types de transformateurs en termes de tension et puissance.

La conception et le poids des transformateurs varient de quelques kg à des milliers de tonnes en fonction de la quantité d'énergie qu'ils peuvent gérer. La puissance nominale d'un transformateur correspond à la puissance qu'il peut délivrer, sans dépasser les limites de température interne de 65°C en moyenne et 80°C sur les points chauds [1]. Comme on peut le voir dans le Tableau 1, les transformateurs utilisés dans la distribution électrique peuvent être divisés en trois types principaux :

Tableau 1 : Résumé schématique des types de transformateurs trouvés dans le réseau électrique.

	Transformateur			
	Générateur	De puissance	De transmission	De distribution
Tension typique	 1 - 25 kV	 400 kV	 90 kV	 33 kV 220 V 
Puissance nominale	800 MVA	1000 MVA	100-300 MVA	2.5-100 MVA

Les matériaux diélectriques isolants sont au cœur de la technologie des transformateurs et déterminent leur durée de vie. Typiquement, la cellulose Kraft est le matériau de choix, alliant

performance et faible coût. Au cours des 70 dernières années, d'importantes recherches ont été menées dans le domaine du vieillissement des isolants Kraft (papiers et cartons), afin de mieux comprendre le processus de vieillissement de ces derniers, prédire la durée de vie restante d'un transformateur de puissance, fournir des paramètres capables de quantifier et contrôler le vieillissement des papiers vieillis.

Le présent travail est le fruit d'un partenariat entre le LGP2 (Laboratoire de Génie des Procédés pour la Bioraffinerie, les Matériaux Biosourcés et l'Impression Fonctionnelle) et le G2Elab (Laboratoire de Génie Electrique de Grenoble). Cette collaboration a combiné deux types d'expertise, le LGP2 a permis de travailler sur les modifications chimiques du papier et le G2Elab a ajouté son expertise sur les propriétés diélectriques des matériaux. Cette combinaison d'expertises a permis d'étudier à l'échelle du laboratoire à la fois les changements chimiques et les changements de propriétés diélectriques lors du vieillissement du papier dans l'huile. L'étude ne s'est pas concentrée sur le comportement de l'huile.

La recherche présentée est divisée en trois chapitres expérimentaux.

Le premier chapitre se concentre sur l'utilisation du méthanol comme marqueur, dosé dans l'huile, représentatif de la dégradation (dépolymérisation) de la cellulose. Une littérature abondante au niveau du laboratoire et du terrain existe sur la méthode, mais la méthode n'a pas encore été normalisée. Dans notre étude, un focus particulier a été porté sur le rôle chimique des principaux composants du papier (cellulose, hémicelluloses, lignine) sur la production de méthanol au cours du vieillissement. Le rôle particulier de la lignine, en relation avec sa structure chimique, a été mis en évidence.

Dans les chapitres suivants, le même ensemble d'échantillons, composé de différents papiers, a été étudié. Il a été choisi pour représenter les variations possibles de la composition organique et inorganique du papier. La variation de la composition organique a été obtenue en utilisant simplement des pâtes cellulosiques de différents types (pâte Kraft de résineux écrue, pâte Kraft de résineux blanchie, pâte de linters de coton). Des variations de composition inorganique ont été obtenues par échange d'ions, pour remplacer certains cations présents dans les pâtes Kraft et enrichir le papier avec d'autres cations métalliques.

Le deuxième chapitre visait à étudier les dommages créés par l'oxydation de la matrice lignocellulosique au cours du vieillissement, et leurs relations avec le test DPv, classiquement appliqué sur les papiers électrotechniques (viscosité degré moyen de polymérisation de la cellulose). L'évaluation des dommages causés par l'oxydation pourrait ajouter des informations supplémentaires, non disponibles avec d'autres méthodes d'évaluation. Seule une petite littérature existe sur le sujet, principalement à l'échelle du laboratoire. Notre étude a mis un accent particulier sur le rôle de la composition du papier par rapport à l'oxydation de la pâte. Elle a également montré des relations claires entre le comportement à l'oxydation de la pâte et sa dépolymérisation.

Le troisième chapitre a évalué certaines propriétés diélectriques de la matrice lignocellulosique au cours du vieillissement. Les changements dans les propriétés diélectriques étaient liés à l'oxydation et cela pourrait être un autre outil pour évaluer l'état de l'isolation Kraft. La méthode de mesure utilisée dans l'étude, la spectroscopie diélectrique de champ, est assez originale et la littérature est peu abondante sur le sujet (essentiellement à l'échelle du laboratoire avec quelques essais de terrain). Le rôle particulier de la formation d'eau, qui accompagne l'oxydation, a également été mis en évidence lors du vieillissement du papier, révélant certaines contradictions

trouvées dans la littérature sur le rôle de l'humidité et du vieillissement dans la réponse diélectrique.

1) Origine de la production de méthanol lors du vieillissement du papier Kraft dans les transformateurs de puissance

a) Contexte

i) L'analyse des gaz dissous

Le processus de vieillissement des matériaux lignocellulosiques dans les transformateurs fera l'objet d'une exploration détaillée, en étudiant l'effet de la composition des fibres de bois sur les produits de dégradation du vieillissement du papier. Grâce à l'analyse des gaz dissous (DGA), certains de ces produits de dégradation sont utilisés comme marqueurs chimiques pour indiquer l'état de l'isolant en papier dans un transformateur en fonctionnement. La lignine, présente sous forme de résidu dans le papier Kraft d'origine, est particulièrement intéressante et pourrait jouer un rôle insoupçonné dans la génération des marqueurs utilisés pour suivre la dépolymérisation de la cellulose. Les marqueurs de gaz dans l'huile peuvent être analysés par HSGC-FID (Chromatographie gazeuse avec espace de tête statique et détecteur par ionisation de flamme).

Le méthanol a récemment été identifié comme marqueur chimique corrélé à la chute du degré de polymérisation moyen viscosimétrique de la cellulose (DP_v) du papier kraft au cours d'un vieillissement thermique de longue durée. Dans le chapitre correspondant, la contribution de la lignine à la production de méthanol est étudiée, en comparant le comportement de la pâte kraft non blanchie, de la pâte kraft blanchie et de la pâte de linters de coton blanchie, puisque les opérations de blanchiment éliminent complètement la lignine de la matrice lignocellulosique, et que seules les pâtes de linters de coton ne contiennent que de la cellulose. En complément, certains composés modèles de lignine et de cellulose seront étudiés, afin d'identifier les groupes fonctionnels contribuant à la génération de méthanol. De plus, l'affinité du papier vis-à-vis du méthanol sera étudiée, en particulier le coefficient de partage méthanol papier/huile en relation avec la présence de lignine dans le papier.

Remarque : la surveillance des gaz dissous (DGA) dans les transformateurs remonte à la fin des années 1920, lorsque les relais Bucholz, installés sur les réservoirs des transformateurs, donnaient la pression du gaz libre généré dans le transformateur. Une augmentation de la pression indiquait un défaut imminent ou en développement. Ce n'est qu'au début des années 1960 que la chromatographie a été appliquée comme technique analytique pour corrélérer la présence d'un gaz spécifique à un défaut particulier. Dans les années 1980, le développement de la chromatographie en phase gazeuse (GC) a permis d'avoir une analyse fiable et rapide de la teneur en gaz dissous dans l'huile. Après extraction par espace de tête, les gaz sont séparés par GC et détectés par spectrométrie de masse (MS) ou détecteurs à ionisation de flamme (FID). Le développement d'une quantification DGA robuste a permis d'envisager sérieusement son utilisation éventuelle pour analyser l'état de dégradation de l'isolant solide kraft, c'est-à-dire la dépolymérisation de la cellulose, en corrélant concentration d'un produit de dépolymérisation dans l'huile à l'évolution à long terme de l'isolant solide inaccessible.

ii) Le méthanol comme indicateur de vieillissement

Le méthanol en tant qu'indicateur chimique de la dépolymérisation de la cellulose a été utilisé pour la première fois par Jalbert et al. en 2007 [2]. Il a été constaté que du méthanol et de l'éthanol étaient détectés en quantité significative lors du vieillissement du papier dans l'huile isolante entre 60 °C et 120 °C. La production de méthanol a été corrélée à la rupture des liaisons 1,4- β -glycosidiques dans la cellulose, c'est-à-dire la dépolymérisation de celle-ci. Cette proposition est venue après des études approfondies du comportement de 50 sous-produits de DGA par HSGC-MS (Headspace Gas Chromatography Mass Spectrometry).

Les premières études ont montré que le principal avantage du méthanol est qu'il est généré par tous les types de papier utilisé comme isolant, c'est-à-dire à la fois le papier Kraft et le papier TU. Les inconvénients sont la forte volatilité du méthanol et l'estérification possible avec des acides de faible masse moléculaire formés avec du papier et de l'huile. La normalisation d'une procédure est un processus long. Pour le méthanol, après 15 ans de recherche scientifique sur le sujet, des comités internationaux (ASTM WG D27 WK30948 et IEC TC10 WG 63025) travaillent sur une norme de normalisation pour l'analyse du méthanol [3]. Même s'il n'existe pas encore de norme, le méthanol est déjà utilisé par les entreprises du monde entier. Pourtant, il reste important d'approfondir les mécanismes amenant à la génération de méthanol, où demeurent des incertitudes.

Il est important de corréliser la production de méthanol au DPv ou la résistance à la traction du papier. L'effet de la température doit également être étudié. Des expériences de « stabilité » et de « coefficient de partage du méthanol » entre huile/papier/gaz peuvent être menées pour comprendre comment le traceur va se comporter dans le transformateur et comment il va se répartir entre les différentes phases à l'intérieur (solide : papier / liquide : huile / gaz : azote). Des expériences complémentaires "d'origine" peuvent donner des indices sur les composants de l'isolant responsables de la production de méthanol.

b) Résultats et discussion

i) Comprendre l'approche expérimentale

Les papiers isolants standards des transformateurs sont constitués d'un seul composant, la pâte kraft de résineux purifiée. Le papier TU kraft contient également des additifs contenant de l'azote en quantités mineures, généralement la dicyandiamide, la mélamine et d'autres composants aminés. La pâte kraft est constituée de 3 macromolécules : la cellulose (75-80 %), les hémicelluloses (15-20 %) et la lignine (< 5 %). La cellulose est un polymère linéaire constitué d'unités d'anhydroglucose (AGU) liées entre elles par des liaisons 1-4- β -glycosidiques. Les hémicelluloses sont une famille de polysaccharides réticulés contenant 5 sucres élémentaires du bois : glucose, mannose, galactose, xylose, arabinose ; et la lignine est un assemblage complexe et variable d'unités phénylpropane (unités C9), qui diffèrent par leur disposition séquentielle, leurs groupes fonctionnels et leurs types de liaison. La chimie de la lignine a été largement étudiée dans le cadre des procédés chimiques de production des pâtes écruées ou blanchies, appliqués sur le bois et les plantes annuelles. Les principales caractéristiques des transformations qui se produisent lors de ces opérations sont actuellement assez bien connues. Cependant, son comportement lors du vieillissement thermique dans les huiles de transformateur n'a pas été spécifiquement approfondi.

Dans cette étude, des investigations ont été menées avec trois approches différentes :

- Des expériences « d'origine » ont examiné le comportement de certains composés modèles sélectionnés, qui représentent les principales structures chimiques de la lignine, de la cellulose et des hémicelluloses. Pour chaque composé modèle, la production de méthanol a été mesurée lors d'expériences de vieillissement.
- Des expériences « de corrélation » ont utilisé des papiers de différentes compositions en polysaccharides et lignine pour examiner l'influence de la composition sur la production de méthanol.
- Des mesures de coefficient de partage huile/papier du méthanol ont permis d'étudier si la présence de lignine, ou les phénomènes de vieillissement, modifient l'affinité du papier pour le méthanol.

ii) Origine du méthanol – Composé modèles

Des expériences sur des composés modèles de lignine visaient à comprendre l'origine de la production de méthanol par la lignine. Les résultats montrent, dans des conditions neutres, que les seuls composés qui produisent une quantité significative de méthanol sont les composés qui contenaient un groupe méthoxy. La seule exception est l'anisole dont le groupe méthoxy n'est activé par aucun substituant sur le cycle aromatique, il est donc beaucoup plus stable. Ceci est également confirmé dans des conditions acides où l'acide sulfurique catalyse l'hydrolyse acide des groupes méthoxy. Dans ce cas, la production de méthanol était proportionnelle au nombre de groupes méthoxy par cycle aromatique, quels que soient les effets activateurs ou désactivant provenant d'autres substituants (Figure 1). Les papiers électrotechniques étant fabriqués avec de la pâte kraft écrue de bois de résineux, dans laquelle la lignine résiduelle (à une teneur de l'ordre de 3 à 5 %) est composée d'unités guaiacyl (1 MeO par unité C6), du méthanol pourrait être potentiellement généré à partir de la lignine pendant un temps de libération très long lors du vieillissement à long terme, en raison de l'augmentation progressive de l'acidité du papier (partiellement mais pas entièrement dissous dans l'huile), qui à son tour augmente le taux de production de méthanol.

Le calcul suivant fournit une preuve de cette dernière affirmation :

En supposant que le papier UKP (pâte kraft écrue de résineux) contient environ 4 % de lignine guaiacyl (avec une masse molaire moyenne de 180 g/mol), 1 g de papier contient $0,04/180 = 222 \mu\text{mol}$ d'unités MeO.

Les échantillons de papier ayant été placés dans des flacons à un rapport papier:huile de 0,4 g de papier:10 mL d'huile, le rapport huile:papier est de 25 mL/g de papier. La capacité totale de libération est donc de $222/25 \times 32 = 284 \mu\text{g}$ de MeOH/mL d'huile, soit 355 μg de MeOH par g d'huile, en supposant la densité de l'huile égale à 0,8. Or en regardant la Figure 47, environ 6 μg de méthanol par g d'huile ont été générés pendant la durée totale de vieillissement (240 h) à 130°C (soit environ 3,75 μmol de méthanol/g de papier). Ainsi, en comparant la quantité de méthanol généré (3,75 μmol) et la quantité d'unités guaiacyl (222 μmol) dans un gramme de papier, seulement 1,7% des groupes guaiacyl dans la lignine ont été déméthylés. Cette valeur est probablement une surestimation du méthanol libéré par la lignine seule, puisqu'une partie du méthanol proviendrait de la dégradation des polysaccharides. En effet, dans les mêmes conditions

de vieillissement (Figure 3), les échantillons de papier BKP (pâte kraft blanchie) produisaient environ 1/6ème du méthanol produit par l'UKP. Ainsi, lors du vieillissement de la pâte UKP, seulement 5/6ème du MeOH produit serait attribuable à la lignine.

Pour conclure, les chiffres ci-dessus montrent que la lignine génère une importante quantité de méthanol, et une libération potentielle de méthanol pendant une très longue période, par rapport à la production de méthanol générée par la dégradation des polysaccharides.

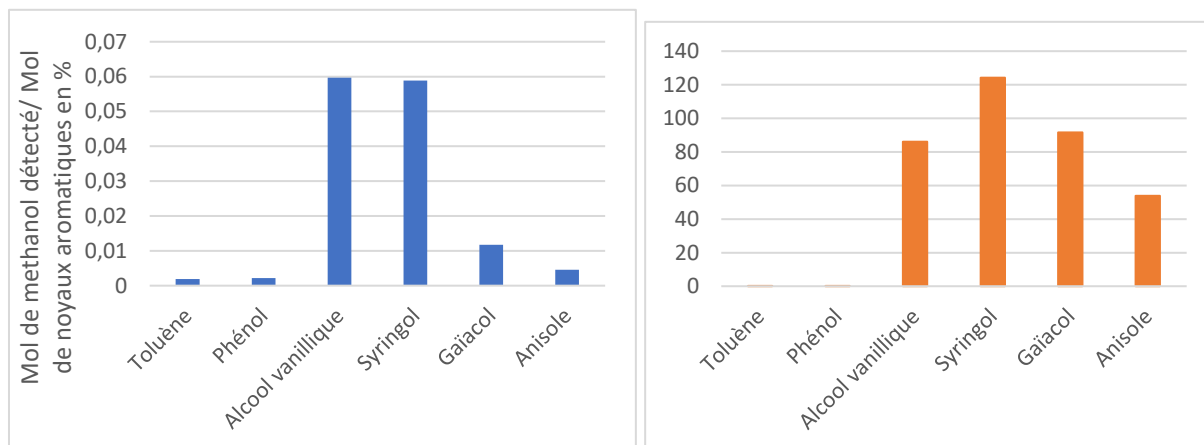


Figure 1: Rapport molaire entre le nombre de molécules de méthanol détectées sur chaque échantillon et le nombre de groupements aromatiques détectés après 24h à 140°C, exprimé en pourcentage. Les résultats sont présentés dans des conditions neutres (a) et acides (b). Echelle Y : représente les moles de méthanol détectées dans l'huile par rapport aux moles de noyaux aromatiques introduits dans l'huile.

De plus, des expériences avec des acides faibles ont confirmé que même une petite augmentation de l'acidité affecte grandement la production de méthanol.

Energie d'activation pour la production de méthanol :

La quantité de méthanol produite pendant le vieillissement à trois températures différentes a été quantifiée et utilisée pour calculer les constantes de vitesse de la réaction de production de méthanol à différentes températures de vieillissement, dont on peut déduire l'énergie d'activation de la réaction en représentant un diagramme d'Arrhenius. Les constantes de vitesse ont été calculées à partir de l'avancement de la réaction après 24 heures à 115, 125 et 135°C.

Le diagramme d'Arrhenius obtenu est représenté sur la Figure 2. L'énergie d'activation peut être estimée à environ 111 kJ/mol, valeur proche de l'énergie d'activation pour l'hydrolyse acide de la cellulose, estimée à environ 109 kJ/mol dans la plupart des articles publiés.

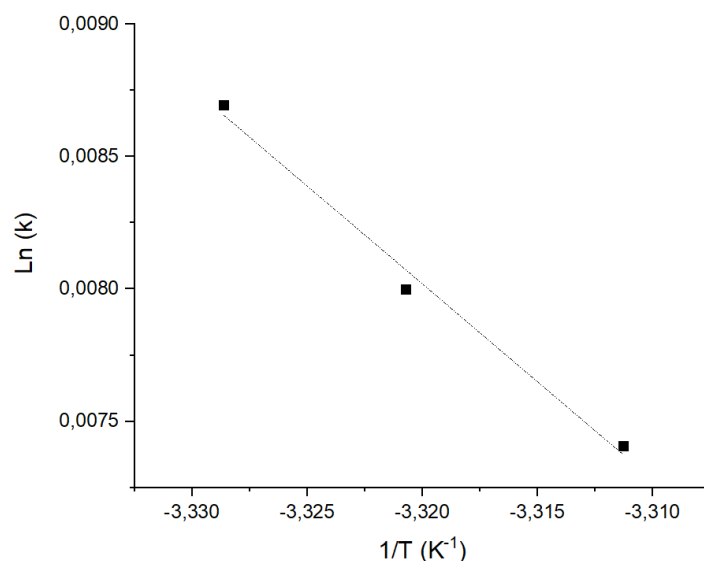


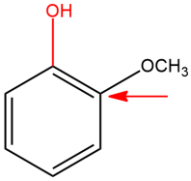
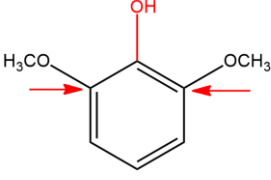
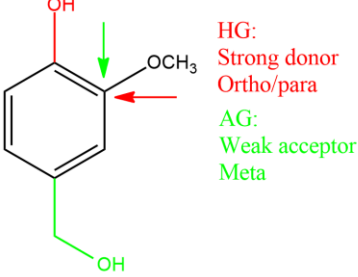
Figure 2: Les expressions d'Arrhenius du tableau des taux de production constants sont visibles ci-dessous pour la production de méthanol issue d'un vieillissement au guaiacyle après 24 heures à 115, 125 et 135 °C. La régression linéaire a une courbe de $y = -13,411x - 3,2125$ avec $R^2=0,9907$.

Vieillissement de composés modèles sélectionnés, représentatifs des polymères lignocellulosiques qui composent la pâte kraft écrue :

Considérant la formule des composés modèles de lignine sélectionnés, il est montré que pour les groupements aromatiques à substitutions multiples, les effets inducteurs et les effets donneur-accepteur des différents substituants peuvent affecter la production de méthanol en activant ou en désactivant les réactions des groupes méthoxy lors de l'hydrolyse acide. Les modèles sélectionnés présentaient trois groupes fonctionnels différents, avec des effets inductifs variables (Tableau 2).

L'effet des groupements fonctionnels présents sur la lignine s'avère conforme aux résultats expérimentaux de la libération de méthanol. Par exemple, dans le cas du syringol, les deux groupements méthoxy du syringol sont fortement activés par le groupement hydroxyle présent sur le cycle aromatique. Cela signifie qu'ils sont plus susceptibles d'être clivés par hydrolyse acide. La libération de méthanol pour le gaiacol n'atteignant pas exactement la moitié de la valeur du syringol, d'autres facteurs pourraient intervenir. En comparant l'alcool vanillique à ses deux homologues, la vanilline et l'acide vanillique, porteurs de carbonyle et carboxyle désactivant du méthoxy sur le cycle aromatique, on constate que l'alcool vanillique produit des quantités plus élevées de méthanol. Dans des conditions fortement acides (Figure 1b), la production de méthanol est proportionnelle au nombre de méthoxy par cycle. Les résultats montrent en effet que le syringol, avec ses deux méthoxy par C6, produit environ deux fois plus de méthanol que l'anisole, le gaiacol et l'alcool vanillique ayant un seul substituant méthoxy par C6. Le toluène et le phénol non-porteurs de substituant méthoxy ne produisent pas de méthanol même en condition acide, confirmant en outre que le groupement méthoxy est le seul à l'origine de la formation de méthanol à partir des composés modèles de lignine.

Tableau 2 : Groupes fonctionnels dans les composés modèles de lignine.

Groupe chimique substitué sur le C6	Type d'effet et position
Groupe hydroxyle (HG)	Fort – donneur (activateur) – ortho/para
Groupe méthoxy (MG)	Moyen– donneur (activateur) – ortho/para
Groupe alkyle (AG)	Faible – donneur (activateur) – ortho/para
Composé modèle	Structure chimique*
Gaïacol	
Syringol	
Alcool vanillique	

iii) Origine du méthanol – Echantillon de papier

Des essais sur les papiers ont poursuivi cette approche en fournissant une quantification directe de la production de méthanol à partir de papier réel, avec et sans lignine (UKP, BKP). Ici, la quantité de méthanol produite par gramme de papier est mise en contraste avec le nombre moyen de scission par chaîne cellulosique, calculé à partir l'équation ci-dessous :

$$\text{Nombre moyen de scission par chaîne} = DP_n \text{ initiale} \times \left(\frac{1}{DP_{n(t)}} - \frac{1}{DP_n \text{ initiale}} \right) \text{Équation 1}$$

Où : $DP_n(t)$ = valeur DP_n de la cellulose après le temps de vieillissement du papier t ; DP_n , initial = DP_n initial de la cellulose avant vieillissement du papier.

Sous l'hypothèse que le rapport DP_v/DP_n reste constant tout au long du processus de dépolymérisation lors du vieillissement du papier, cette formule peut être réécrite :

$$\text{Nombre moyen de scission par chaîne} = DP_v \text{ initiale} \times \left(\frac{1}{DP_{v(t)}} - \frac{1}{DP_v \text{ initiale}} \right) \text{Équation 2}$$

La Figure 3 montre la relation entre la production de méthanol et le nombre moyen de scissions par chaîne. La production de méthanol dépend fortement du substrat. L'UKP produit en fin de vieillissement environ cinq fois plus de méthanol que la pâte BKP ou CL. De telles différences ne peuvent être attribuées qu'à la lignine présente dans l'UKP.

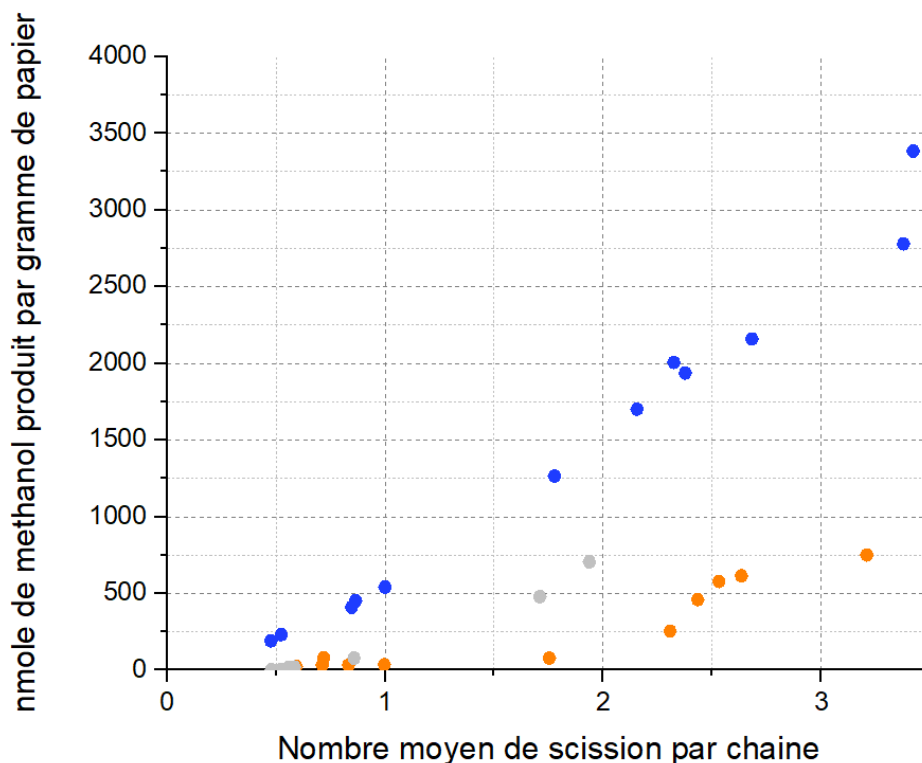


Figure 3: Production de méthanol à partir de différents échantillons cellulosiques en fonction du nombre moyen de scissions par chaîne ; Bourre de coton (●), échantillons de papier kraft écru (●) et blanchi (●) lors d'un vieillissement thermique accéléré dans l'huile (130°C ; 0 à 13 jours), les résultats sont donnés en nmole de méthanol détecté par coupure de chaîne.

Ces résultats montrent très clairement que la lignine influe sur le taux de production de méthanol au cours du vieillissement du papier. En effet, on constate que pour les substrats sans lignine (BKP et CL), la production de méthanol reste plutôt faible jusqu'à un nombre de scission de chaîne d'environ 2. A contrario, pour l'UKP qui contient de la lignine, elle augmente de manière continue et linéaire depuis le début du vieillissement.

Les calculs précédents ont montré que la quantité molaire de méthanol produit en fin de vie du papier (cellulose $DP_v \approx 200$) par la lignine guaiacyl (G) était de l'ordre de 1,7 % du nombre d'unités G). Il reste donc dans l'UKP 98,3% d'unités G non clivées susceptible de produire du méthanol, ce qui semble très important.

De plus, on observe qu'une production linéaire de méthanol commence au début du temps de vieillissement dans le cas de l'UKP. A l'inverse, la formation de méthanol est retardée pour le CL, et encore plus pour le BKP. On peut supposer que cet effet est lié au nombre de groupements réducteurs terminaux des chaînes de polysaccharides, réagissant avec le méthanol produit. Après réaction totale des terminaisons de chaînes accessibles avec le méthanol généré, ce dernier s'accumule. De nouveaux groupes terminaux de chaîne se forment durant la dépolymérisation, mais cela produit néanmoins une accumulation approximativement linéaire de méthanol dans l'huile. Étant donné que l'UKP a une production élevée de méthanol provenant de la lignine, le méthanol peut rapidement saturer les groupements réducteurs accessibles des chaînes de polysaccharides présents initialement. Dans la BKP, du fait de la moindre production de méthanol (absence de lignine) et de la présence d'hémicelluloses accessibles (contenant des groupes réducteurs d'extrémité de chaîne), le méthanol produit par la dépolymérisation des

polysaccharides réagit dans un premier temps avec les terminaisons de chaîne et le relargage de méthanol en solution est retardé. La pâte CL quant à elle ne contient pas d'hémicelluloses et l'effet retard, dû aux terminaisons des chaînes cellulosiques, est moins marqué.

L'augmentation de l'acidité du milieu devrait jouer un triple rôle : en augmentant la production de méthanol à partir de la déméthylation de la lignine, en augmentant la vitesse de dégradation des polysaccharides, et en catalysant la réactivité des groupes terminaux des polysaccharides avec le méthanol.

c) Conclusion

La durée de vie des transformateurs électriques est fortement liée à l'état de l'isolation cellulose. L'utilisation du méthanol comme marqueur de vieillissement de la cellulose dans l'huile a été établie au cours des quinze dernières années de recherche. La génération de méthanol est supposée dépendre linéairement de la dépolymérisation de la cellulose par hydrolyse acide à haute température. Le but de nos expérimentations était de mieux comprendre le rôle de chaque composant du papier kraft lors du processus de génération de méthanol. Des composés modèles lignocellulosiques ont été sélectionnés et vieillis dans l'huile dans les mêmes conditions que les papiers kraft dans des transformateurs à chaud.

Pour résumer, il a été constaté que parmi les trois principaux composants des papiers kraft, la lignine produisait environ cinq fois plus de méthanol que la cellulose et les hémicelluloses. Dans la lignine de résineux, le méthanol provient de la déméthylation des unités gâïacol, un phénomène non lié à la dépolymérisation de la cellulose. La déméthylation des noyaux aromatiques est catalysée par l'acidité du milieu. Ce processus devrait jouer un rôle de plus en plus important à mesure que l'acidité à l'intérieur du papier augmente avec le vieillissement. Dans les polysaccharides, le mécanisme chimique amenant à la production de méthanol à partir de la dépolymérisation de la cellulose n'est pas clairement établi, mais nous avons mis en évidence que le méthanol produit pouvait réagir avec les terminaisons de chaîne réductrices des polysaccharides, effet contribuant à la relation entre la dépolymérisation de la cellulose et la production de méthanol.

En guise de conclusion finale, ce chapitre a mis en évidence que le méthanol détecté dans l'huile lors du vieillissement du papier n'est pas uniquement dû à la dépolymérisation de la cellulose, mais également à la dégradation de la lignine. De nombreux autres paramètres interviennent, tels que la composition du papier, le coefficient de partage du méthanol, l'acidité dans le milieu, ou encore la nature de l'huile, sont à considérer.

2) Oxydation et dépolymérisation des papiers Kraft lors du vieillissement en présence de sels

a) Contexte

La méthode classique pour évaluer l'état de dégradation du papier kraft au cours du vieillissement dans les transformateurs est la mesure du degré de polymérisation moyen viscosimétrique de la cellulose (DP_v). Cependant, l'évaluation de l'état d'oxydation du papier,

paramètre non suivi en général, pourrait également apporter des informations pertinentes. Cet effet est généralement omis car on suppose que la perte de propriétés mécaniques ne provient que de la perte d'enchevêtrement résultant du raccourcissement des chaînes celluloses lors du vieillissement. La dégradation du papier est régie par deux principaux types de réactions ; hydrolyse et oxydation. Bien que l'hydrolyse acide soit considérée comme le principal facteur de dépolymérisation de la cellulose, elle est également liée à l'oxydation des polysaccharides. L'oxydation de l'isolant Kraft dans les transformateurs de puissance en présence d'huile est un sujet complexe qui n'est pas entièrement compris.

L'objectif sera donc d'étudier en parallèle la dépolymérisation et l'oxydation de la pâte, par mesure spectroscopique (FTIR). Pour suivre la dépolymérisation de la cellulose, le test DPv classique ainsi que la chromatographie d'exclusion stérique ont été utilisés. Les échantillons utilisés dans l'étude ont été choisis pour représenter les principaux composants du papier. Le papier vierge est composé d'une combinaison de matières organiques (cellulose, hémicelluloses et lignine) et de composants inorganiques (cations métalliques résiduels et les anions associés) provenant du bois et des procédés de mise en pâte (Ca, Na, Mg et Fe). Lors du vieillissement dans les transformateurs, des ions cuivriques et d'autres ions métalliques et des composants inorganiques pénètrent dans le papier au contact des pièces métalliques (par exemple, papier de guipage des conducteurs en cuivre).

L'objectif de ce chapitre est d'analyser l'impact individuel de chaque composant du papier sur les propriétés d'isolation au cours du processus de vieillissement. Cela se fait en analysant des échantillons de papier de plusieurs compositions (pâte kraft non blanchie (UKP), pâte kraft blanchie (BKP) et pâte blanchie de linters de coton). Des échantillons d'UKP chimiquement modifiés qui ne contiennent qu'un seul type de cation métallique (Ca, Na, Mg, Cu, Fe) ont également été étudiés. Ca et Mg sont introduits lors des étapes de lavage complet de la pâte, par échange d'ions avec le sodium présent dans la pâte kraft écrue, qu'il faut éliminer totalement du papier diélectrique final. Les principaux cations des métaux de transition (Fe et Cu) sont également connus pour avoir un impact significatif sur l'isolation kraft dans les transformateurs.

b) Résultats et discussions

i) Echange d'ions

Les expériences d'échange d'ions ont permis de corriger le profil cationique des pâtes, en conservant un ion métallique et en libérant les autres.

Des pâtes identiques ont été soumises aux mêmes concentrations de chlorures métalliques tout en changeant les contre-ions métalliques. Par conséquent, les différences de concentration en métal dans la pâte finale ne peuvent être attribuées qu'à des différences d'affinité de la pâte pour chaque métal.

Même si le papier électrotechnique résistant est purifié pour contenir très peu d'ions métalliques (en particulier Fe et Cu) par rapport aux papiers Kraft normaux, il existe encore des quantités traçables de fer (et très peu de cuivre), mais les principaux cations sont Mg^{2+} et Ca^{2+} , introduits par les échanges d'ions lors des dernières étapes de lavage de la pâte à l'aide d'eaux environnementales filtrées.

Le premier échantillon testé était l'UKP de référence.

Cet échantillon a montré la concentration ionique attendue pour les pâtes de qualité électrotechnique (Tableau 3).

Tableau 3: Types d'échantillons et leur teneur en ions correspondante mesurée par (ICP/MS).

Samples	Ca ²⁺ (ppm)	±	Na ⁺ (ppm)	±	Mg ²⁺ (ppm)	±	Fe ²⁺ (ppm)	±	Cu ²⁺ (ppm)	±
Référence (UKP)	720	22	49	22	113	13	45	6	11	6
Déminéralisée										
Calcium	641	22								
Sodium	59	4	228	22						
Magnesium	42	4			359	13				
Iron	102	4					1463	6		
Copper	48	4							1435	6

Dans les papiers électrotechniques, une forte teneur en calcium est généralement associée à une faible teneur en sodium, puisque les fabricants de pâte tentent de réduire au maximum la teneur en Na dans les papiers, connue pour diminuer les pertes diélectriques ($\tan \delta$). Le fer et le cuivre sont présents en quantités minimales. Pour les pâtes déminéralisées, sans autre réintroduction d'ions par échange d'ions, aucune cendre n'a été retrouvée après calcination.

Les cations métalliques ont pu être éliminés et remplacés avec succès, comme le montrent les résultats (Tableau 3) des pâtes échangées. Parallèlement à la quantification du métal cible, le calcium résiduel a été mesuré dans chaque échantillon. La diminution observée du calcium montre que les ions initiaux dans UKP ont été éliminés avec succès lors de la première étape de déminéralisation. Il est aussi clairement montré que les métaux principaux (Ca, Mg) ont beaucoup moins d'affinité avec la pâte que les métaux de transition.

ii) Effet de la composition du papier dans la cinétique de la dégradation de la cellulose

L'UKP contient de la lignine, des hémicelluloses et de la cellulose, tandis que la BKP ne contient que des hémicelluloses et de la cellulose, et la pâte CL ne contient qu'un seul composant, la cellulose.

Tous les échantillons ont été vieillis dans les mêmes conditions pour toutes les expériences. L'évolution du DP moyen, calculé à partir des expériences SEC, est présentée dans la figure suivante :

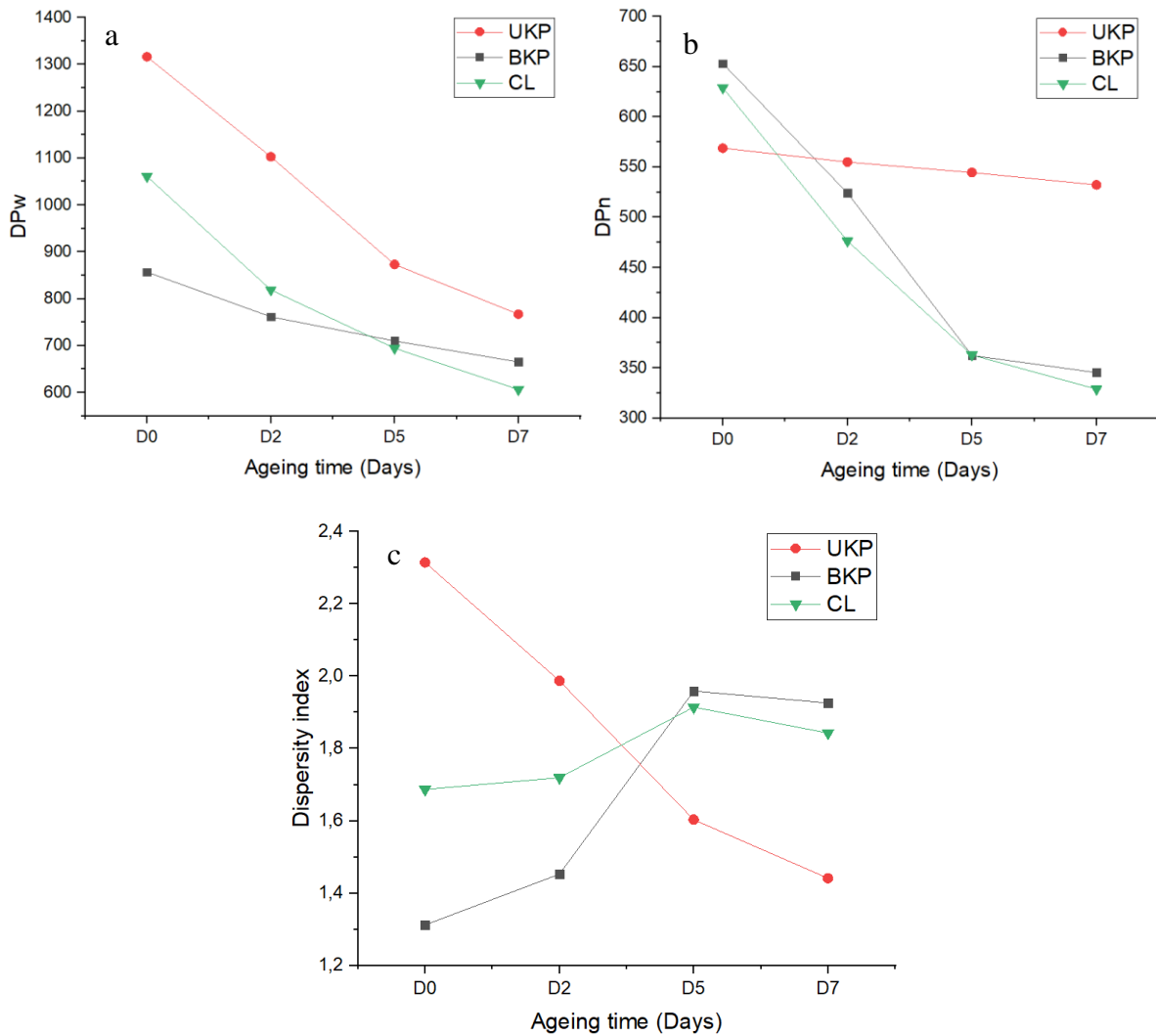


Figure 4: Évolution du DP_w (graphe a), du DP_n (graphe b) et de l'indice de dispersité (\mathcal{D}_M) (graphe c) pour les 7 premiers jours de vieillissement. Les mesures ont été effectuées par SEC après tricarbanilation.

Les figures ci-dessus montrent qu'il existe un contraste important entre les échantillons avec et sans lignine. Les pâtes BKP et CL, qui ne contiennent pas de lignine, présentent une baisse importante de DP_n, alors qu'elle reste beaucoup plus stable pour la pâte contenant de la lignine, l'UKP. Contrairement à cela, la baisse de DP_w suit un schéma assez similaire pour tous les échantillons (bien que la baisse soit légèrement plus prononcée pour l'UKP).

Chaque comportement doit être analysé de manière indépendante.

Pour l'UKP, le DP_w et le DP_v diminuent de manière importante tandis que le DP_n varie beaucoup moins. Par conséquent, il semble que le vieillissement affecte beaucoup plus les chaînes longues de cellulose, qui contribuent principalement aux valeurs initiales élevées de DP_w et DP_v. Au contraire, la lente décroissance de DP_n indique que les chaînes courtes sont moins affectées par le vieillissement, sans une production importante de nouvelles chaînes plus petites. En conséquence, l'indice de dispersité diminue de manière significative, ce qui signifie que la largeur de la distribution de longueur de chaîne est réduite.

Contrairement au comportement décrit ci-dessus, les pâtes BKP et CL présentent des chutes simultanées de DPw et DPn (bien qu'on puisse remarquer que la chute de DPw est moindre pour la BKP que pour la CL). Comme pour l'UKP, les longues chaînes cellulosiques sont dégradées en chaînes plus petites (chute DPw), mais aussi les chaînes plus petites sont dégradées et un nombre important de nouvelles chaînes sont produites (chute DPn). Comme la perte de DPw est plus lente que la perte de DPn, il y a une augmentation de l'indice de dispersité, ce qui signifie une distribution plus large.

La cellulose a une composition polymère unique, et les autres polysaccharides, les hémicelluloses, sont généralement similaires dans une pâte kraft blanchie ou non blanchie (produite dans la même usine suédoise, avec les mêmes essences de bois : un mélange scandinave de résineux du nord dans le cas présent). Par conséquent, le rôle joué par la lignine est important. Il semble que la présence de lignine puisse protéger les chaînes les plus courtes de la dépolymérisation, mais pas les chaînes les plus longues. Certains oligosaccharides peuvent être produits pour des échantillons sans lignine, ce qui apporte un certain effet protecteur. Ces résultats montrent également que le rapport entre le DPw et le DPn n'est pas constant. Cette caractéristique n'a pas été rapportée dans les publications les plus récentes, dans lesquelles un facteur de correction constant a été utilisé pour passer des mesures de DPv aux valeurs de DPn, afin de calculer un nombre de scission de chaîne. Une telle erreur dans les conversions entre DPw et DPn peut entraîner des erreurs dans les modèles mathématiques qui ont été construits, indiquant le taux de scission à différentes températures pour différents types de papier.

iii) Dépolymérisation et oxydation de la cellulose pendant un vieillissement thermique accéléré

Les mesures de degré d'oxydation ont permis de voir que dégradation et oxydation sont liées, mais la dépolymérisation n'est pas nécessairement proportionnelle à l'oxydation.

Un comportement observé sur tous les échantillons est une augmentation puis une diminution des valeurs d'oxydation totale au cours du vieillissement. Contrairement à la dépolymérisation qui s'opère de manière continue, l'oxydation des pâtes augmentait jusqu'à un maximum après 16 jours de vieillissement sur tous les échantillons (sauf UKP qui atteignait son maximum après 6 jours) puis diminuait à nouveau après 35 jours. Certains échantillons ont révélé une réaugmentation après 46 jours. Pour expliquer ce comportement, il convient de noter que le papier n'est pas isolé au cours du vieillissement ; il interagit et échange des sous-produits du vieillissement avec l'huile et indirectement avec la couche de gaz à l'intérieur de la cuve de vieillissement (ou couche de gaz du transformateur dans les applications réelles), ces interfaces échangent en permanence des sous-produits qui peuvent donc sortir ou entrer dans l'isolant Kraft. Les produits oxydés peuvent se décomposer ou se réorganiser dans le papier pour produire des oligosaccharides suffisamment petits pour être dissous dans l'huile. Certains d'entre eux peuvent éventuellement se transformer en gaz qui s'échappent dans la phase gazeuse. On peut postuler qu'au début du vieillissement, l'hydrolyse acide et l'oxydation augmentent l'oxydation globale de la pâte. Lorsqu'une fonction chimique est oxydée, elle peut se décomposer en molécules de plus en plus simple qui, à des températures élevées, peut se décomposer en molécules encore plus petites telles que le méthanol. Pour examiner plus en détail ce changement, l'un des spectres a été analysé jusqu'à 1500 cm^{-1} , permettant de voir le signal les noyaux aromatiques à 1520 cm^{-1} . Les résultats sont visibles sur la Figure 5 ci-dessous :

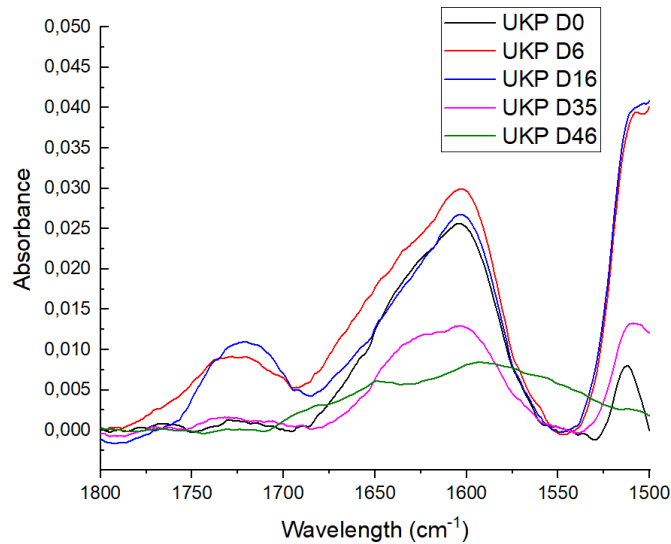
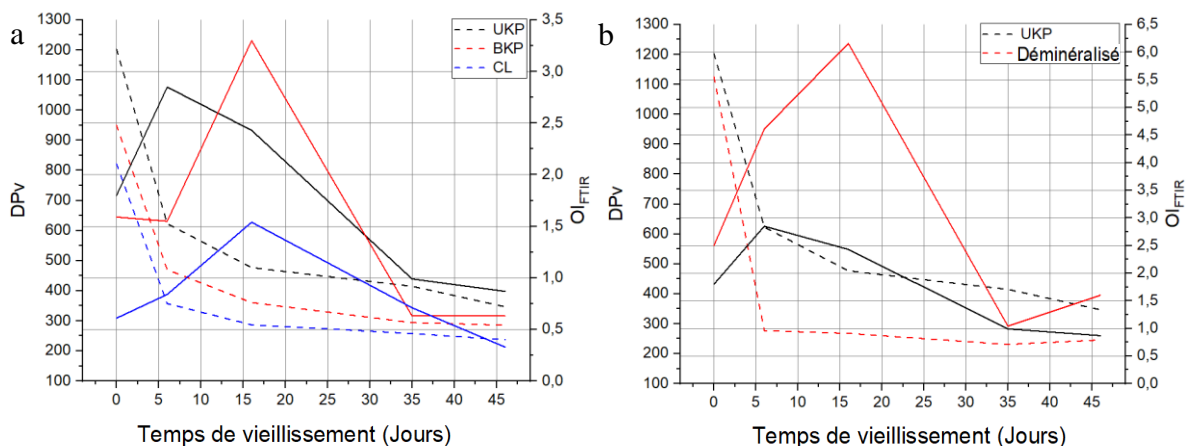


Figure 5: Évolution de la valeur d'absorbance pour les échantillons UKP pendant 46 jours de vieillissement. Ce chiffre inclut les valeurs allant de 1800 à 1500 cm^{-1} pour montrer la dégradation de la lignine visible à 1520 cm^{-1} .

Alors que la valeur globale de l'oxydation augmente jusqu'à 16 jours, puis diminue après, le pic de lignine aromatique (1520 cm^{-1}) diminue après 16 jours de vieillissement. Cela montre que la lignine a été dégradée au cours du vieillissement et l'on peut supposer une extraction des fonctions oxydées de la matrice solide par l'huile. Dans une étude de référence [4], ce comportement en zigzag est également observé pour les échantillons P1 vieillis à 90°C et les échantillons de transformateurs.

Un autre regard du comportement oxydatif de chaque type d'échantillon en fonction de la dépolymérisation est illustré ci-dessous. Le signal OIFTIR représente la valeur intégrale de l'oxydation allant de 1800 à 1500 cm^{-1} . La comparaison avec l'étude de référence précitée [4] est limitée car les températures de vieillissement (90 et 150°C) étaient différentes, alors que les valeurs d'oxydation intégrées étaient du même ordre de grandeur, entre 1 à 4. Il convient de noter OIFTIR est la valeur d'oxydation globale pour le pic des aldéhydes et des acides carboxyliques (1740 cm^{-1}) et le pic des cétones conjuguées (1620 cm^{-1}). Ce signal ne discrimine pas la contribution de chaque pic à la valeur globale. Par conséquent, le rapport d'oxydation entre les deux pics a été calculé pour chaque échantillon. Ci-dessous les valeurs d'oxydation et de dépolymérisation de tous les échantillons présents dans ce chapitre (Figure 6) et le rapport correspondant entre les deux pics (Figure 7) :



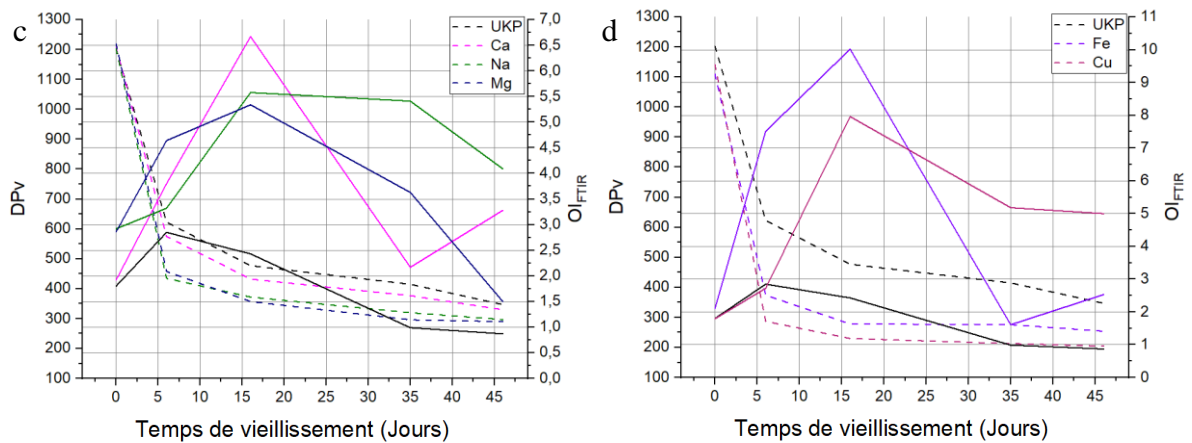


Figure 6: Évolution de la valeur d'absorbance et de dépolymérisation pour l'échange d'ions pendant 46 jours de vieillissement pour des échantillons de compositions multiples (a), des échantillons déminéralisés (b), des échantillons d'échange d'ions avec des métaux principaux (c) et de transition (d). Les lignes pointillées représentent DPV tandis que les lignes droites représentent OI_{FTIR}.

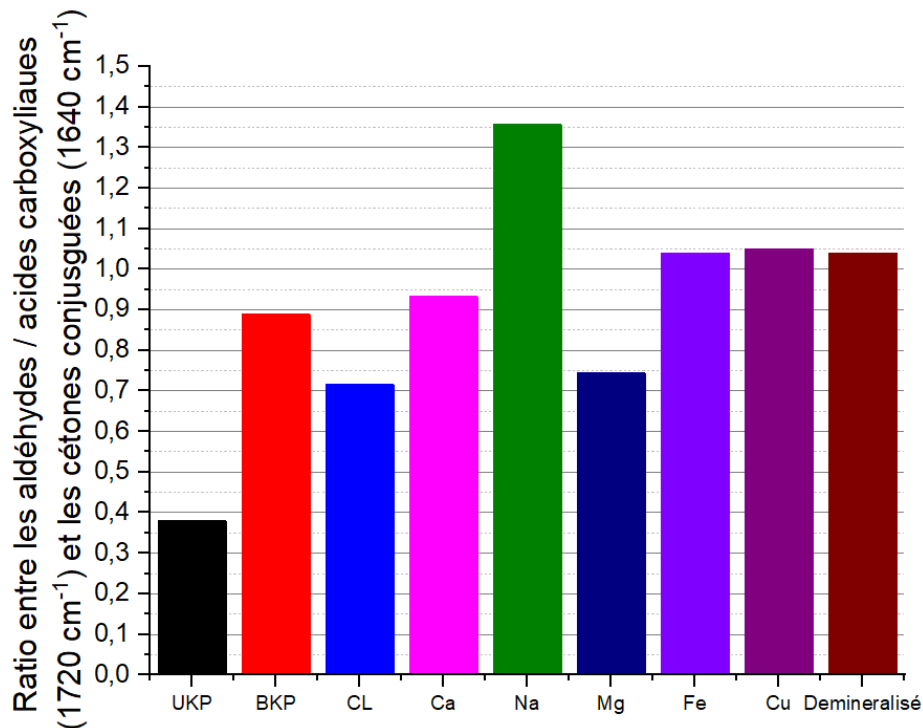


Figure 7 : Évolution du rapport des pics entre les aldéhydes, les acides carboxyliques (1740 cm⁻¹) et les cétones conjuguées (1620 cm⁻¹) pour les échantillons les plus oxydés. Tous les échantillons ont atteint leur valeur d'oxydation la plus élevée après 16 jours, à l'exception de l'UKP qui a atteint sa valeur d'oxydation la plus élevée au 6e jour de vieillissement.

Une vision générale de la dépolymérisation et de l'oxydation montre ainsi une augmentation du signal OI_{FTIR} au moment où chaque échantillon atteint le LODP, puis une diminution de la valeur d'oxydation. On pourrait supposer qu'une partie importante de l'augmentation initiale est le résultat de sous-produits de l'hydrolyse acide initiale des liaisons glycosidiques faibles dans la phase amorphe de la cellulose. Ces sous-produits peuvent ensuite se dégrader davantage et

se dissocier de la pâte. La plupart des signaux semblent rebondir à J46, il est peu probable que ce comportement soit le reflet d'une nouvelle augmentation de l'oxydation et pourrait être davantage attribué à l'aplatissement des signaux FTIR qui rend les intégrations sujettes à erreurs. Néanmoins, tous les échantillons ne se sont pas comportés de la même manière, la composition organique et métallique altérant drastiquement leur comportement au vieillissement. Pour l'UKP, une analyse de la valeur de neutralisation avec KOH a été faite pour les échantillons d'huile utilisés lors du vieillissement, quantifiant la quantité d'acides dissous présents dans l'huile (titrage par KOH). Les résultats sont représentés dans la Figure 8 ci-dessous :

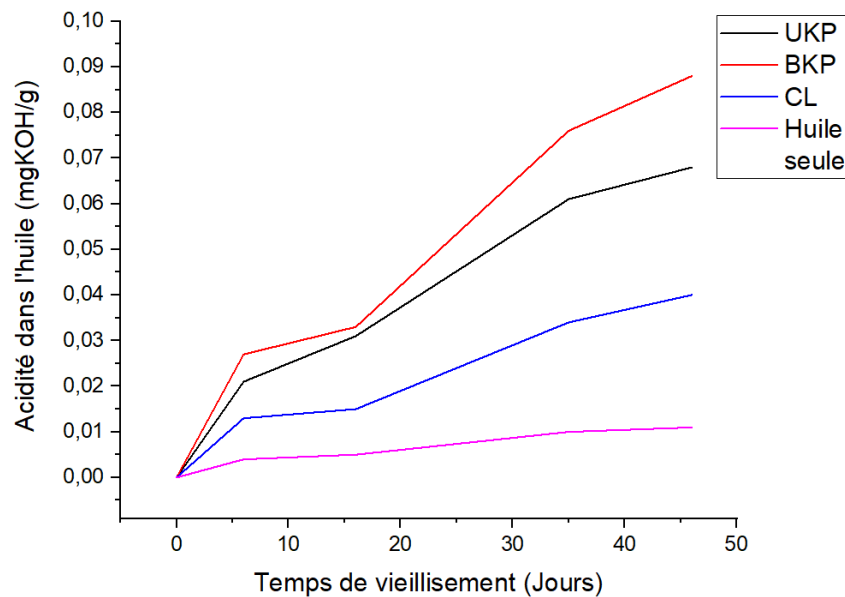


Figure 8: Evolution du niveau d'acidité de l'huile au cours du vieillissement pour UKP, BKP et CL. Un résultat supplémentaire est affiché pour l'huile vieillie sans papier, appelée « huile uniquement ». Les résultats indiqués sont pour la quantité en mg de KOH neutralisé pour chaque g d'huile.

Lors de l'examen de l'acidité de chaque huile, une tendance claire apparaît ; la quantité d'acides dissous dans l'huile augmente rapidement après un plateau vers le 6^{ème} jour, cette augmentation semble retardée pour la BKP et la CL jusqu'au 16^{ème} jour. Pendant ce temps, l'huile sans papier ne montre qu'une petite augmentation de l'acidité. De ces résultats, deux interprétations principales peuvent être tirées. Premièrement, l'augmentation de la teneur en acide correspond à la perte de la valeur d'oxydation OI_{FTIR} , l'acidité croissante de l'huile provenant de l'extraction du papier. L'acidité de l'huile semble présenter un plateau corrélé au pic OI_{FTIR} , puis réaugmente seulement après le 16^{ème} jour pour les pâtes BKP et CL alors qu'elle augmente beaucoup plus tôt pour l'UKP.

Les résultats pour les pâtes UKP, BKP et CL semblent cohérents avec la chimie de leurs composants. Avant le vieillissement, l' OI_{FTIR} ne représente pas les mêmes fonctions chimiques pour les trois échantillons. Lors du vieillissement, chaque échantillon subit un dommage oxydatif propre de ses composants : UKP (cellulose, hémicelluloses et lignine), BKP (cellulose,

hémicelluloses) et CL (cellulose). Les évolutions montrent des différenciations caractéristiques, surtout pour la pâte CL initialement moins riche en fonctions oxydées.

Au cours du vieillissement, il est intéressant d'observer le comportement de la cellulose pure ; la vitesse de dépolymérisation réelle de la pâte CL est plus lente que la BKP tandis que l'oxydation est plus élevée. Compte tenu de sa structure chimique et de leur accessibilité, les hémicelluloses sont intrinsèquement plus sensibles à l'oxydation que la cellulose. La pâte BKP affiche donc un OI_{FTIR} plus élevé que la pâte CL. L'UKP montre la plus petite augmentation du signal OI_{FTIR} , il convient de noter que compte tenu de ce faible taux d'oxydation (0,4), la majeure partie de l'augmentation représente des cétones conjuguées et non des acides comme la BKP et la CL. Seule l'UKP non modifiée a atteint son pic OI_{FTIR} après 6 jours. Ainsi, le rôle protecteur de la lignine vis-à-vis de l'oxydation du papier kraft est pleinement apparent : modification du signal OI_{FTIR} et modification du délai, provenant très probablement de la plus faible quantité d'acides générés.

Les échantillons déminéralisés ont montré une augmentation de la production d'acide par rapport à l'UKP de référence. Quant aux échantillons produits par échanges d'ions, ils produisent avant vieillissement un signal FTIR d'oxydation sensiblement identique.

Pendant le vieillissement, les échantillons d'échange d'ions doivent d'abord être comparés à la fois à l'échantillon UKP de référence et aux échantillons déminéralisés. On voit clairement apparaître un taux d'oxydation avec production d'acides élevé pour Fe, Cu et les échantillons déminéralisés, tandis que Ca et Mg engendrent une oxydation cétonique. Les échantillons avec production d'acides ont également montré les valeurs OI_{FTIR} les plus élevées. Plus important encore, l'oxydation avec production d'acides a engendré une chute complète de DP_v après 6 jours, tandis que les échantillons avec une oxydation cétonique ont pris environ 40 jours. Dans le cas de Na, il y a un taux d'oxydation élevé mais la valeur OI_{FTIR} globale reste similaire au comportement des métaux alcalino-terreux (Ca, Mg), et il en va de même du comportement de dépolymérisation lente. En pratique, l'oxydation de l'échantillon Na semble ne pas affecter le taux de dépolymérisation de la cellulose.

c) Conclusion

Le vieillissement de la cellulose dans l'huile est un processus hétérogène qui entraîne des modifications de propriétés physiques et chimiques du papier et une perte de DP_v de la cellulose. La dégradation du papier dans l'huile ne suit pas un comportement uniforme. L'oxydation affecte les groupements chimiques du papier. Les petites molécules résultant de l'oxydation ou de l'hydrolyse acide peuvent soit être libérées du papier et diffuser dans l'huile, soit rester dans le papier et se dégrader davantage en molécules plus petites. Le processus de dégradation de la cellulose interagit avec l'environnement autour du papier, c'est-à-dire l'huile et la phase gazeuse à l'intérieur du réacteur de vieillissement utilisé au laboratoire.

Une accumulation d'acide dans l'huile est au cours du vieillissement. Le papier immergé dans l'huile produit des quantités importantes de sous-produits acides qui proviennent de la cinétique initiale rapide de dégradation (ordre zéro), puis la production d'acide se ralentit en corrélation avec une dépolymérisation plus lente. Les sous-produits peuvent s'extraire de la matrice, se dégrader en petites molécules oxydées, qui peuvent migrer dans l'huile par diffusion, en deçà d'une certaine taille. La concentration dans l'huile dépend de l'équilibre entre les trois phases.

Il a également été montré que lors de la dépolymérisation du papier kraft, l'indice de dispersité de la cellulose évolue. Cet indice affecte le ratio entre DP_v, DP_w et DP_n, et par conséquent intervient dans les modèles cinétiques où le nombre de scission par chaîne du polymère est déterminé en fonction du temps, caractérisant l'évolution du DP_v.

Un autre fait intéressant, qui sera développé dans la partie suivante, est que l'état d'oxydation de la cellulose est corrélé aux changements des propriétés diélectriques.

3) Caractérisation du vieillissement des isolants Kraft par spectroscopie diélectrique et mesures de claquage

a) Contexte

Le vieillissement de l'isolation kraft des transformateurs de puissance est généralement quantifié en mesurant la dépolymérisation de la cellulose. Les opérateurs sont principalement concernés par les propriétés mécaniques de l'isolation Kraft qui détermineront en fin de compte l'espérance de vie des transformateurs de puissance. L'évolution des propriétés diélectriques au cours du vieillissement est rarement étudiée : la plupart du temps, les auteurs suggèrent que la production d'eau induite par le vieillissement est exclusivement responsable de la dégradation des propriétés diélectriques (pertes diélectriques et tension de claquage).

Une analyse diélectrique de l'isolation kraft a été réalisée, dans le but de voir dans quelle mesure l'oxydation et la dépolymérisation de la pâte affectent les propriétés diélectriques. Les échantillons utilisés dans l'étude étaient les mêmes que ceux du chapitre précédent. Ils représentent la diversité des matières organiques (cellulose, hémicelluloses et lignine) et des métaux résiduels inorganiques (métaux principaux et de transition) que l'on peut trouver dans le papier électrotechnique. Le but de ce chapitre est d'étudier l'effet que chaque composant peut avoir sur les propriétés diélectriques clés.

Cela se fait en analysant des échantillons de papier de plusieurs compositions (UKP, BKP et coton). L'objectif est de développer une compréhension fondamentale de leur rôle sur la réponse diélectrique avant et pendant le vieillissement. La spectroscopie diélectrique de champ (FDS) est principalement utilisée comme méthode d'évaluation pour étudier le vieillissement de l'isolation des transformateurs de puissance. Par rapport aux mesures standard de permittivité et de $\tan \delta$ à une fréquence fixe (généralement 50 Hz), le FDS peut fournir plus d'informations sur l'impact des variations de la composition du matériau. Cette méthode est également intéressante sur le terrain car elle peut être appliquée sur un transformateur à grande échelle et pourrait fournir une méthode non intrusive et rapide pour estimer la teneur en humidité et le vieillissement de l'isolation d'un transformateur de puissance.

b) Résultats et discussions

i) Contexte

Il n'existe pas de consensus clair sur les mécanismes conduisant à la modification des propriétés diélectriques pendant le vieillissement. Le seul consensus couramment cité dans la littérature est que l'eau est principalement responsable de la perte des propriétés diélectriques du papier,

tandis que les acides et autres sous-produits du vieillissement jouent un rôle mineur dans ces changements [5]–[7]. Une autre explication postulée est l'augmentation du contenu polaire de la pâte elle-même, qui à son tour augmenterait la possibilité de porteurs de charge et donc de pertes conductrices.

Dans notre étude, nous approfondirons la question du vieillissement en réalisant des expériences FDS visant à comparer des papiers de différentes compositions et à mesurer l'impact de différents teneurs en ions au cours du vieillissement. Cette étude est rendue possible grâce aux méthodes et analyses chimiques développées à partir des chapitres précédents.

Les échantillons étudiés sont les mêmes que ceux du chapitre précédent, à savoir les pâtes UKP, BKP, CL, ainsi que les échantillons produits par déminéralisation et échange d'ions. Seule l'UKP a été analysée à toutes les températures et à divers degrés de vieillissement. Les échantillons non vieillis ont été séchés, imprégnés et testés avec de l'huile minérale neuve. Pour les échantillons vieillis, la plupart ont été testés dans l'huile dans laquelle ils ont vieilli, mais l'UKP, la BKP et la CL ont été testés avec les trois types décrits précédemment. L'objectif était d'essayer d'identifier l'influence relative de plusieurs phénomènes intervenant au cours du vieillissement : vieillissement de l'huile, vieillissement du papier, présence de sous-produits de vieillissement (dont l'humidité).

ii) Propriétés diélectriques de la pâte écrue (UKP) et de l'huile neuve

Afin de mieux identifier l'origine des pertes dans le papier imprégné, il est intéressant de comparer $\tan \delta$ mesuré dans l'huile seule, le papier seul et le papier imprégné à différentes températures (90, 20 et -30°C), voir Figure 9.

A 90°C, $\tan \delta$ de l'huile et du papier sont identiques à 30 Hz, et $\tan \delta$ du papier imprégné est également logiquement identique à cette fréquence. En dessous et au-dessus de 30 Hz, le papier imprégné présente un $\tan \delta$ intermédiaire entre celui du papier et de l'huile :

- En dessous de 30 Hz, $\tan \delta$ reflète surtout les pertes d'huile (dus à la conduction).
- Au-dessus de 30 Hz, $\tan \delta$ reflète principalement les pertes de papier (dus à la polarisation).

A 20 °C, la situation est similaire, avec une fréquence de « transition » plus faible (environ 1 Hz). A basse température (-30°C) les pertes d'huile deviennent négligeables par rapport à celles du papier, et les pertes du papier imprégné reflètent majoritairement celles du papier.

Le tracé global de $\tan \delta$ du papier imprégné à différentes températures (Figure 9) montre clairement deux zones typiques, en dessous et au-dessus d'une fréquence de « transition » d'environ 30 Hz :

- En dessous de 30 Hz, les pertes sont principalement dues à la conduction dans l'huile, et augmentent beaucoup lorsque la température augmente.
- Au-dessus de 30 Hz, les pertes sont principalement dues à la polarisation dans le papier, et diminuent lorsque la température est élevée.

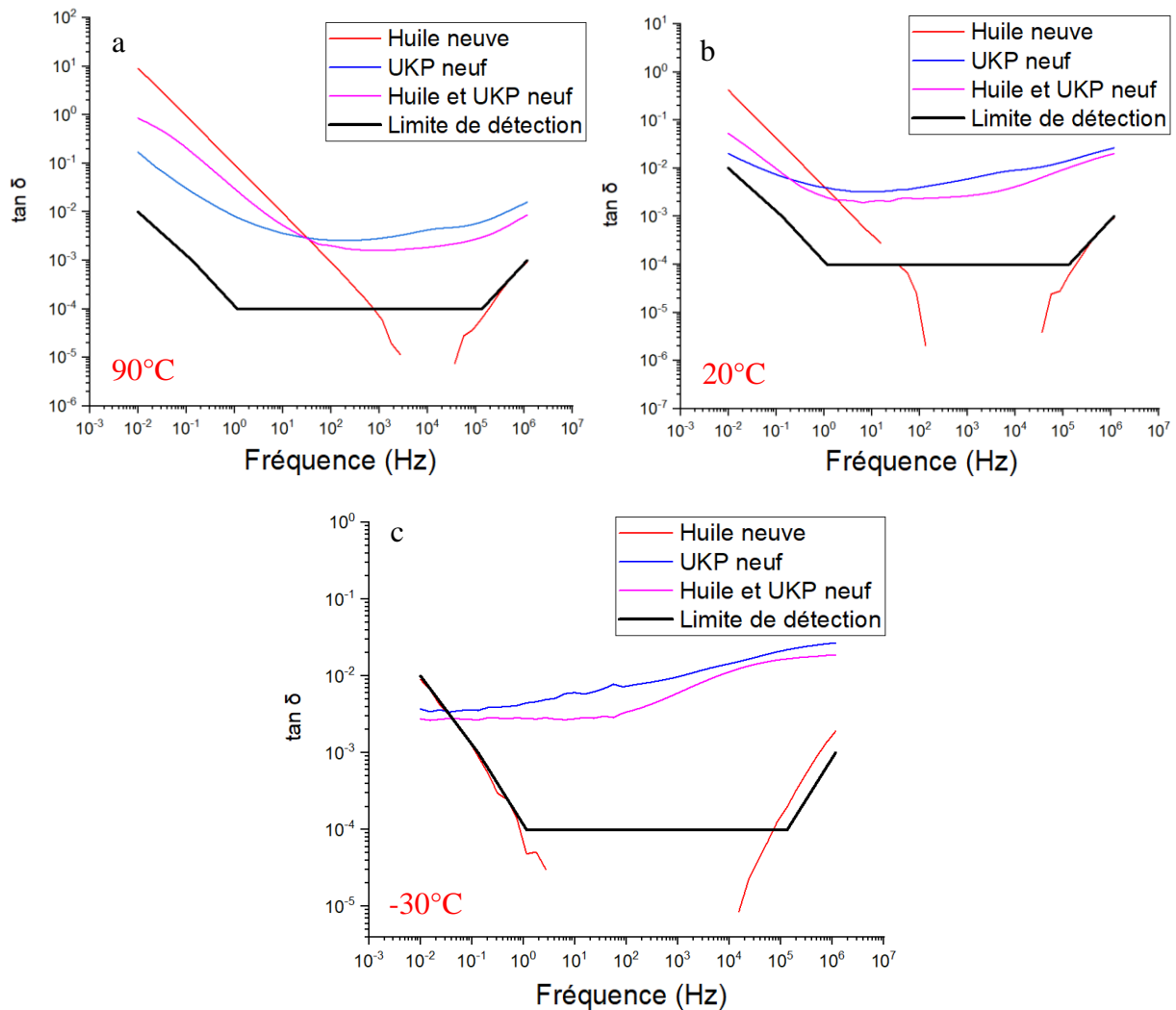


Figure 9: $\tan \delta$ de l'huile non vieillie, du papier UKP et des échantillons UKP imprégnés à haut (a / 90°C), moyen (b / 20°C) et bas (c / -30°C). La teneur en humidité des deux échantillons UKP était de 0,3 %, cette humidité a été mesurée à 21 °C. La limite de détection du spectromètre est indiquée par une ligne noire.

Il n'est cependant pas possible de considérer que le papier imprégné résulte simplement de la "somme" des apports d'huile et de papier, comme le feraient deux condensateurs indépendants en parallèle. Il existe également une interaction entre ces deux matériaux. A basse fréquence et haute température, une forte polarisation des électrodes se produit dans le papier imprégné, induisant une augmentation significative de la permittivité ϵ' (de 2,8 à 4 à 90°C, 10⁻² Hz). Cet effet est beaucoup plus marqué que dans l'huile seule (presque aucune polarisation d'électrode ne se produit dans le papier seul), et met en évidence l'interaction entre les matériaux.

Une interaction bien connue entre le papier transformateur et l'huile minérale est constituée par la « double couche » électrique qui s'établit à leur interface. Cette interaction induit deux couches parallèles de charge. Dans la première couche, les charges positives des impuretés de l'huile sont adsorbées sur l'isolant kraft en raison des interactions chimiques. La deuxième couche est composée d'ions attirés par la charge de surface via la force de Coulomb, masquant électriquement une charge négative en réponse à la première couche. Cette interaction joue un rôle clé dans un phénomène appelé « électrification par flux » qui conduit à une accumulation de charges dans l'isolant kraft suite au flux d'huile. Une telle accumulation de charge peut

conduire à un potentiel local élevé et à un champ électrique, qui peut éventuellement provoquer des décharges partielles ou une panne dans les transformateurs. Ces études se sont concentrées sur la mesure des charges et du potentiel de différents types de papiers et d'huiles, mais presque aucune étude n'a été consacrée à évaluer son rôle sur les mesures de spectroscopie diélectrique. Les conditions existant à l'interface entre la cellulose et l'huile au sein du papier sont certainement très différentes d'une interface papier/huile macroscopique standard : les distances sont beaucoup plus petites, et l'équilibre de charge est probablement différent, et plutôt difficile à prévoir. Cependant, on peut supposer que la présence de charges à l'interface, résultant de l'interaction chimique entre l'huile et la cellulose, peut influencer les mesures FDS du papier imprégné.

iii) Changement des propriétés diélectriques de la pâte écrue lors d'un vieillissement thermique accéléré

Les propriétés diélectriques ont été mesurées au cours du vieillissement, avec des mesures FDS réalisées à intervalles réguliers à une température fixe de 90°C, sans vidange d'huile. Les résultats sont visibles sur la Figure 10:

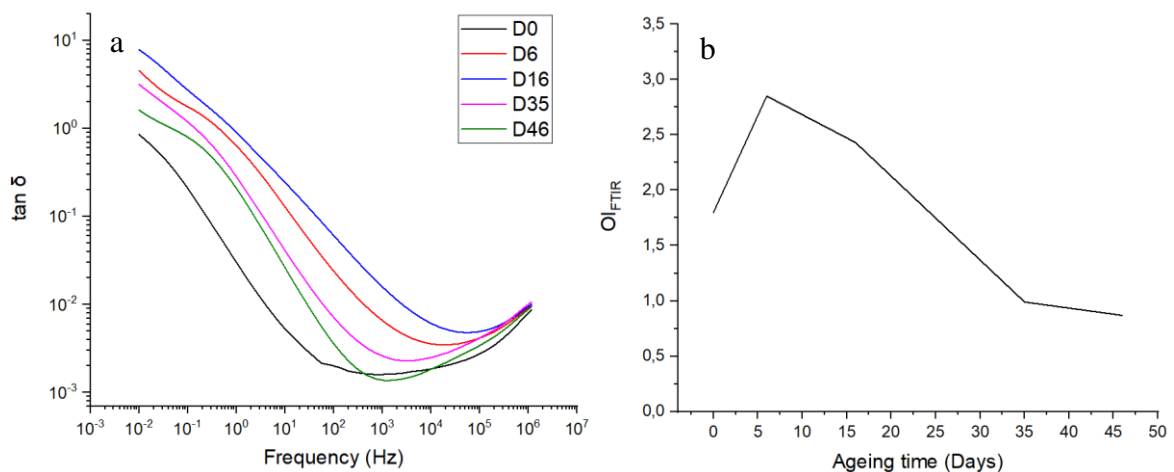


Figure 10: Évolution de $\tan \delta$ (a) et de la valeur d'absorbance (b) des échantillons UKP dans l'huile pour les échantillons non vieillis et vieillis jusqu'à 46 jours. Toutes les mesures de spectroscopie diélectriques ont été faites à 90°C. La teneur en eau des échantillons est visible ci-dessous dans la Figure 11.

Des données intéressantes sont obtenues à partir de ces mesures. L'évolution des propriétés diélectriques en fonction du temps n'est pas progressive : les pertes par conduction augmentent d'abord de J0 à J16, puis diminuent à J35 et J46. Une variation identique au cours du vieillissement a également été observée pour la pâte BKP et la pâte CL. Étant donné que ces résultats étaient quelque peu contre-intuitifs, une autre série de vieillissement de 46 jours dans des conditions identiques a été effectuée et a montré les mêmes résultats. Des vieillissements à J16 et J46 ont également été effectués deux fois pour vérifier qu'il n'y avait pas d'erreurs expérimentales, mais ils ont donné les mêmes résultats.

Un phénomène similaire a d'ailleurs été observé à plusieurs reprises dans la littérature antérieure. La durée réelle après laquelle ϵ'' diminue n'est pas identique dans les différents articles, car les échantillons sont de types différents et vieillis dans des conditions différentes. Dans d'autres études, avec des durées encore plus longues, des inversions multiples ont parfois

été rapportées. L'explication principale postulée est que la tendance non uniforme de la réponse diélectrique est corrélée aux variations de la teneur en humidité de l'huile. Dans ces études, les mesures FDS ont été effectuées à température fixe (55°C ou moins).

Des expériences ont montré que la réponse diélectrique change avec le vieillissement de l'isolant kraft et de l'huile ensemble, bien que le papier et l'huile pris séparément ne montrent étonnamment aucune modification importante. Ceci suggère deux facteurs principaux pour le changement de la réponse diélectrique dû au vieillissement : l'augmentation de la teneur en humidité, et aussi un changement des interactions entre les matériaux présents dans le système : papier, huile et eau. De telles interactions sont loin d'être identifiées et comprises. Un exemple typique d'interaction est la double couche électrique existant entre l'huile et le papier qui pourrait influencer les mesures FDS, bien que de manière imprévisible. L'analyse chimique montrant évidemment des modifications chimiques du papier (oxydation, degré de polymérisation, génération de sous-produits), on peut supposer que de telles interactions pourraient également évoluer (Figure 10b).

Il était donc intéressant d'estimer la teneur en eau de l'huile et du papier au cours du vieillissement. Malheureusement, il n'a pas été possible d'obtenir une mesure directe de ces données. Des échantillons d'huile ont été prélevés aux jours 6, 16, 35 et leur teneur en humidité a été mesurée à température ambiante. Bien que l'équilibre hydrique entre le papier et l'huile change considérablement entre la température ambiante et la température de vieillissement, la teneur en eau de l'huile pendant le vieillissement peut être utilisée pour estimer la teneur en humidité du papier à partir de tracés d'équilibre. Pour ce calcul, on a considéré que l'équilibre ne changeait pas avec le vieillissement. La Figure 11 montre qu'au cours du vieillissement, la teneur en eau du papier augmente d'abord, passe par un maximum d'environ 2,5 % après environ 15 jours, puis diminue. La teneur en eau finale à J = 46 jours est supérieure à celle initiale (0,3 %) et atteint environ 1,5 %, ce qui devrait induire des variations importantes des mesures FDS.

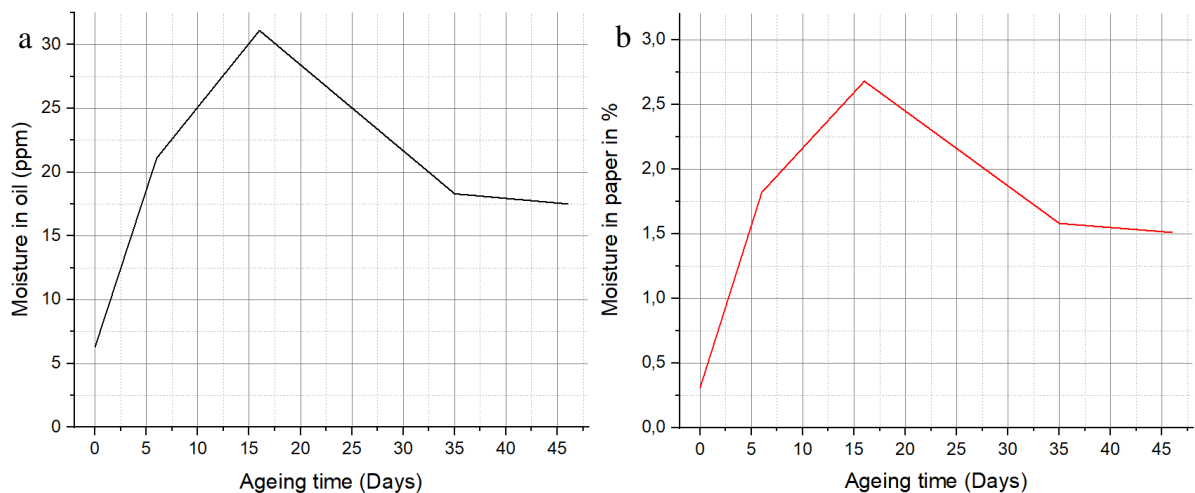


Figure 11: Évolution de la teneur en humidité à 20°C des échantillons d'huile (a) et de papier UKP (b) lors d'un vieillissement à 130°C dans des conditions non oxydantes. La teneur en humidité du papier est représentée par le rapport massique de l'eau divisé par le rapport massique du papier, indiqué en pourcentage. Pour l'huile, la teneur en humidité de l'eau est indiquée en ppm.

La corrélation entre la teneur en eau du papier au cours du vieillissement et les pertes diélectriques est assez évidente, et suggère fortement que les variations de FDS sont en partie

attribuables à l'augmentation de la teneur en eau. Certaines des comportements peuvent être observée après 46 jours :

- Une forte polarisation des électrodes à basse fréquence est observée lorsque la teneur en eau est maximale, induisant une forte augmentation de ϵ' jusqu'à 26 à 90°C au jour 16, soit environ 8 fois la permittivité normale du papier. Une telle augmentation ne peut s'expliquer si les pertes dues au liquide dominant encore.
- Les pertes augmentent beaucoup même à haute fréquence, où la contribution du papier domine.

iv) Effet de la composition du papier sur ses propriétés diélectriques

Les résultats obtenus dans des échantillons non vieillis imprégnés d'UKP, BKP et CL à 90 °C sont visibles sur la Figure 12. Tous les échantillons ont été préparés, séchés et imprégnés d'huile sèche en suivant le même protocole, par conséquent, tout changement dans les résultats doit provenir de différences dans la composition du papier.

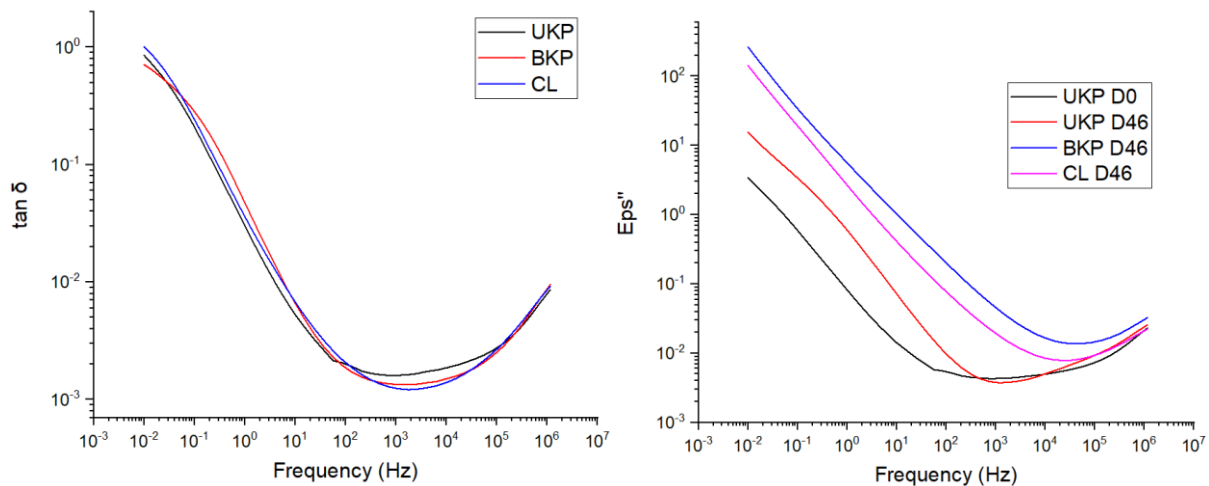


Figure 12 : a : Permittivité réelle (a / ϵ') et imaginaire (b / ϵ'') et $\tan \delta$ (c) comparaison entre la permittivité imaginaire ϵ'' des échantillons UKP, BKP et CL non vieillis. Toutes les mesures FDS ont été faites à 90°C et la teneur en humidité des échantillons est de 0,3%. b : Comparaison entre la permittivité imaginaire ϵ'' d'échantillons UKP, BKP et CL après 46 jours de vieillissement et un échantillon UKP non vieilli. Toutes les mesures de spectroscopie diélectrique ont été effectuées à 90°C.

La composition du papier ne joue pratiquement aucun rôle dans les propriétés diélectriques des échantillons non vieillis. Chimiquement, la pâte UKP contient de la lignine tandis que les pâtes BKP et CL ne contiennent que des polysaccharides (cellulose et hémicelluloses). Cela montre que pour les échantillons non vieillis, la lignine ne joue aucun rôle des échantillons non vieillis.

c) Conclusion

L'isolation kraft imprégnée d'huile constitue un matériau non homogène assez complexe dont la réponse diélectrique est difficile à analyser. Différents composants contribuent à cette

réponse : l'huile, le papier et les interactions entre l'huile et le papier. Le papier étant fortement hygroscopique (contrairement à l'huile), la teneur en eau du papier a également une très grande influence sur les pertes diélectriques. De plus, l'équilibre de l'eau entre l'huile et le papier évolue largement avec la température.

Dans des échantillons secs non vieillis, il a été montré que la réponse diélectrique de l'huile et de l'isolant papier était dominée aux basses fréquences par les pertes de conduction de l'huile et aux hautes fréquences par la polarisation interfaciale solide-liquide. Les pertes de conduction augmentent avec la température.

En comparant les résultats obtenus avec la littérature, il est difficile de donner une réponse universelle sur quel paramètre affecte la réponse diélectrique au cours du vieillissement, car peu d'études ont été réalisées en analyse FDS sur ce sujet, et aussi parce qu'elles ont toutes été réalisées avec différents paramètres. Des modifications de la méthode de mesure telles que la température ou le temps d'équilibrage peuvent modifier considérablement la réponse diélectrique. De plus, le mode de vieillissement peut également modifier significativement la manière dont le papier et l'huile vieillissent et donc la contribution de leur vieillissement. Même dans des conditions fixes et bien définies, les expériences peuvent conduire à des conclusions quelque peu différentes ; par exemple, l'influence dominante du vieillissement du papier ou de la teneur en eau. En revanche, le vieillissement de l'huile dans des conditions non oxydantes n'induit que des variations mineures de ses propriétés diélectriques.

Le rôle des constituants de l'isolant Kraft (lignine, hémicelluloses, cellulose) dans la réponse diélectrique a également été évalué. Pour les échantillons non vieillis, il a été démontré que la lignine a un rôle minime dans les propriétés diélectriques, mais, au fur et à mesure du vieillissement, la lignine protège la pâte de l'oxydation et donc d'une augmentation de la réponse diélectrique. De plus, les hémicelluloses pourraient constituer un maillon faible vis-à-vis de l'oxydation, comme le montre la réponse accrue de la pâte BKP par rapport à la pâte CL.

Conclusion générale

Le processus de vieillissement impliqué dans la dégradation de l'isolation kraft des transformateurs de puissance est un sujet qui malgré plusieurs décennies de recherche demeure très complexe. Cette thèse vise à approfondir le sujet en apportant de nouveaux éléments, par couplage de caractérisations chimiques et diélectriques des papiers kraft.

La fragilisation des isolants à base de papier kraft est généralement corrélée à l'évolution du DPv de la cellulose, polymère constitutif principal. Le mécanisme principal de dépolymérisation de la cellulose est l'hydrolyse acide. La génération de méthanol dans l'huile est récemment apparue comme étant un bon indicateur du DPv de l'isolant cellulosique, mais le mécanisme chimique de sa génération manque de clarté. L'objectif a été ici d'évaluer le rôle possible de la lignine dans la production de méthanol. Des expériences comparant du papier avec et sans lignine ont montré qu'il existe une contribution importante de la lignine à la production de méthanol. Les quantifications sur des composés modèles de lignine (cycles aromatiques méthoxylés) démontrent ainsi que la génération de méthanol provient essentiellement de la déméthylation des unités gaiacyle, favorisée en milieu acide, indépendamment de la dépolymérisation de la cellulose. Il a également été mis en évidence que le méthanol produit pouvait réagir avec les unités réductrices terminales des polysaccharides. En l'absence de lignine, du méthanol est généré au-delà d'un certain seuil de dépolymérisation. Le rôle de la lignine a ainsi été précisé, et les résultats obtenus pourraient guider davantage de recherches sur le sujet.

Les mêmes pâtes (UKP, BKP et CL) ont ensuite été étudiées pour suivre l'oxydation du papier (par FTIR), parallèlement à la dépolymérisation de la cellulose. Certains échantillons ont été produits par déminéralisation acide puis échange d'ions pour les enrichir en différents cations métalliques sélectionnés (Ca, Na, Mg, Fe et Cu).

Lors du vieillissement dans l'huile, il a été observé une augmentation, puis une diminution de l'état d'oxydation du papier et des pertes diélectriques au cours du vieillissement. L'augmentation correspond à la chute initiale rapide de DPv (hydrolyse acide de la phase amorphe de la cellulose), tandis que la diminution correspond à un ralentissement de la dépolymérisation. Le processus initial de dépolymérisation produit également une accumulation de sous-produits d'oxydation, qui se dégradent progressivement et migrent sous formes d'acides dans l'huile. La teneur en eau dans l'huile n'a toutefois pas suivi ce comportement. Le résultat final est que l'oxydation globale et la perte diélectrique diminuent dès que la vitesse de dépolymérisation ralentit.

Concernant l'utilisation de la spectroscopie diélectrique (FDS) comme outil permettant de suivre le vieillissement du papier, différentes conclusions ont été obtenues. Pour expliquer les variations enregistrées en FDS au cours du vieillissement, aucun mécanisme unique ne peut être invoqué : plusieurs résultats indiquent que des changements dans la composition chimique du papier (apparition de sous-produits d'oxydation du papier) sont responsables de l'évolution des pertes, mais l'eau a également une grande influence. Il a également été conclu que le FDS n'est pas en mesure de suivre efficacement la dépolymérisation du papier et montre une faible sensibilité à la composition du papier et à la teneur en ions. Par contre, il est très sensible à la présence d'eau. Ceci fournit des indications et des lignes directrices sur l'intérêt pratique des FDS que l'on peut attendre pour le diagnostic des transformateurs.

Une meilleure compréhension des mesures par spectroscopie diélectrique serait nécessaire pour améliorer le diagnostic de l'isolant cellulosique. Les interactions entre l'huile, le papier et l'eau doivent être mieux caractérisées. L'influence postulée de la double couche électrique à l'interface cellulose/huile pourrait être étudiée en faisant des expériences de spectroscopie diélectrique sur des couches de papier et d'huile en série. Ce phénomène étant fortement dépendant de la nature chimique des matériaux, des expérimentations avec différents matériaux (papiers, huiles), où la double couche est déjà caractérisée, pourraient être entreprises. Concernant l'influence de l'eau, il faudrait mener des expériences dans des situations où l'équilibre est atteint. Les expériences menées dans notre étude n'ont pas permis de s'assurer que l'équilibre était atteint à différentes températures.

Il a également été remarqué que l'indice de dispersité de la cellulose lors du vieillissement de l'UKP n'était pas constant. Ceci n'est pas pris en compte par les modèles mathématiques utilisés pour le vieillissement. En ce qui concerne la composition du papier, les échantillons avant vieillissement contenant de la lignine se sont avérés avoir une valeur d'oxydation similaire aux échantillons sans lignine. Une fois le vieillissement commencé, la lignine protège la pâte de l'oxydation, non seulement en réduisant la valeur globale des dommages oxydatifs, mais également la proportion de composants acides générés lors de l'oxydation. Ceci semble corrélé à l'évolution de la permittivité et à la dépolymérisation, et dans les deux cas, les échantillons avec une oxydation générant des constituants acides correspondaient à la dépolymérisation la plus rapide, et à la perte significative de propriétés diélectriques.

Références

- [1] Nynas, *Transformer oil handbook*. 2010.
- [2] J. Jalbert, R. Gilbert, P. Tétreault, B. Morin, et D. Lessard-Déziel, « Identification of a chemical indicator of the rupture of 1,4- β -glycosidic bonds of cellulose in an oil-impregnated insulating paper system », *Cellulose*, 14/4, 2007
- [3] Jalbert, Rodriguez-Celis, Arroyo-Fernández, Duchesne, et Morin, « Methanol Marker for the Detection of Insulating Paper Degradation in Transformer Insulating Oil », *Energies*, vol. 12/20, 2019.
- [4] J. Bagniuk *et al.*, « How to estimate cellulose condition in insulation transformers papers? Combined chromatographic and spectroscopic study », *Polym. Degrad. Stab.*, vol. 168, 2019.
- [5] G. Xia, G. Wu, B. Gao, H. Yin, et F. Yang, « A New Method for Evaluating Moisture Content and Aging Degree of Transformer Oil-Paper Insulation Based on Frequency Domain Spectroscopy », *Energies*, vol. 10/8, 2017.
- [6] B. Garcia, J. C. Burgos, A. M. Alonso, et J. Sanz, « A Moisture-in-Oil Model for Power Transformer Monitoring—Part I: Theoretical Foundation », *IEEE Trans. Power Deliv.*, vol. 20/2, 2005.
- [7] R. Jadav, C. Ekanayake, et T. Saha, « Understanding the impact of moisture and ageing of transformer insulation on frequency domain spectroscopy », *IEEE Trans. Dielectr. Electr. Insul.*, vol. 21/1, 2014.